UNIVERSITE DE LIMOGES

FACULTE DES SCIENCES ET TECHNIQUES

ECOLE DOCTORALE Sciences et Ingénierie pour l'information

Laboratoire XLIM, Département Composants Circuits

Signaux et Systèmes Hautes Fréquences

Année : 2010 **Thèse N° 69-2010**

THESE

Pour obtenir le grade de

DOCTEUR DE L'UNIVERSITE DE LIMOGES

Discipline : "Electronique des Hautes Fréquences, Photonique et systèmes"

Présentée et soutenue par

ZAHOOR AHMED

Le 2 Décembre 2010

Etude et construction de codes spatio-temporels algébriques dans le contexte des communications asynchrones par relais coopératifs

Directeurs de thèse : Jean Pierre Cances et Vahid Meghdadi

JURY :

Maryline Hélard	***Professeur à l'INSA Rennes***	Président
Gilles Burel	***Professeur à l'université de Bretagne Occidentale***	Rapporteur
Benoît Geller	***Maître de Conférence HDR à l'ENSTA Paris***	Rapporteur
Jean Pierre Cances	***Professeur à l'université de Limoge***	Examinateur
Vahid Meghdadi	***Maître de Conférence HDR à l'université de Limoges***	Examinateur

UNIVERSITE DE LIMOGES

FACULTE DES SCIENCES ET TECHNIQUES

ECOLE DOCTORALE Sciences et Ingénierie pour l'information

Laboratoire XLIM, Département Composants Circuits

Signaux et Systèmes Hautes Fréquences

Année : 2010 **Thèse N° 69-2010**

THESE

Pour obtenir le grade de

DOCTEUR DE L'UNIVERSITE DE LIMOGES

Discipline : "Electronique des Hautes Fréquences, Photonique et systèmes"

Présentée et soutenue par

ZAHOOR AHMED

Le 2 Décembre 2010

Etude et construction de codes spatio-temporels algébriques dans le contexte des communications asynchrones par relais coopératifs

Directeurs de thèse : Jean Pierre Cances et Vahid Meghdadi

JURY :

Maryline Hélard	***Professeur à l'INSA Rennes***	Président
Gilles Burel	***Professeur à l'université de Bretagne Occidentale***	Rapporteur
Benoît Geller	***Maître de Conférence HDR à l'ENSTA Paris***	Rapporteur
Jean Pierre Cances	***Professeur à l'université de Limoge***	Examinateur
Vahid Meghdadi	***Maître de Conférence HDR à l'université de Limoges***	Examinateur

Résumé

Pour faire face à l'évolution grandissante de services de plus en plus exigeants en termes de débits et de fiabilité sur les canaux de communication sans fil, des recherches récentes en théorie de l'information montre que des gains importants en capacité et en fiabilité peuvent être obtenus en exploitant la diversité spatiale. A cette fin, cette technologie, très connue sous le nom de MIMO, consiste à disposer de plusieurs antennes à la fois à l'émetteur et au récepteur. La technologie MIMO offre un certain nombre d'avantages qui nous aident à lutter contre les contraintes imposées par la limitation de puissance, la rareté de la bande passante et les phénomènes de trajets multiples.

Le codage temps-espace en bloc est l'une des techniques les plus utilisée en STC (Space Time Coding). Il est utilisé pour améliorer les performances des systèmes MIMO. Il tire au mieux parti de la diversité spatiale et temporelle et peut éventuellement fournir des gains de codage. Les codes temps-espace en bloc peuvent fournir un gain de diversité sur un système non codé sans sacrifier la bande passante et ainsi augmenter le taux de transmission efficace ainsi que la capacité potentielle du système.

Pour combattre certains inconvénients des Space-Time Block Codes (STBC's) orthogonaux classiques, en particulier la perte de rendement dès que le nombre d'antennes d'émission est supérieur à deux, des STBC's algébriques ont été construits à partir d'architectures en couches qui offrent des rendements de transmission optimaux et une diversité maximale, indépendamment de la constellation et du nombre d'antennes d'émission et de réception.

Toutefois dans certaines applications, il peut ne pas être réalisable ou rentable d'équiper les appareils de poche de petite taille et des capteurs de réseau avec du matériel supplémentaire RF. Pour faire face à ce problème, la diversité coopérative par le biais de la technique de relais peut être utilisée en considérant les relais à proximité des nœuds comme un réseau virtuel d'antennes. Grâce à la présence de ces relais, les nœuds dans un réseau distribué peuvent coopérer ensemble pour la transmission et le traitement de l'information en créant des liens MIMO indépendants.

A cause de la différence entre les différentes distances entre les noeuds de relais et les noeuds de réception dans un système de communications coopératives distribuées, tous les codes dits à taux plein perdent leur fiabilité (à savoir le gain de diversité) en raison de la nature asynchrone de la transmission. Pour éviter ce décalage de synchronisation certains auteurs ont proposé l'utilisation de bandes de garde entre les transmissions successives. Cette technique

peut être applicable pour les codes de courte longueur, mais pour de longs mots de code, l'utilisation de bandes de garde réduit considérablement le taux de codage.

En travaillant sur cette contrainte de délai pour les codes TAST, Damen et Hammons ont introduit une nouvelle classe de codes TAST qui sont robustes en terme de retards et donc adaptés aux réseaux coopératifs asynchrones. Ces codes préservent leur propriété de rang plein pour des retards arbitraires en réception sur les différentes lignes de la matrice de codage.

Bien que les codes distribués TAST mis en place par Damen et Hammons peuvent atteindre le maximum de diversité pour un profil de délai arbitraire, leur longueur temporelle n'est pas optimisée et peut s'avérer prohibitive. Pour aller plus loin dans le travail de Damen et Hammons, notre travail principal de cette thèse a consisté à construire des codes distribués TAST qui pourraient absorber des retards arbitraires et offrir de meilleurs taux de codage avec une longueur minimale. Nos codes proposés sont simples à construire, tolérants en terme de retard, et possèdent une longueur minimale au regard de la taille de la constellation et du nombre d'antennes d'émission et de réception.

Nous présentons différentes techniques pour la construction de codes TAST tolérants en retard. Les analyses mathématiques suivies par des simulations réalisées confirment que nos codes à longueur minimale dépassent les performances des codes existants dans la littérature sans pour autant sacrifier la complexité de décodage.

Abstract

To meet the challenges of rapid growing demands for high data rate and reliability over wireless communication channels, recent research in information theory proves that large gains in capacity and reliability can be achieved by exploiting the spatial diversity. For this purpose the appealing technology is to have multiple antennas both at transmitter and receiver, popularly known as MIMO. The MIMO technology offers a number of benefits that help us to combat against the constraints imposed by power limitation, scarce frequency bandwidth and multi-path fading.

Space-time block coding, one of the STC techniques, is used to improve the performance of MIMO systems. It takes advantages of the spatial and temporal diversity as well as coding gain. STBCs can provide diversity gain over an uncoded system without sacrificing the bandwidth and increase the effective transmission rate as well as the potential system capacity.

To overcome certain draw backs of conventional orthogonal STBCs, algebraic STBCs were constructed from layering/threaded architecture which offer full rate and maximum diversity irrespective of signalling constellation and number of transmit and receive antennas.

However in certain applications, it may not be feasible or cost effective to equip the small pocket size handsets and censor networks with the additional RF hardware. To deal with this problem the cooperative diversity delivered by relaying technology may be benefited by considering the nearby relay nodes as virtual antennas array. By the virtue of this idea, the nodes in a distributed network may cooperate together for transmission and processing of information by generating independent MIMO like channel links between source and destination via the relay channels.

Since the distances between different relay nodes and the receiving nodes in a distributed cooperative communication system may be different, therefore all well-known so-called full rate and fully diverse codes lose their reliability (*viz*. diversity and coding gain) due to the asynchronous nature of transmission. To avoid this destructive effect some authors have proposed the use of guard bands between successive transmissions. This technique may be applicable for short length codes, but for lengthy codewords, the use of guard bands drastically reduces the code rate.

Working on delay constraint of TAST codes, Damen and Hammons introduced a new class of TAST codes which are delay resistant and hence suitable for unsynchronized cooperative network. These codes preserve their rank under arbitrary delays at the reception of different rows of the codeword matrices.

Although the distributed TAST codes introduced by Damen and Hammons can achieve maximum diversity under arbitrary delay profile but their delay time is not gnarly. Extending the work of Damen and Hammons, our principal work in this thesis is to build distributed TAST codes which could absorb arbitrary delays and offer better rates. Our proposed codes are simple in construction, delay tolerant under arbitrary delays, better in rates, feasible in term of constellation size, number of receive/transmit antennas, and decoding complexity.

We introduce different techniques for constructing delay tolerant TAST codes. Mathematical analyses followed by computer simulations confirm that our codes with minimum code lengths outperform the existing codes in the literature without sacrificing decoding complexity and other nice characteristics.

Acknowledgements

I owe a debt of gratitude to all the people who helped and inspired me during my doctoral study in any respect. Without their generosity and assistance, the completion of this thesis would not have been possible.

It is extremely difficult for me to find words of gratitude to my research supervisor, Professor Jean Pierre Cances, who always proved as a springboard for me whenever, I encountered a deep chasm of difficulties and confusion. He devoted his precious time and guided me with valuable instruction and guidance. I have benefited tremendously from his wisdom, vision, inspiring and technical insights. I sincerely appreciate his extensive effort to help me improving my research skills.

I would like to express my deep and sincere gratitude to my co-supervisor, Vahid Meghdadi for his guidance and continuous support and valuable feedbacks throughout my PhD study. His wide knowledge and logical way of thinking have been of great source for completion of this thesis.

It would be my unkindness if I do not mention the kindness of Jean Michel Dumas. I express my special thanks for his precious guidance, encouragement and informative discussion on general issues. I am also thankful to Madam Anne Julien Vergonjanne and Madam Christelle Auptit Berthelemot for their help in my study. I also express my gratitude to Marine Sandrine whom I always used to bother for scanning tasks.

I am thankful to my colleagues and officemates from whom I learned a lot. My special thanks to the secretary of C_2S_2 Marie Claude Lerouge for her help in administrative matters. There are many friends who make my time at univeristé de Limoges enjoyable and memorable, so I would like to say thanks to all of them for their help and fun.

I would like to convey my limitless thanks to the concern authorities in Xlim, HEC and SFERE for their financial support.

At the last but not least, I am forever indebted to my parents for their unconditional love and encouragement. It was their faith in me that drives me so far in life. I also thank my wife because it was her love, patience and support that make me able to stay here in France without her.

List of abbreviations

AF	Amplify and Forward
ARQ	Automatic Repeat Request
AWGN	Additive While Gaussian Noise
BEC	Bit Efficient Code
BER	Bit Error Rate
BPCU	Bit Per Channel Use
BPSK	Binary Phase Shift Keying
CDF	Complementary Distribution Function
CDMA	Code Division Multiple Access
CF	Compressed and Forward
CGD	Code Gain Distance
CSI	Channel State Information
DAST	Diagonal Algebraic Space Time
DF	Decode and Forward
DFE	Decision Feedback Equalization
DS-CDMA	Direct Sequence Code Division Multiple Access
DSSS	Direct Sequence Spread Spectrum
FDMA	Frequency Division Multiple Access
FER	Frame Error Rate
FIR	Finite Impulse Response
HM	Huffman
IID	Independent, Identically Distributed
LDSTBC	Linear Dispersion Space Time Block Code
LHS	Left Hand Side
LOS	Line Of Sight
MIMO	Multi-Input Multi-Output
MISO	Multi-Input Single-Output
MGF	Moment Generating Function

ML	Maximum Likelihood
MMSE	Minimum Mean Square Error
MRC	Maximal-Ratio-Combiner
OSTBC	Orthogonal Space Time Block Codes
PDF	Probability Distribution Function
PEP	Pairwise Error Probability
PN	Pseudo Noise
PSK	Phase Shift Keying
PN	Pseudo Number
QAM	Quadratic Amplitude Modulation
QOSTBC	Quasi Orthogonal Space Time Block Codes
RHS	Right Hand Side
SCM	Shape Coded Modulation
SD	Sphere Decoding
SDF	Selective Decode and Forward
SEC	Symbol Efficient Code
SER	Symbol Error Rate
SIMO	Single-Input Multi-Output
SISO	Single-Input Single-Output
SNR	Signal to Noise Ratio
SOC	Super-Orthogonal Codes
SOSTTC	Super-Orthogonal Space Time Trellis Codes
SQOSTTC	Super-Quasi-Orthogonal Space-Time Trellis Code
SS	Spread Spectrum
SVD	Singular Value Decomposition
TDD	Time Division Duplexing
ST	Space Time
STBC	Space Time Block Codes
STTC	Space Time Trellis Codes
STTTC	Space Time Turbo Trellis Codes
TAST	Threaded Algebraic Space time
TASTBC	Threaded Algebraic Space Time Block Code
TCM	Trellis-Coded Modulation
TDMA	Time Division Multiple Access

TST	Threaded Space Time
UMTS	Universal Mobile Telephone System
UU	Uniform Use
WF	Water Falling
ZF	Zero Forcing

Notations and short words

$\|\cdot\|$	Euclidean norm
$\lfloor\cdot\rfloor$	Floor Function
$\lceil\cdot\rceil$	Ceiling Function
$(\cdot)^*$	Conjugate
$(\cdot)^\dagger$	Hermitian
$(\cdot)^T$	Transpose
$\otimes$	Tensor product
C	Capacity
C_{out}	Outage capacity
Delto	**De**lay **To**lerant
det	Determinant of a matrix
d_H	Hamming distance
$d_{\min}$	Minimum distance
d_P^2	Minimum product distance
E	Expectation
$\boldsymbol{H}$	$N_T \times N_R$ channel matrix
$\mathcal{I}$	Ideal of a ring
$\boldsymbol{I}_{N_T}$	$N_T \times N_T$ Identity matrix
$\Im$	Imaginary part
N_T	Number of transmit antennas
N_R	Number of receive antennas
$\Re$	Real part
$\mathbb{R}$	Set of real numbers
r	Received signal
$\boldsymbol{r}$	$T \times N_R$ received signal

tr	Trace
$\mathbb{Z}$	Set of integers

Table of contents

General introduction

The use of multiple-antennas at the transmitter and/or at the receiver in wireless communication systems has opened a new dimension in reliable communication by improving the system performances substantially. The idea behind MIMO is that the transmit antennas at one end and the receive antennas at the other end are connected and combined in such a way that the quality (the bit error rate, or the data rate) for each user is improved. The core idea in MIMO transmission is space-time signal processing in which signal processing in time is complemented by signal processing in the spatial dimension by using multiple, spatially distributed antennas at both link ends.

Cooperative diversity [19] is benefited to compensate the use of multiple antennas at certain small devices. Another essential problem of the wireless channel is fading, which occurs as the signal follows multiple paths between the transmit and the receive antennas. Fading can be mitigated by diversity, which means that the information is transmitted not only once but several times, hoping that at least one of the replicas will not undergo severe fading. Diversity makes use of an important property of wireless MIMO channels: different signal paths can be often modelled as a number of separate, independent fading channels. These channels can be distinct in frequency domain or in time domain. Several transmission schemes have been proposed that utilize the MIMO channel in different ways, *e.g*. spatial multiplexing, space-time coding or beamforming.

Space time coding [15] has been found a promising technique where the numbers of the transmitted code symbols per time slot are equal to the number of transmit antennas. These code symbols are generated by the space time encoder in such a way that diversity gain, coding gain, as well as high spectral efficiency are achieved.

If we put a view over the past history of space time coding system, this coding system has confronted different constraints during different times. For example after the introduction of Alamouti code [34] in 1998, the main problem was the non-existence of full rate codes for more than two transmit antennas scheme. Quasi-Orthogonal Space Time Block Codes (QOSTBCs) [42] may achieve full rate for more than two transmit antennas schemes but they lose their diversity. Space time trellis codes [15], [49] were invented as a remedial work to overcome this problem but their high decoding complexity do not let them to be propitious codes. Linear Dispersion Space Time Block Codes (LDSTBCs) [46] are easy to encode and

decode but they do not respect the basic condition of orthogonality and are not feasible with respect to number of antennas.

The discovery of TAST codes [63] was considered a great break through to be free from these constraints, but soon it was realized that all the powerful space time codes lose their credibility (*i.e.* diversity and coding gain) when used over asynchronous networks. This point is thoroughly explained in [69]. In fact in a delay constrained cooperative system the data from different relays reach the destination after different delays. It is shown in [69] that the received delayed distributed space-time block codes lose diversity for all well known codes. In [66] the authors study the effects of delay constraints over space-time trellis codes.

In [69], delay tolerant distributed space-time block codes based on threaded algebraic space-time (TAST) codes [63] are designed for unsynchronized cooperative network. The distributed TAST codes of [69] preserve the rank of the space-time codewords under arbitrary delays at the reception of different rows of the codeword matrices.

The principal work of this dissertation focuses the issue of delay constraints in asynchronous cooperative networks. We propose different technique for constructing delay tolerant TAST codes which have the properties to sustain arbitrary delays. Our proposed codes retain to be fully diverse even under arbitrary delay profiles. The mathematical analyses followed by MATLAB simulations confirm that our proposed codes obtain better performances as compare to the codes introduced in [69]. We have also proposed a technique of block layering in TAST codes, in which a series of layers are embedded over a single Diophantine number, and as a result we get a better coding gain by lessening the number of layers. Working on space time coding we have introduced a technique for improving the spectral efficiency of STBC for four transmit antennas scheme. Along with reliability, confidentiality is also a main problem in communication systems. Encrypting the pseudo-noise sequences of CDMA arise serious problem of synchronization. To deal with this issue, we have proposed a relay channel where information is sent in different frequency bands.

This thesis consists of five chapters and three appendices and is organized as follows:

We start with the introduction and performance analysis of MIMO system in chapter 1. The fundamental limits on the capacity of SISO, SIMO, MISO and MIMO were derived and simulated.

Broadcast nature of wireless communication system provides a potential resource for creation of third part's cooperation for transmission of information between source and destination. Chapter 2 thoroughly explains this mechanism in cooperative communication system. Amplify and forward, and decode and forward strategies are discussed in detail both over

single and multiple-hops cooperative networks. At the end of this chapter half duplex and frequency division relay networks are also discussed briefly.

Chapter 3 deals with space-time coding techniques and their performance in slow and fast fading MIMO channels. It provides a systematic discussion of different types of space time codes. Space-time block codes (STBCs) are particularly discussed at large extent. Alamouti code [34] which is considered as a milestone in the evolution of ST coding is also discussed as an example of STB codes. OSTBCs, QOSTBCs,[15] STTCs,[49] STTTCs, SOTTCs [55], LDSTBCs [46] and some more types of space time codes are presented and their performance is evaluated by simulations. A technique for improving the spectral efficiency of STBCs is also discussed in this chapter.

Chapter 4 contributes as principal work in this thesis report. This chapter starts with the introduction of DAST [62] and TAST codes [63]. After achieving the maximum limit in code diversity and rate, delay constraint in asynchronous communication was another emerging problem to suspect the credibility of space time codes. In this chapter we propose different techniques and remedies to deal with this constraint.

The last chapter briefly discusses the application of sphere decoder in multi-antennas scenarios.

The detail derivation for performance analysis of space time codes over slow and fast fading channels are discussed in appendices A and B, respectively, and appendix C describes the trace criteria for construction of space time codes.

Chapter 1

An overview of MIMO wireless systems

1.1 Introduction

The use of multiple antennas at the transmitter and receiver in wireless communication systems, known as MIMO (multiple-input multiple-output) technology, has rapidly gained a lot of popularity since last decade due to its powerful performance enhancing capabilities [1]-[3]. Communication in wireless channels is impaired predominantly by multi-path fading. Multi-path is the arrival of the transmitted signal at an intended receiver through different angles and/or different time delays and/or different frequency (*i.e*. Doppler) shifts due to the scattering of electromagnetic waves in the environment. Consequently, the received signals power fluctuates in space (due to angle spread) and/or frequency (due to delay spread) and/or time (due to Doppler spread) through the random superposition of the impinging multi-path components. This random fluctuation in signal level, known as fading, can severely affect the quality and reliability of wireless communication. Additionally, the constraints posed by limited power and scarce frequency bandwidth make the task of designing high data rate, high reliability wireless communication systems extremely challenging.

MIMO technology is considered a breakthrough in wireless communication system design. The technology offers a number of benefits that help to meet the challenges imposed by both, the impairments in the wireless channel as well as resource constraints. In addition to the time and frequency dimensions that are exploited in conventional SISO (single-input single-output) wireless systems, the leverages of MIMO are realized by exploiting the spatial dimension (provided by the multiple antennas at the transmitter and the receiver).

Figure 1.1 shows the performance of a MIMO system. In this figure the data rate versus the received signal-to-noise ratio (SNR) for an $N_R \times N_T$ (*i.e*. N_R receive and N_T transmit antennas) fading link with N_R = 1, 2, 4 and N_T = 1 are analysed. The channel response is assumed to be constant for a given bandwidth of 100 KHz. Assuming a target receive SNR of 25 dB, a conventional SISO (*i.e*. $N_R = N_T = 1$) system can deliver a data rate of 0.7 Mbps. With N_R = 2 and 4 we can achieve data rates of 1.4 and 2.8 Mbps respectively. This increase in data rate is achieved for no additional power or bandwidth expenditure compared to a SISO system. Equivalently a SISO system can achieve the data rate of 2.8 Mbps with a receive SNR of 25 dB if the bandwidth is increased from 100 KHz to 400 KHz, or alternatively, with the

bandwidth of 100 KHz if the receive SNR is increased to 85 dB. The result presented in this example is based on optimal transceiver design.

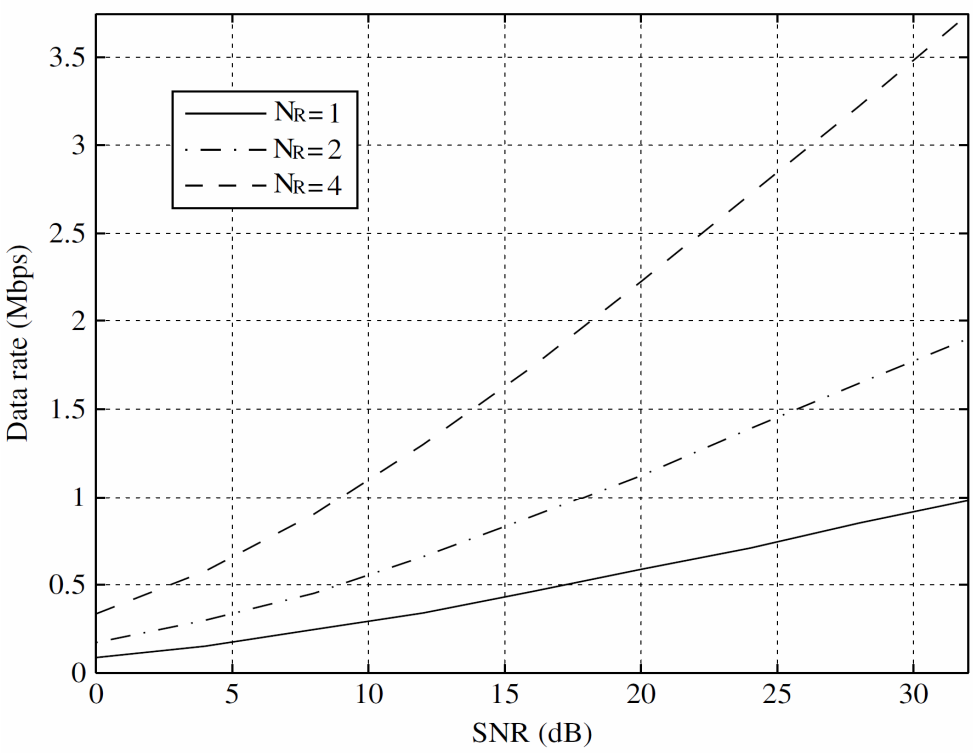

Figure 1.1 Average data rate versus SNR for different antenna configurations.

1.2 Benefits of MIMO technology

The benefits of MIMO technology that help us to achieve such significant performance gains are array gain, spatial diversity gain, spatial multiplexing gain and interference reduction.

1.2.1 Array gain

Array gain is the increase in received SNR that results from the coherent combining effect of the wireless signals at the receiver. The coherent combining may be realized through spatial processing at the receive antenna array and/or spatial pre-processing at the transmit antenna array. Array gain improves resistance to noise, thereby improving the coverage

1.2.2 Spatial diversity gain

As mentioned above, the signal level at the receiver in a wireless system fluctuates or fades. Spatial diversity gain mitigates fading and is realized by providing the receiver with multiple (ideally independent) copies of the transmitted signal in space, frequency or time. With an increasing number of independent copies (the number of copies is often referred to as the diversity order), the probability that at least one of the copies is not experiencing a deep fade increases, thereby improving the quality and reliability of reception. A MIMO channel with N_T transmit antennas and N_R receive antennas potentially offers $N_T N_R$ independently fading links, and hence a spatial diversity order of $N_T N_R$.

1.2.3 Spatial multiplexing gain

MIMO systems offer a linear increase in data rate through spatial multiplexing [1]-[3], *i.e.*, transmitting multiple, independent data streams within the bandwidth of operation. Under suitable channel conditions, such as rich scattering in the environment, the receiver can separate the data streams. Furthermore, each data stream experiences at least the same channel quality that would be experienced by a single-input single-output system, effectively enhancing the capacity by a multiplicative factor equal to the number of streams. In general, the number of data streams that can be reliably supported by a MIMO channel equals the minimum of the number of transmit and receive antennas, *i.e.* $min\{N_T,N_R\}$. The spatial multiplexing gain increases the capacity of a wireless network.

1.2.4 Interference reduction and avoidance

Interference in wireless networks results from multiple users sharing time and frequency resources. Interference may be mitigated in MIMO systems by exploiting the spatial dimension to increase the separation between users. For instance, in the presence of interference, array gain increases the tolerance to noise as well as the interference power, hence improving the signal-to-noise-plus-interference ratio (SINR). Additionally, the spatial dimension may be leveraged for the purposes of interference avoidance, *i.e.*, directing signal energy towards the intended user and minimizing interference to other users. Interference reduction and avoidance improve the coverage and range of a wireless network.

In general, it may not be possible to exploit simultaneously all the benefits described above due to conflicting demands on the spatial degrees of freedom. However, using some combination of the benefits across a wireless network will result in improved capacity, coverage and reliability.

1.3 MIMO channel and signal models

We consider a communication system, where signals are transmitted from N_T transmitters simultaneously. For example, in a wireless communication system, at each time instant t, signals $x_t^i \quad i = 1, 2, \ldots, N_T$ are transmitted simultaneously from N_T transmit antennas. The signals are the inputs of a MIMO channel with N_T outputs. Each transmitted signal goes through the wireless channel to arrive at each of the N_R receivers. In a wireless communication system with N_R receiver antennas, each output of the channel is a linear superposition of the faded versions of the inputs perturbed by noise. Each pair of transmit and receive antennas provides a signal path from the transmitter to the receiver. The coefficient $h_{j,i}$ is the path gain from transmit antenna i to receive antenna j. Figure 1.2 depicts a baseband discrete-time model for a flat fading MIMO channel.

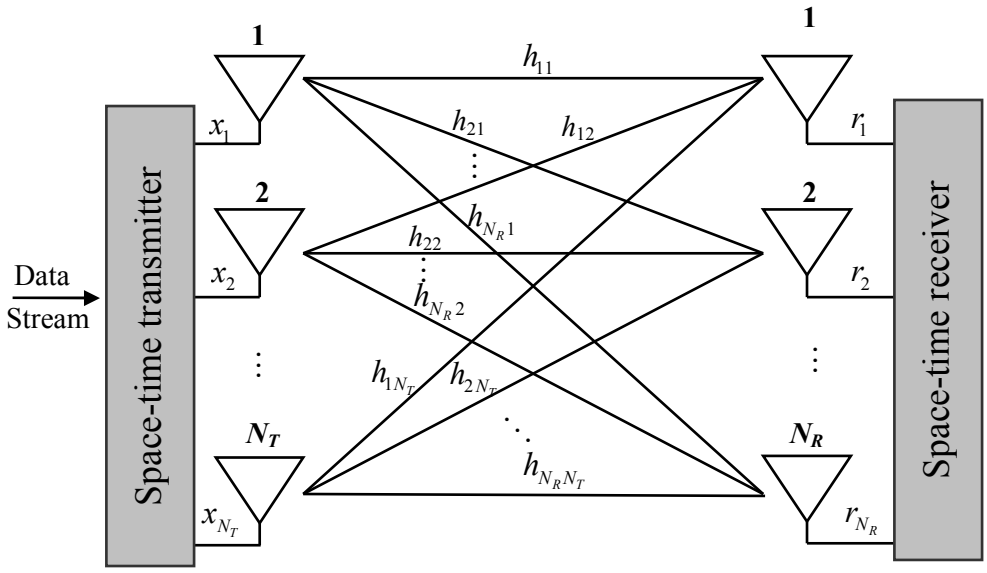

Figure 1.2 MIMO channel model

Based on this model, the signal r_t^j, which is received at time t at antenna j, is given by

$$r_t^j = \sum_{i=1}^{N_T} h_{j,i} x_t^i + n_t^j \tag{1.1}$$

where n_t^j is the noise sample of the receive antenna j at time t. Based on (1.1), a replica of the transmitted signal from each transmit antenna is added to the signal of each receive antenna. Although the faded versions of different signals are mixed at each receive antenna, the existence of the N_R copies of the transmitted signals at the receiver creates an opportunity to provide diversity gain

An important factor in the behaviour of the channel is the correlation between different path gains at different time slots. There are two general assumptions that correspond to two practical scenarios. First, we assume a quasi-static channel, where the path gains are constant over a frame of length T' and change from frame to frame, and as the second case, we consider a correlation between the fades in adjacent time samples. One popular example of such a second-order model is the Jakes model [4].

The value of T' dictates the slow or fast nature of the fading. If a block of data is transmitted over a time frame T that is smaller than T', the fading is slow. In this case, the fades do not change during the transmission of one block of data and the values of path gains in (1.1) are constant for every frame. On the other hand, in a fast fading model, the path gains may change during the transmission of one frame of data, $T > T'$. To form a more compact input-output relationship, we collect the signals that are transmitted from N_T transmit antennas during T time slots in a $T \times N_T$ matrix $\boldsymbol{x}$, as follows:

$$\boldsymbol{x} = \begin{bmatrix} x_{1,1} & x_{2,1} & \cdots & x_{T,1} \\ x_{1,2} & x_{2,2} & \cdots & x_{T,2} \\ \vdots & \vdots & \ddots & \vdots \\ x_{1,N_T} & x_{2,N_T} & \cdots & x_{T,N_T} \end{bmatrix} \tag{1.2}$$

Similarly, we construct a $T \times N_R$ received matrix $\boldsymbol{r}$ that includes all received signals during T time slots:

$$\boldsymbol{r} = \begin{bmatrix} r_{1,1} & r_{2,1} & \cdots & r_{T,1} \\ r_{1,2} & r_{2,2} & \cdots & r_{T,2} \\ \vdots & \vdots & \ddots & \vdots \\ r_{1,N_R} & r_{2,N_R} & \cdots & r_{T,N_R} \end{bmatrix} \tag{1.3}$$

Then, assuming $T < T'$, gathering the path gains in an $N_R \times N_T$ channel matrix $\boldsymbol{H}$

$$\boldsymbol{H} = \begin{bmatrix} h_{1,1} & h_{1,2} & \cdots & h_{1,N_T} \\ h_{2,1} & h_{2,2} & \cdots & h_{2,N_T} \\ \vdots & \vdots & \ddots & \vdots \\ h_{N_R,1} & h_{N_R,2} & \cdots & h_{N_R,N_T} \end{bmatrix} \tag{1.4}$$

results in the following matrix form.

$$\boldsymbol{r} = \boldsymbol{H}.\boldsymbol{x} + \boldsymbol{N} \tag{1.5}$$

where $\boldsymbol{N}$ is the $T \times N_R$ noise matrix defined by

$$\boldsymbol{N} = \begin{bmatrix} n_{1,1} & n_{2,1} & \cdots & n_{T,1} \\ n_{1,2} & n_{2,2} & \cdots & n_{T,2} \\ \vdots & \vdots & \ddots & \vdots \\ n_{1,N_R} & n_{2,N_R} & \cdots & n_{T,N_R} \end{bmatrix} \tag{1.6}$$

Actually (1.4) is mathematical representation of the MIMO system depicted in figure 1.2, where the coefficient $h_{j,i}$ denotes the SISO channel fading between the *j*-th (*j* = 1,2, . . . ,N_R) receive antenna and the *i*-th (*i* = 1, 2, . . . , N_T) transmit antenna. The column vector $\boldsymbol{h}_i = [h_{1,i}, h_{2,i}, ...h_{N_R,i}]^T$ is the single-input multiple-output (SIMO) channel produced by the *i*-th transmit antenna through the N_R receive antennas. The row vector $\boldsymbol{h}_j^T = [h_{j,1}, h_{j,2}, ...h_{j,N_T}]$ is the multiple-input single-output (MISO) channel that represents the different N_T paths arriving to the *j*-th receive antenna.

The rank of the MIMO channel corresponds to the number of independent signals that one may safely transmit through the MIMO system. It is determined by the algebraic rank of the $N_R \times N_T$ channel matrix. A MIMO channel is said rank-deficient if $N_R > N_T$ otherwise full rank.

1.3.1 Independent identically distributed Rayleigh fading channel model

The degree of correlation between the individual $N_T N_R$ channel gains comprising the MIMO channel is a complicated function of the scattering in the environment and antenna spacing at the transmitter and the receiver. Consider a case where all elements at transmitter and receiver are collocated. In such a condition, all the elements of $\boldsymbol{H}$ will be fully correlated and identical, and the spatial diversity order of the channel will be one. Decorrelation between the channel elements will increase with antenna spacing. The typical antenna spacing required for decorrelation is approximately half of the wavelength. Under ideal conditions, when the channel elements are perfectly decorrelated, we have $h_{j,i} \sim i.i.d.\ \mathcal{CN}(0,1)$. In other words, the real and imaginary parts of the path gains at each time slot are *i.i.d.* Gaussian random variables. Therefore, the distribution of the envelope of the path gains $|h_{j,i}|$, is Rayleigh, that is why the channel is called a Rayleigh fading channel.

1.3.2 Time-selective fading and frequency-selective fading channel model

As stated above, the fading is a time varying effect. This variation is characterized by the channel coherence time T_c , that serves as a measure of how fast the channel changes in time. In fact, the coherence time corresponds to the longest interval during which the channel is assumed to be constant. Let the time needed to transmit a symbol and a frame is denote by T_s and T_f respectively. Using these parameters, different channel models could be distinguished.

Ergodic: When $T_c = T_s$, the channel is said to be ergodic. In this case, each transmitted symbol is associated with a new realization of the channel.

Quasi-static: If the channel remains constant during one frame, *i.e.* $T_c = T_f$, the channel is called quasi-static.

Block fading: When fading does not change during $\mathcal{N}$ frame transmissions, the channel is said to be block fading. In this case, $T_c = \mathcal{N}T_f$. Note that a quasi static channel is also a block fading channel with $\mathcal{N}= 1$.

In the wireless channel, the multi-path propagation leads to a time delay spread to receive the different paths. This spread is characterized in the frequency domain by the coherence bandwidth, B_c . Indeed, B_c is a measure of the range of frequencies over which the channel has approximately equal gain.

When the signal bandwidth is comparable or less than B_c , all the frequency components of the transmitted signal undergo the same attenuation, the channel is said to be **flat** or **non-frequency selective** fading.

When the radio channel has different gains within the signal bandwidth, a **frequency selective** fading is experienced.

1.3.3 Ricean fading channel model

In the presence of a line of sight (LOS) component between the transmitter and the receiver, the MIMO channel may be modelled as the sum of a fixed component and a fading component [5], [6].

$$\boldsymbol{H}_{Rice} = \sqrt{\frac{K}{1+K}}\bar{\boldsymbol{H}}_{LOS} + \sqrt{\frac{1}{1+K}}\boldsymbol{H}'_{Rayleigh} \tag{1.7}$$

where $\sqrt{\frac{K}{1+K}}\bar{\boldsymbol{H}} = E[\boldsymbol{H}]$ is line of sight component of the channel and $\sqrt{\frac{1}{1+K}}\boldsymbol{H}'$ is the fading component, assuming uncorrelated fading. In (1.7) $K \geq 0$ is the Ricean K-factor of the channel and is defined as the ratio of the power in the LOS component of the channel to the power in the fading component. When $K = 0$ we have pure Rayleigh fading. At the other extreme $K = \infty$ corresponds to a non-fading channel.

1.3.4 Discrete-time signal model

Like SISO channels, the behaviour of the baseband system depends on the ratio of the signal power and the noise power. Therefore, multiplying the transmission power and noise by the same factor does not affect the characteristics of the system. A fair comparison between two systems consist of the same transmission power, despite the number of transmit antennas, and the same average received signal to noise ratio (SNR). Let us denote the average power of the transmitted symbols, x_t^i, by E_s and assume that the variance of the zero-mean complex Gaussian noise is $N_0/2$ per dimension, that is $Var[\Re\{n_{j,i}\}] = Var[\Im\{n_{j,i}\}] = N_0/2$. Then, the average receive SNR is $\gamma = N_T E_s / N_0$. Since the performance is only a function of SNR, only the ratio of E_s / N_0 is important and not the separate values of E_s and N_0. Therefore, a normalization that removes one of these two values, *i.e.* E_s or N_0 is more compact and useful. One approach to achieve such normalization is to normalize the average transmission power to one. For example, the average power of the transmitted symbols is normalized to $E_s = 1/N_T$. In this case, if the variance of the noise samples is $1/(2\gamma)$ per complex dimension, *i.e.* $N_0 = 1/\gamma$, the average power of the received signal at each receive antenna is 1 and the received SNR is γ.

Another approach for normalizing E_s and N_0 is to use a constellation with an average power of one for transmission symbols and unit-power noise samples. In this case, a normalization factor is considered in the input-output relationship of the MIMO channel as

$$\boldsymbol{r} = \sqrt{\frac{\gamma}{N_T}}\boldsymbol{H}.\boldsymbol{x} + \boldsymbol{N} \tag{1.8}$$

where again γ is the received SNR. Note that (1.5) and (1.8) describe the same system despite the difference in their forms. The main difference between the two equations is the method of normalization.

1.4 MIMO channel diversity

As mentioned above, the use of multiple antennas, sufficiently spaced to ensure independent fading between antennas, produces spatial diversity. This diversity is characterized by the number of independently fading branches, known as *diversity order*. Diversity order can be observed as the slope of the BER versus SNR curve.

Two types of diversity are potentially provided by MIMO channels:

Receive diversity: The use of multiple antennas at the receiver produces a receive-spatial diversity. The diversity order is equal to the number of receive antennas.

Transmit diversity: It consists in sending the same information over different transmit antennas. The diversity order in this case is equal to the number of transmit antennas. Thus the diversity order in MIMO channels is equal to the product of the numbers of transmit and receive antennas.

1.5 MIMO capacity

To determine the capacity of a MIMO channel, we start with the classical information theory introduced by Shannon [7].

Let the random variables $\boldsymbol{x}$ and $\boldsymbol{y}$ be respectively the input and the output of a memoryless wireless channel. The observation of the channel output $\boldsymbol{y}$ gives us information about the variable $\boldsymbol{x}$.

The mutual information $I(\boldsymbol{x}\,;\,\boldsymbol{y})$ is defined by the information theory to measure the amount of information that $\boldsymbol{y}$ contains about $\boldsymbol{x}$. The maximization of the mutual information over all possible input distributions $p(\boldsymbol{x})$ determines the maximum data rate that a channel can support without error, also known as channel capacity. The channel capacity is then measured in bits per channel use. Commonly, it is represented within a unit bandwidth of the channel and it is measured in bits/s/Hz.

For a discrete memoryless channel, the channel capacity is defined as [8].

$$C = \max_{p(\boldsymbol{x})} I(\boldsymbol{x}\,;\,\boldsymbol{y}) \tag{1.9}$$

With a power constraint of P_T at transmitter, (1.9) is written as

$$C = \max_{p(\boldsymbol{x}),E(\boldsymbol{x}^\dagger \boldsymbol{x})\le P_T} I(\boldsymbol{x};\boldsymbol{y}) \tag{1.10}$$

In literature, one can find enough works on MIMO channel capacity derivation in different scenarios. In following sub-sections we find out MIMO capacity for different channel time variations (ergodic and non-ergodic) cases.

1.5.1 Ergodic capacity

To show the gain offered by the use of multiple antennas at both sides in terms of capacity, we begin with fundamental results derived for single antenna (SISO) or multiple antennas at one side (SIMO or MISO) wireless systems.

In the following, we assume that the channel is ergodic and flat fading. Perfect Channel State Information (CSI) is available only at the receiver and the transmitter is constrained in its total power to P_T , *i.e.* $E(\boldsymbol{x}^\dagger \boldsymbol{x}) \le P_T$. The ergodic capacity is defined as the expectation of the instantaneous channel capacity (1.10) over the distribution of the elements of the channel matrix $\boldsymbol{H}$

$$C^{erg} = E_{\boldsymbol{H}}\left\{ \max_{p(\boldsymbol{x}),E(\boldsymbol{x}^\dagger \boldsymbol{x})\le P_T} I(\boldsymbol{x};\boldsymbol{y}) \right\} \tag{1.11}$$

1.5.1.1 The SISO case

For a memoryless SISO system (N_T = N_R = 1), the channel matrix $\boldsymbol{H}$ is reduced to a scalar complex variable *h.* The ergodic capacity is given by

$$C_{SISO}^{erg} = E_h\left\{ \max_{p(x),E(|x|^2)\le P_T} I(x;y) \right\} \tag{1.12}$$

Assuming independent Rayleigh fading channel, the capacity (1.12) can be written as [5]

$$C_{SISO}^{erg} = E_h\left\{\log_2(1+\gamma|h|^2)\right\} \tag{1.13}$$

where γ denotes the average SNR per receive antenna.

If we assume $|h|^2 = 1$, the instantaneous capacity becomes $C_{SISO} = \log_2(1+\gamma)$. It increases gradually with respect to the SNR, according to the logarithm of $(1+\gamma)$.

When the channel gain amplitude $|h|$ is Rayleigh distributed, $|h|^2$ follows a chi-squared distribution with two degrees of freedom [9] which leads to an exponential distribution. Hence (1.13) can then be written as [5]

$$C_{SISO}^{erg} = E_h\left\{\log_2(1+\gamma\chi_2^2)\right\} \tag{1.14}$$

where χ_2^2 is a chi-square distributed random variable with two degrees of freedom.

1.5.1.2 The SIMO case

Consider a SIMO channel $\boldsymbol{h} = [h_{1,1}, h_{2,1}, ..., h_{N_R,1}]$ with a single transmit and N_R receive antennas. The capacity under ergodicity assumption given by [5], [10], [11] is

$$C_{SIMO}^{erg} = E_{\boldsymbol{h}}\left\{\log_2\left(1+\gamma\sum_{j=1}^{N_R}\left|h_{j,1}\right|^2\right)\right\} \tag{1.15}$$

Like that of SISO case, if we assume that $\boldsymbol{h}$ satisfies $\left|h_{j,1}\right| = 1$, j = 1,2,….,N_R, then the instantaneous capacity becomes $C_{SIMO} = \log_2(1+\gamma N_R)$. Thus, the addition of receive antennas only results in a logarithmic increase of the capacity with the SNR.

With optimal combining at the receiver, the capacity of a Rayleigh fading SIMO channel can be expressed as [10]

$$C_{SIMO}^{erg} = E_{\boldsymbol{h}}\left\{\log_2(1+\gamma\chi_{2N_R}^2)\right\} \tag{1.16}$$

where $\chi^2_{N_R}$ is a chi-squared distributed random variable with $2N_R$ degrees of freedom.

1.5.1.3 The MISO case

We consider a MISO channel $\boldsymbol{h} = [h_{1,1}, h_{1,2}, ..., h_{1,N_T}]$ with N_T transmit antennas and a single receive antenna. The capacity for such a set up is given by [5], [10], [11]

$$C_{MISO}^{erg} = E_{\boldsymbol{h}} \left\{ \log_2 \left(1 + \frac{\gamma}{N_T} \sum_{i=1}^{N_T} \left| h_{1,i} \right|^2 \right) \right\} \tag{1.17}$$

If $\left| h_{1,i} \right| = 1$, i = 1, ….,N_T, then the instantaneous capacity is equal to $C_{MISO} = \log_2(1+\gamma)$. There is no gain in capacity over a SISO channel. By comparing equations (1.15) and (1.17) and assuming the same total number of antennas, it is clear that C_{MISO} is lower than C_{SIMO} when CSI is not available at the transmitter.

1.5.1.4 The MIMO case

Let $\boldsymbol{Q} = E(\boldsymbol{x}^{\dagger}\boldsymbol{x})$ be the covariance of the input signal. Then, the capacity is defined as the maximum of the mutual information between the input and output given a power constraint P_T on the total transmission power of the input, *i.e.* $Tr(\boldsymbol{Q}) \le P_T$, where $Tr(\boldsymbol{Q})$ is the trace of a matrix $\boldsymbol{Q}$, then the average capacity of a random ergodic MIMO channel is given by [12]

$$C_{MIMO}^{erg} = E_{\boldsymbol{H}} \left\{ \max_{p(\boldsymbol{x});tr(\boldsymbol{Q}) \le P_T} I(\boldsymbol{x}; \boldsymbol{y}) \right\} \tag{1.18}$$

When the mutual information is maximized for a zero mean circularly symmetric complex Gaussian distributed input, the capacity is then given by [12]

$$C_{MIMO}^{erg} = E_{\boldsymbol{H}}\left\{\log_2\left(\det\left(\boldsymbol{I}_{N_R} + \frac{1}{2No}\boldsymbol{H}^{\dagger}\boldsymbol{Q}\boldsymbol{H}\right)\right)\right\} \tag{1.19}$$

When no CSI is available at the transmitter, the available power P_T can be uniformly distributed among the transmit antennas. For uncorrelated channel, the transmit covariance matrix is equal to $\boldsymbol{Q} = \frac{P_T}{N_T}\boldsymbol{I}_{N_T}$, and the corresponding channel capacity becomes [5]

$$C_{MIMO}^{erg} = E_{\boldsymbol{H}}\left\{\log_2\left(\det\left(\boldsymbol{I}_{N_R} + \frac{P_T}{2N_T N_0}\boldsymbol{H}^{\dagger}\boldsymbol{H}\right)\right)\right\} \tag{1.20}$$

Let $\gamma = \frac{P_T}{2N_0}$ be the average SNR per receive antenna. For optimal combining between N_R antennas at the receiver, the capacity can be written as [10], [12]

$$C_{MIMO}^{erg} = E_{\boldsymbol{H}}\left\{N_T \log_2\left(1 + \frac{\gamma}{N_T}\chi^2_{N_R}\right)\right\} \tag{1.21}$$

By the law of large numbers, the term $\frac{\boldsymbol{H}^{\dagger}\boldsymbol{H}}{N_T} \to \boldsymbol{I}_{N_R}$ as N_T gets larger and N_R remains fixed [13]- [15]. Thus, as a result, the ergodic capacity becomes:

$$C_{MIMO}^{erg} = N_R \log_2(1+\gamma) \tag{1.22}$$

Hence, the capacity reaches an asymptotic value for a fixed N_R. Then it will be unadvantageous to increase indefinitely the number of transmit antennas.

The two figures given below are the simulation results for *i.i.d*. Rayleigh fading ergodic channels for different scenarios of (N_T, N_R) and different power allocation. The input variable x is supposed to be Gaussian distributed. When uniform power allocation is considered (1.20), figure 1.3 shows the channel capacity as a function of the average SNR per receive antenna,

γ. Clearly, the use of multiple antennas increases the achievable rates on fading channels. At moderate to high SNRs, the capacity of an $N_T = N_R = 4$ MIMO channel is about twice the capacity of a 2×2 system and 4 times the capacity of a 1×1 system. The slope of the capacity versus SNR is proportional to min(N_T,N_R). As shown above, the capacity of SIMO system is higher than MISO system for both cases $N_T + N_R = 5$ and $N_T + N_R = 3$. The capacity gain achieved by the following MISO systems: 2×1 and 4×1, over SISO system (1×1) is not significant.

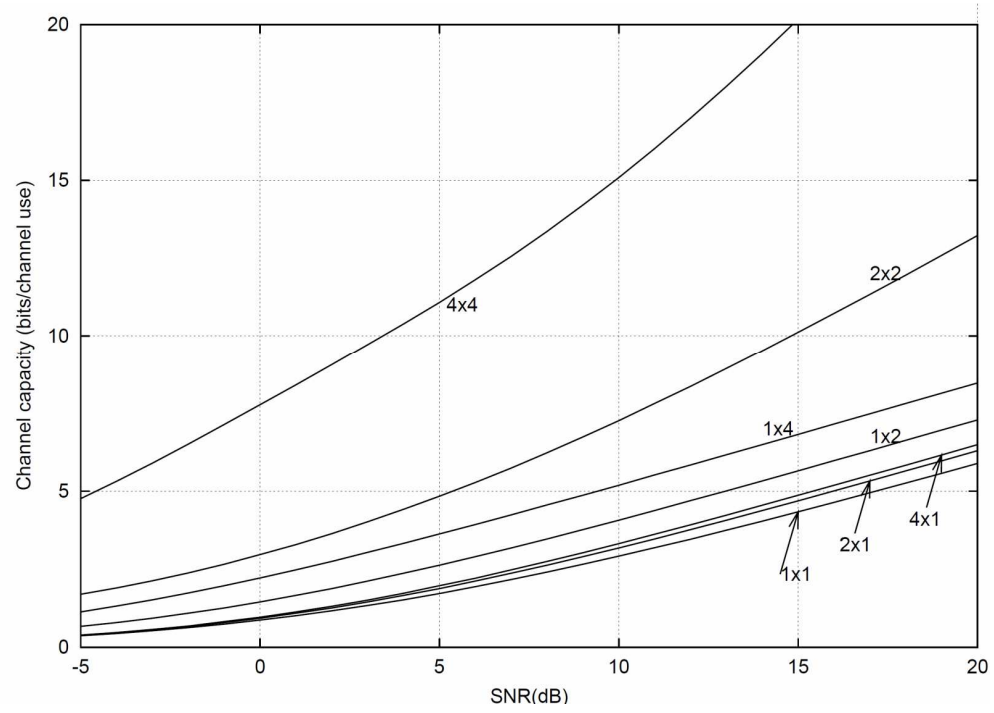

Figure 1.3 MIMO capacity on an *i.i.d*. Rayleigh fading ergodic channel (Gaussian input and uniform power allocation).

Figure 1.4 compares the capacity observed with scheme of two power allocations, *i.e*. uniform power allocation and optimal power allocation based on water-filling algorithm. Both power allocations maintain the capacity proportional to the channel rank which is equal to *min*(N_T,N_R).

However, an SNR gain is noticed while applying the optimal strategy. This gain is more significant at low SNR, especially for 4×4 system.

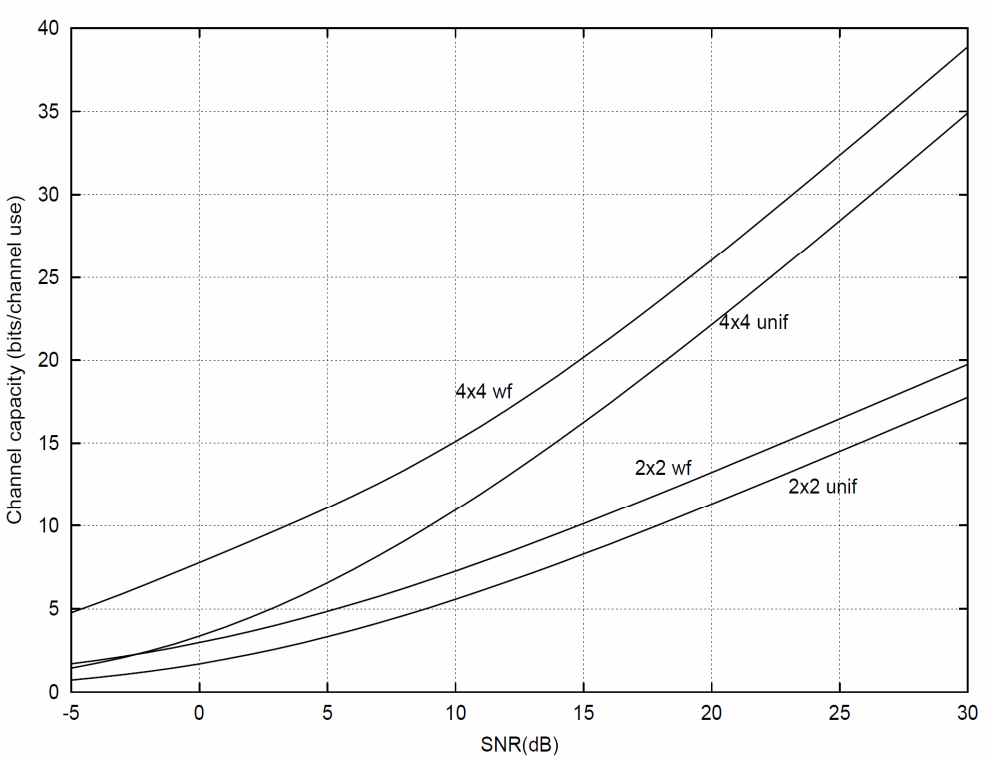

Figure 1.4, MIMO capacity on an *i.i.d*. Rayleigh fading ergodic channel, under uniform power allocation (unif),and optimal power allocation (wf).schemes

Further analysis of the MIMO channel capacity can be conducted by applying the singular value decomposition (SVD) to the channel matrix $\boldsymbol{H}$, interested reader is therein referred to [2], [12], [16].

1.5.2 Outage capacity

In previous section, we discussed the capacity of MIMO channels when the channel is ergodic. But unfortunately for slow-varying or block fading channel, the ergodicity property is not respected and the classical capacity definition is no longer applicable.

Actually in slow fading (quasi-static) channels, the coherence time T_c is much larger than the codeword duration T. The channel thereby remains constant over the duration of a codeword but changes independently from block to block. In such a scenario, the useful parameter for capacity measurement is the outage capacity introduced in [8], [10], [12].

$$P_{out} = \Pr[I < R] \tag{1.23}$$

where *R* is the rate at which reliable communication is possible and *I* is mutual information, or more precisely we can write

$$\mathrm{P}_{out} = \Pr[C < C_{out}] \tag{1.24}$$

Another way of defining the outage probability is to consider the event that the received SNR is below a certain threshold.

$$P_{out} = \Pr\left[\gamma < 2^R - 1\right] = \Pr[\gamma_{SNR} < \gamma_{Threshold}] \tag{1.25}$$

The importance of the outage probability is that if one wants to transmit C_{out} bits/channel use, the capacity of the channel is less than C_{out} with probability P_{out}. In other words, such a transmission is impossible with probability P_{out}. For a stationary channel, if we transmit a large number of frames with a rate of C_{out} bits/channel use, the number of failures is P_{out} times the total number of frames. On the other hand, since with a probability of $1-P_{out}$, the capacity random variable is larger than the outage capacity, the value of the outage capacity C_{out} guarantees that it is possible to transmit C_{out} bits/channel use with a probability of $1-P_{out}$. In what follows, we briefly discuss the outage capacity for different channel setup.

1.5.2.1 The SISO case

We consider the case when we have only one transmit and one receive antenna, $N_T = N_R = 1$. The received signal can be written as

$$r = hx + n \tag{1.26}$$

Let *h* be a zero mean Gaussian random variable with variance 1. Referring to (1.14), with the assumption that the fading is Rayleigh, the outage probability can be written as [17]

$$P_{SISO}^{out}(R) = P\left\{\log_2\left(1+\gamma x_2^2\right) < R\right\} \tag{1.27}$$

where x_2^2 is a chi-square random variable with two degrees of freedom. To achieve one extra bit of capacity, one needs to increase the SNR by 3dB.

By simple algebraic manipulation, (1.27) yields

$$P_{SISO}^{out}(R) = P\left\{x_2^2 < \frac{2^R - 1}{\gamma}\right\} \tag{1.28}$$

We get

$$P_{SISO}^{out}(R) = 1 - \exp\left(\frac{2^R - 1}{\gamma}\right) \tag{1.29}$$

At high SNR which gives

$$P_{SISO}^{out}(R) \approx \frac{2^R - 1}{\gamma} \tag{1.30}$$

We remark that the outage probability asymptotically decays as $1/\gamma$. This channel has diversity order one.

1.5.2.2 The SIMO case

For the case of SIMO, the receiver is assumed to be equipped with an antenna array in order to increase the spatial diversity order of the channel. Here the transmitted vector is in fact a scalar and the channel is a column vector $\boldsymbol{h}$ with N_R components.

The received signal can be written as

$$\boldsymbol{r} = \boldsymbol{h}_{N_R} x + \boldsymbol{n} \tag{1.31}$$

Referring to (1.15), we may write the outage probability for the SIMO case as

$$P_{SIMO}^{out}(R) = P\left\{\log_2\left(1 + \gamma \sum_{j=1}^{N_R} \left|h_{j,1}\right|^2\right) < R\right\} \tag{1.32}$$

Assuming independent Rayleigh fading, the capacity (1.32) can be written as [15]

$$C_{SIMO}^{out} = \log_2\left(1+\gamma\chi_{2N_R}^2\right) \tag{1.33}$$

where $\chi_{2N_R}^2$ is a chi-square random variable with $2N_R$ degrees of freedom.

The corresponding outage probability is given as

$$P_{SIMO}^{out}(R) = P\left(\|h\|^2 < \frac{2^R-1}{\gamma}\right) \tag{1.34}$$

Under Rayleigh fading with each gain, $h_{j,1} \sim i.i.d.\ \mathcal{CN}(0,1)$

$$\|\boldsymbol{h}\|^2 = \sum_{j=1}^{N_R}\left|h_{j,1}\right|^2 \tag{1.35}$$

is the sum of the squares of $2N_R$ independent real Gaussian random variables, each term $\left|h_{j,1}\right|^2$ being the sum of the real and imaginary parts of $h_{j,1}$. It is chi-square distributed with $2N_R$ degrees of freedom, and its PDF is given by [18, ch: 3]

$$p_{\|\boldsymbol{h}\|^2}(x) = \frac{1}{(N_R-1)!}x^{N_R-1}e^{-x} \tag{1.36}$$

For small x, the probability density function of $\|\boldsymbol{h}\|^2$ is approximately

$$p_{\|h\|^2}(x) \approx \frac{1}{(N_R-1)!}x^{N_R-1} \tag{1.37}$$

So we get

$$P\left\{\|h\|^2(x)<1/\gamma\right\}\approx\int_0^{\frac{1}{\gamma}}\frac{1}{(N_R-1)!}x^{N_R-1}dx=\frac{1}{N_R!}\frac{1}{\gamma^{N_R}} \tag{1.38}$$

By applying (above) to the expression of the outage probability at high SNR, we get

$$P_{SIMO}^{out}(R)=\frac{\left(2^R-1\right)^{N_R}}{N_R!\gamma^{N_R}} \tag{1.39}$$

The outage probability asymptotically decays as $1/\gamma^{N_R}$, hence N_R is the diversity order of this channel.

Figure 1.5 shows the outage probability plotted against SNR for an outage capacity of C_{out} = 2 bits/(s/Hz) for one transmit antenna and N_R =2, 3, 4 receive antennas.

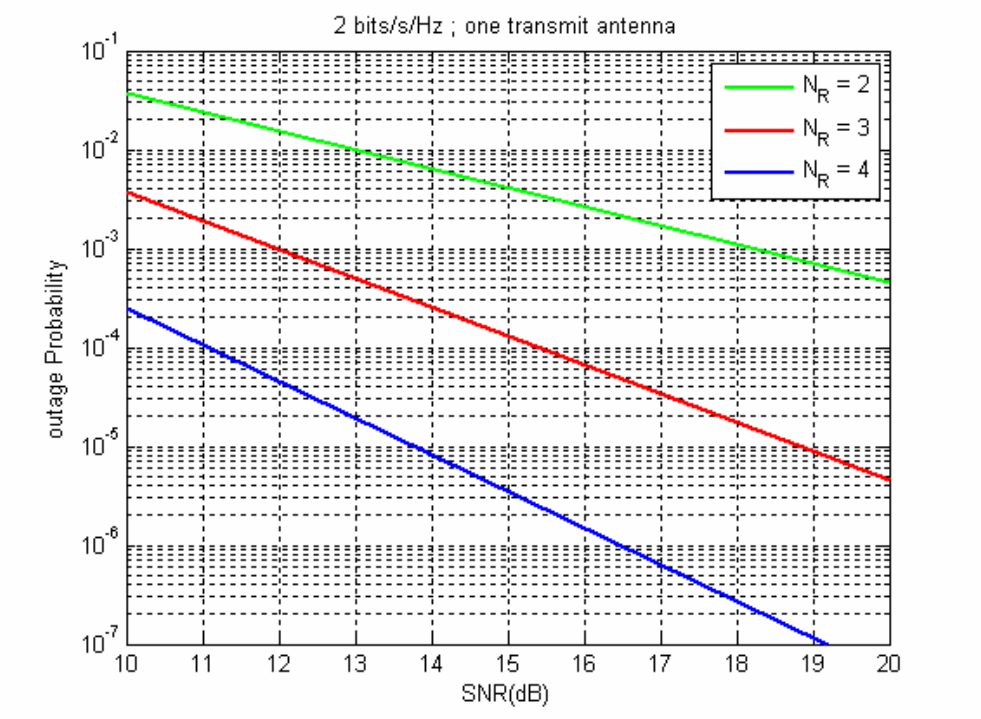

Figure 1.5 C_{out} = 2 bits/(s/Hz); N_R receive antennas, one transmit antenna.

1.5.2.3 The MISO case

Similarly for a system with N_T transmit antennas and one receive antenna, the received signal can be written as

$$r = \boldsymbol{h}_{1\times N_T}\boldsymbol{x} + n \tag{1.40}$$

the channel is a row vector $\boldsymbol{h}$ with N_T components, which are assumed to be *i.i.d*. zero-mean Gaussian. The outage probability for the MISO case from equation (1.17) can be written as

$$P_{MISO}^{out} = P\left\{\log_2\left(1+\frac{\gamma}{N_T}\sum_{i=1}^{N_T}\left|h_{1,i}\right|^2\right) < R\right\} \tag{1.41}$$

Assuming independent Rayleigh fading, the capacity (1.41) can be written as [15]

$$P_{out} = \log_2(1+(\gamma/N_T).x_{2N_T}^2) \tag{1.42}$$

where $x_{2N_T}^2$ is a chi-square random variable with $2N_T$ degrees of freedom.

The corresponding outage probability is given as

$$P_{MISO}^{out} = P\left(x_{2N_T}^2 < N_T\frac{2^R-1}{\gamma}\right) \tag{1.43}$$

The same calculation as we did in case of SIMO, yields

$$P_{MISO}^{out}(R) = \frac{{N_T}^{N_T}\left(2^R-1\right)^{N_T}}{N_T!\gamma^{N_T}} \tag{1.44}$$

enlightening a transmit diversity order equal to N_T

Figure 1.6 shows the outage probability plotted against SNR for an outage capacity C_{out} = 2 bits/(s Hz) for N_T = 2, 3, 4 transmit antennas and one receive antenna. As it is clear from above discussion that for a given outage capacity, a system with N_T transmit antennas and one receive antenna requires N_T times more signal-to-noise ratio to provide the same outage probability as a system with $N_R = N_T$ receive antennas and one transmit antenna. This is due to the fact that the capacity formulas are derived for the same total transmission power in both cases. Mathematically, the $N_T \times 1$ channel and the $1 \times N_R$ channel provide a similar capacity for $N_R = N_T$ if the transmitted power over each path is the same. However for a fair comparison, the total transmission power needs to be divided among the N_T transmit antennas. Therefore, the received signal-to-noise ratio is affected by a factor of N_T.

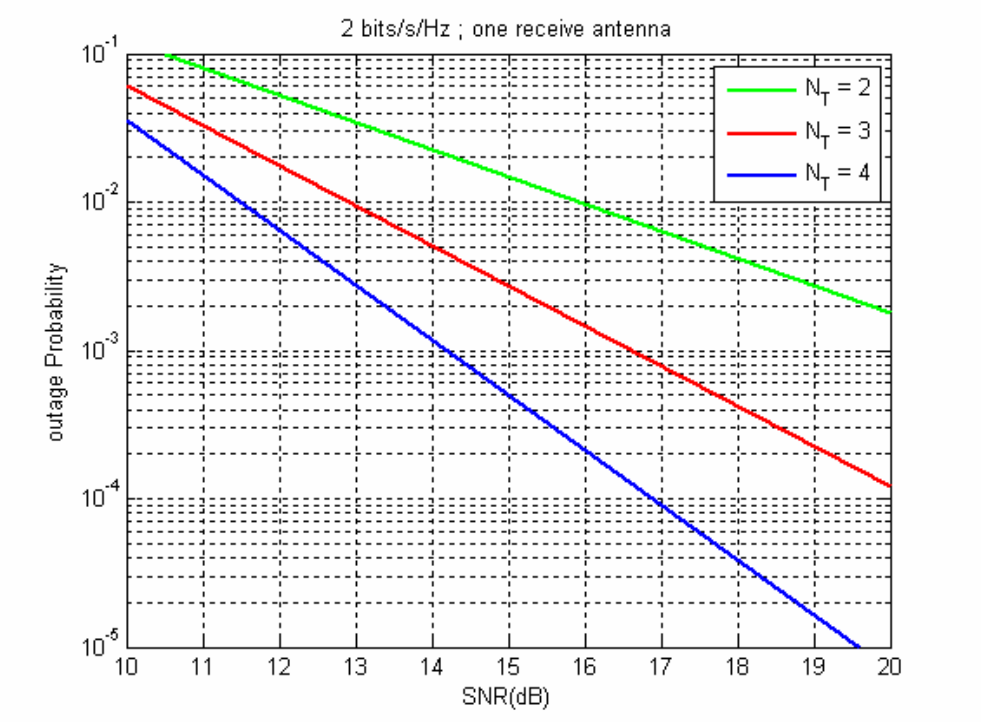

Fig. 1.6, C_{out} = 2 bits/(s Hz); N_T transmit antennas, one receive antenna.

1.5.2.4 The MIMO case

The calculation of the outage probability for the MIMO case is more difficult than for the previous case. In the MIMO case, the channel matrix $\boldsymbol{H}$ is an $N_R \times N_T$ matrix with zero-mean Gaussian *i.i.d.* components.

Let $q = \min\{N_R, N_T\}$. Then the outage probability is given by [17],[18]

$$P_{MIMO}^{out}(R) = P\left\{\sum_{i=1}^{q}\log_2\left(1+\frac{\gamma}{M}\lambda_i^2\right) < R\right\} \quad (1.45)$$

where λ_i is the singular values of the matrix $\boldsymbol{H}$. The MIMO channel exhibits q modes of transmission, each corresponding to an instantaneous SNR equal to $(\gamma\lambda_i^2)/N_T$.

The channel diversity order obtained from the outage probability calculation in the MIMO case is $N_R N_T$.

1.6 Conclusion

In this chapter, we discussed the fundamental limits on the capacity of MIMO channels for both single and multi-user systems. We briefly discussed the ergodic and outage capacity gains for different channel set up and realized their performances by simulation results.

The capacity gains derived for such systems can be realized in some cases, but realistic assumptions about channel knowledge and the underlying channel model can significantly mitigate these gains.

For single-user systems the capacity under perfect CSI at the transmitter and receiver is relatively straightforward and predicts that capacity grows linearly with the number of antennas. However backing off from the perfect CSI assumption makes the capacity calculation much more difficult, and under such scenarios the capacity gains highly depend on the nature of the CSI, the channel SNR, and the antenna element correlations.

One of the main constraints of MIMO system is the installation of more than one antenna over a small pocket size mobile apparatus. The broadcast nature of wireless channels helps us to overcome this problem by the introduction of relay networks. In next chapter we study the effects of relay networks which provide us a MIMO-like channel link between source and destination via relay nodes, to be considered as a set of distributed antennas in MIMO communication system.

Chapter 2

Introduction and performance analysis of cooperative relay networks

2.1 Introduction

In traditional communication systems data transmissions take place directly between the transmitter and the receiver. No user solicits the assistance of others. However, in a general communication networks, there are many intermediate nodes that might be requested for help in transmitting the source message to the intended destination. For example in wireless networks, when one node broadcasts its messages, all nearby nodes overhear this transmission. Processing and forwarding these messages to the intended destination, system performance, whether it be throughput, lifetime, or coverage area, can be improved. Such a communication system where the intermediate nodes (generally called as relays) cooperate with source in transmitting his message to the intended destination, is called *cooperative network*, and for the first time, was introduced by Van der Meulen [19] in 1968.

Figure 2.1 represents a simple cooperative network in which the source node transmits a signal to the destination node via the relay node. The link between the source and the relay and the relay and the destination is commonly referred to as the relay link whereas the link between the source and the destination is referred as direct link.

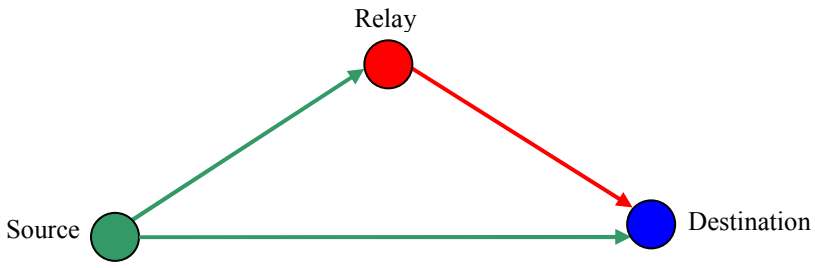

Figure 2.1 A single node relay network

Now the question arises that how cooperative communications in wireless networks are possible. Note that the wireless channel is broadcast by nature. This implies that many nearby nodes or users can “hear” and receive transmissions from a source and hence can help the source for better transmission if needed. In other words, the broadcast nature, long considered as a vast waste of energy causing interference to others, is now regarded as a potential resource for possible assistance. For example, it is well known that the wireless channel is quite bursty, *i.e.* when a channel is in a severe fading state, it is likely to stay in the state for a while. Therefore, when a source cannot reach its destination due to severe fading, it will not

be much helpful to keep trying by leveraging repeating transmission protocols such as automatic repeat request (ARQ). If a third party that receives the information from the source could help via a channel that is independent from the source–destination link, the chances for a successful transmission would be brighten, thus improving the overall performance.

In fact after the emergence of MIMO technology with the constraint of installing multiple antennas on pocket size mobile handsets, the relaying technology has gained much attention by considering these nodes as a set of distributed antennas in MIMO communication system. Adopting this point of view, nodes in the network may cooperate together for distributed transmission and processing of information. Indeed, cooperative communications can be thought of as a generalized MIMO concept with different reliabilities in antenna array elements by generating independent MIMO-like channel links between a source and destination via the introduction of relay channels. This idea of using the broadcast nature of the wireless channels to make communicating nodes help each other, implementing the communication process in a distribution fashion, and gaining the same advantages as those found in MIMO systems has birth various new communication techniques that improve communication capacity, speed, performances and coverage area.

In this chapter, we study the effects and performance enhancing capacity of relay networks by using different protocol operations over single and multi-hop relaying system. We provide capacity limits both for half and full duplex mode of communication. At the end of this chapter we provide a technique of information hiding over orthogonal Gaussian relay channel.

2.2 Network performance analysis through channel capacity

For the sake of completeness and ease to understand, we put a bird eye view over information theory which is an important tool in analysing the achievable rates and performances of a communication network. The information theory deals with the information provided by the outcome of a random variable.

Suppose that X and Y are two random variables representing the input and output of a communication channel, respectively.

The information provided by the outcome x of a discrete random variable X is defined as [8]

$$I_X(x) = \log \frac{1}{\Pr[X = x]} = -\log \Pr[X = x] \tag{2.1}$$

where $\Pr[X = x]$ is the probability of the outcome $X = x$

It is clear to judge that, rarer is event, the more information it provides. Since the communication process is inherently a process relating more than one random variable (*e.g.* the input and output of a channel), so it is important to define a magnitude relating the information shared by two random variables. This magnitude is the mutual information, which for two discrete random variables X and Y is defined as

$$I(X;Y) = \sum_{x \in X} \sum_{y \in Y} \Pr[X = x, Y = y] \log \frac{\Pr[X = x, Y = y]}{\Pr[X = x] \Pr[Y = y]} \tag{2.2}$$

where $\Pr[X = x, Y = y]$ is the joint probability mass function and $\Pr[X = x]$ and $\Pr[Y = y]$ are marginal probability mass functions.

According to Bayes theorem, the mutual information can be written as

$$I(X;Y) = \sum_{x \in X} \sum_{y \in Y} \Pr[X = x, Y = y] \log \frac{\Pr[X = x \mid Y = y]}{\Pr[X = x]} \tag{2.3}$$

Furthermore, we can write

$$\begin{aligned} I(X;Y) &= -\sum_{x \in X} \Pr[X = x] \sum_{y \in Y} \Pr[X = x, Y = y] + \sum_{x \in X} \sum_{y \in Y} \Pr[X = x, Y = y] \log \Pr[X = x \mid Y = y] \\ &= -\sum_{x \in X} \Pr[X = x] \log \Pr[X = x] + \sum_{x \in X} \sum_{y \in Y} \Pr[X = x, Y = y] \log \Pr[X = x \mid Y = y] \end{aligned} \tag{2.4}$$

The first term in (2.4) is called the entropy of the random variable X

$$H(X) = -\sum_{x \in X} \Pr[X = x] \log \Pr[X = x] \tag{2.5}$$

and the second term in (2.4) can be written in term of the conditional entropy of X

$$H(X \mid Y) = -\sum_{x \in X} \Pr[X = x, Y = y] \log \Pr[X = x \mid Y = y] \tag{2.6}$$

Considering (2.1), the entropy of the random variable can also be read as the mean value of the information provided by all its outcomes. Likewise, the conditional entropy can be regarded as the mean value of the information provided by all the outcomes of a random variable (X) given than the outcome of a second random variable (Y) is known, or in other words how much uncertainty about a random variable (X) remains after knowing the outcome of the second random variable (Y). Therefore, the mutual information in (2.4) can now be written as

$$I(X;Y) = H(X) - H(X \mid Y) \tag{2.7}$$

In information theory, one of the main measures of performance is the capacity of the system. When the random variations of the channel are stationary and ergodic process, it is possible to consider the traditional notion of capacity as introduced by Claude Shannon [7]. In this case, coding is assumed to be done using arbitrary long blocks. The capacity of an AWGN channel over fast fading, when the receiver has perfect channel information is given as [20]

$$C = E\left[\log\left(1+\frac{|h|^2 P}{N_0}\right)\right] \tag{2.8}$$

where $E[\cdot]$ is expectation operator, P is the power of transmitted signal, N_0 is the variance of noise and $|h|^2$ is the envelope of the channel attenuation.

Although the notion of Shannon capacity is quite useful, but there are some other design parameters where the assumptions of using arbitrary long codes or that the channel is a stationary and ergodic random process do not hold. In such cases, Shannon capacity may not yield useful results. For example, in the case of a non-ergodic slow fading channel following a Rayleigh distribution, the Shannon capacity is arbitrary small or zero. This is because of the fact that the channels are affected by deep fades realizations. Therefore, for such cases it is more appropriate to consider the notion of outage capacity, as discussed in previous chapter.

The outage capacity is tied to the concept of an outage event. From an information theory point of view, an outage event is defined as the set of channel realizations that cannot support reliable transmission at rate R. In other words, the outage event is the set of channel realizations with an associated capacity less than the transmit rate R. Now considering a setup that leads to (2.8) corresponds to a non-ergodic channel, the outage condition for a realization of the fading can be written as

$$\log\left(1+\frac{|h|^2 P}{N_0}\right) < R \tag{2.9}$$

From here, the outage probability is calculated as the one associated with the outage event

$$P_{out} = \Pr\left[\log\left(1+\frac{|h|^2 P}{N_0}\right) < R\right] \tag{2.10}$$

Once we have introduced the concepts of outage event and outage probability, the outage capacity, C_{out}, is defined as the information rate that can be reliably communicated with a probability $1-\Pr_{out}$,*i.e.*

$$\Pr[C \le C_{out}] = \mathrm{P}_{out} \tag{2.11}$$

where C is the Shannon capacity associated with the channel

Equivalently the outage probability may be defined as in (1.25)

$$P_{out} = \Pr\left[\gamma < 2^R - 1\right] = \Pr[\gamma_{SNR} < \gamma_{Threshold}] \tag{2.12}$$

2.3 Basic model of relay channel

A cooperative communication takes place in two phases. In both phases users transmit signals through orthogonal channels by using TDMA, FDMA, or CDMA. In this section we consider a simple single relay model as depicted in figure 2.2.

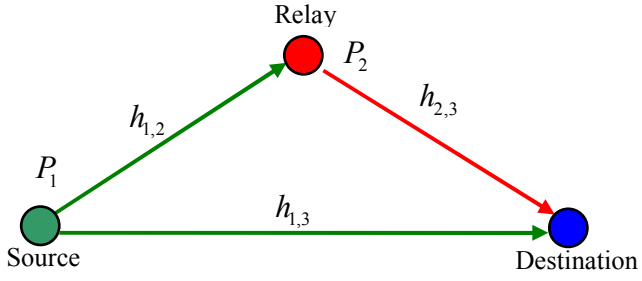

Figure 2.2 A simple cooperative model

In phase-I: the source broadcasts its information to both, the destination and the relay. The received signals at the destination $y_{1,3}$ and at the relay $y_{1,2}$ can be expressed as

$$y_{1,3} = \sqrt{P_1} h_{1,3} x + n_{1,3} \tag{2.13}$$

and

$$y_{1,2} = \sqrt{P_1} h_{1,2} x + n_{1,2} \tag{2.14}$$

where P_1 and P_2 are transmitted powers from the source and the relay, respectively, x is transmitted symbol, $n_{1,3}$ and $n_{1,2}$ are additive noises, and $h_{1,3}$ and $h_{1,2}$ are channel coefficients from source to the destination and to the relay, respectively, and are modelled as zero mean complex Gaussian random variables with variance $\sigma_{1,3}^2$ and $\sigma_{1,2}^2$, respectively. The noise term $n_{1,3}$ and $n_{1,2}$ are zero mean complex Gaussian random variables with variance N_0.

In phase-II: the relay forwards a processed version of the source's signal to the destination, and this can be represented as

$$y_{2,3} = h_{2,3} q(y_{1,2}) + n_{2,3} \tag{2.15}$$

where $q(\cdot)$ is the process performed at the relay.

2.4 Cooperation protocols

A key aspect of the cooperative communication is the processing of the signal received from the source node at the relay. There are different processing schemes resulting in different cooperative communications protocols. Cooperative communications protocols can be generally classified into fixed relaying schemes and adaptive relaying schemes. In fixed relaying, the channel resources are divided between the source and the relay in a fixed (deterministic) manner. In a fixed amplify-and-forward (AF) relaying protocol [21], the relay simply scales the received signal and transmits an amplified version of it to the destination. Another possibility of processing at the relay node is to decode the received signal, re-encode it and then transmit it to the receiver. This kind of relaying is referred a fixed decode-and-forward (DF) relaying protocol [21]. Fixed relaying has the advantage of easy implementation, but the disadvantage of low bandwidth efficiency. This is because half of the channel resources are allocated to the relay for transmission, which reduces the overall rate. This is true especially when the source-destination link is not very bad in a sense that the

destination can decodes the source message correctly without the help of relay and hence the relay's transmission will be useless. Adaptive relaying technique which comprises selective and incremental relaying may compensate this problem to some extent.

In selective relaying, if the signal-to-noise ratio of the received signal at the relay exceeds a certain threshold, the relay performs decode-and-forward operation on the message, otherwise it remains idle. Moreover, if the source knows that the destination does not decode correctly, then the source may repeat to transmit the information to the destination or the relay may help in forwarding the information, which is termed as incremental relaying. In this case, a feedback channel from the destination to the source and the relay is necessary.

In literature one can find numerous cooperation protocols introduced by different researchers. To discuss each and every protocol is beyond the scope of this report, in what follows, we elaborate two principal protocols from fixed relaying scheme and two from adaptive relaying scheme.

2.4.1 Fixed cooperation strategies

2.4.1.1 Amplify and Forward (AF) strategy

In an AF relaying, the relay amplifies the signal received from the source and forwards it to the destination ideally to equalize the effect of the channel fade between the source and the relay. The relay does that by simply scaling the received signal by a factor that is inversely proportional to the received power, which is denoted by [20]

$$\alpha = \frac{\sqrt{P_2}}{\sqrt{P_1 \left| h_{1,2} \right|^2 + N_0}} \tag{2.16}$$

The signal transmitted from the relay is thus given by $\alpha y_{1,2}$ and has the same power as that of the source. To calculate the mutual information between the source and the destination, we need to calculate the total instantaneous SNR at the destination. The SNR received at the destination is the sum of the SNRs from the source and the relay. The SNR from the source link is given by

$$SNR_{1,3} = \gamma \left| h_{1,3} \right|^2 \tag{2.17}$$

where $\gamma = P_1 / N_0$

Now we calculate the received SNR from the relay link. In phase-II the relay amplifies the received signal and forwards it to the destination with transmitted power P_2. The received signal at the destination in phase-II from (2.15) and (2.16) can be written as

$$y_{2,3} = \frac{\sqrt{P_2}}{\sqrt{P_1 \left| h_{1,2} \right|^2 + N_0}} h_{2,3} y_{1,2} + n_{2,3} \tag{2.18}$$

where $h_{2,3}$ is the channel coefficient from the relay to the destination and $n_{2,3}$ is an additive noise. More specifically, the received signal $y_{2,3}$ in this case is

$$y_{2,3} = \frac{\sqrt{P_1 P_2}}{\sqrt{P_1 \left| h_{1,2} \right|^2 + N_0}} h_{2,3} h_{1,2} x + n'_{2,3} \tag{2.19}$$

where

$$n'_{2,3} = \frac{\sqrt{P_2}}{\sqrt{P_1 \left| h_{1,2} \right|^2 + N_0}} h_{2,3} n_{1,2} + n_{2,3} \tag{2.20}$$

Assume that the noise terms $n_{1,2}$ and $n_{2,3}$ are independent then the equivalent noise $n'_{2,3}$ is a zero-mean, complex Gaussian random variable with variance.

$$N'_0 = \left(\frac{P_2 \left| h_{2,3} \right|^2}{P_1 \left| h_{1,2} \right|^2 + N_0} + 1 \right) N_0 \tag{2.21}$$

This is due to fact that the relay amplifies not only the received signal, but the noise as well. The destination receives two copies of the signal *x* through the source and relay links. There are different techniques to combine the two signals. The optimal technique that maximizes the overall signal-to-noise ratio is the maximal ratio combiner (MRC). Note that MRC combining requires a coherent detector that has knowledge of all channel coefficients. We know that the SNR at the output of the MRC is equal to the sum of the received SNRs from both branches.

With knowledge of the channel coefficients $h_{1,3}$, $h_{1,2}$ and $h_{2,3}$ the output of the MRC detector at the destination can be written as

$$y = a_1 y_{1,3} + a_2 y_{2,3} \tag{2.22}$$

The combining factors a_1 and a_2 should be designed to maximize the combined SNR, which can be done by formulating an optimization problem and selecting these factors correspondingly. An easier way to design them is by resorting to signal space and detection theory principles [6]. Since, the AWGN noise terms span the whole space, to minimize the noise effects the detector should project the received signals $y_{1,3}$ and $y_{1,2}$ to the desired signal spaces. Hence, $y_{1,3}$ and $y_{1,2}$ should be projected along the directions of $h_{1,3}$ and $h_{2,3}$ $h_{1,2}$, respectively, after normalizing the noise variance terms in both received signals. Therefore, a_1 and a_2 are given by [20].

$$a_1 = \frac{\sqrt{P_1} h_{1,3}^*}{N_0} \quad \text{and} \quad a_2 = \frac{\sqrt{\dfrac{P_1 P_2}{P_1 \left|h_{1,2}\right|^2 + N_0}} h_{1,2}^* h_{1,3}^*}{\left(\dfrac{P_2 \left|h_{2,3}\right|^2}{P_1 \left|h_{1,2}\right|^2 + N_0} + 1 \right) N_0} \tag{2.23}$$

By assuming that the transmitted symbol x in (2.13) has average energy 1, the instantaneous SNR of the MRC output is

$$\Gamma = \Gamma_1 + \Gamma_2 \tag{2.24}$$

where

$$\begin{aligned} \Gamma_1 &= \frac{\left|a_1 \sqrt{P_1} h_{1,3}\right|^2}{\left|a_1\right|^2 N_0} \\ &= \frac{P_1 \left|h_{1,3}\right|^2}{N_0} \end{aligned} \tag{2.25}$$

and

$$\Gamma_2 = \frac{\left| a_2 \dfrac{\sqrt{P_1 P_2}}{\sqrt{P_1 \left|h_{1,2}\right|^2 + N_0}} h_{2,3} h_{1,2} \right|^2}{\left|a_2\right|^2 N_0'}$$

$$= \frac{\dfrac{P_1 P_2}{P_1 \left|h_{1,2}\right|^2 + N_0} \left|h_{1,2}\right|^2 \left|h_{2,3}\right|^2}{\left(\dfrac{P_2 \left|h_{2,3}\right|^2}{P_1 \left|h_{1,2}\right|^2 + N_0} + 1 \right) N_0}$$

$$= \frac{1}{N_0} \frac{P_1 P_2 \left|h_{1,2}\right|^2 \left|h_{2,3}\right|^2}{P_1 \left|h_{1,2}\right|^2 + P_2 \left|h_{2,3}\right|^2 + N_0} \tag{2.26}$$

From the above, the instantaneous mutual information as a function of the fading coefficients for AF strategy is given by

$$I_{AF} = \frac{1}{2} \log\left(1 + \Gamma_1 + \Gamma_2\right) \tag{2.27}$$

Substituting for the values of the SNR of both links, we can write the mutual information as

$$I_{AF} = \frac{1}{2} \log\left(1 + \gamma \left|h_{1,3}\right|^2 + f(\gamma \left|h_{1,2}\right|^2, \gamma \left|h_{2,3}\right|^2)\right) \tag{2.28}$$

where

$$f\left(x, y\right) \triangleq \frac{xy}{x + y + 1} \tag{2.29}$$

The outage probability can be obtained by averaging over the exponential channel gain distribution, as follows

$$\Pr\left[I_{AF} < R\right] = E_{h_{1,3}, h_{1,2}, h_{2,3}} \left[\frac{1}{2} \log\left(1 + \gamma \left|h_{1,3}\right|^2 + f(\gamma \left|h_{1,2}\right|^2, \gamma \left|h_{2,3}\right|^2)\right) < R \right] \tag{2.30}$$

Calculating the above integration, the outage probability at high SNR is given by [20], [22].

$$\Pr\left[I_{AF} < R\right] \simeq \left(\frac{\sigma_{1,2}^2 + \sigma_{2,3}^2}{2\sigma_{1,3}^2\left(\sigma_{1,2}^2\sigma_{2,3}^2\right)}\right)\left(\frac{2^{2R}-1}{\gamma}\right)^2 \tag{2.31}$$

where, the multiplicative factor of 2 in $2R$ is because half of the bandwidth is lost in cooperation by allocating them to the relay. The outage expression decays as γ^{-2} which means that the AF protocol achieves diversity 2.

Figure 2.3 shows the simulation results of outage probability versus SNR in dB for a fixed rate of 2 bps/Hz, for an AF protocol. For comparison we have included the simulation result of direct transmission. The channel variance $\sigma_{1,3}$ between source and destination is taken as 1, whereas for source-relay and relay-destination as 0.5. The noise variance is one. One can see from the graph that AF protocol achieves a diversity of 2.

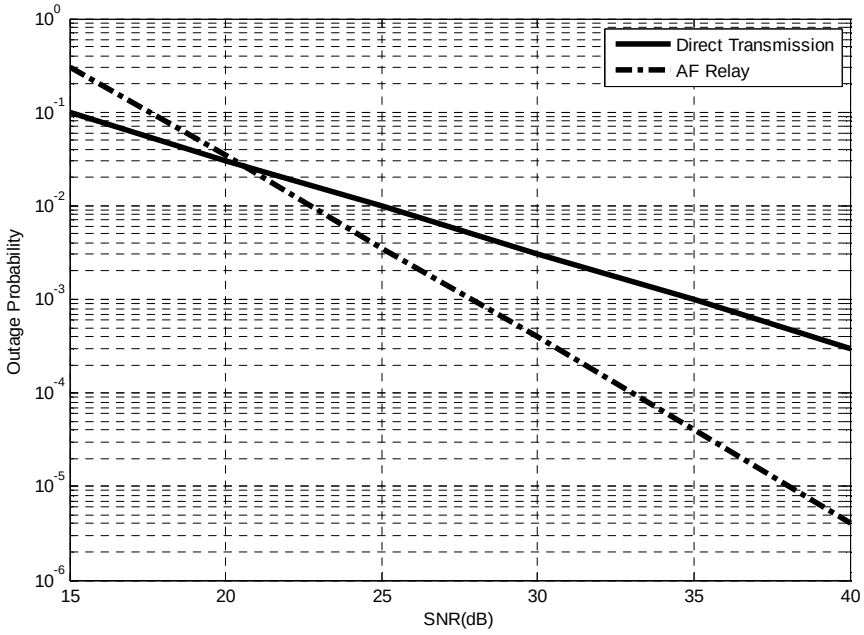

Figure 2.3 Outage probability versus SNR

In figure 2.4 the outage probability is depicted versus spectral efficiency in bps/Hz for a fixed SNR of 40 dB. The reason for selection of such a high SNR is to study the effect of increasing the rate making it free from the effect of SNR. It is clear from the graph that the performance degrades with increasing R, but it degrades faster for AF because of the inherent loss in the spectral efficiency. At high enough R, direct transmission becomes more efficient than cooperation.

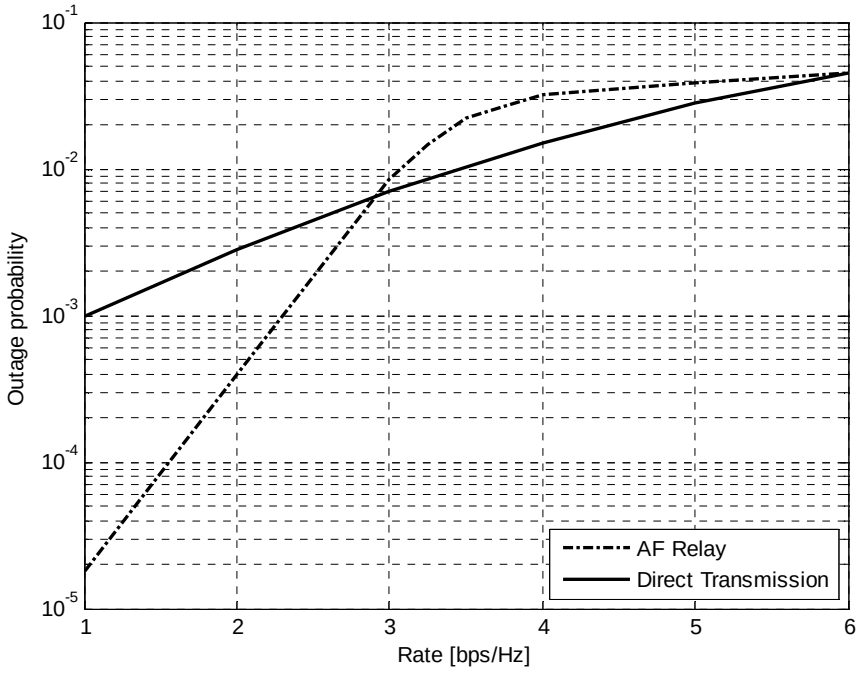

Figure 2.4 Outage probability versus spectral efficiency

Symbol Error Rate (SER) Analysis for AF Protocol

The SER of an uncoded M-PSK and M-QAM modulations can be written as [20], [23]

$$\Psi_{PSK}(\rho) \triangleq \frac{1}{\pi}\int_0^{(M-1)\pi/M} \exp\left(-\frac{b_{PSK}\rho}{\sin^2\theta}\right) d\theta \tag{2.32}$$

$$\Psi_{QAM}(\rho) \triangleq 4KQ\left(\sqrt{b_{QAM}\rho)}\right) - 4K^2Q^2\left(\sqrt{b_{QAM}\rho)}\right) \tag{2.33}$$

where ρ is SNR, and $b_{PSK} = \sin^2/(\pi/M)$, $K = 1-\left(1/\sqrt{M}\right)$, $b_{QAM} = 3/(M-1)$, and Q is the Gaussian Q-function.

From (2.26), the instantaneous SNR Γ_2 can be tightly upper bounded as

$$\Gamma_2 \le \tilde{\Gamma}_2 \triangleq \frac{1}{N_0}\frac{P_1P_2\left|h_{1,2}\right|^2\left|h_{2,3}\right|^2}{P_1\left|h_{1,2}\right|^2 + P_2\left|h_{2,3}\right|^2} \tag{2.34}$$

Now if we approximate (2.24) as $\Gamma \approx \Gamma_1 + \tilde{\Gamma}_2$, then for an M-PSK modulation, the conditional SER of an AF cooperation system with the channel coefficients $h_{1,3}$, $h_{1,2}$ and $h_{2,3}$ can be written as

$$P_{\mathrm{PSK}}^{h_{1,3},h_{1,2},h_{2,3}} = \psi_{\mathrm{PSK}}(\Gamma) \tag{2.35}$$

Similarly in case of M-QAM, it is written as

$$P_{\mathrm{QAM}}^{h_{1,3},h_{1,2},h_{2,3}} = \psi_{\mathrm{QAM}}(\Gamma) \tag{2.36}$$

Now substituting (2.32) into (2.35), and (2.33) into (2.36), the conditional SER for AF cooperation for M-PSK and M-QAM modulations respectively, can be expressed as

$$P_{\mathrm{PSK}}^{h_{1,3},h_{1,2},h_{2,3}} \approx \frac{1}{\pi}\int_0^{(M-1)\pi/M} \exp\left(-\frac{b_{PSK}(\Gamma_1+\tilde{\Gamma}_2)}{\sin^2\theta}\right)d\theta \tag{2.37}$$

$$P_{\mathrm{QAM}}^{h_{1,3},h_{1,2},h_{2,3}} \approx 4KQ\left(\sqrt{b_{\mathrm{QAM}}(\Gamma_1+\tilde{\Gamma}_2)}\right) - 4K^2Q^2\left(\sqrt{b_{\mathrm{QAM}}(\Gamma_1+\tilde{\Gamma}_2)}\right) \tag{2.38}$$

Now let us denote the moment generating function (MGF) of a random variable Z as

$$\mathcal{M}_Z(s) = \int_{-\infty}^{\infty} \exp(-sz)Pz(z)dz \tag{2.39}$$

for any real number s. By averaging the conditional SER in (2.37) and (2.38) over Rayleigh fading channels $h_{1,3}$, $h_{1,2}$ and $h_{2,3}$, we get the SER of AF cooperation with M-PSK and M-QAM in term of MGF $\mathcal{M}_{\Gamma_1}(s)$ and $\mathcal{M}_{\tilde{\Gamma}_2}(s)$, as follows [20]:

$$P_{\mathrm{PSK}} \approx \frac{1}{\pi}\int_0^{(M-1)\pi/M} \mathcal{M}_{\Gamma_1}\left(\frac{b_{\mathrm{PSK}}}{\sin^2\theta}\right)\mathcal{M}_{\tilde{\Gamma}_2}\left(\frac{b_{\mathrm{PSK}}}{\sin^2\theta}\right)d\theta \tag{2.40}$$

$$P_{\mathrm{QAM}} \approx \left[\frac{4K}{\pi}\int_0^{\pi/2} - \frac{4K^2}{\pi}\int_0^{\pi/4}\right]\mathcal{M}_{\Gamma_1}\left(\frac{b_{\mathrm{QAM}}}{2\sin^2\theta}\right)\mathcal{M}_{\tilde{\Gamma}_2}\left(\frac{b_{\mathrm{QAM}}}{2\sin^2\theta}\right)d\theta \tag{2.41}$$

As the term $\Gamma_1 = P_1 \left|h_{1,3}\right|^2 / N_0$ has an exponential distribution with parameter $N_0 /(P_1\sigma_{1,3}^2)$, the MGF of Γ_1 can be simplified as

$$\mathcal{M}_{\Gamma_1}(s) = \frac{1}{1+\frac{sP_1\sigma_{1,3}^2}{N_0}} \tag{2.42}$$

As we can see that the expression (2.34) is harmonic mean of two random variables $P_1 \left|h_{1,2}\right|^2 / N_0$ and $P_2 \left|h_{2,3}\right|^2 / N_0$, hence the MGF of $\tilde{\Gamma}_2$ may be calculated as [24].

$$\mathcal{M}_{\tilde{\Gamma}_2}(s) = \frac{16\beta_1\beta_2}{3(\beta_1+\beta_2+2\sqrt{\beta_1\beta_2}+s)}\left[\frac{4(\beta_1+\beta_2)}{(\beta_1+\beta_2+2\sqrt{\beta_1\beta_2}+s)} \times {}_2F_1\left(3,\frac{3}{2};\frac{5}{2};\frac{\beta_1+\beta_2-2\sqrt{\beta_1\beta_2}+s}{\beta_1+\beta_2+2\sqrt{\beta_1\beta_2}+s}\right)\right.$$
$$\left. + {}_2F_1\left(2,\frac{1}{2};\frac{5}{2};\frac{\beta_1+\beta_2-2\sqrt{\beta_1\beta_2}+s}{\beta_1+\beta_2+2\sqrt{\beta_1\beta_2}+s}\right)\right] \tag{2.43}$$

where $\beta_1 = N_0 /(P_1\sigma_{1,2}^2)$, $\beta_2 = N_0 /(P_2\sigma_{2,3}^2)$ and ${}_2F(\cdot,\cdot;\cdot;\cdot)$ is the Gauss hypergeometric function. The SER of AF cooperation systems with M-PSK and M-QAM modulations can be tightly approximated as [20]

$$P_s \approx \frac{VN_0^2}{b^2}\frac{1}{P_1\sigma_{1,3}^2}\left(\frac{1}{P_1\sigma_{1,2}^2}+\frac{1}{P_2\sigma_{2,3}^2}\right) \tag{2.44}$$

where in case of M-PSK $V = \frac{3(M-1)}{8M} + \frac{\sin\frac{2\pi}{M}}{4\pi} - \frac{\sin\frac{4\pi}{M}}{32\pi}$ and $b = b_{PSK}$ and in case of M-QAM $V = \frac{3(M-1)}{8M} + \frac{K^2}{\pi}$ and $b = b_{QAM/2}$. For detail and proof the interested reader is referred to [20].

Figure 2.5 shows the comparative graph of the simulation results between SER derived in (2.40) and tightly approximation in (2.44). For simulation we have assumed that $P_1 / P = 2/3$ and $P_2 / P = 2/3$, where $P = P_1 + P_2$, and $\sigma_{1,3}^2 = \sigma_{1,2}^2 = \sigma_{2,3}^2 = 1$, $N_0 = 1$

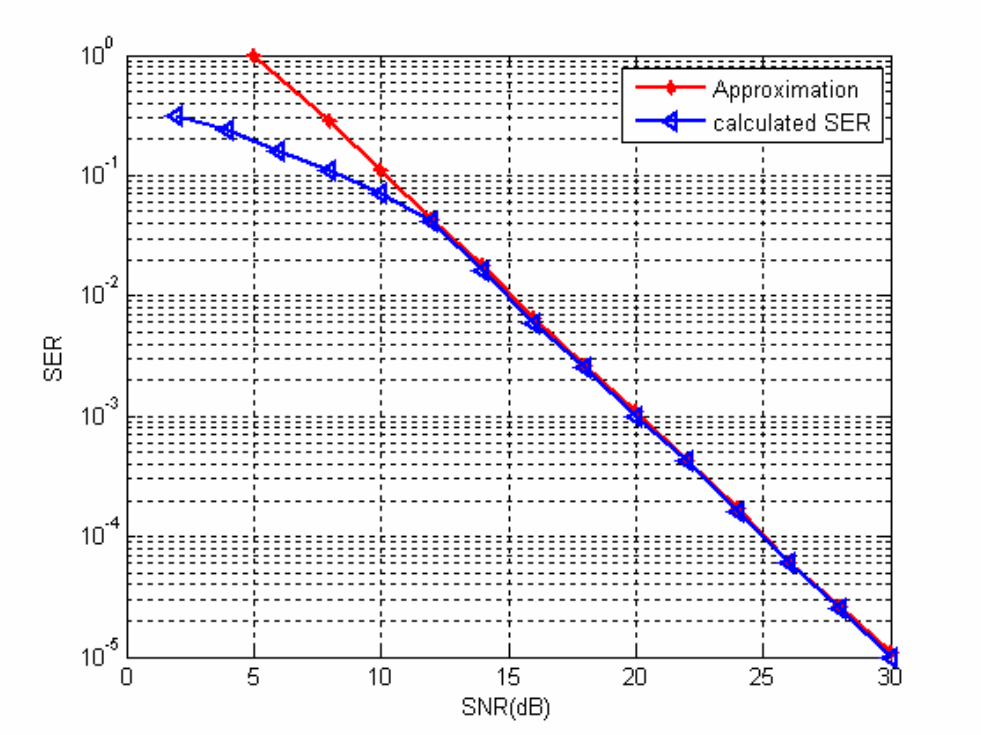

Figure 2.5 The SER and the upper bound comparison for AF cooperation using QPSK

2.4.1.2 Decode and Forward (DF) strategy

In this strategy of relaying, the relay node decodes the received signal, re-encode it, and then transmit it to the destination. If the decoded signal at the relay is denoted by $\hat{x}$, the transmitted signal from the relay can be denoted by $\sqrt{P_2}\hat{x}$ given that $\hat{x}$ has unit variance. Note that the decoded signal at the relay may be incorrect. If an incorrect signal is forwarded to the destination, the decoding at the destination is meaningless. It is clear that for such a scheme the diversity achieved is only one, because the performance of the system is limited by the worst link from the source–relay and source–destination. This is the main draw back of DF relaying because forwarding erroneously detected signals to the destination may cause error propagation that can decline the system performance. The mutual information between the source and the destination is limited by the mutual information of the weakest link between the source–relay and the combined channel from the source–destination and relay–destination. More specifically, the mutual information for DF transmission in terms of the channel fades can be written as

$$I_{DF} = \frac{1}{2}\min\left\{\log\left(1+\gamma\left|h_{1,2}\right|^2\right), \log\left(1+\gamma\left|h_{1,3}\right|^2+\gamma\left|h_{2,3}\right|^2\right)\right\} \tag{2.45}$$

where the "min" operator takes into account the fact that the relay only transmits if decoded correctly, hence the performances is limited by the weakest link between the source destination and source–relay.

The outage probability for DF relaying scheme is given by $\Pr[I_{DF} < R]$. By simple algebraic manipulation, we may write

$$\min\left\{|h_{1,2}|^2, |h_{1,3}|^2 + |h_{2,3}|^2\right\} < \frac{2^{2R}-1}{\gamma} \tag{2.46}$$

The outage probability can be written as:

$$\Pr[I_{DF} < R] = \Pr\left\{|h_{1,2}|^2 < \frac{2^{2R}-1}{\gamma}\right\} + \Pr\left\{|h_{1,2}|^2 > \frac{2^{2R}-1}{\gamma}\right\} \Pr\left\{|h_{1,3}|^2 + |h_{2,3}|^2 < \frac{2^{2R}-1}{\gamma}\right\} \tag{2.47}$$

Since the channel is Rayleigh fading, the above random variables are all exponential random variables with parameter one. Averaging over the channel conditions, the outage probability for DF strategy at high SNR is given by

$$\Pr[I_{DF} < R] \simeq \frac{1}{\sigma_{1,2}^2} \frac{2^{2R}-1}{\gamma} \tag{2.48}$$

Figure 2.6 shows the simulation result of outage probability versus SNR for a fixed rate of 2 bps/Hz for a DF scheme. The channel variance $\sigma_{1,3}$ between source and destination is taken as 1, whereas for source-relay and relay-destination as 0.5. The noise variance is one. It is clear from the graph that the diversity order of DF scheme is one, *i.e*. no diversity gain.

In figure 2.7 the outage probability is depicted versus spectral efficiency in bps/Hz for a fixed SNR of 40 dB. One can see that the performance degrades with increasing R. Again in term of diversity DF do not have any advantage. To gain diversity, selective DF strategy can be preferably.

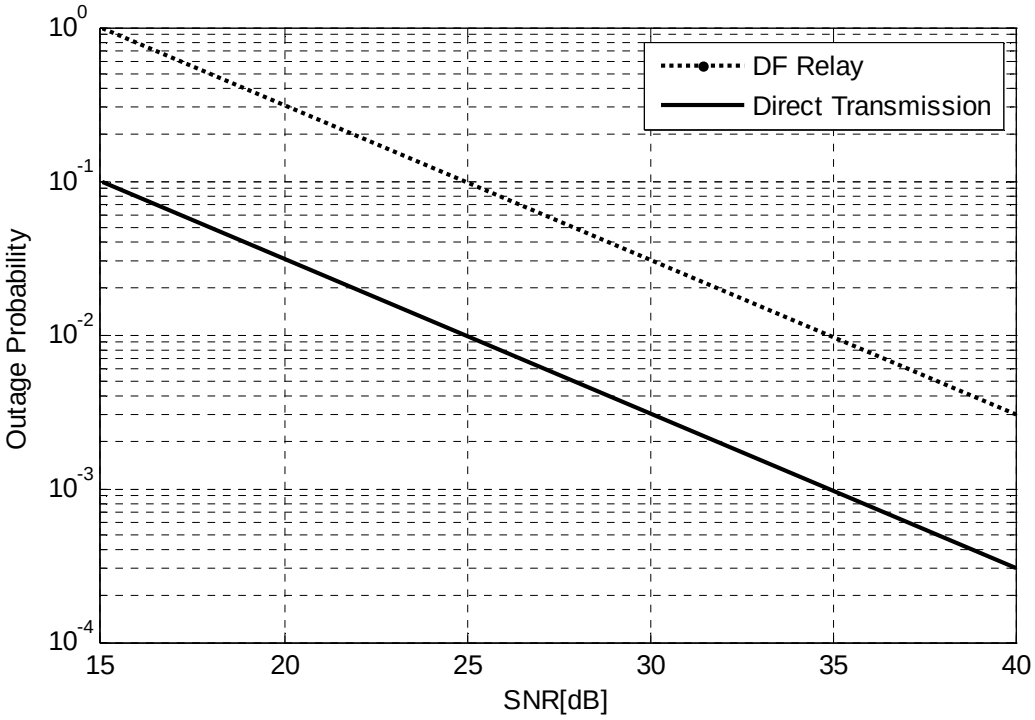

Figure 2.6 Outage probability versus SNR

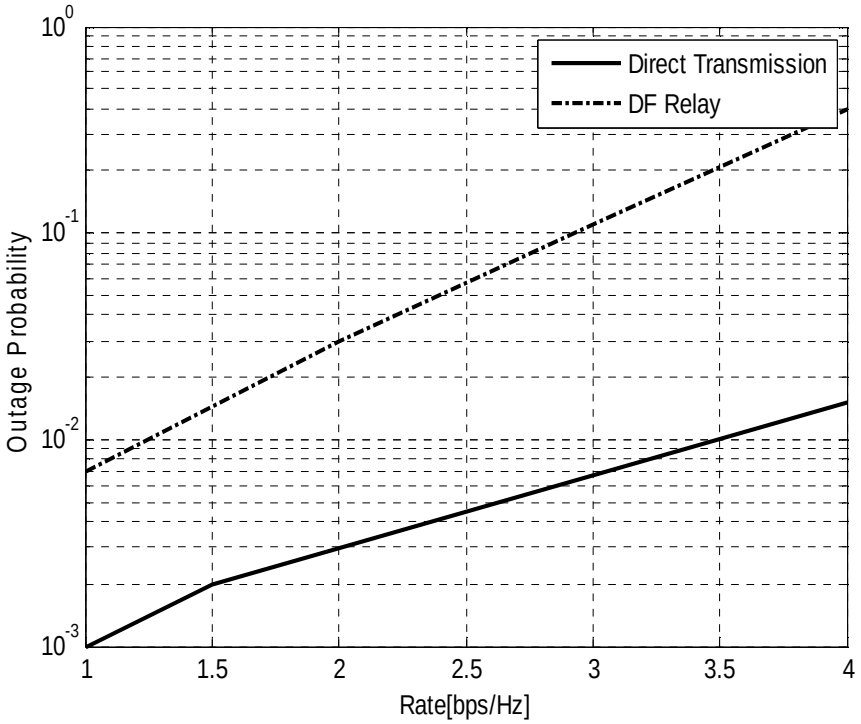

Figure 2.7 Outage probability versus spectral efficiency

Symbol Error Rate (SER) analysis for DF protocol

In Phase-II, if the relay is able to decode the transmitted symbol correctly, then the relay forwards the decoded symbol with power P_2 to the destination, otherwise it remains idle. The received signal at the destination in this case can be represented as

$$y_{2,3} = \sqrt{\tilde{P}_2} h_{2,3} x + n_{2,3} \tag{2.49}$$

where $\tilde{P}_2 = P_2$ if the relay decodes and forwards the transmitted signal, otherwise $\tilde{P}_2 = 0$. For practical applications, one may predefine a certain SNR threshold at relay. Of course selection of higher threshold at the relay assures the detection error propagation near to zero. For example figure 2.8 shows DF performances with different SNR thresholds at the relay where system performance improves by increasing the SNR thresholds.

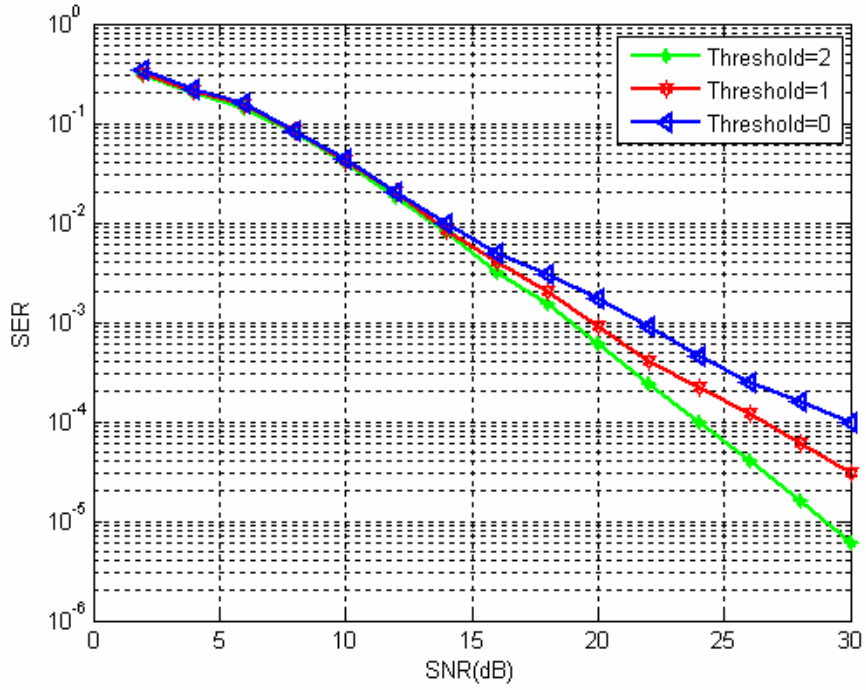

Figure 2.8 Performance analysis with different SNR threshold

With knowledge of the channel coefficients from source and destination links, the destination detects the transmitted symbols by combining the signals transmitted by the source (2.13) and the relay (2.49).The combined signal at the MRC detector can be written as

$$y = a_1 y_{1,3} + a_2 y_{2,3} \tag{2.50}$$

where the factor a_1 and a_2 are determined such that the SNR of the MRC output is maximized, and are given by $a_1 = \sqrt{P_1} h_{1,3}^* / N_0$ and $a_2 = \sqrt{\tilde{P}_2} h_{2,3}^* / N_0$.

With the assumption that the transmitted symbol x in (2.13) and (2.49) has average energy 1, the SNR of the MRC output is given by

$$\Gamma = \frac{P_1 \left| h_{1,3} \right|^2 + \tilde{P}_2 \left| h_{2,3} \right|^2}{N_0} \tag{2.51}$$

Now if we use M-PSK modulation in DF system with the instantaneous SNR Γ in (2.51), the conditional SER of the system with the channel coefficients $h_{1,3}$, $h_{1,2}$ and $h_{2,3}$ can be written as

$$P_{\text{PSK}}^{h_{1,3}, h_{1,2}, h_{2,3}} = \psi_{\text{PSK}}(\Gamma) \tag{2.52}$$

In case of M-QAM modulation, it can be expressed as

$$P_{\text{QAM}}^{h_{1,3}, h_{1,2}, h_{2,3}} = \psi_{\text{QAM}}(\Gamma) \tag{2.53}$$

As discussed above there are two possible cases at relay, *i.e.*

- It decodes correctly, $\tilde{P}_2 = P_2$.
- It cannot decode, and goes idle, $\tilde{P}_2 = 0$

The chances of incorrect decoding at the relay for an M-PSK/M-QAM symbols are $\Psi_{\text{PSK/QAM}}\left(P_1 \left| h_{1,2} \right|^2 / N_0 \right)$ and the chances for correct decoding are $1 - \Psi_{\text{PSK/QAM}}\left(P_1 \left| h_{1,2} \right|^2 / N_0 \right)$.

Taking into account the two cases, *i.e.* (i) $\tilde{P}_2 = P_2$ and (ii) $\tilde{P}_2 = 0$, we calculate the conditional SER in (2.52) as

$$P_{\mathrm{PSK}}^{h_{1,3},h_{1,2},h_{2,3}} = \psi_{\mathrm{PSK}}(\Gamma)|_{\tilde{P}_2=0}\,\Psi_{\mathrm{PSK}}\left(\frac{P_1|h_{1,2}|^2}{N_0}\right)+\psi_{\mathrm{PSK}}(\Gamma)|_{\tilde{P}_2=P_2}\left[1-\Psi_{\mathrm{PSK}}\left(\frac{P_1|h_{1,2}|^2}{N_0}\right)\right]$$

$$=\frac{1}{\pi}\int_0^{(M-1)\pi/M}\exp\left(-\frac{b_{\mathrm{PSK}}P_1|h_{1,3}|^2}{N_0\sin^2\theta}\right)d\theta\int_0^{(M-1)\pi/M}\exp\left(-\frac{b_{\mathrm{PSK}}P_1|h_{1,2}|^2}{N_0\sin^2\theta}\right)d\theta$$

$$+\frac{1}{\pi}\int_0^{(M-1)\pi/M}\exp\left(-\frac{b_{\mathrm{PSK}}P_1|h_{1,3}|^2+P_2|h_{2,3}|^2}{N_0\sin^2\theta}\right)d\theta\times\left[1-\frac{1}{\pi}\int_0^{(M-1)\pi/M}\exp\left(-\frac{b_{\mathrm{PSK}}P_1|h_{1,2}|^2}{N_0\sin^2\theta}\right)d\theta\right] \tag{2.54}$$

Since the fading channels $h_{1,3}$, $h_{1,2}$ and $h_{2,3}$ are independent of each other, and

$$\int_0^{\infty}\exp\left(-\frac{b_{\mathrm{PSK}}P_1 z}{N_0\sin^2\theta}\right)P|h|^2(z)dz=\frac{1}{1+\frac{b_{\mathrm{PSK}}P_1\sigma_h^2}{N_0\sin_2\theta}} \tag{2.55}$$

hence if we average the conditional SER in (2.54) over Rayleigh fading channels $h_{1,3}$, $h_{1,2}$ and $h_{2,3}$ with variances $\sigma_{1,3}$, $\sigma_{1,2}$ and $\sigma_{2,3}$, respectively, we get the SER of DF cooperation with M-PSK as follows:

$$P_{\mathrm{PSK}}=\mathcal{G}_1\left(1+\frac{b_{\mathrm{PSK}}P_1\sigma_{1,3}^2}{N_0\sin^2\theta}\right)\mathcal{G}_1\left(1+\frac{b_{\mathrm{PSK}}P_1\sigma_{1,2}^2}{N_0\sin^2\theta}\right)+\mathcal{G}_1\left(\left(1+\frac{b_{\mathrm{PSK}}P_1\sigma_{1,3}^2}{N_0\sin^2\theta}\right)\left(1+\frac{b_{\mathrm{PSK}}P_2\sigma_{2,3}^2}{N_0\sin^2\theta}\right)\right)\times\left[1-\mathcal{G}_1\left(1+\frac{b_{\mathrm{PSK}}P_1\sigma_{1,2}^2}{N_0\sin^2\theta}\right)\right] \tag{2.56}$$

where

$$\mathcal{G}_1(x(\theta))=\frac{1}{\pi}\int_0^{(M-1)\pi/M}\frac{1}{x(\theta)}d\theta \tag{2.57}$$

Similarly for M-QAM

$$P_{\mathrm{QAM}} = \mathcal{G}_2\left(1+\frac{b_{\mathrm{QAM}}P_1\sigma_{1,3}^2}{2N_0\sin^2\theta}\right)\mathcal{G}_2\left(1+\frac{b_{\mathrm{QAM}}P_1\sigma_{1,2}^2}{2N_0\sin^2\theta}\right)+\mathcal{G}_2\left(\left(1+\frac{b_{\mathrm{QAM}}P_1\sigma_{1,3}^2}{2N_0\sin^2\theta}\right)\left(1+\frac{b_{\mathrm{QAM}}P_2\sigma_{2,3}^2}{2N_0\sin^2\theta}\right)\right)\times\left[1-\mathcal{G}_2\left(1+\frac{b_{\mathrm{QAM}}P_1\sigma_{1,2}^2}{2N_0\sin^2\theta}\right)\right] \tag{2.58}$$

where

$$\mathcal{G}_2(x(\theta)) = \frac{4K}{\pi}\int_0^{\pi/2}\frac{1}{x(\theta)}d\theta - \frac{4K^2}{\pi}\int_0^{\pi/4}\frac{1}{x(\theta)}d\theta \tag{2.59}$$

Upper bound for DF cooperation with M-PSK

Removing the negative term in (2.56), we get

$$P_{\mathrm{PSK}} \le \mathcal{G}_1\left(1+\frac{b_{\mathrm{PSK}}P_1\sigma_{1,3}^2}{N_0\sin^2\theta}\right)\mathcal{G}_1\left(1+\frac{b_{\mathrm{PSK}}P_1\sigma_{1,2}^2}{N_0\sin^2\theta}\right)+\mathcal{G}_1\left(\left(1+\frac{b_{\mathrm{PSK}}P_1\sigma_{1,3}^2}{N_0\sin^2\theta}\right)\left(1+\frac{b_{\mathrm{PSK}}P_2\sigma_{2,3}^2}{N_0\sin^2\theta}\right)\right) \tag{2.60}$$

One can see that by putting $\sin^2\theta = 1$ in RHS of above inequality, we get maximum value. Hence substituting $\sin^2\theta = 1$ into (2.60), we get

$$P_{\mathrm{PSK}} \le \frac{(M-1)^2}{M^2}\frac{N_0^2}{(N_0+b_{\mathrm{PSK}}P_1\sigma_{1,3}^2)(N_0+b_{\mathrm{PSK}}P_1\sigma_{1,2}^2)}+\frac{M-1}{M}\frac{N_0^2}{(N_0+b_{\mathrm{PSK}}P_1\sigma_{1,3}^2)(N_0+b_{\mathrm{PSK}}P_2\sigma_{1,3}^2)}$$

$$= \frac{(M-1)N_0}{M^2}\frac{Mb_{\mathrm{PSK}}P_1\sigma_{1,2}^2+(M-1)b_{\mathrm{PSK}}P_2\sigma_{2,3}^2)+(2M-1)N_0}{(N_0+b_{\mathrm{PSK}}P_1\sigma_{1,3}^2)(N_0+b_{\mathrm{PSK}}P_1\sigma_{1,2}^2)(N_0+b_{\mathrm{PSK}}P_2\sigma_{2,3}^2)} \tag{2.61}$$

Similar proof can be derived for QAM modulation.

Theorem: The SER of DF cooperation systems with M-PSK or M-QAM modulation can be upper bounded as

$$P_s \le \frac{(M-1)N_0}{M^2}\frac{MbP_1\sigma_{1,2}^2+(M-1)bP_2\sigma_{2,3}^2)+(2M-1)N_0}{(N_0+bP_1\sigma_{1,3}^2)(N_0+bP_1\sigma_{1,2}^2)(N_0+bP_2\sigma_{2,3}^2)} \tag{2.62}$$

where $b = b_{\mathrm{PSK}}$ for M-PSK signals and $b = b_{\mathrm{QAM}}/2$ for M-QAM signals.

Figure 2.9 shows the comparative performance of the simulation between the SER (2.56) and upper bound (2.62). For simulation we have assumed that $P_1/P = 2/3$ and $P_2/P = 2/3$, where $P = P_1 + P_2$, and $\sigma_{1,3}^2 = \sigma_{1,2}^2 = \sigma_{2,3}^2 = 1$, $N_0 = 1$

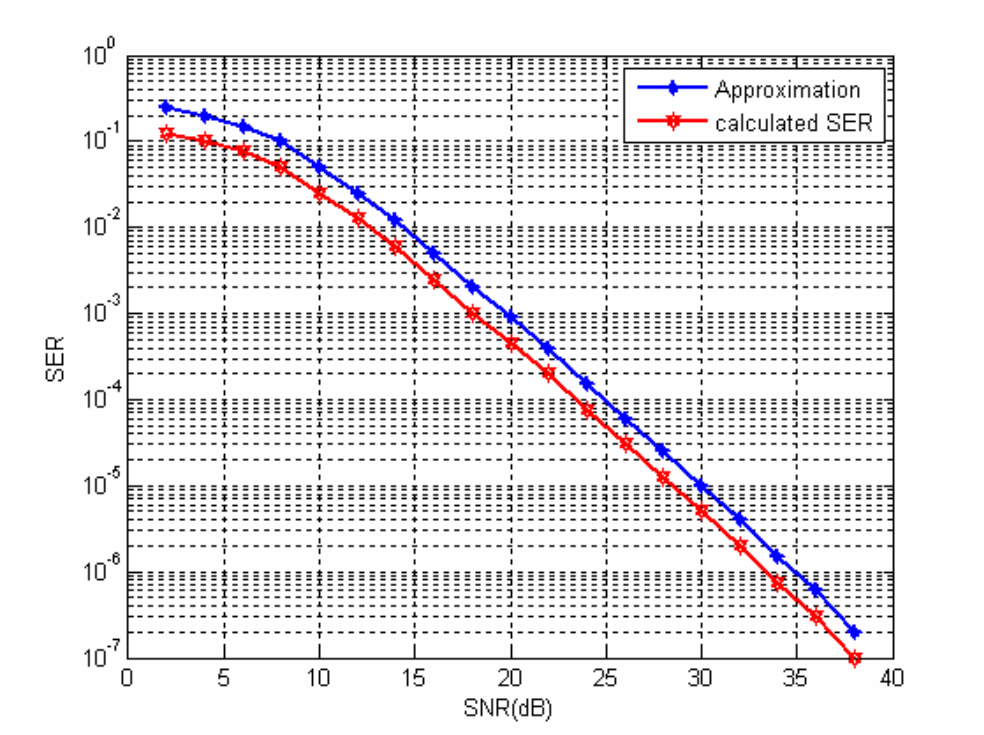

Figure 2.9 The SER and the upper bound comparison of DF cooperation with QPSK

2.4.2 Adaptive cooperation strategies

Fixed relaying suffers from deterministic loss in the transmission rate, for example, there is 50% loss in the spectral efficiency with transmissions in two phases. Moreover, fixed DF relaying suffers from the fact that the performance is limited by the weakest source-relay and relay-destination channels which reduces the diversity gains to one. To overcome this problem, adaptive relaying protocols can be used to improve the inefficiency. In following two sub-sections, we briefly define selective DF and incremental relaying.

2.4.2.1 Selective DF strategy

In a selective DF relaying scheme, if the SNR of a signal received at the relay exceeds a certain threshold, the relay decodes the received signal and forwards the decoded information to the destination. On the other hand, if the channel between the source and the relay suffers a

severe fading such that the SNR falls below the threshold, the relay remains idle. Selective relaying improves the performances of fixed DF relaying, as the threshold at the relay can be determined to overcome the inherent problem in fixed DF relaying in which the relay forwards all decoded signals to the destination although some decoded signals may be incorrect. In [20] it was proved that at high SNR selective DF achieves same diversity gain as AF relaying.

2.4.2.2 Incremental relaying

For incremental relaying, it is assumed that there is a feedback channel from the destination to the relay. The destination sends an acknowledgement to the relay if it was able to receive the source's message correctly in the first transmission phase, so the relay does not need to transmit. This protocol has the best spectral efficiency among the previously mentioned protocols because the relay does not always need to transmit, and hence the second transmission phase becomes opportunistic depending on the channel state condition of the direct channel between the source and the destination. In incremental relaying, if the source transmission in the first phase was successful, then there is no second phase and the source transmits new information in the next time slot. On the other hand, if the source transmission was not successful in the first phase, the relay can use any of the fixed relaying protocols to transmit the source signal from the first phase. The transmission rate in incremental relaying is random. If the first phase was successful, the transmission rate is R, if the first transmission was in outage the transmission rate becomes $R/2$ as in fixed relaying.

2.4.3 Multi-hop cooperative communication

In previous sections, we discussed some frequently used cooperative communication strategies with single hop between source and destination. In this section we discuss two main protocols *i.e.* decode and forward, and amplify and forward protocols in multi-hop scenario. We derive SERs for both cases and present the simulation results.

2.4.3.1 Multi-hop decode and forward strategy

We consider an arbitrary N-relays wireless network, where information is to be transmitted from a source to a destination. Due to the broadcast nature of the wireless channel, some

relays can overhear the transmitted information and thus can cooperate with the source to send its data. The wireless link between any two nodes in the network is modelled as a Rayleigh fading channel with additive white Gaussian noise.

We further assume that the relays are spatially well separated so that the channel fades for different links are assumed to be statistically independent. The additive noise at all receiving terminals is modelled as zero-mean, complex Gaussian random variables with variance N_0. For medium access, the relays are assumed to transmit over orthogonal channels, thus no inter-relay interference is considered in the signal model.

We consider a selective DF protocol at the relaying nodes by predefining a certain threshold. Each relay can measure the received SNR and forwards the received signal if the SNR is higher than the threshold. For mathematical tractability of symbol error rate calculations we assume the relays can judge whether the received symbols are decoded correctly or not, and only forward the signal if decoded correctly otherwise remains idle.

In multi-hop cooperative relaying scenario various possibilities for cooperation among the relays arise. A general scenario is denoted by $C(n)$ $(1 \le n \le N-1)$, in which each relay combines the signals received from the n previous relays and the source.

Figure 2.10 shows a cooperative scenario for $C(N-1)$ environment, where each relay combine the signals received from the source and n previous relays. Another possible scenario is $C(1)$ depicted in figure 2.11, where each relay combines the signals received from the source his immediate neighbour.

The $C(1)$ scenario is simple to analysis and has been well explored in literature, for example [25], [26]. Therefore in what follows, we discuss $C(N-1)$ scenario as illustrated in fig. 2.10.

In $C(n)$, $1 \le n \le N-1$ scenario, each relay decodes the information after combining the signals received from the source and the previous n relays. The cooperation protocols have (N+1) phases. In phase-I the source transmits the information and the received signal at the destination and i-th relay can be modelled respectively, as.

$$y_{1,3} = \sqrt{P_1} h_{1,3} x + n_{1,3} \tag{2.63}$$

$$y_{1,2_i} = \sqrt{P_1} h_{1,2_i} x + n_{1,2_i} \qquad 1 \le i \le N \tag{2.64}$$

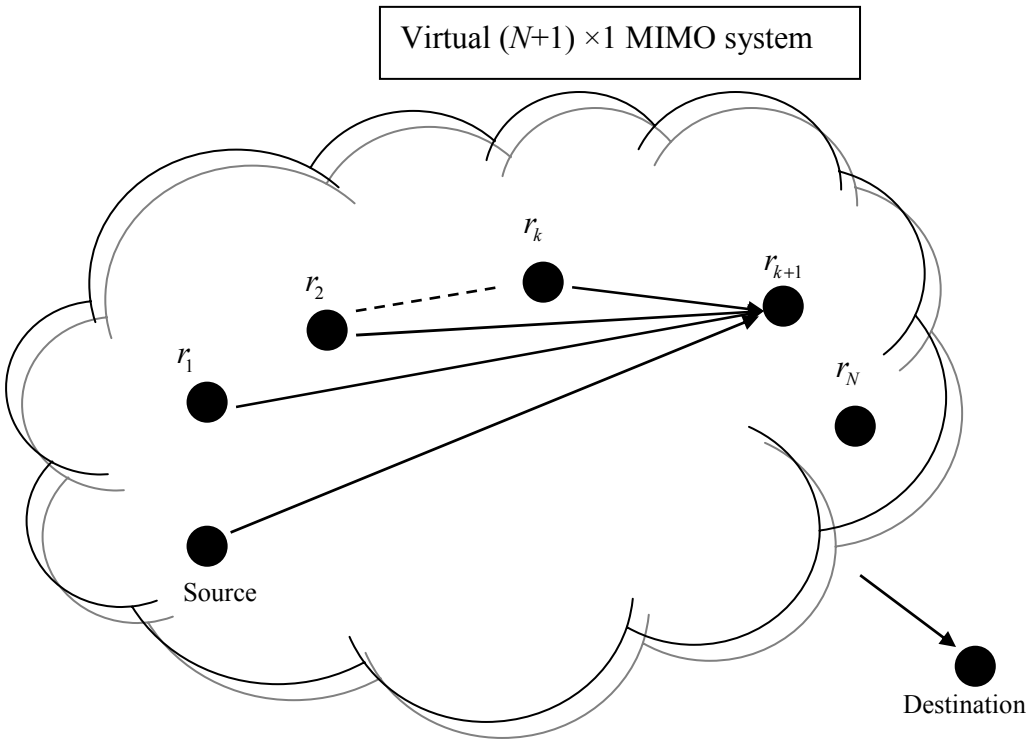

Figure 2.10 Cooperation under C(N-1) scenario: the (k+1)-th relay combines the signals received from the source and all of the previous relays.

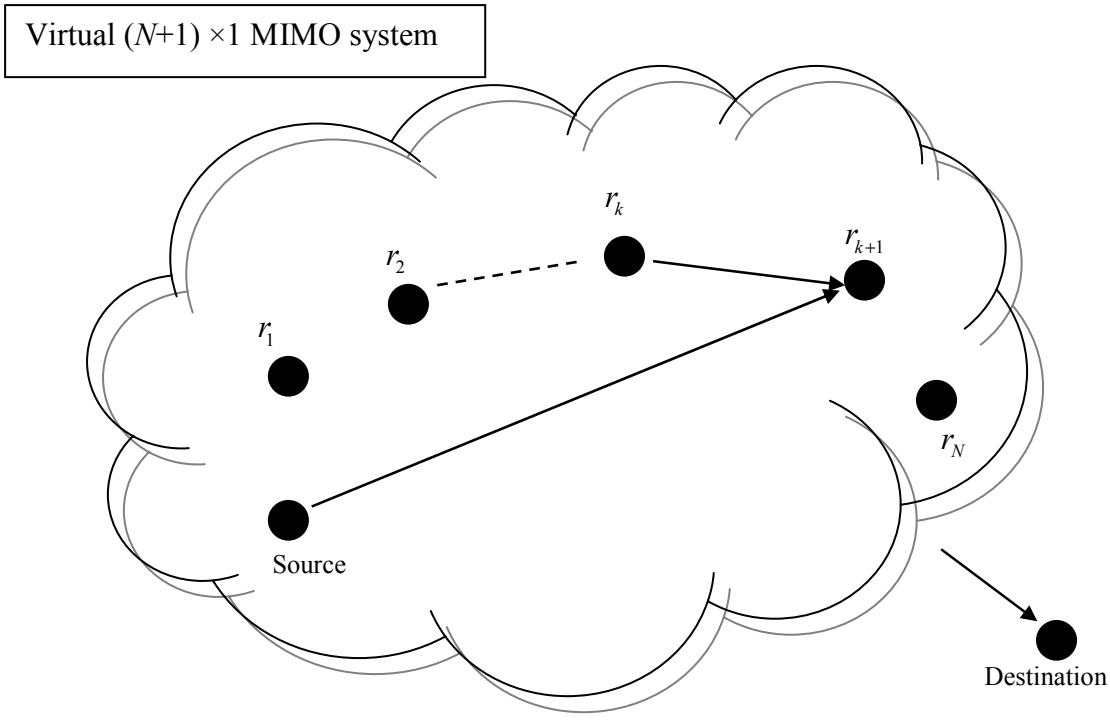

Figure 2.11 Cooperation under *C*(1) scenario: the (*k*+1)-th relay combines the signals received from the source and the *k*-th relay.

In (2.63) and (2.64), P_1 is the power transmitted at the source, x is the transmitted symbol with unit power, $h_{1,3} \sim CN(0,\sigma_{1,3}^2)$ and $h_{1,2_i} \sim CN(0,\sigma_{1,2_i}^2)$ are the channel fading coefficients between the source and the destination, and *i*-th relay, respectively, and $\mathcal{CN}(\alpha,\sigma^2)$ denotes a circularly symmetric complex Gaussian random variable with mean α and variance σ^2. $n_{1,3}$ and $n_{1,2_i}$ denote the AWGN from source to destination and source to *i*-th relay. In phase-II, if the first relay decodes correctly, it forwards the decoded symbol with power P_1 to the destination, otherwise it remains idle.

In general, during phase m, $2 \le m \le N$, the *m*-th relay combines the received signals from the source and the previous $\min(n, m-1)$ relays using an MRC as follows.

$$y_{2_m} = \sqrt{P_1} h_{1,2_m}^* y_{1,2_m} + \sum_{i=\max(1,m-n)}^{m-1} \sqrt{\hat{P}_i} h_{2_i,2_m}^* y_{2_i,2_m} \tag{2.65}$$

Note that $\max(1, m-n)$ function is used to make sure that if $m < n$, then the combining starts at the first relay.

In (2.65) the $h_{2_i,2_m} \sim CN(0,\sigma_{2_i,2_m}^2)$ is the channel fading coefficient between the *i*-th and the *m*th relays, and the term $y_{2_i,2_m}$ denotes the signal received at the *m*-th relay from the *i*-th relay, and can be modelled as

$$y_{2_i,2_m} = \sqrt{\hat{P}_i} h_{2_i,2_m} x + n_{2_i,2_m} \tag{2.66}$$

where $\hat{P}_i$ is the power transmitted at relay *i* in phase (*i* + 1), and $\hat{P}_i = P_i$ if relay *i* correctly decodes the transmitted symbol, otherwise $\hat{P}_i = 0$. The *m*-th relay uses y_{2_m} in (2.65) as the detection statistics. If relay *m* decodes correctly it transmits with power $\hat{P}_m = P_m$ in Phase (*m*+1), otherwise it remains idle. Finally, in phase (*N*+1), the destination coherently combines all the received signals using an MRC as follows

$$y_3 = \sqrt{P_1} h_{1,3}^* y_{1,3} + \sum_{i=1}^{N} \sqrt{\hat{P}_i} h_{2_i,3}^* y_{2_i,3} \tag{2.67}$$

total transmitted power is fixed as $P_1 + \sum_{i=1}^{N} P_i = P$

Symbol Error Rate (SER) performance analysis

We present the SER performance analysis for a general cooperative scheme $C(n)$, $1 \le n \le N-1$, both for M-PSK and M-QAM modulation system.

As stated above each relay has two states, whether it decodes correctly or not.

We define a $1 \times l$, $1 \le l \le N$ vector $\boldsymbol{S}_l$ to represent the states of the first l relays for a given transmission. The k-th entry of the vector $\boldsymbol{S}_l$ denotes the state of the k-th relay as follow

$$\boldsymbol{S}_l[k] = \begin{cases} 1 & \text{if relay } k \text{ decodes correctly} \\ 0 & \text{otherwise} \qquad\qquad 1 \le k \le l \end{cases} \tag{2.68}$$

Since the decimal value of the binary vector $\mathbf{S}_l$ can take any value from 0 to 2^{l-1}, for convenience we denote the state of the network by an integer decimal number. Let

$$\boldsymbol{D}_{z,l} = \left(\boldsymbol{D}_{z,l}[1], \boldsymbol{D}_{z,l}[2], ..., \boldsymbol{D}_{z,l}[l]\right) \tag{2.69}$$

be the $1 \times l$ binary representation of a decimal number z, with $\boldsymbol{D}_{z,l}[1]$ being the most significant bit. So $\boldsymbol{S}_N = \boldsymbol{D}_{z,N}$ indicates that the k-th relay, $1 \le k \le N$, is in state $\boldsymbol{S}_N[k] = \boldsymbol{D}_{z,N}[k]$.

We consider a general cooperation scheme $C(n)$, $1 \le n \le N-1$, in which the k-th $(1 \le k \le N)$ relay coherently combines the signals received from the source along with the signals received from the previous $\min(n, k-1)$ relays. The state of each relay in this scheme depends on the states of the previous n relays, *i.e.* whether these relays have decoded correctly or not. This is due to the fact that the number of signals received at each relay depends on the number of relays that decoded correctly from the previous n relays. Hence, the joint probability of the states is given by

$$P(\boldsymbol{S}_N) = P(S_N[1])P(S_N[2]/(S_N[1])....P(S_N[N]/S_N[N-1],...,S_N[N-n]) \tag{2.70}$$

Conditioning on the network state, which can take 2^N values, the probability of error at the destination given the CSI can be calculated using the law of total probability as follows: [20]

$$P_e = \sum_{i=0}^{2^N-1} Pr(e \mid \boldsymbol{S}_N = \boldsymbol{D}_{i,N}) \Pr(\boldsymbol{S}_N = \boldsymbol{D}_{i,N}) \tag{2.71}$$

where, *e* denotes the event that the destination decoded in error.

The destination collects the copies of the signal transmitted in the previous phases using MRC (2.67) and the resulting SNR at the destination can be computed as

$$SNR_3 = \frac{P_1 \left|h_{1,3}\right|^2 + \sum_{j=1}^{N} P_j D_{i,N}[j] \left|h_{2_j,3}\right|^2}{N_0} \tag{2.72}$$

where $D_{i,N}[j]$ takes value 1 or 0 and determines whether the *j*-th relay has decoded correctly or not. The *k*-th relay coherently combines the signals received from the source and the previous *n* relays. The resulting SNR can be calculated as

$$SNR_{2k}^{n} = \frac{P_1 \left|h_{1,2_k}\right|^2 + \sum_{j=\max(1,k-n)}^{k-1} P_j D_{i,N}[j] \left|h_{2_j,2_k}\right|^2}{N_0} \tag{2.73}$$

If M-PSK modulation is used, with instantaneous SNR Γ, the SER with the CSI from (2.32) can be written as

$$P_{\mathrm{PSK}} = \psi_{\mathrm{PSK}}(\Gamma) \triangleq \frac{1}{\pi} \int_0^{(M-1)\pi/M} \exp\left(-\frac{b_{\mathrm{PSK}}\Gamma}{\sin^2(\theta)}\right) d\theta \tag{2.74}$$

where $b_{\mathrm{PSK}} = \sin^2(\pi / M)$.

In case of M-QAM modulation the corresponding conditional SER from (2.33) can be written as

$$P_{\text{QAM}} = \psi_{\text{QAM}}(\Gamma) \triangleq 4KQ\left(\sqrt{b_{\text{QAM}}\Gamma}\right) - 4K^2Q^2\left(\sqrt{b_{\text{QAM}}\Gamma}\right) \tag{2.75}$$

where $K = 1 - 1/\sqrt{M}$ and $b_{\text{QAM}} = 3/(M-1)$, and $Q(x)$ is the complementary distribution function (CDF) of the Gaussian distribution.

In what follows, we mainly focus M-PSK modulation and the same procedure can be straightforwardly applied to M-QAM modulation.

From (2.70) for a given network state $\boldsymbol{S}_N = \boldsymbol{D}_{i,N}$, the conditional SER at the destination can be computed as

$$\Pr(e \mid \boldsymbol{S}_N = \boldsymbol{D}_{i,N}) = \psi_{\text{PSK}}(SNR_3) \tag{2.76}$$

From (2.73) the conditional probability that the *k*-th relay is in state $D_{i,N}[k]$ given the states of the previous *n* relays by $P_{k,i}^n$ is computed as follow

$$\begin{aligned} P_{k,i}^n &\triangleq \Pr(S_N[k] = D_{i,N}[k] \mid S_N[k-1] = D_{i,N}[k-1], ..., S_N[k-n] = D_{i,N}[k-n] = D_{i,N}[k-n]) \\ &= \begin{cases} \psi_{\text{PSK}}(SNR_{2_k}^n, & \text{if } D_{i,N}[k] = 0 \\ 1 - \psi_{\text{PSK}}(SNR_{2_k}^n & \text{if } D_{i,N}[k] = 1 \end{cases} \end{aligned} \tag{2.77}$$

To compute the average SER, we need to average the probability in (2.71) over all channel realizations, *i.e.* $P_{\text{SER}}(n) = E[P_e]$. Using (2.70), (2.76), and (2.77), $P_{\text{SER}}(n)$ can be expanded as

$$P_{\text{SER}}(n) = \sum_{i=0}^{2^N-1} E\left[\psi_{\text{PSK}}(SNR_d)\prod_{k=1}^{N} P_{k,i}^n\right] \tag{2.78}$$

Since the channel fades between different pairs of nodes in the network are statistically independent by the virtue that different nodes are not co-located, the quantities inside the expectation operator in (2.78) are functions of independent random variables, and thus can be further decomposed as

$$P_{\mathrm{SER}}(n)=\sum_{i=0}^{2^N-1}\left\{E\left[\psi_{\mathrm{PSK}}(SNR_d)\right]\prod_{k=1}^{N}E\left[P_{k,i}^{n}\right]\right\} \tag{2.79}$$

Note that (2.79) is equivalently applicable for M-QAM modulation system by replacing the function $\psi_{\mathrm{PSK}}(\cdot)$ by $\psi_{\mathrm{QAM}}(\cdot)$

Since the channels between the nodes are modelled as Rayleigh fading channels, the absolute norm square of any channel realization $h_{j,i}$ between any two nodes j and i in the network has an exponential distribution with mean $\sigma_{j,i}^2$. Hence, $E\left[\psi_q(\gamma)\right]$ can be expressed as

$$E[\psi_u(\Gamma)]=\int_{\gamma}\psi_u(\Gamma)f(\Gamma)d\Gamma \tag{2.80}$$

where $f(\Gamma)$ is the probability density function of the random variable Γ, and u is 1or 2 for M-PSK and M-QAM respectively. If Γ is an exponentially distributed random variable with mean $\overline{\Gamma}$, then it can be shown that $E\left[\psi_u(\Gamma)\right]$ is given by [20]

$$E[\psi_u(\Gamma)]=F_u\left(1+\frac{b_u\overline{\Gamma}}{\sin^2(\theta)}\right) \tag{2.81}$$

where $F_u(\cdot)$ and the constant b_u are defined as

$$F_1(x(\theta))=\frac{1}{\pi}\int_0^{(M-1)\pi/M}\frac{1}{x(\theta)}d\theta \qquad b_1=b_{\mathrm{PSK}} \tag{2.82}$$

and

$$F_2(x(\theta))=\frac{4K}{\pi}\int_0^{\pi/2}\frac{1}{x(\theta)}d\theta-\frac{4K^2}{\pi}\int_0^{\pi/4}\frac{1}{x(\theta)}d\theta \qquad b_2=\frac{b_{\mathrm{QAM}}}{2} \tag{2.83}$$

In order to get the SER formulation in above expressions, two special properties of the Gaussian *Q*-function are needed as follows [20]

$$Q(x)=\frac{1}{\pi}\int_0^{\pi/2}\exp\left(-\frac{x^2}{2\sin^2(\theta)}\right)d\theta \tag{2.84}$$

$$Q^2(x)=\frac{1}{\pi}\int_0^{\pi/4}\exp\left(-\frac{x^2}{2\sin^2(\theta)}\right)d\theta \tag{2.85}$$

for $x \geq 0$

Averaging over all the Rayleigh fading channel realizations, the SER at the destination for a given network state $\boldsymbol{D}_{i,N}$ is given by

$$E(\psi_u(SNR_3))=F_u\left[\left(1+\frac{b_u P_1\sigma_{1,3}^2}{N_0\sin^2(\theta)}\right)\prod_{j=1}^{N}\left(1+\frac{b_u D_{i,N}[j]P_j\sigma_{2_j,3}^2}{N_0\sin^2(\theta)}\right)\right] \tag{2.86}$$

Similarly, the probability that the *k*-th relay is in state $D_{i,N}[k]$ given the states of the previous *n* relays is given by

$$E[P_{k,i}^n]=B_k^n\left(D_{i,N}[k]\right) \tag{2.87}$$

where $B_k^n(\cdot)$ is defined as

$$B_k^n(x)=\begin{cases}F_u\left[\left(1+\dfrac{b_u P_1\sigma_{1,2_k}^2}{N_0\sin^2(\theta)}\right)\displaystyle\prod_{j=\max(1,k-n)}^{k-1}\left(1+\dfrac{b_u D_{i,N}[j]P_j\sigma_{2_j,2_k}^2}{N_0\sin^2(\theta)}\right)\right] \\ \text{if } x=0 \\ 1-F_u\left[\left(1+\dfrac{b_u P_1\sigma_{1,2_k}^2}{N_0\sin^2(\theta)}\right)\displaystyle\prod_{j=\max(1,k-n)}^{k-1}\left(1+\dfrac{b_u D_{i,N}[j]P_j\sigma_{2_j,2_k}^2}{N_0\sin^2(\theta)}\right)\right] \\ \text{if } x=1\end{cases} \tag{2.88}$$

So we conclude that the SER of an *N*-relay DF cooperative diversity network using protocol $C(n)$, $1 \leq n \leq N-1$ for M-PSK and M-QAM can be written as

$$P_{\mathrm{SER}}(n)=\sum_{i=0}^{2^N-1}F_u\left[\left(1+\frac{b_u P_1\sigma_{1,2k}^2}{N_0\sin^2(\theta)}\right)\prod_{j=1}^{N}\left(1+\frac{b_u D_{i,N}[j]P_j\sigma_{2_j,2_k}^2}{N_0\sin^2(\theta)}\right)\right]\prod_{k=1}^{N}B_k^n(D_{i,N}[k]) \qquad (2.89)$$

where $F_u(.)$ and $B_k^n(.)$ are defined in (2.82) and (2.88), respectively.

To evaluate performance analysis, we consider two cases in figure 2.12 for $C(1)$ scenario using Q-PSK modulation. Firstly under the assumption that the relays correctly judge whether the received signal is decoded correctly or not *i.e.* no error propagation (NEP), as analysed above. Secondly we predefine a certain threshold and each relay compares the instantaneous received SNR to the threshold and decides whether to forward the received signal or not *i.e.* error propagation (EP). In simulation the threshold is taken as 3 dB. For sake of simplicity we restrict up to three relays.

Figure 2.13 depicts the comparative performance between $C(N-1)$ and $C(1)$ strategies both for Q-PSK and 16-QAM modulation. For sake of simplicity we limit N to 3. It can be seen from the graph that there is a very small gap between the SER performance of scenarios $C(1)$ and $C(N-1)$, and that they almost merge together at high enough SNR. This confirms that utilizing scenario $C(1)$ can deliver the required SER performance for a fairly wide range of SNR.

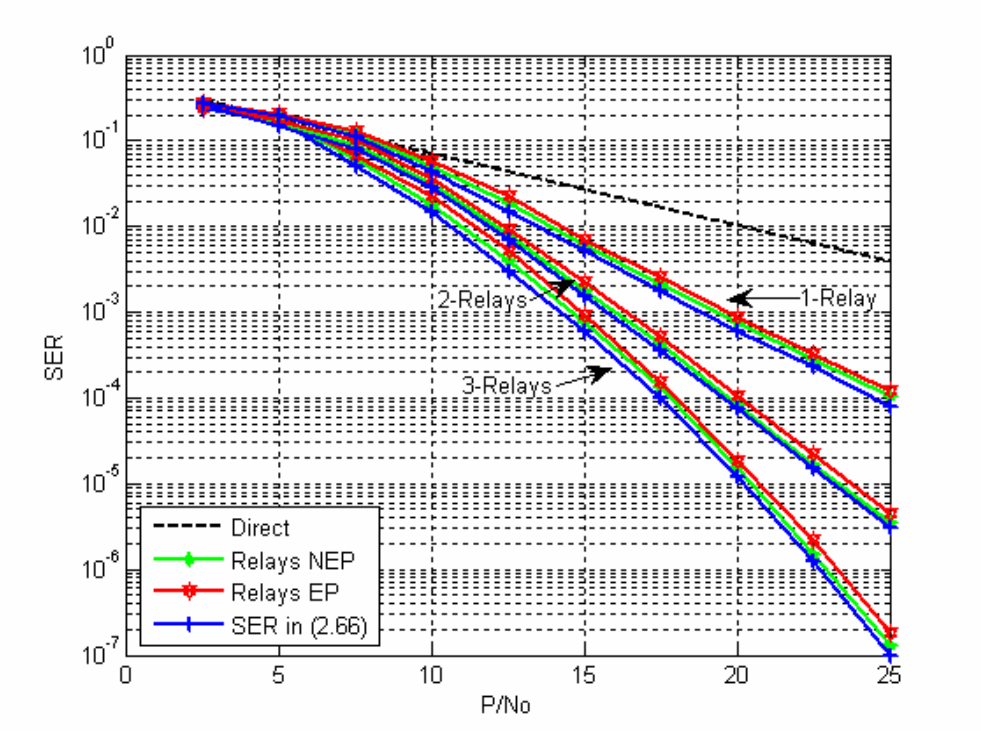

Figure 2.12 SER versus SNR for 3-different scenarios

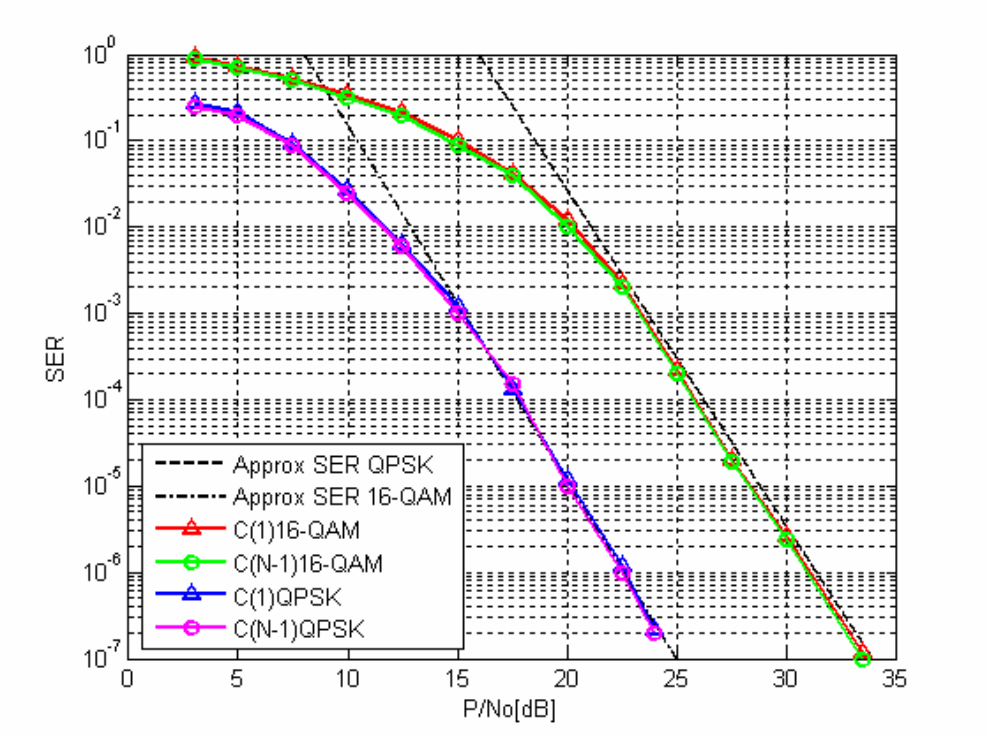

Figure 2.13, Comparison between $C(1)$ and $C(N\text{-}1)$ for QPSK and 16-QAM for $N = 3$

2.4.3.2 Multi-hop amplify and forward strategy

Recall that in AF scheme, the relay scales the received version of the signal and transmits an amplified version to the destination or to next relay in case of multi-hop relays. As contrast to DF protocol, an AF protocol does not suffer from the error propagation problem because the relays do not perform any hard-decision operation on the received signal. An AF strategy in a multi-hop scenario is depicted below in figure 2.14.

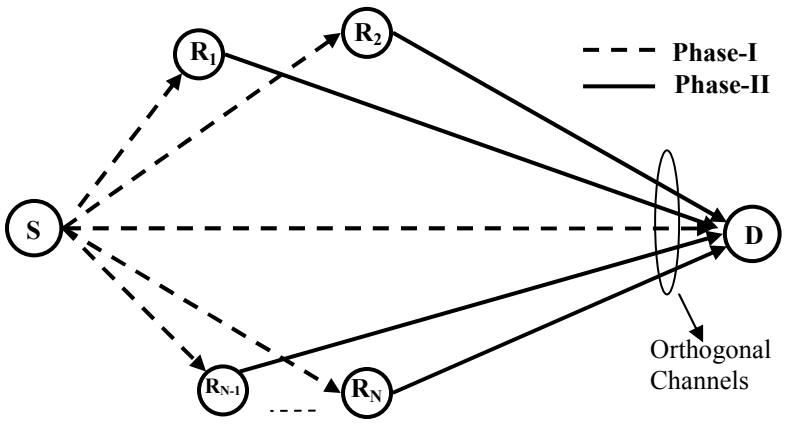

Figure 2.14 Multi-hop AF system model.

As we saw from the previous section that in multi-hop scenario more than one relaying strategy is possible. For example in DF strategy we studied two cases as depicted in figure 2.10 and 2.11. Similarly in case of AF, two strategies are possible. In first scenario, each relay forwards only the source's signal to the destination and in second scenario each relay forwards a combined signal from the source and the previous relays.

Here we discuss only the first case because the second case is not of much importance as in that case the relay combines the same signal in different phases and as a result noise propagation problem causes severe degradation in the system performance [20].

In first scenario, the cooperation is done in two phases as highlighted in figure 2.14 by dot and ray lines. In phase-I, the source broadcasts his information to the destination and N relays nodes whereas in phase-II each relay forward the received signal to destination.

The received signal at the destination and i-th relay in phase-I can be respectively written as

$$y_{1,3} = \sqrt{P_1} h_{1,3} x + n_{1,3} \tag{2.90}$$

$$y_{1,2_i} = \sqrt{P_1} h_{1,2_i} x + n_{1,2_i} \tag{2.91}$$

for $i = 1, 2, ..., N$, where P_1 is the transmitted source power, $n_{1,3}$ and $n_{1,2_i}$ denote the AWGN at the destination and i-th relay respectively, $h_{1,3}$ and $h_{1,2_i}$ are the channel coefficients from the source to the destination, and i-th relay, respectively. In second phase of transmission, each relay re-transmits an amplified version of the received signal to the destination. The relays amplify the received signal by a factor that is inversely proportional to the received power at i-th relay as given in (2.16). The received signal at the destination in phase-II from i-th relays can be represented as

$$y_{2_i,3} = \frac{\sqrt{P_i}}{\sqrt{P_1 \left| h_{1,2_i} \right|^2 + N_0}} h_{2_i,3} y_{1,2_i} + n_{2_i,3} \tag{2.92}$$

where P_i is the i-th relay node power. The channel coefficients $h_{1,3}$, $h_{1,2_i}$ and $h_{2_i,3}$ are modelled as zero-mean, complex Gaussian random variables with variances $\sigma^2_{1,3}, \sigma^2_{1,2_i}$ and $\sigma^2_{2_i,3}$ respectively.

The noise terms are modelled as zero-mean, complex Gaussian random variables with variance N_0. Jointly combining the signal received from the source in phase-I and those from the relays in phase-II, the destination detects the transmitted symbols by the use of MRC.

Symbol Error Rate (SER) performance analysis

Like DF strategy, here we also try to derive SER expression with M-PSK and M-QAM signals. With the knowledge of the Channel State Information (CSI), the output of the MRC detector at the destination can be written as

$$y_3 = \alpha_1 y_{1,3} + \sum_{i=1}^{N} \alpha_i y_{2_i,3} \tag{2.93}$$

where

$$a_1 = \frac{\sqrt{P_1} h_{1,3}^*}{N_0} \qquad \text{and} \qquad a_i = \frac{\sqrt{\dfrac{P_1 P_i}{P_1 \left|h_{1,2_i}\right|^2 + No}}\, h_{1,2_i}^* h_{2_i,3}^*}{\left(\dfrac{P_i \left|h_{2_i,3}\right|^2}{P_1 \left|h_{1,2_i}\right|^2 + N_0} + 1\right) N_0} \tag{2.94}$$

If we assume that the transmitted symbol x has an average energy of 1, then the SNR at the MRC detector output is

$$\Gamma_3 = \Gamma_1 + \sum_{i=1}^{N} \Gamma_i \tag{2.95}$$

where $\Gamma_1 = P_1 \left|h_{1,3}\right|^2 / N_0$, and

$$\Gamma_i = \frac{1}{N_0} \frac{P_1 P_i \left|h_{1,2_i}\right|^2 \left|h_{2_i,3}\right|^2}{P_1 \left|h_{1,2_i}\right|^2 + P_i \left|h_{2_i,3}\right|^2 + N_0} \tag{2.96}$$

The instantaneous SNR Γ_i can be tightly upper bounded as

$$\tilde{\Gamma}_i = \frac{1}{N_0} \frac{P_1 P_i \left|h_{1,2_i}\right|^2 \left|h_{2_i,3}\right|^2}{P_1 \left|h_{1,2_i}\right|^2 + P_i \left|h_{2_i,3}\right|^2} \tag{2.97}$$

which is the harmonic mean of $P_1\left|h_{1,2_i}\right|^2/N_0$ and $P_i\left|h_{2_i,3}\right|^2/N_0$. The SER of M-PSK and M-QAM conditional on the CSI are defined in (2.74) and (2.75), respectively.

Let us denote the MGF of a random variable *Z* as [20]

$$M_Z(s)=\int_{-\infty}^{\infty}\exp(-sz)P_Z(z)dZ \tag{2.98}$$

Averaging the conditional SER over the Rayleigh fading channels, the SER of the M-PSK signals and M-QAM signals can be given, respectively, as

$$P_{\text{SER}}\approx\frac{1}{\pi}\int_0^{(M-1)\pi/M}M_{\Gamma_s}\left(\frac{b_{\text{PSK}}}{\sin^2\theta}\right)\prod_{i=1}^{N}M_{\tilde{\Gamma}_i}\left(\frac{b_{\text{PSK}}}{\sin^2\theta}\right)d\theta \tag{2.99}$$

$$P_{\text{QAM}}\approx\frac{4C}{\pi}\int_0^{\pi/2}M_{\Gamma_s}\left(\frac{b_{\text{QAM}}}{2\sin^2\theta}\right)\prod_{i=1}^{N}M_{\tilde{\Gamma}_i}\left(\frac{b_{\text{QAM}}}{2\sin^2\theta}\right)d\theta$$

$$-\frac{4C^2}{\pi}\int_0^{\pi/4}M_{\gamma_s}\left(\frac{b_{\text{QAM}}}{2\sin^2\theta}\right)\prod_{i=1}^{N}M_{\tilde{\gamma}_i}\left(\frac{b_{\text{QAM}}}{2\sin^2\theta}\right)d\theta \tag{2.100}$$

The MGF of Γ_s is same as given in (2.42), and to get the MGF of $\tilde{\gamma}_i$, we suppose that X_1 and X_2 are two independent exponential random variables with parameters β_1 and β_2 respectively, and $Z=\dfrac{X_1X_2}{X_1+X_2}$ is the harmonic mean of X_1 and X_2, then the MGF of *Z* is

$$M_Z(s)=\frac{(\beta_1+\beta_2)^2+(\beta_1+\beta_2)s}{\Delta^2}+\frac{2\beta_1\beta_2 s}{\Delta^3}\ln\frac{(\beta_1+\beta_2+s+\Delta)^2}{4\beta_1\beta_2} \tag{2.101}$$

where $\Delta=\sqrt{(\beta_1+\beta_2)^2+2(\beta_1+\beta_2)s+s^2}$

With $\beta_1=N_0/P_1\sigma_{1,2_i}^2$ and $\beta_2=N_0/P_i\sigma_{2_i,3}^2$ at high SNR, for any relay both β_1 and β_2 go to zero, and Δ goes to *s*. Thus, the MGF in (2.101) can be approximated as

$$M_Z(s) \approx \frac{\beta_1 + \beta_2}{s} + \frac{2\beta_1\beta_2}{s^2} \ln \frac{s^2}{\beta_1\beta_2} \tag{2.102}$$

At enough high SNR, the MGF can be further simplified as [24]

$$M_Z(s) \approx \frac{\beta_1 + \beta_2}{s} \tag{2.103}$$

Substituting the above MGF approximation into (2.99), we conclude that:

at enough high SNR, the SER of AF cooperative protocol with N relay nodes employing M-PSK or M-QAM signals can be approximated as:

$$P_{\text{SER}} \approx \frac{g(N)N_0^{N+1}}{b^{N+1}} \cdot \frac{1}{P_1\sigma_{1,3}^2} \prod_{i=1}^{N} \frac{P_1\sigma_{1,2_i}^2 + P_i\sigma_{2_i,3}^2}{P_1P_i\sigma_{1,2_i}^2\sigma_{2_i,3}^2} \tag{2.104}$$

where in case of M-PSK, $b = b_{PSK}$ and

$$g(N) = \frac{1}{\pi}\int_0^{(M-1)\pi/M} \sin^{2(N+1)}\theta d\theta \tag{2.105}$$

and in case of M-QAM, $b = b_{\text{QAM}}/2$ and

$$g(N) = \frac{4C}{\pi}\int_0^{\pi/2} \sin^{2(N+1)}\theta d\theta - \frac{4C^2}{\pi}\int_0^{\pi/4} \sin^{2(N+1)}\theta d\theta \tag{2.106}$$

Figure 2.15 shows the performance of the AF relaying protocol with QPSK modulation up to three relay nodes in different channel conditions. From the graph one can observe that AF protocol achieves full diversity of order N+1.

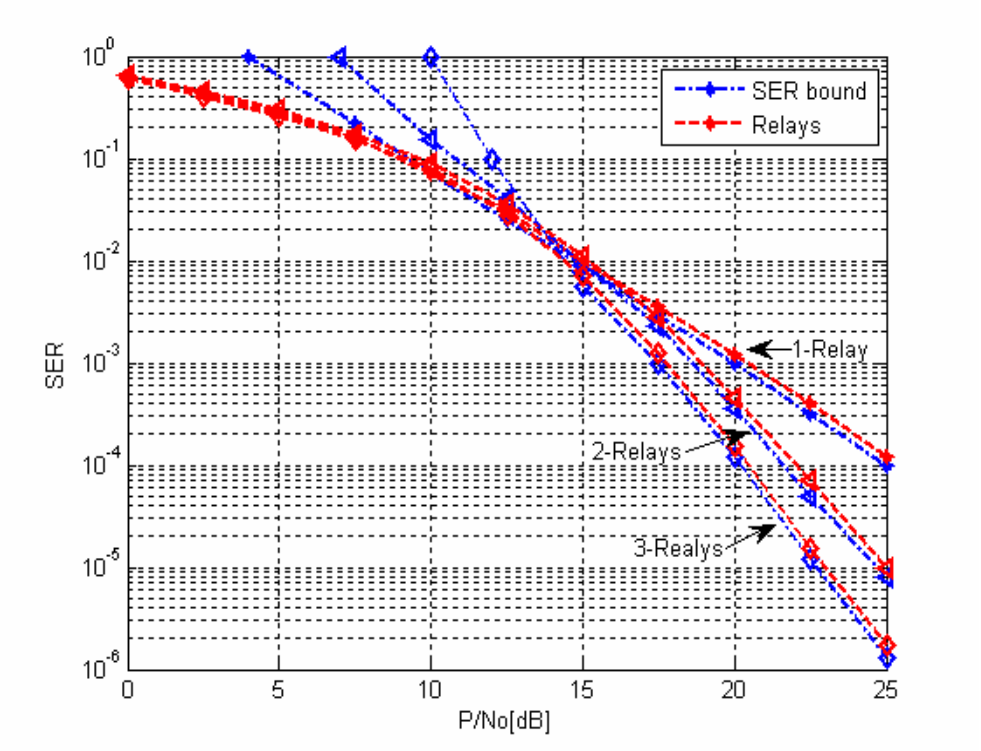

Figure 2.15 SER performances for QPSK constellation with equal power $(\sigma_{1,3}^2 = 1, \sigma_{1,2_i}^2 = 1, \sigma_{2_i,3}^2 = 1)$

2.5 Half duplex Gaussian relay channels

In previous sections, we assumed that the relays are full-duplex. Although it is possible to design full duplex RF radios, but the design of such radios need precise and expensive components. In this section, we consider a half-duplex relay and study the impact of half-duplex operation on relaying protocols and achievable rates.

We consider a discrete memoryless communication system where the intermediate relay node operates in TDD mode when transmitting and sending in same frequency band.

For sake of simplicity we consider a half-duplex relay network with single hop relay node, although same idea can be extended to multi-hop relay networks. We model a half-duplex operation using the state variable Q that controls the relay operation. Q takes the value q_1 if the relay is listening and q_2 if the relay is transmitting. We also consider fixed protocols, in which the relay listens for a fixed time interval fraction t $(0 \le t \le 1)$ and then transmits in the remaining portion $(1-t)$ as shown in figure 2.16.

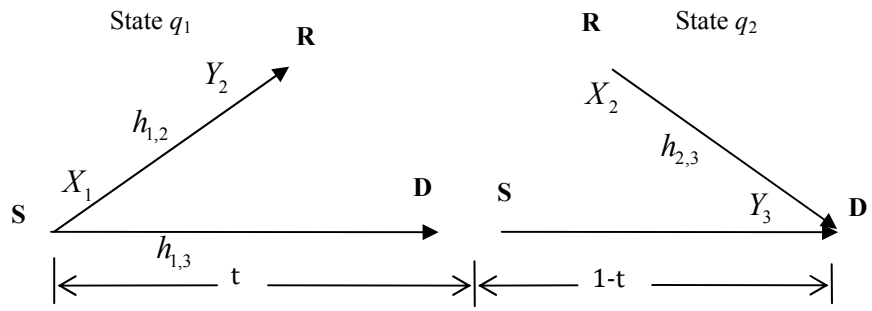

Figure 2.16, two-modes of operation

According to [25] the rate

$$R_{DF} = \max_{t,0\le t\le 1} \min\{tI(X_1;Y_2/q_1)+(1-t)I(X_1;Y_3 \mid X_2,q_2),$$
$$tI(X_1;Y_3/q_1)+(1-t)I(X_1,X_2;Y_3/q_2)\} \quad (2.107)$$

is achievable for a fixed input distribution and a fixed t, can be maximized over all input distributions, $t\in[0,1]$. The first term in (2.107) is the sum of two mutual information expressions. The first one indicates the amount of information the relay can decode in t fraction of the time. The second is the mutual information the destination collects from the source during the time when the relay is transmitting. The second term in (2.107) is also a sum of two terms, the first of which is the mutual information at the destination while the relay is silent, and the second is the rate at which the source and the relay can together send in 1-t fraction of time. Like full-duplex case, if the half-duplex relay channel is physically degraded, then the above rate is capacity achieving.

The real Gaussian noise half duplex relay channel is very similar to the full-duplex case, but in half-duplex case the relay cannot transmit and receive at the same time. So we can write

$$Y_{2,1} = h_{1,2}X_{1,1} + N_{2,1} \quad (2.108)$$

$$Y_{3,1} = h_{1,3}X_{1,1} + N_{3,1} \quad (2.109)$$

When the channel is in q_1 state, and

$$Y_{3,2} = h_{1,3}X_{1,2} + h_{2,3}X_{2,2} + N_{3,2} \quad (2.110)$$

When the channel is in q_2 state.

Note that the second number in subscript in (2.108) - (2.110) show the channel state q_1 and q_2. where $h_{1,2}$, $h_{1,3}$ and $h_{2,3}$ are channel fading from source to relay, source to destination and relay to destination, respectively, and are assumed to be constant. N_2 and N_3 are AWGN at relay and destination respectively.

For Gaussian half duplex relay channel the DF achievable rate becomes [28]

$$R_{DF} = \max_{\rho,t\in[0,1]} \min\left\{\frac{t}{2}\log\left(1+\left|h_{1,2}\right|^2 P_{1,1}\right)+\frac{1-t}{2}\log\left(1+\rho\left|h_{1,3}\right|^2 P_{1,2}\right), \frac{t}{2}\log\left(1+\left|h_{1,3}\right|^2 P_{1,1}\right)\right.$$
$$\left.+\frac{1-t}{2}\log\left(1+\left|h_{1,3}\right|^2 P_{1,2}+\left|h_{2,3}\right|^2 P_2+2\sqrt{(1-\rho)\left|h_{1,3}\right|^2 P_{1,2}\left|h_{2,3}\right|^2 P_2}\right)\right\} \quad (2.111)$$

In AF strategy, the relay simply scales Y_2 according to its own power constraint and forwards $X_2 = \alpha Y_2$ to the destination, where $\alpha \le \sqrt{P_2/\left(\left|h_{1,2}\right|^2 P_1+1\right)}$. Assuming α is equal to its upper bound, the AF protocol achieves the rate [25]

$$R_{AF} = \frac{1}{4}\log\left(1+\left|h_{1,3}\right|^2 P_1+\frac{\left|h_{1,2}\right|^2 P_1\left|h_{2,3}\right|^2 P_2}{1+\left|h_{1,2}\right|^2 P_1+\left|h_{2,3}\right|^2 P_2}\right) \quad (2.112)$$

2.6 Cryptographic relay networks

When talking about relay networks although cryptography seems somewhat alien but yet it possesses some interesting applications in this field. Particularly the encryptions of PN sequences in Spread Spectrum (SS) communications birth certain problems that seek its solution in relay networks. In fact the classical PN sequences used in spread spectrum have short periodic sequences with small periods, and are repeated as many times as needed. This property of PN sequences is used to synchronize the transmission by the search of peaks of correlations [31], [32]. But unfortunately when someone wants to encrypt the PN sequences, he/she will lose this basic and necessary property.

In what follows, we propose the use of a relay network with orthogonal channels from the source to relay, and from the source/relay to the receiver. In other words source-relay link uses a different frequency band from the source-destination and relay-destination link.

The basic principle of an ordinary Direct Sequence Spread Spectrum (DSSS) communication which takes binary data sequences and multiplies it by a higher rate pseudorandom binary sequence is depicted below in figure 2.17.

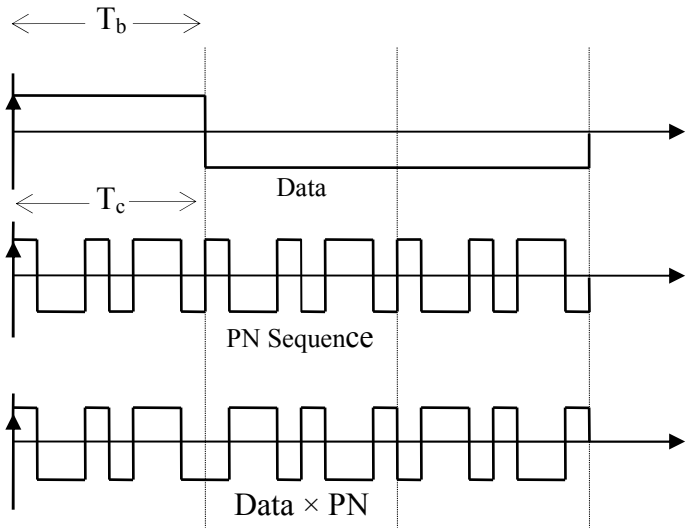

Figure 2.17 Spread spectrum operation

If we denote the data bit duration of DSSS signal as T_b , then the data waveform can be represented as

$$d(t) = d_n \text{ , with } nT_b \le t < (n+1)T_b \text{ and } d_n \in \{1,-1\} \tag{2.113}$$

where (d_n) is the binary data sequence. For example in figure 2.17, (d_n) =1,-1,-1.....

For simplification, we use $\{1,-1\}$ in lieu of $\{0,1\}$.

For practical application, the data clock and the PN sequence clock must be synchronized, moreover the bit duration T_b must be the multiples of the chip duration T_c. The ratio $N = T_b / T_c$ is referred as the spreading factor. For example in figure 2.17 N = 8 and PN sequence is (1,-1,-1,1,-1,1,1,-1.....).

We assume that the data $D=(d_t)$ is transmitted with bit duration T_b and the data $D'=(d'_t)$ with chip duration T_c, where D' is obtained from D by repeating each bit d_t, N times.

Then the data transmitted is $C=D'\times \mathrm{PN}$ with chip time T_c.

To recover the original message, the receiver multiplies C by the pseudorandom sequence PN in order to get D' and then decodes D.

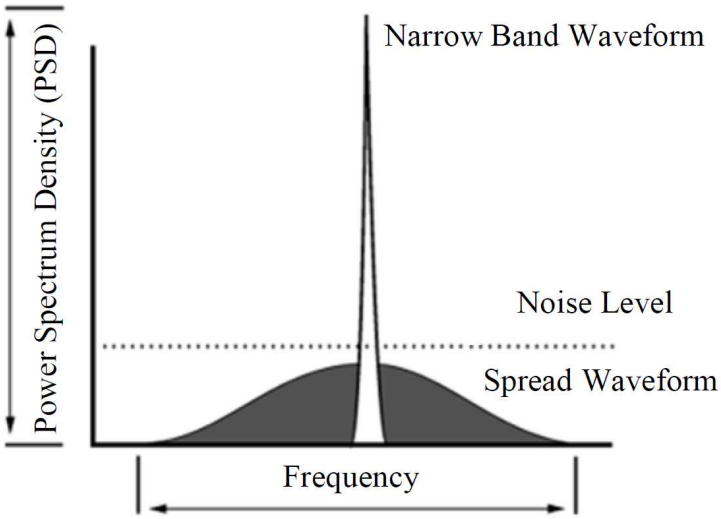

Figure 2.18 Spread spectrum signal spreading below noise level

Spread spectrum communication owns many advantages. For example the frequency band is much larger and the power density of the signal is much lower as compare to an ordinary signal. The signal is more resistant to interferences, because after multiplication by the PN sequence, these interferences look like white Gaussian noise. Figure 2.18 represents a signal view of SS communication.

As one can see from the figure that the power density is smaller than the noise density, therefore it becomes difficult to detect the signal without multiplication by the PN sequence.

The spread spectrum techniques are particularly used in Code Division Multiple Access (CDMA) where each user has its own PN sequence, which allows them to transform the signals of other users into white noise. Another advantage of the spread spectrum is the fact that it is possible to use it with a very low SNR by increasing the value of N. It can make the signal undetectable if the PN sequence is not known to compute the cross-correlation. Therefore to make the communication absolutely secure one may desire to encrypt the PN sequence.

Spread Spectrum and cryptography

In symmetric cryptography (*i.e*. cryptography with a secret key shared by the sender and the receiver), there are two methods of encryption, *i.e*. the block ciphers and the stream ciphers. In this sequel we consider the latter. The principle is very simple. We use modulo 2 addition of a random symbol k_t to each symbol d_t of the binary data.

Now let the

Message is denoted by $M = (d_t)_{t=1}^{n}$

Shared secret key: $K = (k_t)_{t=1}^{n}$, and

Cryptogram $C = (d_t \oplus k_t)_{t=1}^{n}$ (2.114)

To recover the source message *M*, receiver needs to compute $C \oplus K$. If the secret key is randomly chosen and used only once (*e.g*. one-Time Pad) then such a method is absolutely secure. However it is not possible to use a secret key having the same size as the message. So we replace the random sequence *K* by a sequence generated by a pseudorandom generator initialized by a smaller key.

We further propose that instead of adding a random sequence with good cryptographic properties to the data before transmission, we use directly such a pseudorandom sequence as PN sequence of spread spectrum.

Suppose we want to transmit the message $M = (d_t)$ with a spreading factor $N = T_b / T_c$ and a PN sequence $S = (s_t)$, then the transmitted cryptogram will be $C' = M' \oplus S$, where M' is the message *M* with *N* repetition of each bit $\left(d'_t = d_{\lceil t/N \rceil}\right)$.

Another advantage of our this approach is that since the energy of the spread signal is lower than the energy of the ambient noise, so it becomes nearly impossible to recover the cryptogram $C' = M' \oplus S$ without the knowledge of *S*. Indeed, the correlation of the received signal with *S* is needed to eliminate the ambient noise.

However, the main draw back of such a system is the problem of synchronization, as indicated above. In what follows, we propose some solutions to deal this issue.

In ordinary cryptography, a cryptogram sent over the channel is not secret. However in some particular cases, one may want not only to have a cryptographic secure transmission but also to keep it secret. One method to achieve this goal is to use the proposed communication with a large signal spectrum spreading *N* to mask the message inside the ambient noise. However,

by doing so the problem of synchronizations cannot be avoided. A second solution lies in masking the secret SS signal with a classical unimportant communication. The secret signal is then synchronized with the classical communication. This method is more robust than the classical steganography. Because even the secret signal is detected, it is not possible to recover the initial message without the knowledge of the PN sequence.

As an example, let the non-secret communication is denoted by

$$M = (D_n) \ , \ D_n \in \{0,1\} \tag{2.115}$$

and the transmitted signal is represented by

$$\Phi(t) = A\cos(\omega t + D(t)\pi) \tag{2.116}$$

where, A= amplitude of the signal, $1/\omega$ = is the frequency of the signal, and $D(t) = D_n$ with $n = \lfloor t/T_b \rfloor$. Now let the hidden message

$$m = (d_n) \ , \ d_n \in \{0,1\} \tag{2.117}$$

is transmitted with amplitude α, chip times t_c a divisor of T_b and bit chip t_b a multiple of T_b. The pseudorandom sequence is denoted by (k_n) , $k_n \in \{0,1\}$

Hence the secret communication is represented by

$$\phi(t) = \alpha\cos(\omega t + (d(t) + k(t)\pi) \tag{2.118}$$

where $d(t) = d_n$ with $n = \lfloor t/t_b \rfloor$ denotes instantaneous hidden message, $k(t) = d_{n'}$ with $n' = \lfloor t/t_c \rfloor$ denotes PN sequence, α = amplitude, and $1/\omega$ = is the frequency of the signal.

Combining (2.116) and (2.118), the transmitted message can be written as

$$X(t) = \Phi(t) + \phi(t) \ \text{with} \ \alpha << A \tag{2.119}$$

The receiver uses the known message to synchronize the communication, recovers the signal $\Phi(t)$ and then recovers the secret message using the classical spread spectrum methods. Note that the secret message is smaller than the noise and is not detectable if the PN sequence is not used to compute the correlation. For external viewers, the transmitted message looks like a slightly perturbed in amplitude BPSK signal.

$$\Phi(t) = (A \pm \varepsilon(t))\cos(\omega t + D(t)\pi) \quad , \qquad 0 \le \varepsilon(t) \le \alpha \tag{2.120}$$

However, again the main problem with this method is that if an error occurs on message *M*, this error induces a very high noise on T_b / t_c chips, and equivalent may induces some errors on secret message *m*.

To overcome this problem we use orthogonal relay channels where the two messages are transmitted orthogonally in different frequency bands.

Hence the transmitted messages (2.116) and (2.118) can be written as, respectively

$$\Phi(t) = A\cos(\omega t + D(t)\pi) \tag{2.121}$$

$$\phi(t) = \alpha \sin(\omega t + (d(t) + k(t))\pi) \tag{2.122}$$

With a small abuse of the notation, we denote the source message as X_1, and the orthogonal components as X_Φ and X_ϕ.

Definition 1 : A discrete memoryless relay channel denoted by $(\mathcal{X}_1 \times \mathcal{X}_2, p(y_3, y_2 / x_1, x_2), \mathcal{Y}_3 \times \mathcal{Y}_2)$ consists of a sender $X_1 \in \mathcal{X}_1$, a receiver $Y_3 \in \mathcal{Y}_3$, a relay sender $X_2 \in \mathcal{X}_2$, a relay receiver $Y_2 \in \mathcal{Y}_2$, and a family of conditional probability mass function $p(y_3, y_2 / x_1, x_2)$ on $\mathcal{Y}_3 \times \mathcal{Y}_2$, one for each $(x_1, x_2) \in \mathcal{X}_1 \times \mathcal{X}_2$.

Definition: 2 A discrete memoryless relay channel is said to have orthogonal components if the sender alphabet $\mathcal{X}_1 = \mathcal{X}_\Phi \times \mathcal{X}_\phi$ and the channel can be expressed as $p(y_3, y_2 \mid x_1, x_2) = p(y_3 \mid x_\Phi, x_2)\, p(y_2 \mid x_\phi, x_2)$ for all $(x_\Phi, x_\phi, x_2, y_3, y_2) \in \mathcal{X}_\Phi \times \mathcal{X}_\phi \times \mathcal{X}_2 \times \mathcal{Y}_3 \times \mathcal{Y}_2$.

The capacity of such a relay channel with orthogonal components is given by [33]

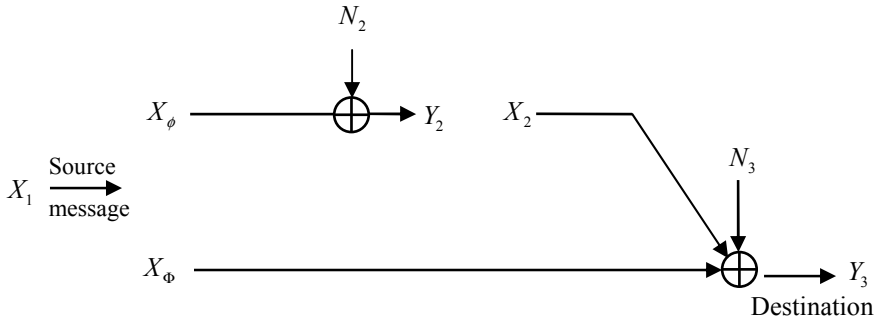

Fig 2.19. Frequency division AWGN relay channel

$$C \le \max_{p(x_2)p(x_\Phi|x_2)p(x_\phi|x_2)} \min\left\{I(X_\Phi, X_2; Y_3), I(X_\phi; Y_2 \mid X_2) + I(X_\Phi; Y_3 \mid X_2)\right\} \tag{2.123}$$

For proof we use max-flow min-cut upper bound [21]

$$C \le \max_{p(x_1,x_2)} \min\left\{I(X_1, X_2; Y_3), I(X_1; Y_3, Y_2 \mid X_2)\right\} \tag{2.124}$$

We show that any $R<C$ is achievable using the generalized block Markov encoding scheme. Substituting $X_1 = (X_\Phi, X_\phi)$ and assuming joint probability mass function of the form $p(x_2)p(x_\phi \mid x_2)p(x_\Phi \mid x_2)$, we get

$$\begin{aligned} I(X_1, X_2; Y_3) &= I(X_\phi, X_\Phi, X_2; Y_3) \\ &= I(X_\Phi, X_2; Y_3) + I(X_\phi; Y_3 \mid X_\Phi, X_2) \\ &= I(X_\Phi, X_2; Y_3) \end{aligned}$$

and

$$\begin{aligned} I(X_1; Y_3, Y_2 \mid X_2) &= I(X_\Phi, X_\phi; Y_3, Y_2 \mid X_2) \\ &= I(X_\Phi, X_\phi; Y_2 \mid X_2) + I(X_\Phi, X_\phi; Y_3 \mid X_2, Y_2) \\ &= I(X_\phi; Y_2 \mid X_2) + I(X_\Phi; Y_2 \mid X_2, X_\phi) + I(X_\Phi, X_\phi; Y_3 \mid X_2, Y_2) \end{aligned}$$

It follows that $X_\Phi \to (X_2, X_\phi) \to Y_2$ form a Markov chain

$$\begin{aligned} &= I(X_\phi; Y_2 \mid X_2) + I(X_\Phi, X_\phi; Y_3 \mid X_2, Y_2) \\ &= I(X_\phi; Y_2 \mid X_2) + H(Y_3 \mid X_2, Y_2) - H(Y_3 \mid X_2, X_\Phi, X_\phi, Y_2) \end{aligned}$$

It follows that $(X_\phi, Y_2) \to (X_2, X_\Phi) \to Y_3$ form a Markov chain

$$\begin{aligned} &= I(X_\phi; Y_2 \mid X_2) + H(Y_3 \mid X_2, Y_2) - H(Y_3 \mid X_2, X_\Phi) \\ &\le I(X_\phi; Y_2 \mid X_2) + H(Y_3 \mid X_2) - H(Y_3 \mid X_2, X_\Phi) \\ &= I(X_\phi; Y_2 \mid X_2) + I(X_\Phi; Y_3 \mid X_2) \end{aligned}$$

Thus we showed that

$$C \le \max_{p(x_\Phi, x_\phi, x_2)} \min\left\{I(X_\Phi, X_2; Y_3), I(X_\phi; Y_2 \mid X_2) + I(X_\Phi; Y_3 \mid X_2)\right\} \tag{2.125}$$

2.7 Conclusion

Cooperative communication system is a communication paradigm that generalizes MIMO communications to much broader applications. In this system, the terminals dispersed in a wireless network cell can be thought of as distributed antennas. Through cooperation among these nodes, MIMO-like gains can be achieved by increasing the diversity gains of the system. In literature one can find numerous cooperative protocols proposed by different authors. In this chapter we mainly focused on two principal cooperative strategies, *i.e*. decode and forward, and amplify and forward from fixed relaying concept and selective DF and incremental strategy from adaptive relaying concept. We computed exact SER for DF and AF strategies, both over single and multi-hop scenarios. We described the performance of these algorithms through calculating outage capacity and characterizing diversity gains. The performance of adaptive relaying techniques in general outperforms the fixed relaying techniques because of the extra information utilized in implementing the protocols, for example, knowledge of the received SNR in selective relaying and the feedback from the destination in incremental relaying. On the other hand, fixed relaying techniques are simple to implement.

The multi-hop cooperative strategies consist of schemes in which each relay can combine the signals arriving from an arbitrary but fixed number of previous relays along with that received from the source. We derived exact SER expressions for DF and AF cooperation schemes both for M-PSK and M-QAM modulations. At high SNR, the performance of a simple cooperation scenario in which each relay combines the signals arriving from the previous relay(s) and the source is asymptotically exactly the same as that for the most complicated scenario in which each relay combines the signals arriving from all the previous relays and the source.

In this chapter, we also studied the capacity analysis for a half duplex Gaussian relay channels operating in TDD mode when transmitting and sending information in same frequency band. Although the capacity of such a relay channel is less than the capacity of full duplex relay channel, however the lower bound on the capacity show that even it can gain higher capacity with respect to direct link.

At the end of this chapter we introduced a technique of cryptography in cooperative communication system. Actually our cryptographic system in a conventional communication system encountered the problem of synchronization. To seek the solution of this problem we

proposed a frequency division AWGN relay channel where the information is sent orthogonally in different frequency bands.

As discussed in chapter 1, to meet our fast growing demands for reliable communication, the use of multiple antennas at transmitter and receiver is inevitable. But without the presence of some efficient protocols, one cannot fully exploit the benefits tendered by a MIMO system. Until now it is believed that space time coding system is most pertinent and ideal technique to be used to exploit the available resources in a MIMO system. So in forthcoming chapter we study different techniques for construction of space time codes for getting maximum diversity and rates over the MIMO channels.

Chapter 3

Space time coding performance analysis and design criteria

3.1 Introduction

In chapter 1, we showed that the information capacity of wireless communication systems can be increased considerably by employing multiple transmit and receive antennas. For a system with a large number of transmit and receive antennas and an independent flat fading channel known at the receivers, the capacity grows linearly with the minimum number of antennas.

An effective and practical way to approach the capacity of MIMO wireless channels is to employ Space-Time (ST) coding [34], [35]. Space-time coding is a coding technique designed for use with multiple transmit antennas. Coding is performed in both spatial and temporal domains to introduce correlation between signals transmitted from various antennas at various time periods. The spatial-temporal correlation is used to exploit the MIMO channel fading and minimize transmission errors at the receiver. Space-time coding can achieve transmit diversity and power gain over spatially uncoded systems without sacrificing the bandwidth. There are various approaches in ST coding structures, including Space Time Block Codes (STBCs), Space-Time Trellis Codes (STTCs), Super Orthogonal Space-Time Trellis Codes (SOSTTCs) and Space-Time Turbo Trellis Codes (STTTCs). A central issue in all these schemes is the exploitation of multi-path effects in order to achieve high spectral efficiencies and performance gains.

In this chapter, we study and evaluate error probability upper bounded over flate fading Rayleigh channels. These bounds will provide us a better orientation for designing space time codes with high performances. We also study different aspects of design criteria for space time codes. We provide some construction techniques for achieving better diversity, maximum rate and spectral efficiency. We present a technique to enhance the spectral efficiency of STBCs. At the end of this chapter, we provide the simulation results for the performance of some interesting type of space time codes, e.g. STBCs, STTCs, and SOTTCs.

3.2 Basic concept in space-time coding system

We consider a baseband space-time coded communication system with N_T transmit and N_R receive antennas, as shown in figure 3.1

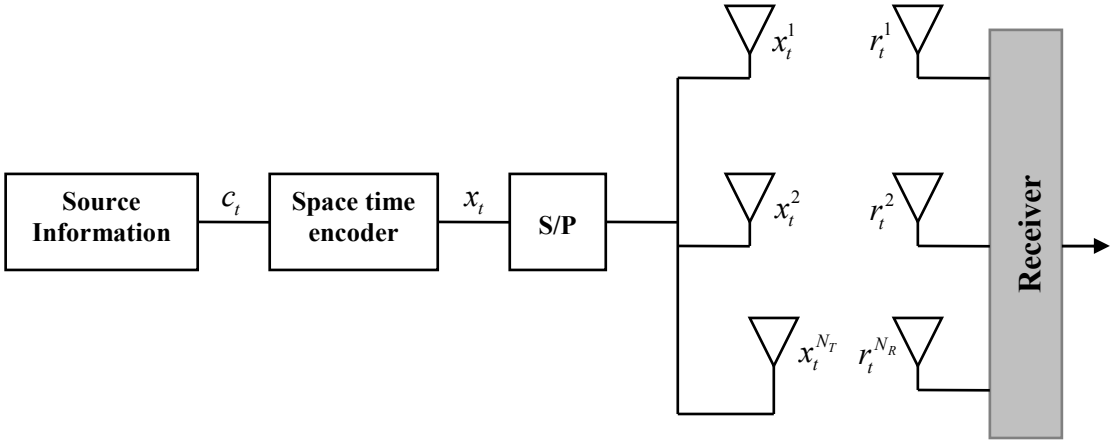

Figure 3.1 Space time coding system

The transmitted data are encoded by a space-time encoder. At each time instant *t*, a block of *m* binary information symbols, denoted by

$$\boldsymbol{c}_t = \left[c_t^1, c_t^2, ..., c_t^m \right] \tag{3.1}$$

is fed into the space-time encoder. The space-time encoder maps the block of *m* binary input data into N_T modulation symbols from a signal set of $M = 2^m$ points. The coded data are applied to a Serial-to-Parallel (S/P) converter producing a sequence of N_T parallel symbols, arranged into an $N_T \times 1$ column vector:

$$\boldsymbol{x}_t = \left[x_t^1, x_t^2, ..., x_t^{N_T} \right]^T \tag{3.2}$$

where $(\cdot)^T$ denotes the transposition. The N_T parallel outputs are simultaneously transmitted by N_T-different antennas, whereby symbol x_t^i, $1 \le i \le N_T$, is transmitted by antenna *i* and all transmitted symbols have the same duration of T_{Sec}. The vector of coded modulation symbols from different antennas, as shown in (3.2), is called a space-time symbol.

The MIMO channel with N_T transmit and N_R receive antennas can be represented by an $N_R \times N_T$ channel matrix $\boldsymbol{H}_t$.

$$\boldsymbol{H}_t = \begin{bmatrix} h_{1,1}^t & h_{1,2}^t & \cdots & h_{1,N_T}^t \\ h_{2,1}^t & h_{2,2}^t & \cdots & h_{2,N_T}^t \\ \vdots & \vdots & \ddots & \vdots \\ h_{N_R,1}^t & h_{N_R,2}^t & \cdots & h_{N_R,N_T}^t \end{bmatrix} \tag{3.3}$$

where $h_{j,i}^t$ represents the fading attenuation coefficient for the path from transmit antenna *i* to receive antenna *j* at time *t*.

In the analysis, we assume that the fading coefficients $h_{j,i}^t$ are independent complex Gaussian random variables with zero mean and variance 1/2 per dimension, implying that the amplitudes of the path coefficients are modelled as Rayleigh fading. In terms of the coefficient variation speed, we consider fast and slow fading channels. For slow fading, it is assumed that the fading coefficients are constant during a frame and vary from one frame to other. In a fast fading channel, the fading coefficients are constant within each symbol period and vary from one symbol to another.

At the receiver, the signal at each of the N_R receive antennas is a noisy superposition of the N_T transmitted signals degraded by channel fading. At time *t*, the received signal at antenna *j* , $j = 1, 2, ...N_R$, denoted by r_t^j is given by

$$r_t^j = \sum_{i=1}^{N_T} h_{j,i}^t x_i^t + n_t^j \tag{3.4}$$

where n_t^j is the noise component of receive antenna *j* at time *t*, which is an independent sample of the zero-mean complex Gaussian random variable.

We represent the received signals from N_R receive antennas at time *t* by an $N_R \times 1$ column vector as

$$\boldsymbol{r}_t = \left[r_t^1, r_t^2, \ldots, r_t^{N_R} \right]^T \tag{3.5}$$

and the noise at the receiver can be described by an $N_R \times 1$ column vector as:

$$\boldsymbol{N}_t = \left[n_t^1, n_t^2, \ldots, n_t^{N_R} \right]^T \tag{3.6}$$

So the received signal vector can be represented as

$$\boldsymbol{r}_t = \boldsymbol{H}_t \boldsymbol{x}_t + \boldsymbol{N}_t \tag{3.7}$$

We assume that the decoder at the receiver uses a maximum likelihood algorithm to estimate the transmitted information sequence and that the receiver has ideal CSI on the MIMO channel whereas the transmitter has no information about the channel. At the receiver, the decision metric is computed based on the squared Euclidean distance between the hypothesized received sequence and the actual received sequence as

$$\sum_t \sum_{j=1}^{N_R} \left| r_t^j - \sum_{i=1}^{N_T} h_{j,i}^t \hat{x}_t^i \right|^2 \tag{3.8}$$

The decoder selects a codeword with the minimum decision metric as the decoded sequence.

3.3 Performance analysis of space-time codes

In the performance analysis we assume that the transmitted data frame length is L symbols for each antenna. We define an $N_T \times L$ space-time codeword matrix, obtained by arranging the transmitted sequence in an array, as

$$\boldsymbol{X} = \left[\boldsymbol{x}_1, \boldsymbol{x}_2, \ldots, \boldsymbol{x}_L \right] = \begin{bmatrix} x_1^1 & x_2^1 & \ldots & x_L^1 \\ x_1^2 & x_2^2 & \ldots & x_L^2 \\ \vdots & \vdots & \ddots & \vdots \\ x_1^{N_T} & x_2^{N_T} & \ldots & x_L^{N_T} \end{bmatrix} \tag{3.9}$$

where the i-th row $\boldsymbol{x}^i = \left[x_1^i, x_2^i, \ldots, x_L^i \right]$ is the data sequence transmitted from the i-th transmit antenna, and the t-th column $\boldsymbol{x}_t = \left[x_t^1, x_t^2, \ldots, x_t^{N_T} \right]^T$ is the space-time symbol at time t.

The Pairwise Error Probability (PEP) $P\left(\boldsymbol{X},\hat{\boldsymbol{X}}\right)$ is the probability that the decoder selects as its estimate an erroneous sequence $\hat{\boldsymbol{X}}=\left(\hat{\boldsymbol{x}}_1,\hat{\boldsymbol{x}}_2,\ldots,\hat{\boldsymbol{x}}_L\right)$ whereas the transmitted sequence was in fact $\boldsymbol{X}=\left(\boldsymbol{x}_1,\boldsymbol{x}_2,\ldots,\boldsymbol{x}_L\right)$. In maximum likelihood decoding, this occurs if

$$\sum_{t=1}^{L}\sum_{j=1}^{N_R}\left|r_t^j-\sum_{i=1}^{N_T}h_{j,i}^t x_t^i\right|^2\geq\sum_{t=1}^{L}\sum_{j=1}^{N_R}\left|r_t^j-\sum_{i=1}^{N_T}h_{j,i}^t\hat{x}_t^i\right|^2 \tag{3.10}$$

The inequality (3.10) is equivalent to

$$\sum_{t=1}^{L}\sum_{j=1}^{N_R}2\Re\left\{\left(n_t^j\right)^*\sum_{i=1}^{N_T}h_{j,i}^t\left(\hat{x}_t^i-x_t^i\right)\right\}\geq\sum_{t=1}^{L}\sum_{j=1}^{N_R}\left|\sum_{i=1}^{N_T}h_{j,i}^t\left(\hat{x}_t^i-x_t^i\right)\right|^2 \tag{3.11}$$

where $\Re$ means the real part of a complex number.

Assuming that perfect information is available at the receiver, for a given realization of the fading variable matrix sequence $\boldsymbol{H}=\left(\boldsymbol{H}_1,\boldsymbol{H}_2,\ldots,\boldsymbol{H}_L\right)$, the term on the right hand side of (3.11) is a constant equal to $d_h^2\left(\boldsymbol{X},\hat{\boldsymbol{X}}\right)$ and the term on the left hand side of (3.11) is a zero mean Gaussian random variable. $d_h^2\left(\boldsymbol{X},\hat{\boldsymbol{X}}\right)$ is the modified Euclidean distance between the two space-time codeword matrices $\boldsymbol{X}$ and $\hat{\boldsymbol{X}}$, given by

$$\begin{aligned}d_h^2\left(\boldsymbol{X},\hat{\boldsymbol{X}}\right)&=\sum_{t=1}^{L}d_h^2\left(\boldsymbol{x}_t,\hat{\boldsymbol{x}}_t\right)\\&=\sum_{t=1}^{L}\left\|\boldsymbol{H}_t.\left(\hat{\boldsymbol{x}}_t-\boldsymbol{x}_t\right)\right\|^2\\&=\sum_{t=1}^{L}\sum_{j=1}^{N_R}\left|\sum_{i=1}^{N_T}h_{j,i}^t\left(\hat{x}_t^i-x_t^i\right)\right|^2\end{aligned} \tag{3.12}$$

The PEP conditioned on $\boldsymbol{H}$ is given by

$$P\left(\boldsymbol{X},\hat{\boldsymbol{X}}\mid\boldsymbol{H}\right)=Q\left(\sqrt{\frac{E_s}{2N_0}d_h^2\left(\boldsymbol{X},\hat{\boldsymbol{X}}\right)}\right) \tag{3.13}$$

where E_s is the energy per symbol at each transmit antenna and $Q(x)$ is the complementary error function defined by

$$Q(x) = \frac{1}{2\pi}\int_x^\infty e^{-t^2/2}dt \tag{3.14}$$

By using the inequality

$$Q(x) \le \frac{1}{2}e^{-x^2/2}, \qquad x \ge 0 \tag{3.15}$$

The conditional PEP (3.13) can be upper bounded by

$$P\left(\boldsymbol{X}, \hat{\boldsymbol{X}} \mid \boldsymbol{H}\right) \le \frac{1}{2}\exp\left(-d_h^2\left(\boldsymbol{X}, \hat{\boldsymbol{X}}\right)\frac{E_s}{4N_0}\right) \tag{3.16}$$

3.3.1 Slow fading channels

In case of slow fading channels, the fading coefficients of the channel are constant during a frame length L. It means the fading $h_{j,i}^t$ does not depend on temporal superscript t, *i.e.* $h_{j,i}^t = h_{j,i}$ during the transmission of one frame.

So the expression (3.12) for calculating Euclidean distance between two sequences of space time codes can be written as:

$$d_h^2\left(\boldsymbol{X}, \hat{\boldsymbol{X}}\right) = \sum_{t=1}^{L}\sum_{j=1}^{N_R}\left|\sum_{i=1}^{N_T} h_{j,i}\left(\hat{x}_t^i - x_t^i\right)\right|^2 \tag{3.17}$$

Let $\boldsymbol{B}$ is defined as codeword difference matrix between two sequences of space time symbols $\boldsymbol{X}$ and $\hat{\boldsymbol{X}}$:

$$\boldsymbol{B}\left(\boldsymbol{X},\hat{\boldsymbol{X}}\right)=\boldsymbol{X}-\hat{\boldsymbol{X}}=\begin{bmatrix} x_1^1-\hat{x}_1^1 & x_2^1-\hat{x}_2^1 & \dots & x_L^1-\hat{x}_L^1 \\ x_1^2-\hat{x}_1^2 & x_2^2-\hat{x}_2^2 & \dots & x_L^2-\hat{x}_L^2 \\ \vdots & \vdots & \ddots & \vdots \\ x_1^{N_T}-\hat{x}_1^{N_T} & x_2^{N_T}-\hat{x}_2^{N_T} & \dots & x_L^{N_T}-\hat{x}_L^{N_T} \end{bmatrix} \tag{3.18}$$

Now the matrix $\boldsymbol{A}$, called as distance matrix with $N_T \times N_T$ dimension, can be constructed as [15], [16]

$$\boldsymbol{A}\left(\boldsymbol{X},\hat{\boldsymbol{X}}\right)=\boldsymbol{B}\left(\boldsymbol{X},\hat{\boldsymbol{X}}\right).\boldsymbol{B}^{\dagger}\left(\boldsymbol{X},\hat{\boldsymbol{X}}\right) \tag{3.19}$$

where $(\cdot)^{\dagger}$ denotes the conjugate transpose.

If we denote r_A as the rank of matrix $\boldsymbol{A}$, then matrix $\boldsymbol{A}$ contains exactly $N_T - r_A$ zero eigenvalues λ_i. At high SNR, the upper bound on PEP becomes:

$$P(\boldsymbol{X},\hat{\boldsymbol{X}}) \le \left[\underbrace{\left(\prod_{i=1}^{r_A} \lambda_i \right)^{\frac{1}{r_A}}}_{\text{Coding gain}} \frac{E_s}{4N_0} \right]^{\underbrace{-r_A N_R}_{\text{Diversity order}}} \tag{3.20}$$

Detail is deferred to Appendix-A

Note that in case of slow fading channel the diversity order of the system is equivalent to $r_A N_R$. The matrix $\boldsymbol{B} = \boldsymbol{X} - \hat{\boldsymbol{X}}$ has the same rank r_A as that of matrix $\boldsymbol{A}$. Furthermore, the coding gain (independent of SNR) is determined by the r_A order root of the product of nonzero eigenvalues λ_i of $\boldsymbol{A}$. In case if $r_A = N_T$, the product of eigenvalues $\prod_{i=1}^{r_A} \lambda_i$ is also equivalent to determinant of matrix $\boldsymbol{A}$.

3.3.2 Fast fading channels

In case of fast fading channel, the channel fading coefficients $h_{j,i}^{t}$ varies from one symbol to other. Let $d_H(\boldsymbol{X},\hat{\boldsymbol{X}})$ be the Hamming distance between two sequences $\boldsymbol{X}$ and $\hat{\boldsymbol{X}}$ of length L.

$$d_H(\boldsymbol{X},\hat{\boldsymbol{X}}) = \sum_{t=1}^{L} h(\boldsymbol{x}_t,\hat{\boldsymbol{x}}_t) \tag{3.21}$$

where h is defined as

$$h(\boldsymbol{x}_t,\hat{\boldsymbol{x}}_t) = \begin{cases} 0 & \text{if } \boldsymbol{x}_t = \hat{\boldsymbol{x}}_t \\ 1 & \text{otherwise} \end{cases} \tag{3.22}$$

Furthermore, note that the product distance d_P^2 is defined as to be the Euclidean product distance between space time symbols of two sequences of length L when these symbols are different. So the product distance can be written as

$$d_p^2(\boldsymbol{X},\hat{\boldsymbol{X}}) = \prod_{\substack{t=1 \\ x_t \neq \hat{x}_t}}^{L} d_E^2(\boldsymbol{x}_t,\hat{\boldsymbol{x}}_t) = \prod_{\substack{t=1 \\ x_t \neq \hat{x}_t}}^{L} \left(\sum_{i=1}^{N_T} \left| x_t^i - \hat{x}_t^i \right|^2 \right) \tag{3.23}$$

At high SNR, the error probability bound can be simplified as (for proof see Appendix-B)

$$P(\boldsymbol{X},\hat{\boldsymbol{X}}) \leq \left[\underbrace{\left(d_p^2(\boldsymbol{X},\hat{\boldsymbol{X}}) \right)^{1/d_H(\boldsymbol{X},\hat{\boldsymbol{X}})}}_{\text{Coding gain}} \frac{E_s}{4N_0} \right]^{\overbrace{-d_H(\boldsymbol{X},\hat{\boldsymbol{X}})N_R}^{\text{Diversity order}}} \tag{3.24}$$

The term $d_H(\boldsymbol{X},\hat{\boldsymbol{X}})N_R$ is the diversity gain of the system obtained over Rayleigh fast fading channel. The coding gain (independent of SNR) is determined by the $d_H(\boldsymbol{X},\hat{\boldsymbol{X}})$ order root of the product distance $d_P^2(\boldsymbol{X},\hat{\boldsymbol{X}})$.

3.4 Space-time code design criteria

3.4.1 Rank and determinant criteria

Taking into account the error rates, as discussed above, Tarokh et al. [35] developed two criteria for analysing the performance of the codes by optimizing the probability of error in a slow fading channel. The two criteria are, rank and determinant criteria.

From rank criterion, we determine maximum diversity of the code. In section (3.3.1) in case of slow fading channel we showed that the diversity factor depends the product of the minimum rank and the number of receive antennas, $r_A N_R$. Hence to maximize the diversity order means that the space time code $\boldsymbol{A}(\boldsymbol{X}, \hat{\boldsymbol{X}})$ should be of full rank, *i.e.* $r_A = N_T$. Note that the difference matrix $\boldsymbol{B}$ has also same rank r_A as that of matrix $\boldsymbol{A}$. In addition, to minimize the error probability, the minimum product of nonzero eigenvalues $\prod_{i=1}^{r} \lambda i$ of matrix $\boldsymbol{A}(\boldsymbol{X}, \hat{\boldsymbol{X}})$ along the pairs of codewords with the minimum rank should be maximized.

Similarly, with assumption that the matrix $\boldsymbol{A}(\boldsymbol{X}, \hat{\boldsymbol{X}})$ is of full rank, the product of the nonzero eigenvalues $\prod_{i=1}^{r} \lambda i$ or equivalently the determinant of the matrix $\boldsymbol{A}(\boldsymbol{X}, \hat{\boldsymbol{X}})$ will help us to maximize the coding gain of the code.

Note that $\prod_{i=1}^{r} \lambda i$ is the absolute value of the sum of determinants of all the principal $r_A \times r_A$ cofactors of matrix $\boldsymbol{A}(\boldsymbol{X}, \hat{\boldsymbol{X}})$ [16].

The two criteria for slow Rayleigh fading channels can be summarized as follow:

- **Rank criteria:** The matrix $\boldsymbol{B}(\boldsymbol{X}, \hat{\boldsymbol{X}})$ should be of full rank for all pair of possible sequences of symbols $\boldsymbol{X}$ and $\hat{\boldsymbol{X}}$. In this way a maximum diversity of $N_T N_R$ can be achieved.
- **Determinant criteria:** For a maximum diversity code, the minimum determinant of the matrix $\boldsymbol{A}(\boldsymbol{X}, \hat{\boldsymbol{X}})$ calculated over all possible sequences of symbol $\boldsymbol{X}$ and $\hat{\boldsymbol{X}}$ should be maximize. Denoting this parameter by $\det_{min}(\boldsymbol{A})$, the error probability (3.20) for slow fading channel, can be simplified as

$$P(\boldsymbol{X},\hat{\boldsymbol{X}}) \le \left[\left(\det_{\min}(\boldsymbol{A}) \right)^{1/N_T} \frac{E_s}{4N_0} \right]^{-N_T N_R} \tag{3.25}$$

3.4.2 Hamming and product distance criteria

In (3.24) it was shown that code diversity depends on the product of number of receive antennas and hamming distance $d_H(\boldsymbol{X},\hat{\boldsymbol{X}})$ between the sequence $\boldsymbol{X}$ and $\hat{\boldsymbol{X}}$. Therefore to maximize the diversity, one must maximize the distances between all possible sequences $\boldsymbol{X}$ and $\hat{\boldsymbol{X}}$. Another factor to be kept in mind while designing space time codes is the coding gain which also needs to be maximized, can be determined by the product distance $d_p^2(\boldsymbol{X},\hat{\boldsymbol{X}})$.

Shortly, the space-time codes design criteria for fast fading as proposed by Tarokh [35] is summarized as follow:

- **Distance criteria:** The minimum Hamming distance $d_H(\boldsymbol{X},\hat{\boldsymbol{X}})$ between any two sequences of symbols $\boldsymbol{X}$ and $\hat{\boldsymbol{X}}$ should be maximized.
- **Product distance criteria:** The minimum product distance $d_p^2(\boldsymbol{X},\hat{\boldsymbol{X}})$ between any two sequences of symbols $\boldsymbol{X}$ and $\hat{\boldsymbol{X}}$ should be maximized. If we denote the minimum product distance by $d_{p_{\min}}^2(\boldsymbol{X},\hat{\boldsymbol{X}})$, then PEP can be written as [36]

$$P(\boldsymbol{X},\hat{\boldsymbol{X}}) \le \left[\left(d_{P_{\min}}^2(\boldsymbol{X},\hat{\boldsymbol{X}}) \right)^{1/d_{H_{\min}}(\mathbf{X},\hat{\mathbf{X}})} \frac{E_s}{4N_0} \right]^{-d_{H_{\min}}(\boldsymbol{X},\hat{\boldsymbol{X}})N_R} \tag{3.26}$$

One can see that increasing the number of receive antennas may help to alleviate the probability of error.

3.4.3 Trace criteria

Trace is another important parameter in designing powerful space time codes. In fact the sum of all eigenvalues of a square matrix equal to the sum of all the elements on the main diagonal, which is called the *trace of the matrix*, and is given by [38].

$$tr\left(\boldsymbol{A}\left(\boldsymbol{X},\hat{\boldsymbol{X}}\right)\right)=\sum_{i=1}^{r_A}\lambda_i=\sum_{i=1}^{N_T}A^{i,i} \tag{3.27}$$

where $A^{i,i}$ are the elements on the main diagonal of matrix $\boldsymbol{A}(\boldsymbol{X},\hat{\boldsymbol{X}})$. Since

$$A^{i,j}=\sum_{t=1}^{L}(x_t^i-\hat{x}_t^i)(x_t^j-\hat{x}_t^j)^* \tag{3.28}$$

Substituting (3.28) into (3.27), we get

$$tr\left(\boldsymbol{A}\left(\boldsymbol{X},\hat{\boldsymbol{X}}\right)\right)=\sum_{i=1}^{N_T}\sum_{t=1}^{L}\left|x_i^t-\hat{x}_i^t\right|^2 \tag{3.29}$$

(3.29) shows that the trace of matrix $\boldsymbol{A}(\boldsymbol{X},\hat{\boldsymbol{X}})$ is equivalent to the squared Euclidean distance between the codewords $\boldsymbol{X}$ and $\hat{\boldsymbol{X}}$, *i.e.*

$$tr\left(\boldsymbol{A}\left(\boldsymbol{X},\hat{\boldsymbol{X}}\right)\right)=\sum_{i=1}^{r_A}A_{ii}=\sum_{i=1}^{r_A}\sum_{t=1}^{L}\left|x_i^t-\hat{x}_i^t\right|^2=\sum_{t=1}^{L}d_E^2\left(\boldsymbol{x}_t,\hat{\boldsymbol{x}}_t\right) \tag{3.30}$$

Detail are deferred to Appendix-C

We summarize the trace criteria as follow:

- **Trace criteria :** For a large number of antennas, typically $N_TN_R\geq 4$, the minimum trace of the matrices $\boldsymbol{A}(\boldsymbol{X},\hat{\boldsymbol{X}})$ among all possible sequences of symbols $\boldsymbol{X}$ and $\hat{\boldsymbol{X}}$ should be maximized.

Here one can see that this criteria does not depend the type of channel, *viz* fast fading or slow fading channels, then the hypothesis are used for elimination the attenuation coefficient of the channel. Note that the term $\sum_{i=1}^{N_T}\left|x_i^t-\hat{x}_i^t\right|^2=d_E^2\left(x_t-\hat{x}_t\right)$ in (3.30) can also be found in the formula of product distance (3.23). So we can say that the codes having large trace may also have large product distance, and can offer a good performance over fast fading channels.

3.5 Space time block codes

In space time block coding system, the modulated symbols are split into packets of P size, and regrouped into an $N_T \times P$ coding matrix $\boldsymbol{X}$, where N_T is the number of transmit antennas. The first Space Time Block Code (STBC) is the well known Alamouti code [34]. This code has two transmit antennas and may have one or more than one receiver antennas. Symbols are transmitted in orthogonal blocks. In following subsections we study in detail the structure of Alamouti code, and present some other orthogonal and non-orthogonal STBCs.

3.5.1 Orthogonal space time block codes

In this section we study the design of STBCs having N_T transmit antennas and N_R receive antennas. Orthogonal codes achieve maximum diversity of $N_R N_T$, maximum coding gain, and highest possible throughput [35]. In 1998 Alamouti [34] developed such an Orthogonal Space Time Block Code (OSTBC) with two transmit antennas.

In what follows, we discuss in more detail different types of orthogonal space time coding system.

3.5.1.1 Alamouti code

The Alamouti code [34] is historically the first and the most well-known space-time code which provides full transmit diversity for a system with two transmit antennas. It is also well known for its simple structure and fast ML decoding.

We consider a modulation signal constellation S having 2^m points. At each time interval, the binary signal encoder takes m bits of source information to generate a complex system $x_i \in S$.

For example in case of Q-PSK constellation, in each symbol interval, the encoder takes 2 bits of source information to generate a complex system x_i belonging to $(1, j, -1, -j)$

Then in each encoding operation, the ST encoder takes a block of two modulated symbols x_1 and x_2 and maps them to two transmit antennas according to following codeword matrix.

$$\boldsymbol{X} = \begin{bmatrix} x_1 & -x_2^* \\ x_2 & x_1^* \end{bmatrix} \tag{3.31}$$

The encoders outputs are transmitted in two consecutive transmission period from two transmit antennas. During the first transmission period, two signals x_1 and x_2 are transmitted simultaneously from antenna one and two respectively. In second transmission period, $-x_2^*$ is transmitted from antenna one and x_1^* from antenna two.

It is easy to see that the two columns/rows of $\boldsymbol{X}$ are orthogonal. This design scheme is also called the 2×2 orthogonal design. Further more, with the power constraints $|x_1|^2+|x_2|^2=1$, $\boldsymbol{X}$ is actually a unitary matrix with determinant 1.

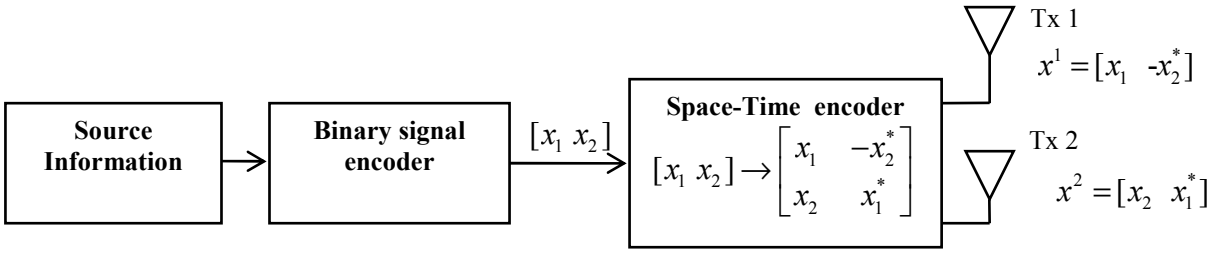

Figure 3.2 Alamouti transmit scheme

In other words, the code matrix has the property

$$\boldsymbol{X}.\boldsymbol{X}^{\dagger}=\begin{bmatrix} |x_1|^2+|x_2|^2 & 0 \\ 0 & |x_1|^2+|x_2|^2 \end{bmatrix}$$
$$=\left(|x_1|^2+|x_2|^2\right)\boldsymbol{I}_2 \qquad (3.32)$$

where I_2 is 2×2 identity matrix, and $(\cdot)^{\dagger}$ is the Hermitian transpose.

3.5.1.2 Simple decoding

The Alamouti scheme is applicable for a system with two transmit and N_R receive antennas. We assume that the channel fading coefficients are constant during the transmission of a block of two symbols.

Let $r_{j,1}$ and $r_{j,2}$ be the signals received by receiving antenna j at time t and $t+T$ respectively.

where, T denotes the symbol duration. So we have

$$r_{j,1} = h_{j,1}.x_1 + h_{j,2}.x_2 + n_{j,1}$$
$$r_{j,2} = -h_{j,1}.x_2^* + h_{j,2}.x_1^* + n_{j,2} \quad (3.33)$$

where $h_{j,i}$, i=1,2 and j=1,2,……,N_R is the channel fading coefficient from transmit antenna i to receiving antenna j and $n_{j,1}$, $n_{j,2}$ are the AWGN from receiving antenna j during time instant t and t+T, respectively. Equation (3.33) can be written in matrix form as

$$\boldsymbol{r}_j = \begin{bmatrix} r_{j,1} & r_{j,2} \end{bmatrix} = \begin{bmatrix} h_{j,1} & h_{j,2} \end{bmatrix} \begin{bmatrix} x_1 & -x_2^* \\ x_2 & x_1^* \end{bmatrix} + \begin{bmatrix} n_{j,1} & n_{j,2} \end{bmatrix} \quad (3.34)$$

Note that

$$r_{j,2}^* = h_{j,2}^*.x_1 - h_{j,1}^*.x_2 + n_{j,2}^* \quad (3.35)$$

Equivalently we can write as

$$\boldsymbol{r}_j' = \begin{bmatrix} r_{j,1} \\ r_{j,2}^* \end{bmatrix} = \begin{bmatrix} h_{j,1} & h_{j,2} \\ h_{j,2}^* & -h_{j,1}^* \end{bmatrix} \cdot \begin{bmatrix} x_1 \\ x_2 \end{bmatrix} + \begin{bmatrix} n_{j,1} \\ n_{j,2}^* \end{bmatrix}$$

$$\boldsymbol{r}_j' = \boldsymbol{H} \cdot \boldsymbol{x} + \boldsymbol{N} \quad (3.36)$$

Multiplying (3.36) by $\boldsymbol{H}^\dagger$ on left, we get

$$\boldsymbol{H}^\dagger.\boldsymbol{r}_j' = \boldsymbol{H}^\dagger \boldsymbol{H}.\boldsymbol{x} + N$$
$$= \left(\left| h_{j,1} \right|^2 + \left| h_{j,2} \right|^2 \right).\boldsymbol{x} + N \quad (3.37)$$

Assume that all the signals in the modulation constellation are equiprobable, a maximum likelihood decoder choose a pair of signal $\hat{x}_1$ and $\hat{x}_2$ from the signal modulation constellation to minimize the distance metric

$$\hat{\boldsymbol{x}} = \begin{bmatrix} \hat{x}_1 \\ \hat{x}_2 \end{bmatrix} = \underset{\boldsymbol{x} \in S^2}{\operatorname{argmin}} \left(\sum_{j=1}^{N_R} \left\| \tilde{r}_{j,1} - \left(\left| h_{j,1} \right|^2 + \left| h_{j,2} \right|^2 \right) . \boldsymbol{x} \right\|^2 \right) \tag{3.38}$$

where $\tilde{\boldsymbol{r}}_j = \boldsymbol{H}^{\dagger} . \boldsymbol{r}_j'$

Considering a memoryless source information, the modulated symbols x_1 and x_2 are independent to each other, we can separately decode each of the symbols by calculating

$$\hat{\boldsymbol{x}} = \begin{bmatrix} \hat{x}_1 \\ \hat{x}_2 \end{bmatrix} = \begin{bmatrix} \underset{x \in S}{\operatorname{argmin}} \left(\sum_{j=1}^{N_R} \left| \tilde{r}_{j,1} - \left(\left| h_{j,1} \right|^2 + \left| h_{j,2} \right|^2 \right) . x_1 \right|^2 \right) \\ \underset{x \in S}{\operatorname{argmin}} \left(\sum_{j=1}^{N_R} \left| \tilde{r}_{j,2} - \left(\left| h_{j,1} \right|^2 + \left| h_{j,2} \right|^2 \right) . x_2 \right|^2 \right) \end{bmatrix} \tag{3.39}$$

3.5.1.3 Performance of Alamouti code

Due to the orthogonality between the sequences transmitted from the two transmit antennas, the Alamouti encoding scheme can achieve a gain of maximum diversity equal to $N_T.N_R = 2N_R$. Let us consider any two distinct code sequences $\boldsymbol{X}$ and $\boldsymbol{X}'$ generated by the inputs (x_1, x_2) and (x_1', x_2'), respectively, where $(x_1, x_2) \neq (x_1', x_2')$. So the codeword difference matrix $\boldsymbol{B}$ is given by

$$\boldsymbol{B}(\boldsymbol{X}, \boldsymbol{X}') = \begin{bmatrix} x_1 - x_1' & -x_2^* + x_2^* \\ x_2 - x_2' & x_1^* - x_1'^* \end{bmatrix} \tag{3.40}$$

Since the rows of the codeword matrix $\boldsymbol{X}$ are orthogonal, the rows of the codeword difference matrix $\boldsymbol{B}$ are also orthogonal. The distance matrix $\boldsymbol{A}$ is given by

$$\boldsymbol{A}(\boldsymbol{X},\boldsymbol{X}') = \boldsymbol{B}(\boldsymbol{X},\boldsymbol{X}').\boldsymbol{B}^{\dagger}(\boldsymbol{X},\boldsymbol{X}') = \begin{bmatrix} |x_1 - x_1'|^2 + |x_2 - x_2'|^2 & 0 \\ 0 & |x_1 - x_1'|^2 + |x_2 - x_2'|^2 \end{bmatrix} \quad (3.41)$$

Since $(x_1, x_2) \neq (x_1', x_2')$, it is clear that the distance matrix $\boldsymbol{A}$ is full rank equal to two. In other words, the Alamouti scheme can achieve a gain of maximum diversity of $N_T.N_R = 2N_R$. The determinant of difference matrix $\boldsymbol{A}$ is given by

$$\det \boldsymbol{A}(\boldsymbol{X},\boldsymbol{X}') = (|x_1 - x_1'|^2 + |x_2 - x_2'|^2)^2 \quad (3.42)$$

It is obvious from distance matrix (3.41) that for the Alamouti scheme, the codeword distance matrix has two identical eigenvalues. These common eigenvalues $\lambda_1 = \lambda_2 = \left(\det \boldsymbol{A}(\boldsymbol{X},\boldsymbol{X})\right)^{1/2}$ is equal to the minimum squared Euclidean distance of the signal constellation. This implies that for the Alamouti scheme, the minimum distance between any two transmitted code sequences remains the same as in the uncoded system. Therefore, the Alamouti scheme does not provide any coding gain relative to the uncoded modulation scheme, *i.e.*

$$G_c = \frac{(\lambda_1\lambda_2)^{1/2}}{d_u^2} = 1 \quad (3.43)$$

The performance of the Alamouti code on slow Rayleigh fading channels is evaluated by simulation in figure 3.3. One receive antenna and a system of Q-PSK constellation is taken into account for the simulation. We further assumed that fading from each transmit antenna to each receive antenna is mutually independent and that the receiver has the perfect knowledge of the channel coefficients.

One can see from the figure that the performance of Alamouti code with two transit antennas is better than that with a single transmit antenna. At a BER of 10^{-3} the Alamouti code outperform by a gain of about 11dB.

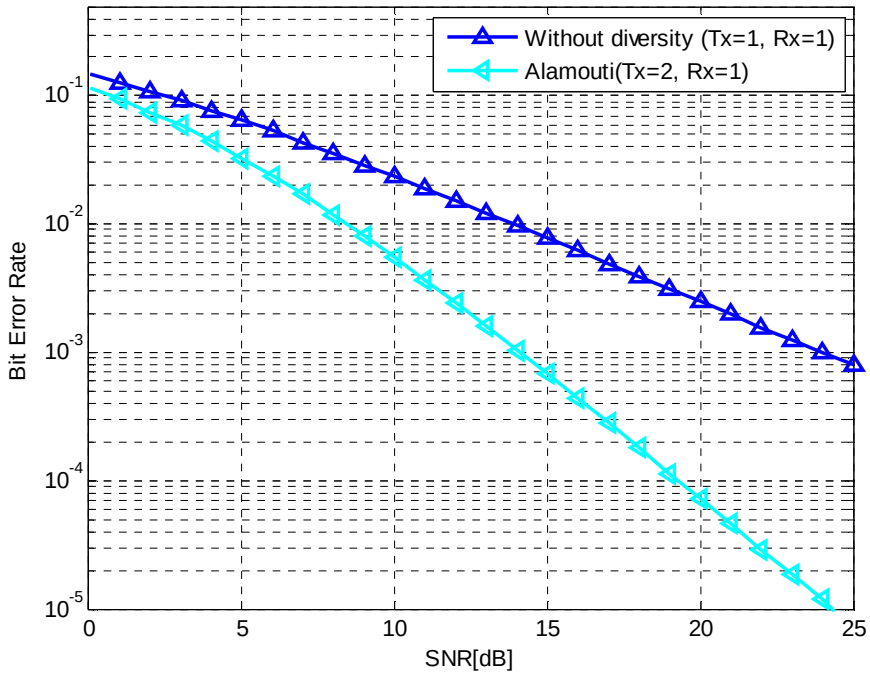

Figure 3.3 Performance of Alamouti code

To conclude our discussion on Alamouti code, we can say that Alamouti code has two important properties.

- **Simple decoding:** Each modulated symbol can be decoded separately by simple maximum likelihood decoder.
- **Maximum diversity:** The Alamouti code satisfies rank criteria, hence may offer a maximum diversity gain.

3.5.2 Extended orthogonal STBCs

The key of success of Alamouti code lies in the property of its orthogonality between the sequences of signals transmitted from two transmit antennas. In [35] the scheme of encoding of orthogonal design was generalized for any number of transmit antennas by compromising with the code rate. In [37] it was proved that rate one codes do not exist for generalized complex orthogonal designs. However recently some authors have proved that it is possible to construct rate one code irrespective of number of transmit antennas or input alphabet size at the cost of decoding complexity and/or diversity order. We talk in more detail about such codes in forthcoming sections.

3.5.2.1 STBC encoder

Figure 3.4 represents the structure of a STBC encoder. In general a STBC is defined by an $N_T \times P$ transmission matrix $\boldsymbol{X}$. Where N_T represents the number of transmit antennas and P represents the number of time periods for transmission of one block of coded symbols.

We assume that the signal constellation consists of 2^m points. In each encoding operation, a block of Km information bits are mapped into the signal constellation to select K modulated signals $x_1, x_2, ..., x_K$, where each group of m bits selects a constellation signal.

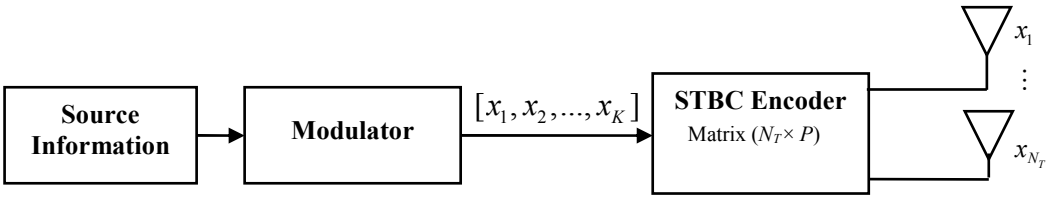

Figure 3.4 STBC encoder

The K modulated signals are encoded by a STBC encoder to generate N_T parallel signal sequences of length P according to the transmission matrix $\boldsymbol{X}$. These sequences are transmitted simultaneously through N_T transmit antennas in P time periods. In STB coding system, the number of symbols the encoder takes as its input in each encoding operation is K. The number of transmission periods required to transmit the space-time coded symbols through the multiple transmit antennas is P. In other words, there are P space-time symbols transmitted from each antennas for each block of K input symbols.

The rate of a STBC is defined as the ratio between the number of symbols the encoder takes as its input and the number of space-time coded symbols transmitted from each antenna. It is given by

$$R = \frac{K}{P} \tag{3.44}$$

The spectral efficiency of the STBC is given by

$$\eta = \frac{Km}{P} \text{ bits/s/Hz} \tag{3.45}$$

or more precisely

$$\eta = \frac{r_b}{B} = \frac{r_s m R}{r_s} = \frac{Km}{P} \tag{3.46}$$

where r_b and r_s are bit and symbol rates, respectively and B is the bandwidth.

The elements of the codeword matrix $\boldsymbol{X}$ are linear combination of K modulated symbols $x_1, x_2, ..., x_K$ and their conjugates $x_1^*, x_2^*, ..., x_K^*$. In order to achieve the maximum diversity of N_T, the transmission matrix $\boldsymbol{X}$ is constructed based on orthogonal designs such that [35].

$$\boldsymbol{X} \cdot \boldsymbol{X}^{\dagger} = c\left(|x_1|^2 + |x_2|^2 + \cdots + |x_K|^2\right)\boldsymbol{I}_{N_T} \tag{3.47}$$

where c is a constant.

The i-th row of $\boldsymbol{X}$ represents the symbols transmitted from the i-th transmit antenna consecutively in P transmission periods, while the j-th column of $\boldsymbol{X}$ represents the symbols transmitted simultaneously through N_T transmit antennas at time j.

Note that orthogonal designs are applied to construct STBC. The rows of the transmission matrix $\boldsymbol{X}$ are orthogonal to each other. This means that in each block, the signal sequences from any two transmit antennas are orthogonal. For example, if we assume that $x_i = (x_{i,1}, x_{i,2}, ...x_{i,p}) \in \mathbb{C}_{1\times P}$ is the transmitted sequence from the i-th antenna, i =1,2,…., N_T, we get

$$< \boldsymbol{x}_i \cdot \boldsymbol{x}_j >= \sum_{t=1}^{P} x_{i,t} \cdot x_{j,t}^* = 0, \quad i \neq j, \quad i, j \in \{1, 2, ..., N_T\} \tag{3.48}$$

where, $x_i . x_j$ shows the inner product of the sequences x_i and x_j. This condition of orthogonality (3.48) enables us to have a communication system with maximum transmit diversity for a given number of transmit antennas. In addition, it allows the receiver to decouple the signals transmitted from different antennas by simple ML decoder, based on linear processing of the received signals.

Based on type of signal constellation, STBCs can be classified into STBCs with real signals and STBCs with complex signals.

3.5.2.2 STBCs for real signal constellations

An OSTBC is said to be real if all its coefficients in matrix $\boldsymbol{X}$ are real. *i.e.*

$$\boldsymbol{X} \cdot \boldsymbol{X}^{\dagger} = c\left(x_1^2 + x_2^2 + \ldots\ldots + x_k^2\right)\boldsymbol{I}_{N_T} \tag{3.49}$$

where $x_k \in \mathbb{R}$ with $1 \le k \le K$ and $c \in \mathbb{R}$

Let $\boldsymbol{X}_{N_T}$ denote the codeword matrix $\boldsymbol{X}$ having N_T transmit antennas. For sake of simplicity we consider STBCs with a square matrices *i.e.* $P = N_T$. An OSTBC with minimum possible block length P and corresponding STBC is called delay-optimal [35].

For any arbitrary real signals constellation, such as M-ASK, space-time block codes with $N_T \times N_T$ square transmission matrix $\boldsymbol{X}_{N_T}$ exist if and only if the number of transmit antennas N_T = 2, 4, or 8 [35]. These codes are of full rate R = 1 and offer the full transmit diversity of N_T. The transmission matrices are given by [16]

$$\boldsymbol{X}_2 = \begin{bmatrix} x_1 & -x_2 \\ x_2 & x_1 \end{bmatrix} \tag{3.50}$$

For N_T = 2 transmit antennas

$$\boldsymbol{X}_4 = \begin{bmatrix} x_1 & -x_2 & -x_3 & -x_4 \\ x_2 & x_1 & x_4 & -x_3 \\ x_3 & -x_4 & x_1 & x_2 \\ x_4 & x_3 & -x_2 & x_1 \end{bmatrix} \tag{3.51}$$

For N_T = 4 transmit antennas

$$\boldsymbol{X}_8 = \begin{bmatrix} x_1 & -x_2 & -x_3 & -x_4 & -x_5 & -x_6 & -x_7 & -x_8 \\ x_2 & x_1 & -x_4 & x_3 & -x_6 & x_5 & x_8 & -x_7 \\ x_3 & x_4 & x_1 & -x_2 & -x_7 & -x_8 & x_5 & x_6 \\ x_4 & -x_3 & x_2 & x_1 & -x_8 & x_7 & -x_6 & x_5 \\ x_5 & x_6 & x_7 & x_8 & x_1 & -x_2 & -x_3 & -x_4 \\ x_6 & -x_5 & x_8 & -x_7 & x_2 & x_1 & x_4 & -x_3 \\ x_7 & -x_8 & -x_5 & x_6 & x_3 & -x_4 & x_1 & x_2 \\ x_8 & x_7 & -x_6 & -x_5 & x_4 & x_3 & -x_2 & x_1 \end{bmatrix} \tag{3.52}$$

For N_T = 8 transmit antennas.

It is desirable to construct full rate code $R=1$ transmission schemes for any number of transmit antennas, since full rate codes are bandwidth efficient. In general, for N_T transmit antenna, the minimum value of transmission periods P to achieve the full rate is given by [16]

$$P = \min(2^{4c+d}) \tag{3.53}$$

where the minimization is taken over the set

$$0 \le c \qquad 0 \le d \le 4 \qquad \text{and } 8c+2d \ge N_T$$

For $N_T \le 8$, the minimum values of P are given in table 3.1

Table 3.1 (values of P for different N_T)

N_T	2	3	4	5	6	7	8
P	2	4	4	8	8	8	8

These values provide guidelines to construct full rate STBCs. A full rate and full diversity space time block code for 3 transmit antennas is

$$\boldsymbol{X}_3 = \begin{bmatrix} x_1 & -x_2 & -x_3 & -x_4 \\ x_2 & x_1 & x_4 & -x_3 \\ x_3 & -x_4 & x_1 & x_2 \end{bmatrix} \tag{3.54}$$

3.5.2.3 STBCs for complex signal constellations

An orthogonal space time block code is said to be complex if certain coefficients of matrix $\boldsymbol{X}$ are complex. *i.e.*

$$\boldsymbol{X} \cdot \boldsymbol{X}^{\dagger} = c\left(|x_1|^2 + |x_2|^2 + \cdots + |x_K|^2\right)\boldsymbol{I}_{N_T} \tag{3.55}$$

where $x_k \in \mathbb{C}$ with $1 \le k \le K$ and $c \in \mathbb{R}$

The Alamouti code is unique STBC with an $N_T \times N_T$ complex transmission matrix to achieve the full rate [38]. If the number of the transmit antennas is larger than two, the code design goal is to construct high rate complex transmission matrices with low decoding complexity

that achieve full diversity. In addition, similar to real orthogonal designs, the value of P must be minimized in order to minimize the decoding delay.

For an arbitrary complex signal constellation, there are STBCs that can achieve a rate of 1/2 for any given number of transmit antennas. Following are two OSTBCs complex matrices which could attain a maximum rate of 3/4 [35].

$$\boldsymbol{X}=\begin{bmatrix} x_1 & -x_2^* & \frac{x_3^*}{\sqrt{2}} & \frac{x_3^*}{\sqrt{2}} \\ x_2 & x_1^* & \frac{x_3^*}{\sqrt{2}} & -\frac{x_3^*}{\sqrt{2}} \\ \frac{x_3}{\sqrt{2}} & \frac{x_3}{\sqrt{2}} & \frac{(-x_1-x_1^*+x_2-x_2^*)}{2} & \frac{(x_1-x_1^*+x_2+x_2^*)}{2} \end{bmatrix} \tag{3.56}$$

$$\boldsymbol{X}=\begin{bmatrix} x_1 & -x_2^* & \frac{x_3^*}{\sqrt{2}} & \frac{x_3^*}{\sqrt{2}} \\ x_2 & x_1^* & \frac{x_3^*}{\sqrt{2}} & -\frac{x_3^*}{\sqrt{2}} \\ \frac{x_3}{\sqrt{2}} & \frac{x_3}{\sqrt{2}} & \frac{(-x_1-x_1^*+x_2-x_2^*)}{2} & \frac{(x_1-x_1^*+x_2+x_2^*)}{2} \\ \frac{x_3}{\sqrt{2}} & \frac{-x_3}{\sqrt{2}} & \frac{(x_1-x_1^*-x_2-x_2^*)}{2} & \frac{(-x_1-x_1^*-x_2+x_2^*)}{2} \end{bmatrix} \tag{3.57}$$

Another example of rate 3/4 space-time block code with three transmit antennas over complex signal constellations given in [39] is:

$$\boldsymbol{X}=\begin{bmatrix} x_1 & x_2^* & x_3^* & 0 \\ -x_2 & x_1^* & 0 & -x_3^* \\ -x_3 & 0 & x_1^* & x_2^* \end{bmatrix} \tag{3.58}$$

As mentioned above that rate 1/2 codes exist for any number of transmit antennas [35], such a code is given below for three transmit antennas.

$$\boldsymbol{X}=\begin{bmatrix} x_1 & -x_2 & -x_3 & -x_4 & x_1^* & -x_2^* & -x_3^* & -x_4^* \\ x_2 & x_1 & x_4 & -x_3 & x_2^* & x_1^* & x_4^* & -x_3^* \\ x_3 & -x_4 & x_1 & x_2 & x_3^* & -x_4^* & x_1^* & x_2^* \end{bmatrix} \tag{3.59}$$

Table 3.2 provides maximum possible code rates for complex orthogonal design for different transmit antennas.

Table 3.2 (Possible code rates wrt to number of transmit antennas)

No. of transmit antennas (N_t)	**Symbols (K)**	**Block length (P)**	**Rate (K/P)**
$N_T = 2$	2	2	1
$N_T = 3$	3	4	3/4
$N_T = 4$	6	8	3/4
$N_T = 5$	10	15	2/3
$N_T = 6$	20	30	2/3
$N_T = 7$	35	56	5/8
$N_T = 8$	70	112	5/8
$N_T = 9$	126	210	3/5
$N_T = 10$	252	420	3/5
$N_T = 11$	462	792	7/12
$N_T = 12$	924	1584	7/12
$N_T = 13$	1716	3003	4/7
$N_T = 14$	3432	6006	4/7
$N_T = 15$	6435	11440	9/16
$N_T = 16$	12870	22880	9/16
$N_T = 17$	24310	43758	5/9
$N_T = 18$	48620	87516	5/9

In [40], the authors developed an algorithm for systematic construction of high rate complex OSTBCs for any number of transmit antennas.

3.5.2.4 Performance of STBCs

The performances of different space time block codes given in (3.31, 3.56 ,3.57) over fast Rayleigh fading channel are shown in figure 3.5, using a single receive antenna. To have same spectral efficiency of 3 bits/s/Hz, we use 8-PSK modulation for a code with 2 transmit

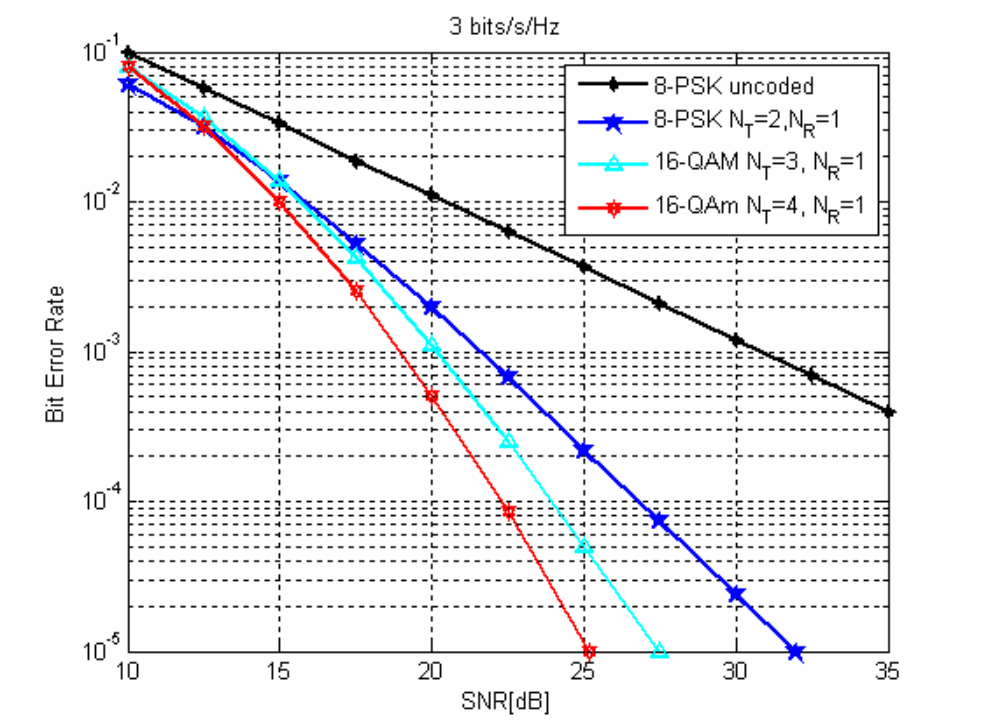

Figure 3.5 Performance of OSTBC with a spectral efficiency of 3 bits/s/Hz in slow fading channel

antennas and 16-QAM modulation is used for code rate of 3/4 for three and four transmit antennas. At a BER of 10^{-5}, the code with four antennas obtains a gain of about 7dB and 4.5 dB as compare to the codes with two and three antennas, respectively. The simulation results show that increasing the number of transmit antennas can provide a significant performance gain. The increase in decoding complexity for STBCs with a large number of transmit antennas is very little due to the fact that only linear processing is required for decoding.

3.5.2.5 Efficiency bound limit of OSTBCs

From above discussion, we observed that the maximum code rate for complex signal constellation is possible only in case of two transmit antennas. In case where we have more than two transmit antennas, it has been proved in [41] that the maximum rate for a square

matrix is 3/4. Xue-Bin in [37] has also proved that the maximum rate for any STBC with N_T transmit is

$$R_{\max} = \frac{n_0 + 1}{2n_0} \tag{3.60}$$

where $n_0 = \left\lceil \frac{N_T + 1}{2} \right\rceil$

In general, we always try to construct a code having maximum rate. As these codes have a longer block length P, so this is not practically possible that the receiver should wait until the end of transmission of P symbols to start decoding. In other words larger block length increases the receiver delay time. For example a particular OSTBC having a rate of 9/16 for 16 transmit enumerated in table 3.2 has a block length of 22880.

In the following section, we see that relaxing the constraint of orthogonality of the codes, we can get STBCs with better rate at the cost of diversity order.

3.5.3 Quasi-orthogonal STBCs

The main characteristics of an orthogonal design are their simple separate decoding, full rate and full diversity. But unfortunately one can not have all these three properties for more than two transmit antennas scheme. Therefore in a system with more than two transmit antennas, we have to sacrifice one or the other of these nice characteristics. Quasi Orthogonal Space-Time Block Codes (QOSTBCs) introduced by Jaffarkhani [42], is a class of STBC which offers full rate at the cost of decoding complexity. In QOSTBCs decoding is done independently in pairs of symbols.

Here we lay down the basic idea of Jaffarkhani for constructing a code for four transmit antennas using the code structure of Alamouti. We consider the transmission of a block having four symbols, x_1, x_2, x_3 and x_4. We use a pattern very like that of Alamouti for encoding these four symbols in pair, and we get following two generator matrices.

$$\boldsymbol{X}_{12} = \begin{bmatrix} x_1 & -x_2^* \\ x_2 & x_1^* \end{bmatrix} \quad \text{and} \quad \boldsymbol{X}_{34} = \begin{bmatrix} x_3 & -x_4^* \\ x_4 & x_3^* \end{bmatrix} \tag{3.61}$$

Applying Alamouti code for second time over these two matrices, we get another code matrix for four transmit antennas as follow:

$$\boldsymbol{X} = \begin{bmatrix} x_{12} & -x_{34}^{*} \\ x_{34} & x_{12}^{*} \end{bmatrix} \tag{3.62}$$

Expanding (3.62) we get

$$\begin{bmatrix} x_1 & -x_2^{*} & -x_3^{*} & x_4 \\ x_2 & x_1^{*} & -x_4^{*} & -x_3 \\ x_3 & -x_4^{*} & x_1^{*} & -x_2 \\ x_4 & x_3^{*} & x_2^{*} & x_1 \end{bmatrix} \tag{3.63}$$

One may notice that the rows of (3.63) are not orthogonal to each other. For example the first and last rows and the second and third rows of matrix are not orthogonal. That is why it is called quasi orthogonal code. The decoding is done in pair of symbols rather than separate symbol. x_1 is decoded with x_4, and x_2 is decoded with x_3.

Therefore now we can say that the code given in (3.63) for four transmit antennas is also full rate, but unfortunately its diversity is not maximum.

To get maximum diversity, different constellations for different transmit signals can be used [15]. For example in case of QPSK constellation, the signal x_3 and x_4 are rotated by $\pi/4$ before transmission. To get maximum diversity, there are many different techniques of signal rotation discussed in [43], [44] and [45]. Note that such type of codes can be constructed for large number of transmit antennas using same technique.

3.5.4 Linear dispersion space time block codes

A linear code is defined as a set of codewords that are linear in the scalar input symbols. Since linear codes are easier to encode and decode, so one may desire to use linear codes for information transmission, but unfortunately the linearity of STBCs are limited to certain number of transmit and/ or receive antennas. In previous sections, we saw that full rate linear codes are available only for two transmit antennas. For higher number of transmit antennas,

full diversity OSTBCs may be constructed but they do not attain full rate. On the other hand QOSTBCs may achieve full rate but they lose their maximum diversity. In [46] Hassibi and Hochwald find out the remedy of this problem by introducing Linear Dispersion Space Time Block Codes (LDSTBCs). LDSTBCs do not respect the constraint of orthogonality and are designed for specific number of receive antennas.

Complex valued $N_T \times T$ spatio-temporal matrices $\{\mathbf{A}_k\}_{k=1}^{K}$ are used to spread the input information symbols over $N_T T$ spatio-temporal dimensions. The real and imaginary part of each input symbol x_k is modulated separately with the matrices $\mathbf{A}_k$ and $\mathbf{A}_{k+K/2}$. Define $s_k = \Re x_k$ and $s_{k+K/2} = \Im x_k$ where $1 \le k \le K$. The modulated matrices are summed to obtain the $N_T \times T$ codeword $\boldsymbol{X}$ as follows:

$$\mathbf{X} = \sum_{k=1}^{K/2} \left(\mathbf{A}_k \Re x_k + \mathbf{A}_{k+K/2} \Im x_k \right) = \sum_{k=1}^{K} \mathbf{A}_k s_k \tag{3.64}$$

The number of modulation matrices K is usually upper bounded by the total number of spatio-temporal degrees of freedom $2N_T T$. When $K < 2N_T T$, the modulation matrices can be designed to be orthogonal, however for optimal capacity performance, in general $K = 2N_T T$ and the modulation matrices are not orthogonal.

For example using the dispersion technique, the matrix given in (3.63) can be re-written as:

$$A_1 = \begin{bmatrix} 1 & 0 & 0 & 0 \\ 0 & 0 & 0 & 0 \\ 0 & 0 & 0 & 0 \\ 0 & 0 & 0 & 1 \end{bmatrix}, \; A_2 = \begin{bmatrix} 0 & 0 & 0 & 0 \\ 1 & 0 & 0 & 0 \\ 0 & 0 & 0 & -1 \\ 0 & 0 & 0 & 0 \end{bmatrix}, \; A_3 = \begin{bmatrix} 0 & 0 & 0 & 0 \\ 0 & 0 & 0 & -1 \\ 1 & 0 & 0 & 0 \\ 0 & 0 & 0 & 0 \end{bmatrix}, \; A_4 = \begin{bmatrix} 0 & 0 & 0 & 1 \\ 0 & 0 & 0 & 0 \\ 0 & 0 & 0 & 0 \\ 1 & 0 & 0 & 0 \end{bmatrix}$$

$$A_5 = \begin{bmatrix} 0 & 0 & 0 & 0 \\ 0 & 1 & 0 & 0 \\ 0 & 0 & 1 & 0 \\ 0 & 0 & 0 & 0 \end{bmatrix} \; A_6 = \begin{bmatrix} 0 & -1 & 0 & 0 \\ 0 & 0 & 0 & 0 \\ 0 & 0 & 0 & 0 \\ 0 & 0 & 1 & 0 \end{bmatrix}, \; A_7 = \begin{bmatrix} 0 & 0 & -1 & 0 \\ 0 & 0 & 0 & 0 \\ 0 & 0 & 0 & 0 \\ 0 & 1 & 0 & 0 \end{bmatrix} \; A_8 = \begin{bmatrix} 0 & 0 & 0 & 0 \\ 0 & 0 & -1 & 0 \\ 0 & -1 & 0 & 0 \\ 0 & 0 & 0 & 0 \end{bmatrix}$$

Of course the construction of such dispersion matrices is the main headache in generalization of orthogonal codes. In [47] Health and Paulraj have also discussed some other types of linear dispersion codes.

3.5.5 Spectral efficient STBCs

As we saw that in previous sections our main focus was on the design of space time codes offering full rate and/or maximum diversity. In this section we address spectral efficiency of the codes and propose some technique to ameliorate the spectral efficiency of STBCs having four transmit antennas. Here we may add that same technique may be straightforwardly extended for higher number of transmit antennas. Our proposed scheme carries more information symbols in each transmission block as compare to his brother code, and yet retains the property of simple decoding.

We define the code efficiency η as the ratio of the number of useful bits and the total number of bits in that codeword matrix. To make it clear, consider the following codeword matrix for four transmit antennas

$$\begin{bmatrix} x_1 & x_2 & x_3 & x_4 \\ -x_2 & x_1 & -x_4 & x_3 \\ -x_3 & x_4 & x_1 & -x_2 \\ -x_4 & -x_3 & x_2 & x_1 \end{bmatrix} \tag{3.65}$$

The useful symbols are enumerated in first row of (3.65) whereas all other symbols are redundant and completely depend on four useful symbols. So the code efficiency is $\eta = 4/16 = 0.25$. Full efficient code $\eta = 1$, is only possible when the redundant symbols would have dual functionality *i.e.* at the same time they could be used as redundant symbols and as well as information symbols. But as our original data is random, so the probability of getting such a code pattern is $2^8 / 2^{32} = 0.6^{-9}\%$ which is too small and practically near to zero probability.

In what follows, we discuss two simple techniques for improving code efficiency η.

3.5.5.1 Bit efficient technique

If we write codeword matrix (3.65) by its corresponding bit representation by assuming, $x_1 = e^{j\pi 0}$, $x_2 = e^{\frac{j\pi}{2}}$, $x_3 = e^{j\pi}$ and $x_4 = e^{\frac{j3\pi}{2}}$, we get

$$\begin{bmatrix} 00 & 01 & 11 & 10 \\ 10 & 00 & 01 & 11 \\ 00 & 10 & 00 & 10 \\ 01 & 00 & 10 & 00 \end{bmatrix} \tag{3.66}$$

This technique is very similar to [48], which was developed for increasing the spectral efficiency of Alamouti code [34]. The original data stream is divided into group of nine bits. The first eight bits are arranged as useful bits in matrix form as in (3.66) and for the transmission of ninth bit, we use two different 4-PSK constellations as shown below in figures 3.6 and 3.7. For example if ninth bit is 1, we choose the constellation A, shown in

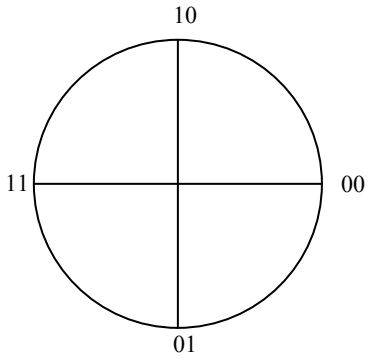

Fig 3.6 QPSK constellation 'A'

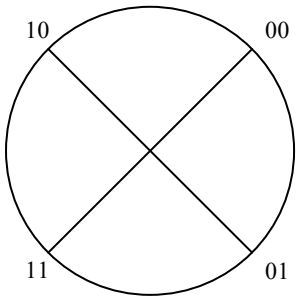

Fig 3.7 QPSK constellation 'B'

figure 3.6, otherwise constellation B shown in figure 3.7. It turns out that the transmission matrix has the same format as that of (3.66) but now each transmission block contains nine information bits instead of eight. So the code efficiency increases to 9/32 = 0.28125. As the code efficiency increases by a single bit we call this technique, Bit Efficient Code (BEC).

3.5.5.2 Symbol efficient technique

In this technique we divide the source binary data in to group of ten bits and then convert them into two binary substream by a serial to parallel converter. For simplicity we show these five, 2-bits parallel bit stream by $[x_1\ x_2\ x_3\ x_4\ x_5]$.

Before and after passing the symbols through signal constellation we tally the fifth symbol with other four symbols by its corresponding bit representation and find out the symbol which is same as fifth symbol. In case if there are more than one matching symbol, then we take the first one and in case if there is no any matching symbol then we ignore the fifth symbol for that specific transmission. For transmission of fifth symbol, we use same technique of two

constellations as above. We assume that in each block of transmission we find a matching symbol. In this case the code efficiency increases to 10/32 = 0.3125. As the code efficiency is increased by a symbol, we call this technique as Symbol Efficient Code (SEC).

Let $s_5 \in \{x_1\ x_2\ x_3\ x_4\}$ denotes the fifth symbol and $\{x_1\ x_2\ x_3\ x_4\} \in A, B$

Then the transmission matrix (3.65) can be represented as:

$$\begin{bmatrix} x_1 e^{j\frac{\pi}{2}s_5} & x_2 e^{j\frac{\pi}{2}s_5} & x_3 e^{j\frac{\pi}{2}s_5} & x_4 e^{j\frac{\pi}{2}s_5} \\ -x_2 e^{j\frac{\pi}{2}s_5} & x_1 e^{j\frac{\pi}{2}s_5} & -x_4 e^{j\frac{\pi}{2}s_5} & x_3 e^{j\frac{\pi}{2}s_5} \\ -x_3 e^{j\frac{\pi}{2}s_5} & x_4 e^{j\frac{\pi}{2}s_5} & x_1 e^{j\frac{\pi}{2}s_5} & -x_2 e^{j\frac{\pi}{2}s_5} \\ -x_4 e^{j\frac{\pi}{2}s_5} & -x_3 e^{j\frac{\pi}{2}s_5} & x_2 e^{j\frac{\pi}{2}s_5} & x_1 e^{j\frac{\pi}{2}s_5} \end{bmatrix} \tag{3.67}$$

At the receiving end, s_5 is decided by the location of $r_i = 1,...,4$ which is closer to the decision boundary. Maximum likelihood decoding of $s_i = 1,...,4$ can be decoupled

$$\hat{s}_i = \arg\min_{s \in \mathcal{A}} \left\{ \left| r_i - s_i e^{j\frac{\pi}{2}s_5} \right|^2 \right\} \tag{3.68}$$

The minimum Euclidean distance between two QPSK constellations is the same as that of 8PSK constellation. Therefore in worse case the BER performance of the efficient STBC will be slightly worse due to additional error in fifth bit/symbol, as compare to 8PSK modulation. But on the contrary, if the recovery of fifth symbol/bit is perfect *i.e.* the number of errors related to fifth symbol/bit is zero, then the selection of the QPSK constellation at the receiver is always correct, and the minimum Euclidean distance turns out to be the same as that of a QSPK constellation. Thus in the best case, the BER performance of efficient STBC will be slightly better as compare to ordinary STBCs.

Simulation result in figure 3.8 shows that our proposed code outperforms conventional STBCs. Table 3.3 shows some specific results of neat comparison between STBCs, BEC-STBCs, SEC-STBCs over QPSK modulation.

Table 3.3 (Performance of different coding schemes)

Scheme	Efficiency	R bits/s/Hz	BER
4-QPSK	0.25	2	Low
4-PSK SEC	0.282	2.25	↓
4-PSK BEC	0.32	0.5	
8-PSK	0.25	3	High

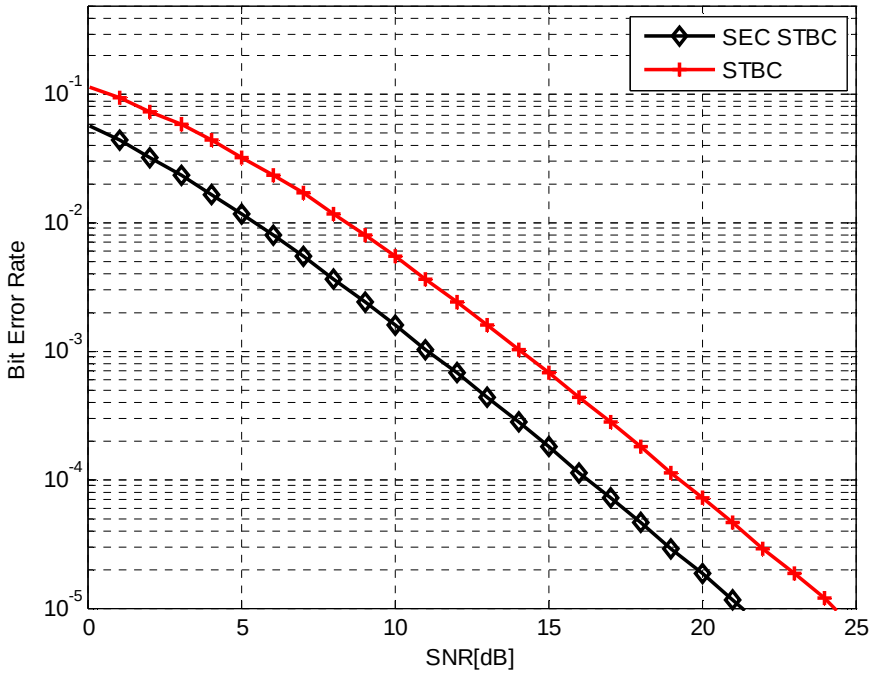

Figure 3.8 Performances of SEC STBC and STBC

3.6 Space time trellis codes

Space-time block codes can achieve maximum possible diversity with simple decoding, and are much attractive because of their simple structures. However, STBCs have the demerit that they do not provide coding gain, and non-full rate space-time block codes introduce bandwidth expansion.

In this section, we discuss Space Time Trellis Codes (STTCs) which combine the modulation and trellis coding to transmit information over multiple transmit antennas and MIMO channels. STTCs was first introduced by Tarokh,et al.[38]. Now they have been widely

discussed and explored in literature. STTCs simultaneously offer a substantial coding gain, spectral efficiency, and diversity improvement on flat fading channels.

3.6.1 STTC encoder

In space time trellis codes, the encoder maps binary data to module symbols, where the mapping function is described by a trellis diagram.

In figure 3.9, we illustrate an example of STTC with two transmit antennas.

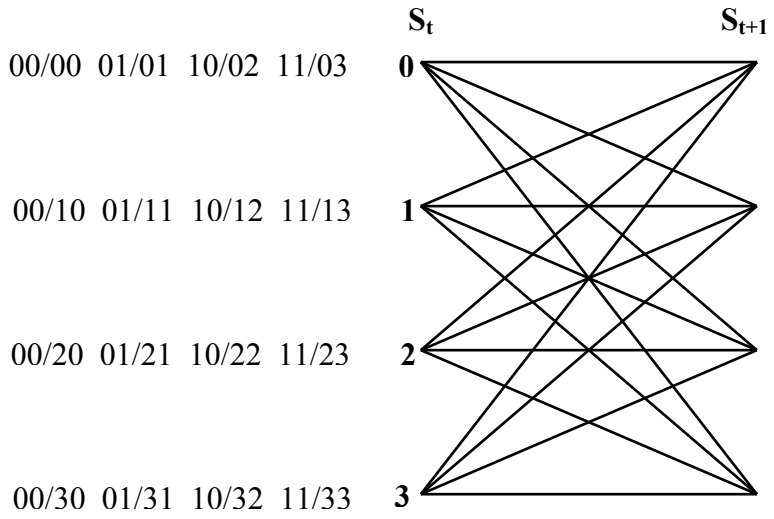

Figure 3.9 4-state STTC using 4-PSK with 2 transmit antennas, and r =2 bits/s/Hz

The STTCs that send b bits/s/Hz of information, 2^m branches leave every state. A set of 2^m pairs of indices next to every state represents the 2^m pairs of symbols for 2^m outgoing branches from top to bottom. For example, figure 3.9 illustrates a rate one space-time trellis code to transmit r = 2 bits/s/Hz. The code uses a 4-PSK constellation, *i.e.* m = 2, that includes indices 0, 1, 2, 3 to represent $1, j, -1, -j$, respectively

The encoder takes m = 2 bits as its input at each time. There are 2^m = 4 branches leaving from each state corresponding to four different input patterns. Each branch is labelled by $x_t^1 \; x_t^2 / y_t^1 \; y_t^2$ where x_t^1 and x_t^2 are a pair of encoder input bits and y_t^1 and y_t^2 represent two coded QPSK symbols transmitted through antennas 1 and 2, respectively. The row listed next to a state node in figure. 3.9 indicates the branch labels for transitions from that state corresponding to the encoder inputs 00, 01, 10, and 11, respectively

For example if we want to transmit the binary input sequence

$x = [10\ 01\ 10\ 11\ 00\ 01.....]$

the successive transitions between the states of encoder are:

$$\mathbf{0} \rightarrow \mathbf{2} \rightarrow \mathbf{1} \rightarrow \mathbf{2} \rightarrow \mathbf{3} \rightarrow \mathbf{0} \rightarrow \mathbf{1}.....$$

So the symbols transmitted from first antenna are:

0, 2, 1, 2, 3, 0……

and the symbols transmitted from second antenna are:

2, 1, 2, 3, 0, 1……..

Although the code has been designed manually, there is a logic behind it that guarantees full diversity. All branches diverging from a state contain the same symbol for the first antenna while all branches merging to a state contain the same symbol for the second antenna. Using a similar method, one can manually design full rate full diversity STTCs for other constellations and trellises [16].

All the codes proposed in [16], [28] are represented over trellis structure. Of course such type of code structure is easy to understand for small state STTCs but could be much difficult for the codes having large number of states. Working on this problem, in 2000, Baro et al.[49], developed STTCs in matrix form. So by the dint of this technique of code construction, it is possible to represent STTCs in general form for any number of transmit antennas. Figure 3.10 depicts a view of such a STTC.

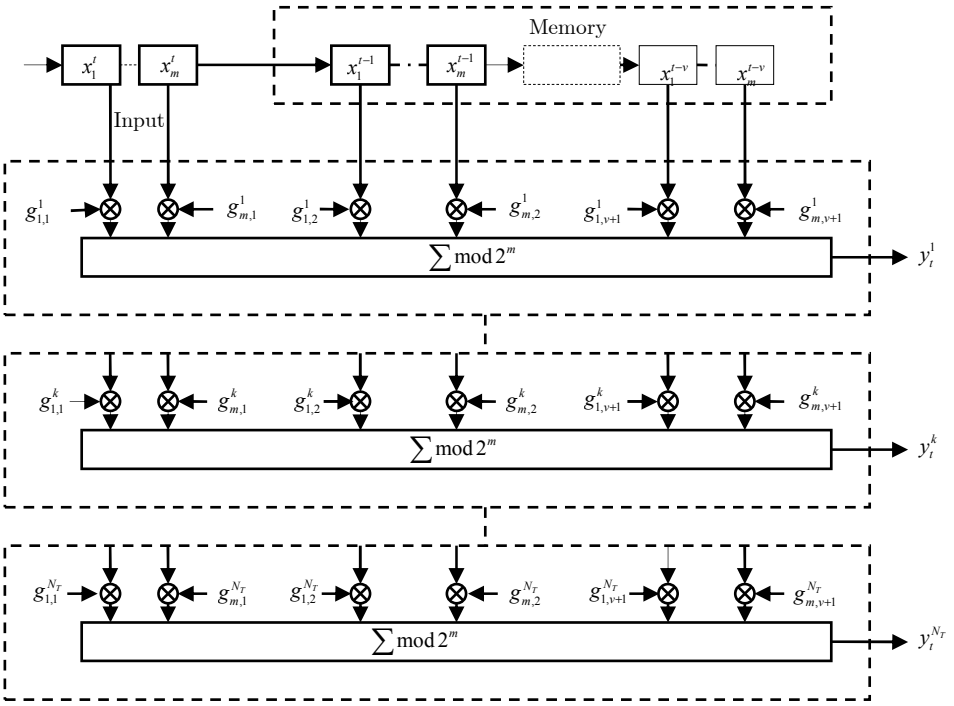

Figure 3.10 2^m-PSK STTC encoder for N_T transmit antennas

The encoder takes a block of *m* bits as input and *v* memory blocks of *m* bits (2^{mv} states). The *k*-th input sequence $x^k = (x_1^k, x_2^k, ...x_t^k, ...)$, $k = 1, 2, ...m$ is passed to the *k*-th shift register and multiplied by an encoder coefficient set. The multiplier outputs from all shift registers are added modulo 2^m, giving the encoder output $y = (y^1, y^2, ..., y^{N_T})$. The connection between the shift register elements and modulo 2^m adder can be described by the following matrix [36]

$$G = \begin{bmatrix} g_{1,1}^1 & \cdots & g_{m,1}^1 & \cdots & g_{1,v+1}^1 & \cdots & g_{m,v+1}^1 \\ \vdots & & & \cdots & & & \vdots \\ g_{1,1}^k & & g_{m,1}^k & \cdots & g_{1,v+1}^k & \cdots & g_{m,v+1}^k \\ \vdots & & & \cdots & & & \vdots \\ g_{1,1}^{N_T} & \cdots & g_{m,1}^{N_T} & \cdots & g_{1,v+1}^{N_T} & \cdots & g_{m,v+1}^{N_T} \end{bmatrix} \tag{3.69}$$

where $g_{i,j}^k$, $k = 1....N_T$, j=1,2,...,mv , i=1,2,....,m is an element of the 2^m-PSK constellation and *mv* is the memory order of the *k*-th shift register.

The encoder output at time *t* for transmit antenna *k*, denoted by y_t^k can be computed as

$$y_t^k = \sum_{i=1}^{m} \sum_{j=1}^{v+1} x_i^{t-j+1} g_{i,j}^k \qquad \bmod 2^m \tag{3.70}$$

For example, the code presented by trellis diagram in fig. 3.9 can be written in matrix form as:

$$G = \begin{bmatrix} 0 & 0 & 2 & 1 \\ 2 & 1 & 0 & 0 \end{bmatrix} \tag{3.71}$$

and the corresponding diagram is depicted in figure 3.11

As we said above that initially the encoder will be in zero state, so it means at the beginning of transmission all the four states are filled with zero. As an example we use the same binary input sequence, as we did above.

i.e. $x = [10\ 01\ 10\ 11\ 00\ 01.....]$

and the output symbols are:

$$y_1^1 y_1^2 = [1 \quad 0 \quad 0 \quad 0]G^T \qquad \bmod 4 = [0 \quad 2]$$

$$y_2^1 y_2^2 = [0 \quad 1 \quad 1 \quad 0]G^T \qquad \bmod 4 = [2 \quad 1]$$

$$y_3^1 y_3^2 = [1 \quad 0 \quad 0 \quad 1]G^T \qquad \bmod 4 = [1 \quad 2]$$

$$y_4^1 y_4^2 = [1 \quad 1 \quad 1 \quad 0]G^T \qquad \bmod 4 = [2 \quad 3]$$

$$y_5^1 y_5^2 = [0 \quad 0 \quad 1 \quad 1]G^T \qquad \bmod 4 = [3 \quad 0]$$

$$y_6^1 y_6^2 = [0 \quad 1 \quad 0 \quad 0]G^T \qquad \bmod 4 = [0 \quad 1]$$

So it is shown that trellis codes can be represented in matrix form as well.

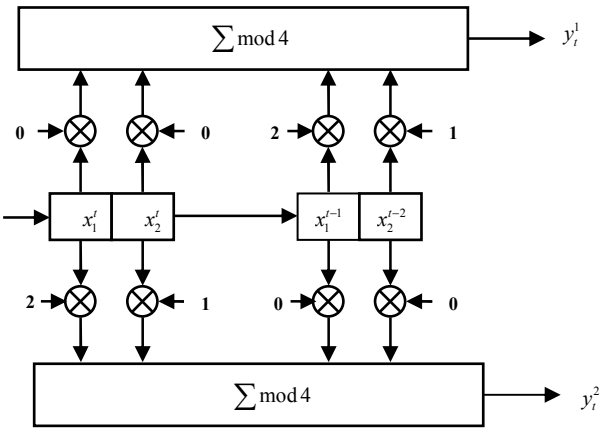

Figure 3.11 4-PSK STTC encoder with 2 transmit antennas

3.6.2 STTC decoder

The maximum-likelihood decoding finds the most likely valid path that starts from state zero and merges to state zero after L time interval

We assume that the received signals from receive antenna j at time interval L are $r_{t,j}$, $t = 1, 2, ..., L$. Similar to the case of Trellis Coded Modulation (TCM) the Viterbi algorithm can be used for the ML decoding of STTCs. Suppose at receiver we have complete CSI, if the estimated symbols transmitted from N_T antennas at time instant t are : $\hat{s}_1^t, \hat{s}_2^t, ..., \hat{s}_{N_T}^t$, the corresponding branch metric is given by:

$$\sum_{j=1}^{N_R}\left| r_{t,j} - \sum_{i=1}^{N_T} h_{i,j}^{t}\hat{s}_i^{t}\right|^2 \tag{3.72}$$

Then, the path metric of a valid path is the sum of the branch metrics for the branches that form the path. The most likely path is the one which has the minimum path gain. The ML decoder finds the set of constellation symbols that construct a valid path and solves the following minimization problem:

$$\min_{\{s_i\}} \sum_{t=1}^{L}\sum_{j=1}^{N_R}\left| r_{t,j} - \sum_{i=1}^{N_T} h_{i,j}^{t}s_i^{t}\right|^2 \tag{3.73}$$

3.6.3 Performance of STTCs

After introduction of STTCs by Tarokh [38], many researchers have worked on this area for obtaining better performances. Most of the researchers have focused to determine new STTCs optimized on slow fading channels. Some authors have developed codes with better coding gain than that introduced in [38], under the rank criteria. In 2001 Chen [50] carried out a research on STTCs over slow fading channels meeting the condition of trace criteria. Here we may add that the criteria of trace do not depend on type of channel. So it means that the codes of Chen in slow fading channels are as optimal as in fast fading channels. The codes of Firmanto-Vuceutic [51] are also result of a systematic research according to Hamming distance and product distance criteria, which are criteria for code construction on fast fading channels.

In following tables we have enumerated some codes, their principal characteristics and authors' names developed for two transmit antennas with QPSK constellation. Tables 3.4, 3.5 and 3.6 contain STTCs of 4, 8 and 16 states respectively. In these tables the necessary parameters of the codes performances like their minimum rank (Rank), minimum determinant (Det), minimum Hamming distance (d_H), minimum product distance (d_p^2), minimum trace (Trace) are enumerated. To help us to better understand the impact of these different parameters on codes' performance, we have simulated these codes over fast and slow fading channels. Simulation results are provided in next section.

Table 3.4 8-States QPSK STTCs with two transmit antennas

Code	No. of States	Generating matrix	Rank	Det	d_H	d_p^2	Trace
Tarokh [38]	8	$\begin{bmatrix} 0 & 0 & 2 & 1 & 0 & 2 \\ 2 & 1 & 0 & 0 & 0 & 2 \end{bmatrix}$	2	12	2	16	8
Yan [52]	8	$\begin{bmatrix} 0 & 2 & 1 & 0 & 2 & 0 \\ 2 & 1 & 0 & 2 & 2 & 0 \end{bmatrix}$	2	16	3	24	10
Baro [49]	8	$\begin{bmatrix} 2 & 0 & 2 & 1 & 0 & 2 \\ 2 & 1 & 0 & 0 & 0 & 2 \end{bmatrix}$	2	12	2	32	8
Firmanto [51]	8	$\begin{bmatrix} 2 & 0 & 1 & 1 & 0 & 2 \\ 2 & 2 & 2 & 3 & 0 & 0 \end{bmatrix}$	2	8	2	48	10
Jung-Lee [54]	8	$\begin{bmatrix} 2 & 0 & 2 & 3 & 0 & 2 \\ 2 & 1 & 0 & 2 & 0 & 2 \end{bmatrix}$	2	12	2	32	8
Yi Hong [53]	8	$\begin{bmatrix} 1 & 2 & 2 & 3 & 0 & 0 \\ 2 & 0 & 0 & 1 & 0 & 2 \end{bmatrix}$	2	16	2	24	10
Chen [50]	8	$\begin{bmatrix} 2 & 2 & 2 & 1 & 0 & 0 \\ 2 & 0 & 1 & 2 & 0 & 2 \end{bmatrix}$	2	8	2	48	12

Table 3.5 16-States QPSK STTCs with two transmit antennas

Code	No. of States	Generating matrix	Rank	Det	d_H	d_p^2	Trace
Tarokh [38]	16	$\begin{bmatrix} 0 & 0 & 2 & 1 & 0 & 2 \\ 2 & 1 & 0 & 2 & 2 & 0 \end{bmatrix}$	2	12	3	16	8
Yan [52]	16	$\begin{bmatrix} 0 & 2 & 1 & 1 & 2 & 0 \\ 2 & 2 & 1 & 2 & 0 & 2 \end{bmatrix}$	2	32	3	64	12
Baro [49]	16	$\begin{bmatrix} 1 & 2 & 2 & 0 & 0 & 2 \\ 2 & 0 & 1 & 2 & 2 & 0 \end{bmatrix}$	2	20	3	48	12
Firmanto [51]	16	$\begin{bmatrix} 2 & 0 & 1 & 0 & 0 & 2 \\ 0 & 2 & 2 & 1 & 2 & 2 \end{bmatrix}$	2	20	3	64	14
Jung-Lee [54]	16	$\begin{bmatrix} 2 & 0 & 2 & 3 & 3 & 2 \\ 2 & 1 & 0 & 2 & 2 & 2 \end{bmatrix}$	2	16	3	32	10
Yi Hong [53]	16	$\begin{bmatrix} 2 & 0 & 2 & 3 & 2 & 2 \\ 2 & 2 & 1 & 2 & 0 & 2 \end{bmatrix}$	2	32	3	64	12
Chen [50]	16	$\begin{bmatrix} 2 & 1 & 2 & 1 & 2 & 3 \\ 0 & 2 & 2 & 3 & 0 & 2 \end{bmatrix}$	2	8	3	128	16

Table 3.6 4-States QPSK STTCs with two transmit antennas

Code	No. of States	Generating matrix	Rank	Det	d_H	d_p^2	Trace
Tarokh [38]	4	$\begin{bmatrix} 0 & 0 & 2 & 1 \\ 2 & 1 & 0 & 0 \end{bmatrix}$	2	4	2	4	4
Yan [52]	4	$\begin{bmatrix} 2 & 0 & 1 & 2 \\ 2 & 2 & 2 & 1 \end{bmatrix}$	2	8	2	16	8
Baro [49]	4	$\begin{bmatrix} 2 & 0 & 1 & 3 \\ 2 & 2 & 0 & 1 \end{bmatrix}$	2	8	2	8	6
Vucetic [16]	4	$\begin{bmatrix} 2 & 0 & 1 & 0 \\ 2 & 2 & 0 & 1 \end{bmatrix}$	2	8	2	8	6
Firmanto [51]	4	$\begin{bmatrix} 2 & 3 & 0 & 2 \\ 2 & 1 & 2 & 1 \end{bmatrix}$	2	4	2	24	10
Jung-Lee [54]	4	$\begin{bmatrix} 2 & 0 & 3 & 2 \\ 2 & 2 & 1 & 2 \end{bmatrix}$	1	0	2	16	8
Yi Hong [53]	4	$\begin{bmatrix} 0 & 2 & 2 & 3 \\ 2 & 2 & 1 & 2 \end{bmatrix}$	2	8	2	16	8
Chen [50]	4	$\begin{bmatrix} 0 & 2 & 1 & 2 \\ 2 & 3 & 2 & 0 \end{bmatrix}$	2	4	2	24	10

3.6.3.1 Performance of STTCs in slow fading channels

Here we illustrate the simulation results of performances of different STTCs discussed in previous sections. We suppose a quasi static slow Rayleigh fading channel. The different channel coefficients are complex Gaussian random variable, fixed during the transmission of a data frame. The frame length taken for simulation is 130 symbols.

Figure 3.12 shows the simulation results of 4-state STTCs having two transmit antennas and with 1, 2 and 4 receive antennas, developed by Tarokh [38]. As we see from the graph that the code performance increases with increasing the number of receive antennas. Hence it can be deduced that the diversity of the system will increase with the performance of the code.

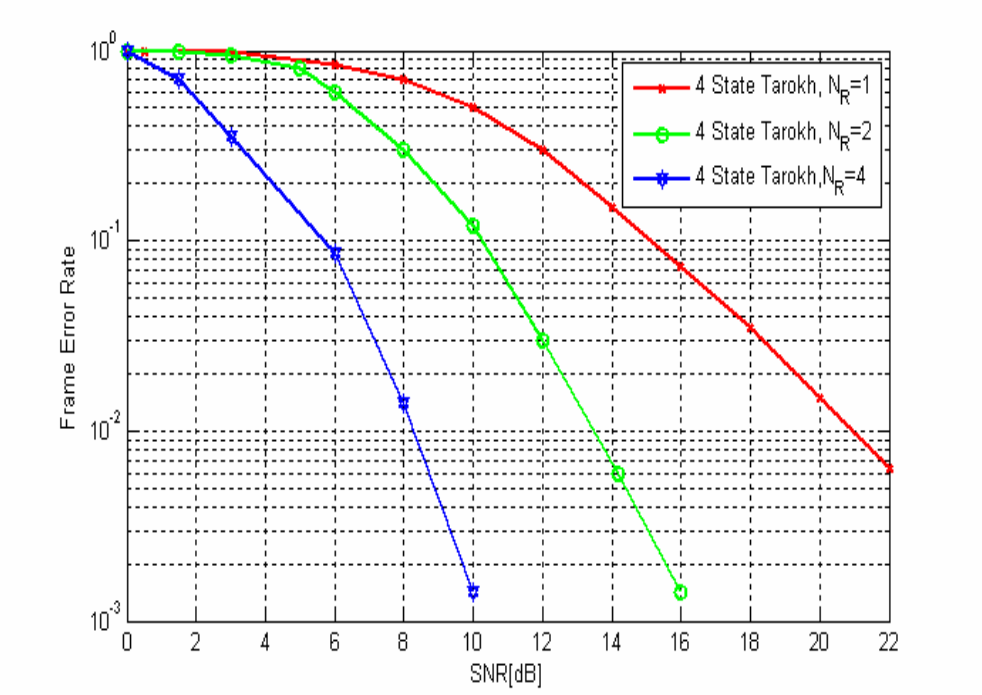

Figure 3.12 Performance of 4-states STTC in slow fading channel with two transmit antennas and with 1, 2 and 4 receive antennas using QPSK.

Figure 3.13 shows the simulation results of different STTCs with 4, 8 and 16 states and two transmit antennas, as proposed by Tarokh [38]. At the receiving end, we have two antennas.

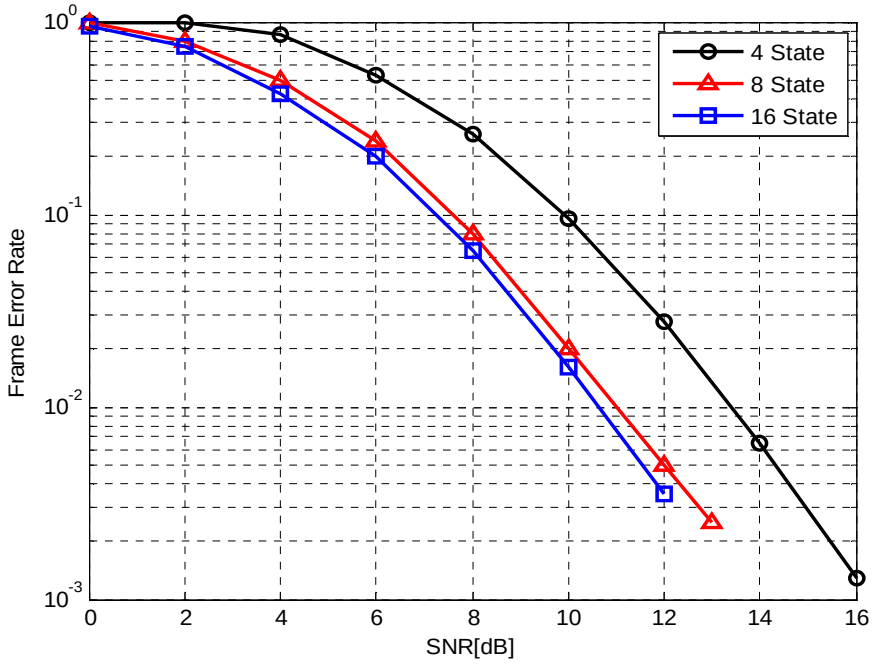

Figure 3.13 Performance of 4,8 and 16-states STTC in slow fading channel with two transmit antennas and two receive antennas using QPSK

One can see from the graph that the performance of the code increases with increasing the number of states.

Figure 3.14 show the simulation results of different STTCs with 4-states proposed by different authors (listed in table 3.6) with a single receive antenna. All the codes simulated in figure 3.14 have same minimum rank of two but their minimum determinants are different. We simulated three codes and among them, the code of Baro [49] having highest determinant has a better performance than others. This confirms the rank and determinant criteria as discussed in section 3.4.1 for slow fading channels. From the figure, one can notice that the code of Chen [50] having 4-states is not optimal with a single receive antenna.

The different codes listed in table 3.6 with 4-states are also simulated and tested with different number of receive antennas. Their simulation results are illustrated in figure 3.15. In this set up the $r_A N_R$ product is superior or equal to 4. Therefore the codes with higher values of minimum trace offer better coding gains. So one can deduce that the code of Chen [50] with higher minimum trace have better performance.

Figure 3.16 show the simulation results of 16-states STTCs proposed by Tarokh [38] and Chen [50] (table 3.5) with one and two receive antennas. Again we can observe that for two receive antennas, the code of Chen [50] following the trace criteria obtains a better performance over slow fading channels.

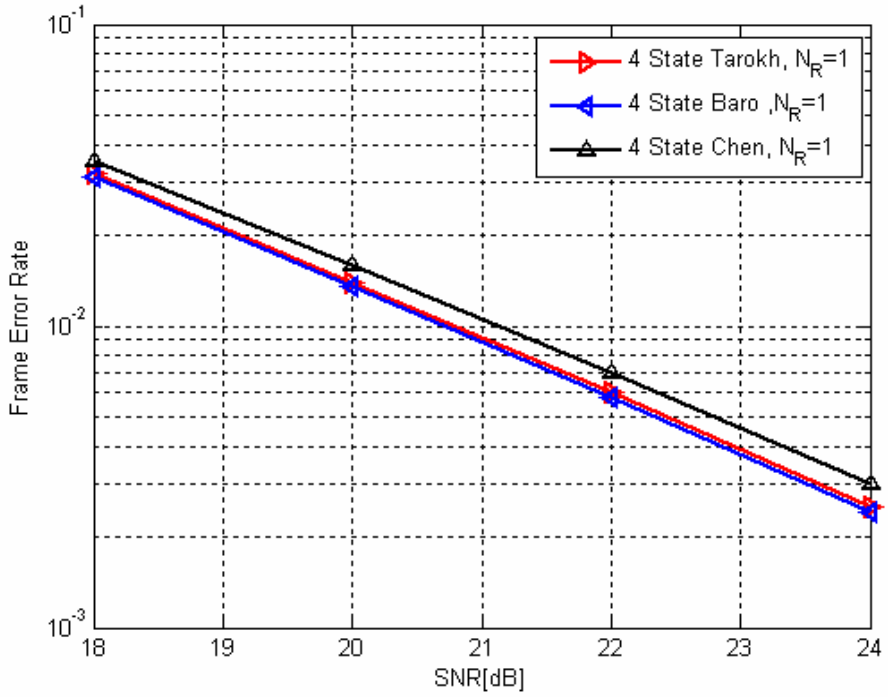

Figure 3.14 Performance of 4-states STTCs in slow fading channel with a single receive antenna using QPSK

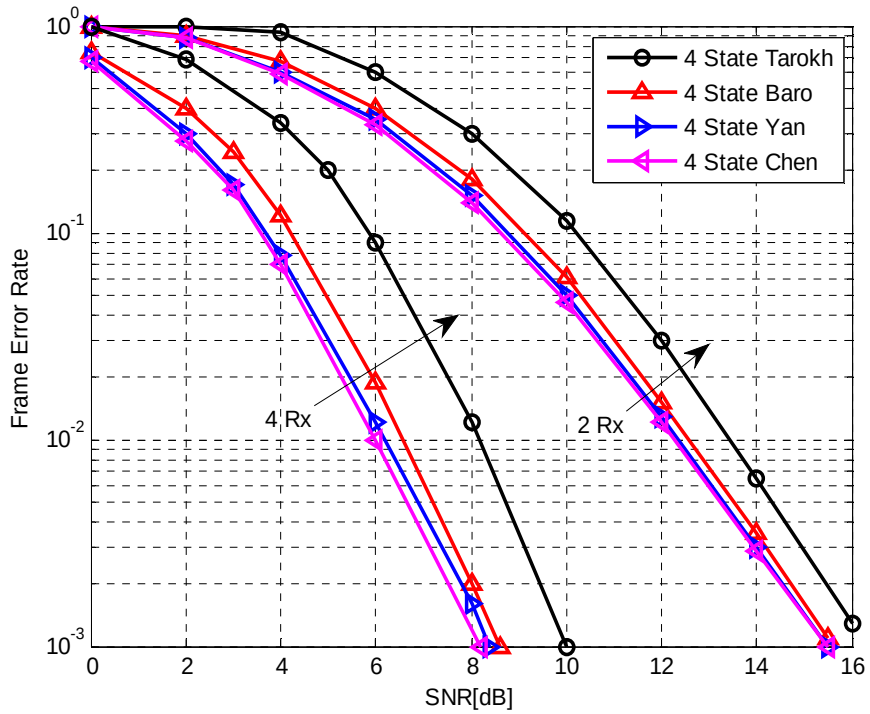

Figure 3.15 Performance of 4-states STTC in slow fading channel with different number of receive antennas using QPSK

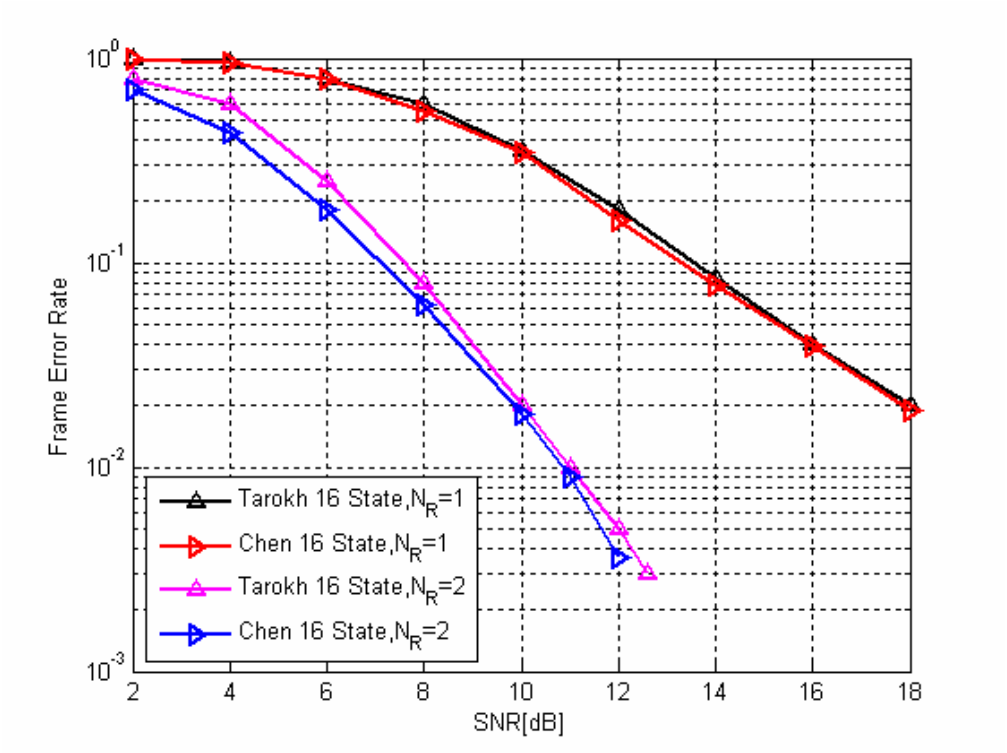

Figure 3.16 Performance of 16-states STTCs in slow fading channel using QPSK

3.6.3.2 Performance of STTCs in fast fading channels

In this section we analysis the performances of STTCs over fast Rayleigh fading channels through computer simulation. The different channel coefficients are complex Gaussian random variables, and are assumed to be constant during a symbol time and vary from symbol to symbol. We consider a frame length of 130 symbols.

Figure 3.17 illustrates the simulation results of different codes having 4-states as listed in table 3.6, with a single receive antenna. In this case, the different values of product distance d_p^2 results different coding gain. Confirming the product distance criteria, the codes proposed by Chen [50] and Firmanto [51] have better performances on fast fading channels.

Figure 3.18 combines the simulation results of different codes having 4-states (as listed in table 3.6) with 2 and 4 receive antennas. In this configuration the product $r_A N_R$ is greater or equal to 4. The codes with higher values of minimum trace have better coding gain. So we deduce that the code of Chen [50] and Firmanto [51] offer better performance.

The performance graphs of different codes having 16-states (table 3.5) are depicted in figure 3.19. Following the trace criteria, the code of Chen [50] using two receive antennas offers better performances.

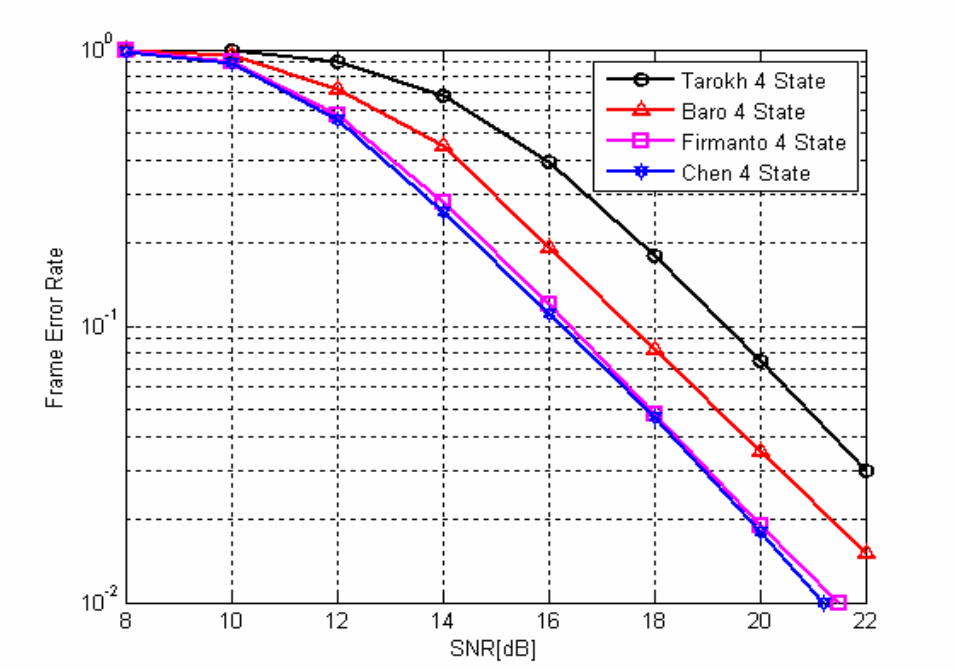

Figure 3.17 Performance of 4-states STTC in fast fading channel with a single receive antenna using QPSK

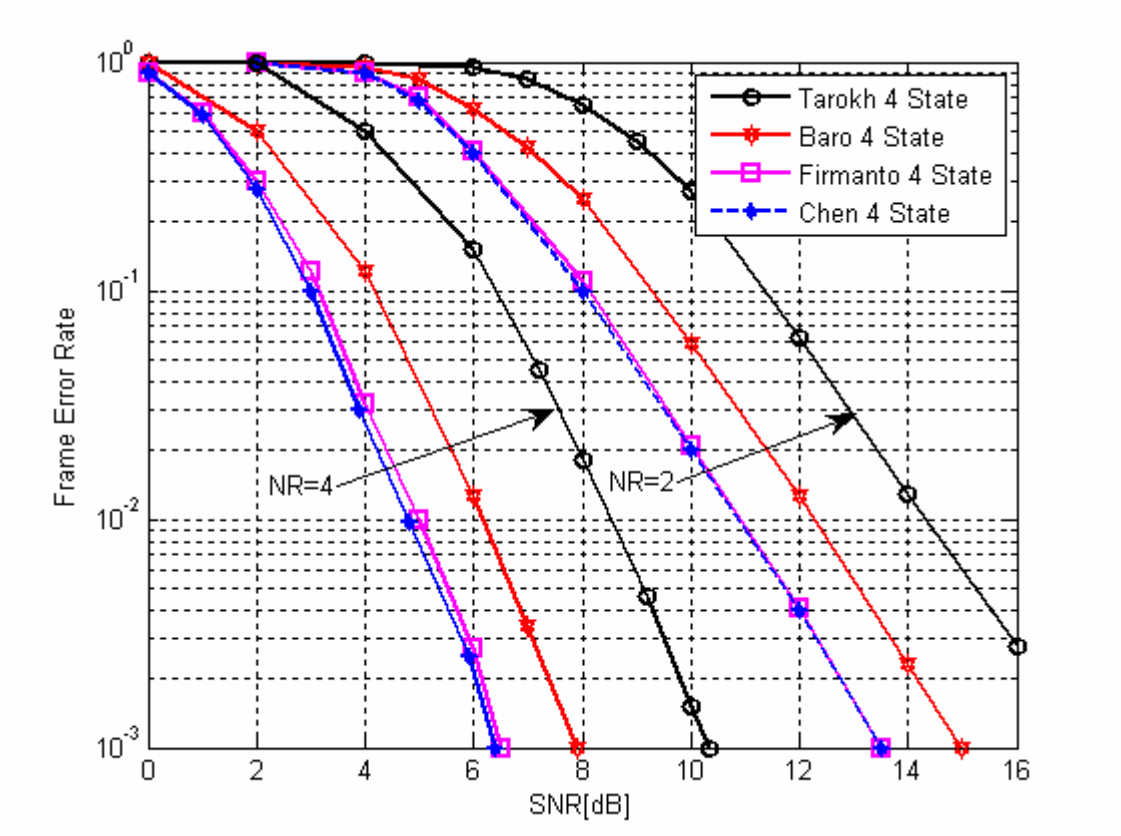

Figure 3.18 Performance of 4-states STTC in fast fading channel with 2 and 4 receive antennas using QPSK

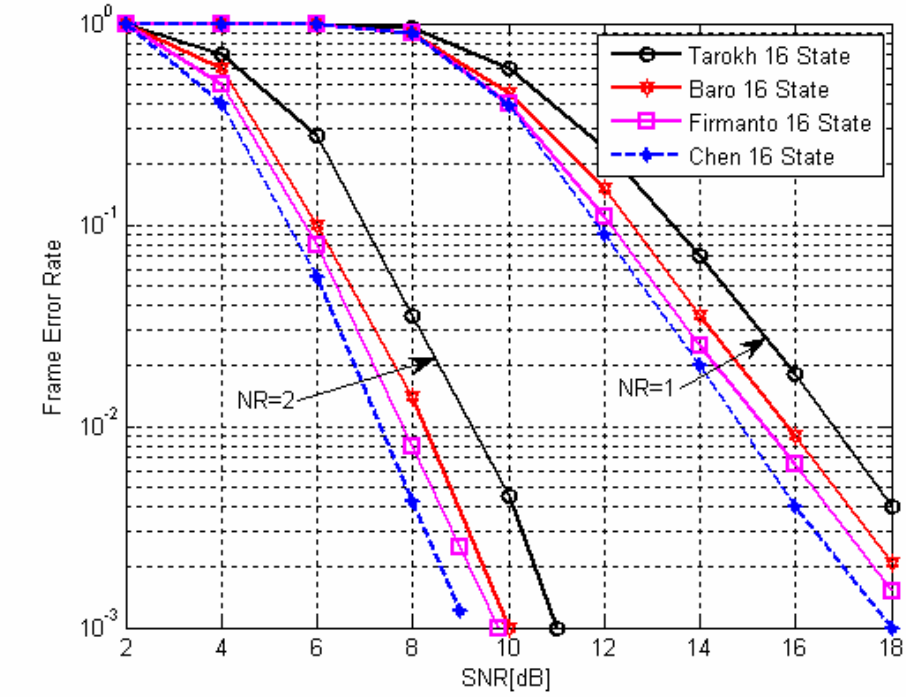

Figure 3.19 Performance of 16-states STTC in fast fading channel using QPSK

Concluding our discussion on construction criteria of space time codes, we can say that the performance curves of optimized codes following the trace criteria outperform both on slow and fast fading channels.

3.7 Super orthogonal space time trellis codes

As we saw from foregoing sections that the STBCs provide full diversity and small decoding complexity. STBCs have the advantage that they can be used as modulation scheme for a system with any number of transmit antennas but their negative aspect is that they do not provide coding gains. Another disadvantage of STBCs as discussed in section 3.5 is their non-existence of full rate for every possible number of transmit antennas.

On the other hand, STTCs can achieve full diversity and high coding gains at the cost of higher decoding complexity.

In [55] Jaffarkhani proposed an idea of combining the principal advantages of these two coding schemes. He called it Super-Orthogonal Space Time Trellis Codes (SOSTTCs). The SOSTTCs are simply concatenation of outer trellis code with STBCs. Here we may add that each codeword generated by a STBC represents a point of MIMO constellation. In STTCs a point of MIMO constellation is represented by a vector of space time symbols whereas in SOSTTCs a point of MIMO constellation is represented by codeword matrix generated by STBCs

The role of outer trellis code is to select one signal point from MIMO constellation points based on the current state and the input bits. In [56], it is shown that for slow fading channels, the trellis code should be based on the set partitioning concepts of Ungerboeck [57].

The main idea behind SOSTTCs is to consider STBCs as modulation scheme for the trellis. Therefore we assign a STBC with specific constellation symbols, for example QPSK constellation, to all the transitions arising from a state of a given trellis. Therefore, in general for a $P \times N_T$ space-time block code, picking up a trellis branch from a state is equivalent of transmitting N_T symbols from P transmit antennas in T time intervals. By doing so, it is guaranteed that we get the diversity of the corresponding STBC.

In following section we discuss in detail SOSTTCs, their construction and performances.

3.7.1 Super orthogonal codes

Alamouti code [34] is a well known example of a full-rate full-diversity complex STBC, which is defined by the following generator matrix

$$\mathcal{G}(x_1, x_2) = \begin{bmatrix} x_1 & x_2 \\ -x_2^* & x_1^* \end{bmatrix} \tag{3.74}$$

The code is designed for two transmit antennas and any number of receive antennas. Using a constellation with 2^m points, the code transmits $2m$ bits every two symbol intervals. For each block, $2m$ bits arrive at the encoder and the encoder chooses two modulation symbols x_1 and x_2. The encoder transmits x_1 from antenna one and x_2 from antenna two in first time interval. In second time interval, the encoder transmits $-x_2^*$ from antenna one and x_1^* from antenna two. This scheme provides diversity gain, but no additional coding gain.

There are other codes whose behaviours are similar to those of (3.74) for the same rate and number of transmit antennas. In fact multiplying an OSTBC codeword matrix with a unitary matrix births another OSTBC codeword matrix [15]. The set of all such codes which only use x_1, x_2, and their conjugates with positive or negative signs are listed below

$$\begin{bmatrix} x_1 & x_2 \\ -x_2^* & x_1^* \end{bmatrix} \quad \begin{bmatrix} -x_1 & x_2 \\ x_2^* & x_1^* \end{bmatrix} \quad \begin{bmatrix} x_1 & -x_2 \\ x_2^* & x_1^* \end{bmatrix} \quad \begin{bmatrix} x_1 & x_2 \\ x_2^* & -x_1^* \end{bmatrix}$$

$$\begin{bmatrix} -x_1 & -x_2 \\ x_2^* & -x_1^* \end{bmatrix} \quad \begin{bmatrix} -x_1 & x_2 \\ -x_2^* & -x_1^* \end{bmatrix} \quad \begin{bmatrix} x_1 & -x_2 \\ -x_2^* & -x_1^* \end{bmatrix} \quad \begin{bmatrix} -x_1 & -x_2 \\ -x_2^* & x_1^* \end{bmatrix} \tag{3.75}$$

The union of all these codes is given the name “super-orthogonal code” and is denoted by C. Using just one of the constituent codes from C, for example the code in (3.74), one cannot create all possible 2×2 orthogonal matrices for a given constellation. To make this point more evident, let us concentrate on the BPSK constellation for now. We show that it is possible to build all possible 2×2 orthogonal matrices (whose elements are 1, -1 for case of BSPK) using two of the codes in C. For example, one can generate the following four 2×2 constellation matrices using the code in (3.74)

$$\begin{bmatrix} 1 & 1 \\ -1 & 1 \end{bmatrix} \quad \begin{bmatrix} -1 & -1 \\ 1 & -1 \end{bmatrix} \quad \begin{bmatrix} -1 & 1 \\ -1 & -1 \end{bmatrix} \quad \begin{bmatrix} 1 & -1 \\ 1 & 1 \end{bmatrix} \tag{3.76}$$

There are four other possible distinct orthogonal 2×2 matrices which are listed below:

$$\begin{bmatrix} -1 & 1 \\ 1 & 1 \end{bmatrix} \quad \begin{bmatrix} 1 & -1 \\ -1 & -1 \end{bmatrix} \quad \begin{bmatrix} 1 & 1 \\ 1 & -1 \end{bmatrix} \quad \begin{bmatrix} -1 & -1 \\ -1 & 1 \end{bmatrix} \tag{3.77}$$

To create these four additional matrices (3.77), one can use the following code from the set *C*:

$$\begin{bmatrix} -x_1 & x_2 \\ x_2^* & x_1^* \end{bmatrix} = \begin{bmatrix} x_1 & x_2 \\ -x_2^* & x_1^* \end{bmatrix} \cdot \begin{bmatrix} -1 & 0 \\ 0 & 1 \end{bmatrix} \tag{3.78}$$

Which represents a phase shift of the signals transmitted from antenna one by π. We denote a set including all 2×2 orthogonal matrices from (3.76) and (3.77) as $\mathcal{O}_2$. By using more than one code from set *C*, we can create all possible 2×2 orthogonal matrices from $\mathcal{O}_2$. Each codewords matrix of $\mathcal{O}_2$ can be seen as a point in a MIMO constellation.

Therefore, the scheme provides a sufficient number of constellation matrices to design a trellis code with the highest possible rate.

As mentioned above that multiplying an orthogonal STBC by a unitary matrix from the left or right results in another orthogonal STBC. In what follows, we consider multiplying the generator matrix from the right by the following unitary matrix:

$$U = \begin{bmatrix} e^{j\theta} & 0 \\ 0 & 1 \end{bmatrix} \tag{3.79}$$

Multiplying on right hand side of the OSTBC matrix by *U* results in rotation the symbols of the first column, preserving the property of orthogonalities. The matrix *U* itself is not an orthogonal matrix but it can be used to get other orthogonal matrices. In the following section we see how it is possible.

A parameterized class of STBCs

Considering the multiplication of the Alamouti code (3.74) from the right by the unitary matrix *U* (3.79), we obtain the following new orthogonal matrix:

$$\mathcal{G}(x_1, x_2, \theta) = \mathcal{G}(x_1, x_2).U = \begin{bmatrix} x_1 e^{j\theta} & x_2 \\ -x_2^* e^{j\theta} & x_1^* \end{bmatrix} \tag{3.80}$$

Note that if $\theta = 0$ we get the same code as given in (3.74). So, here we can write that $\mathcal{G}(x_1, x_2, 0) = \mathcal{G}(x_1, x_2)$.

Transmissions take place very similar to that of an ordinary OSTBC code, *i.e.* during first time interval, the symbols $x_1 e^{j\theta}$ and x_2 are transmitted respectively from antenna one and two. In second time interval, the symbols $-x_2^* e^{j\theta}$ and x_1^* are transmitted respectively from antenna one and two.

We want that the multiplication of STBC matrix by *U* would not expand the constellation size, and all the modulated symbols should leave from same constellation as well. To have this property, the value of θ need to be well determined (*i.e.* θ should not take any value). In other words we should select the value θ, so ingeniously that whatever be the symbol from original constellation, his rotation by an angle of θ would not tweak it out of constellation.

For example for an *M*-PSK, the constellation signals can be represented by $e^{j2\pi k/M}$, $k = 0,1,....,M-1$, in this case, to avoid constellation expansion, one can pick $\theta = 2\pi k'/M$ where $k' = 0,1,....M-1$,[15]. By this selection, the resulting transmitted signals are also members of the *M*-PSK constellation. To be more specific, we use $\theta \in \{0, \pi\}$ for BPSK modulation and $\theta \in \{0, \pi/2, \pi, 3\pi/2\}$ for QPSK modulation.

By using $\mathcal{G}(x_1, x_2, 0)$ and $\mathcal{G}(x_1, x_2, \pi)$ in case of BPSK constellation, one can generate all 2×2 orthogonal matrices in $\mathcal{O}_2$ as discussed above. In fact, $\mathcal{G}(x_1, x_2, 0)$ represents the code in (3.74) and $\mathcal{G}(x_1, x_2, \pi)$ represents the code in (3.78). The combination of these two codes coins the name "Super-Orthogonal Code" (SOC).

In general, a SOC consists of the union of a few orthogonal codes, like the ones in (3.78). A special case is, when the SOC consists of only one orthogonal code, for example only $\theta = 0$. Therefore, the set of orthogonal codes is a subset of the set of super-orthogonal codes. Obviously, the number of orthogonal matrices that a SOC provides is more than, or in the worst case equal to, the number of orthogonal matrices that an orthogonal code provides. Therefore, the super-orthogonal codes do not extend the constellation alphabet of the

transmitted signals, but expands the number of available orthogonal matrices. This is the main point of interest for constructing full rate and maximum diversity trellis codes

3.7.2 Set partitioning for orthogonal codewords

In this section we explain the basic principle of "set partitioning" for the codewords of an orthogonal code and show that how one can maximize the coding gain.

Very similar to the set partitioning of the TCM proposed by Ungerboeck [57], we partition all the codewords of MIMO Constellation, which are orthogonal matrices generated by an OSTBC in various levels of subsets. In our case, each orthogonal matrix of the MIMO constellation correspond a modulated symbol of the constellation in case of TCM modulation.

The main objective of set partitioning is to partition all sets of codewords in such a way that at each level of partition, the minimum Euclidean distance should increase.

For a full diversity code, the coding gain corresponds to minimum determinant of the matrix $A\left(\boldsymbol{X}_i,\boldsymbol{X}_j\right)=B\left(\boldsymbol{X}_i,\boldsymbol{X}_j\right).B^{\dagger}\left(\boldsymbol{X}_i,\boldsymbol{X}_j\right)$ over all possible pairs of distinct codewords X_i and X_j.

In [15, ch: 3] , the author defines Code Gain Distance (CGD) between two codewords X_i and X_j as the determinant of the matrix, $\det\left(A\left(\boldsymbol{X}_i,\boldsymbol{X}_j\right)\right)$. The author uses CGD in lieu of Euclidean distance, the later term was used in [57] for case of TCM. Here we may add that it is also possible to use minimum trace of $A\left(\boldsymbol{X}_i,\boldsymbol{X}_j\right)$, $i\neq j$ as the measuring parameter for set partitioning.

3.7.2.1 Set partitioning for Alamouti code over BPSK constellation

Here we give an example of set partitioning of the codewords created from Alamouti code (3.74) using modulated symbols from a BPSK constellation. The P set of these codewords is $\boldsymbol{P}=\left\{\boldsymbol{X}_{00},\boldsymbol{X}_{01},\boldsymbol{X}_{10},\boldsymbol{X}_{11}\right\}$,

where

$$\boldsymbol{X}_{00} = \mathcal{G}\left(x_1 = 1, x_2 = 1\right) = \begin{bmatrix} 1 & 1 \\ -1 & 1 \end{bmatrix} \tag{3.81}$$

$$\boldsymbol{X}_{01} = \mathcal{G}\left(x_1 = 1, x_2 = -1\right) = \begin{bmatrix} 1 & -1 \\ 1 & 1 \end{bmatrix} \tag{3.82}$$

$$\boldsymbol{X}_{10} = \mathcal{G}\left(x_1 = -1, x_2 = 1\right) = \begin{bmatrix} -1 & 1 \\ -1 & -1 \end{bmatrix} \tag{3.83}$$

$$\boldsymbol{X}_{11} = \mathcal{G}\left(x_1 = -1, x_2 = -1\right) = \begin{bmatrix} -1 & -1 \\ 1 & -1 \end{bmatrix} \tag{3.84}$$

To do set partitioning for set *P*, first of all we calculate $CGD = \det\left(A\left(\boldsymbol{X}_i, \boldsymbol{X}_j\right)\right)$ between all the pairs of the elements of *P*. For example

$$\begin{aligned} CGD\left(X_{01}, X_{10}\right) &= \det A\left(\boldsymbol{X}_{01}, \boldsymbol{X}_{10}\right) \\ &= \det\left(\boldsymbol{X}_{01} - \boldsymbol{X}_{10}\right)\left(\boldsymbol{X}_{01} - \boldsymbol{X}_{10}\right)^{\dagger} \\ &= \det\begin{bmatrix} 2 & -2 \\ 2 & 2 \end{bmatrix}.\begin{bmatrix} 2 & 2 \\ -2 & 2 \end{bmatrix} \\ &= \det\begin{bmatrix} 8 & 0 \\ 0 & 8 \end{bmatrix} = 64 \end{aligned} \tag{3.85}$$

The calculated result of CGD between all pairs of elements of *P* created from (3.74) are listed below in table 3.7

Table 3.7 CGD between codewords

CGD	$\boldsymbol{X}_{00}$	$\boldsymbol{X}_{01}$	$\boldsymbol{X}_{10}$	$\boldsymbol{X}_{11}$
$\boldsymbol{X}_{00}$	0	16	16	64
$\boldsymbol{X}_{01}$	16	0	64	16
$\boldsymbol{X}_{10}$	16	64	0	16
$\boldsymbol{X}_{11}$	64	16	16	0

We can see from the table that the minimum CGD calculated between all the pairs of different elements of P is 16.

According to principle of set partitioning, the set P should be partitioned in subsets in such a way that the minimum CGD calculated among all the pairs of the elements of the subset, should be maximum. So as first step, P is partitioned into two subsets P_0 and P_1, the only possible partition is to put the two codewords X_{00} with X_{11} in P_0 and X_{01} with X_{10} in P_1. With this process in first level of set partitioning, we get the largest CGD of 64.

In second step of partitioning we again partition P_0 and P_1 in two subsets. At the end of second level of set partitioning, we get four subsets P_{00} , P_{11} , P_{01} and P_{10} with only one codeword per subset.

The partition of P containing the codewords generated by Alamouti code (3.74) for a BPSK constellation is illustrated in figure 3.20.

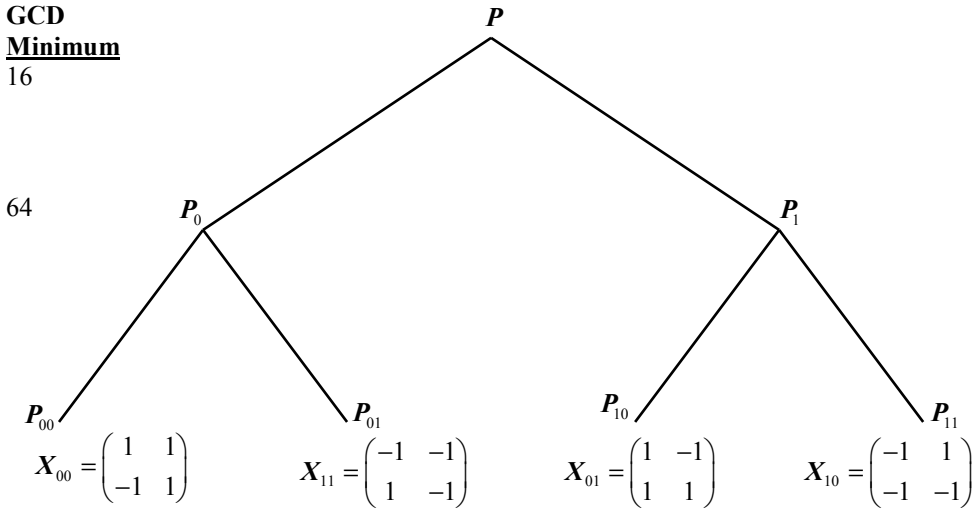

Figure 3.20 Set partitioning for BPSK modulation

A more compact view of this set partitioning is given in figure 3.21. In this compact representation, instead of writing the codeword matrices at the root of the tree, we have just written a pair of BPSK indices for symbols x_1 and x_2 to be incorporated in codeword matrix.

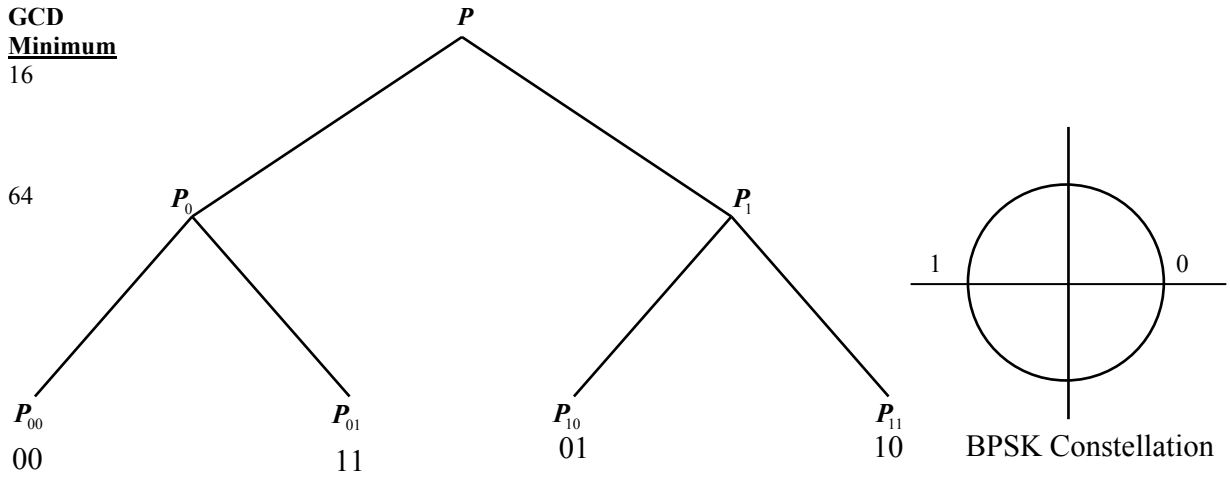

Figure 3.21 A compact representation of set partitioning for BPSK

In BPSK modulation, the index 0 represents the modulated symbol 1 whereas and the index 1 represents the symbol -1. For example the codewords matrix

$$\boldsymbol{X}_{01} = \mathcal{G}\left(x_1 = 1, x_2 = -1\right) = \begin{bmatrix} 1 & -1 \\ 1 & 1 \end{bmatrix} \tag{3.86}$$

can be represented in a compact way by a pair of indices '01' which corresponds to two modulated symbols $x_1 = 1$ and $x_2 = -1$ to incorporate in matrix (3.74)

From the given set partition, we can construct trellis codes by respecting the following regulations very similar to that proposed by Ungerboeck [57].

- All subsets should be used an equal number of times in the trellis.
- Transitions originating from the same state or merging into the same state in the trellis should be assigned subsets that are separated by the largest Euclidean distance.
- Parallel[1] paths, if they occur, should be assigned signal points separated by the largest Euclidean distance

According to these rules, we construct a 4-states trellis code (given in fig 3.22) based on the set partitioning of figure 3.21.

[1] In a trellis, the parallel branches correspond to branches leaving from the same state of the encoder at time 't' and arriving to same state at time t+1.

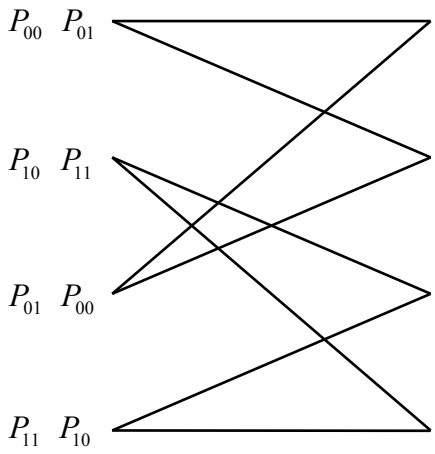

Figure 3.22, 4-state trellis set partitioning

The rate of such a code is 0.5 bit/s/Hz using a BPSK constellation, and this code cannot transmit the maximum possible rate of 1 bit/s/ Hz.

3.7.2.2 Set partitioning for Alamouti code over M-PSK constellation

In last section we laid down a simple strategy of set partitioning for Alamouti code using BSPK constellation. In this section we present a general technique of set partitioning for *M*-PSK modulation.

The best set partitioning is the one for which the minimum CGD of the sets at each level of the tree is maximum among all possible cases. To establish basic guidelines for partitioning the sets, one needs to develop formulas to calculate CGD. For an M-PSK constellation, let each signal be represented by $x = e^{j2\pi k/M}$, $k = 0,1,.....M-1$. We consider two distinct pairs of constellation symbols ($x_1^1 = e^{j2\pi k_1/M}, x_2^1 = e^{j2\pi l_1/M}$) and $x_1^2 = e^{j2\pi k_2/M}, x_2^2 = e^{j2\pi l_2/M}$, and the corresponding 2×2 orthogonal codewords X_1 and X_2. The codeword difference matrix B between these two codewords can be written as:

$$B(\boldsymbol{X}_1, \boldsymbol{X}_2) = \boldsymbol{X}_1 - \boldsymbol{X}_2 = \begin{pmatrix} e^{j2\pi k_1/M} - e^{j2\pi k_2/M} & e^{j2\pi l_1/M} - e^{j2\pi l_2/M} \\ e^{-j2\pi l_2/M} - e^{-j2\pi l_1/M} & e^{j2\pi k_1/M} - e^{-j2\pi k_2/M} \end{pmatrix} \tag{3.87}$$

So the CGD is

$$
\begin{aligned}
CGD &= \det A\left(\boldsymbol{X}_1, \boldsymbol{X}_2\right) \\
&= \det\left(B\left(\boldsymbol{X}_1, \boldsymbol{X}_2\right).B\left(\boldsymbol{X}_1, \boldsymbol{X}_2\right)\right)^{\dagger} \\
&= \left\{4 - 2\cos\left[\frac{2\pi}{M}\left(k_2 - k_1\right)\right] - 2\cos\left[\frac{2\pi}{M}\left(l_2 - l_1\right)\right]\right\}^2
\end{aligned} \tag{3.88}
$$

Here we have considered only one transition. However to calculate the minimum CGD of a trellis code, one needs to consider codewords that include more than one trellis transition.

If we consider two codewords that diverge from state zero and remerge after P trellis transitions, the size of the corresponding difference matrix B is $2\times 2\mathrm{P}$. In fact, such a difference matrix B can be represented as the concatenation of P difference matrices corresponding to the P transitions that construct the path.

For p-th transition, let us denote the set of constellation symbols for the first codeword by $\left(x_1^1, x_2^1\right)^p = (e^{j2\pi k_1^p/M}, e^{j2\pi l_1^p/M})$, $p = 1, 2, ..., P$ and $\left(x_1^2, x_2^2\right)^p = (e^{j2\pi k_2^p/M}, e^{j2\pi l_2^p/M})$ $p = 1, 2, ..., P$ for the second codeword. We also define B_p as the difference matrix of the p-th transition and $A_p = B_p.B_p^{\dagger}$. For the above two codewords, for P transitions, we get

$$
B = \left[B_1 B_2 .....B_P\right] \tag{3.89}
$$

Using (3.89) one can calculate the matrix A as :

$$
A = B.B^{\dagger} = \sum_{p=1}^{P} A_p \tag{3.90}
$$

Therefore, matrix A is still a 2×2 diagonal matrix, *i.e.* $A_{12} = A_{21} = 0$. The CGD between the above codewords that differ in P transitions can be calculated as [36]

$$
\det(A) = \left\{\sum_{p=1}^{P}\left\{4 - 2\cos\left[\frac{2\pi}{M}\left(k_2^p - k_1^p\right)\right] - 2\cos\left[\frac{2\pi}{M}\left(l_2^p - l_1^p\right)\right]\right\}\right\}^2 \tag{3.91}
$$

Note that (3.91) contains a sum of P non-negative terms. Therefore, the following inequality holds

$$\det(A) \geq \sum_{p=1}^{P} \left\{ 4 - 2\cos\left[\frac{2\pi}{M}\left(k_2^p - k_1^p\right)\right] - 2\cos\left[\frac{2\pi}{M}\left(l_2^p - l_1^p\right)\right] \right\}^2 = \sum_{p=1}^{P} \det(A_p) \qquad (3.92)$$

Based on the CGD calculated in (3.88) and (3.91), one can show that the coding gain of such a STTC is dominated by parallel transitions. So it justifies the need to maximize the CGD between codeword in each transition in trellis codes. The optimal set partitioning for QPSK is demonstrated in figures 3.23. For QPSK modulation, the indices 0,1,2,3 correspond to phase values $0,\ \pi/2,\ \pi$ and $3\pi/2$, respectively.

It is clear from figures 3.21 and 3.23, that the minimum CGD increases (or remains the same) as we go down in the tree. The branches at each level can be used to design a trellis code with a specific rate. Higher coding gain necessitates the use of redundancy resulting in reduced rate. In the following section, we show how to design STTCs without sacrificing the rate

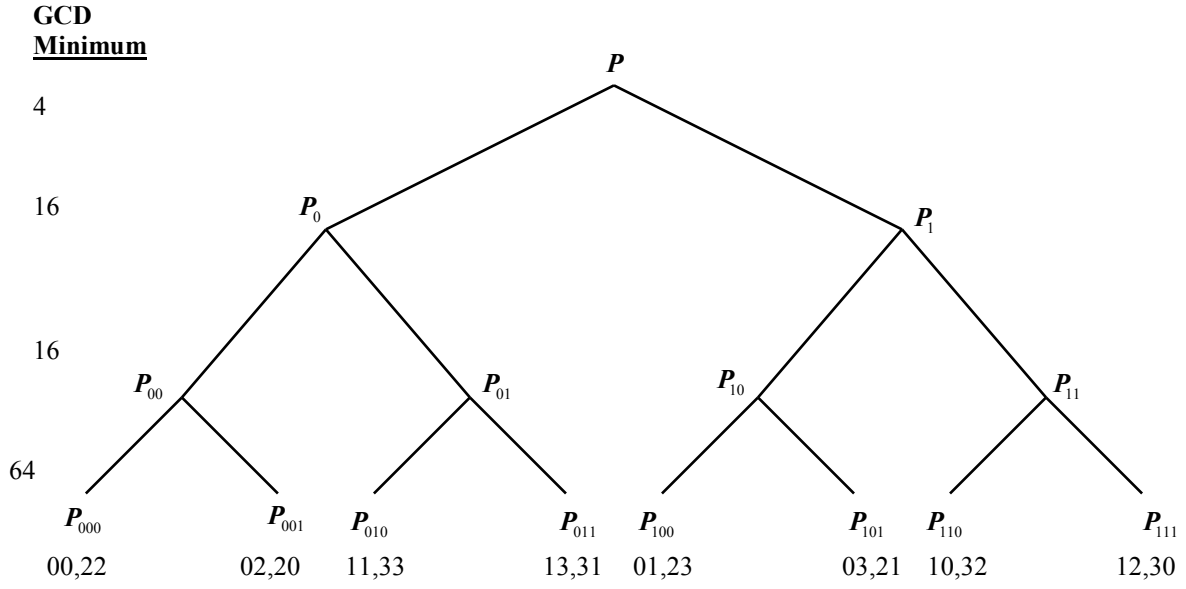

Figure 3.23 Set partitioning for QPSK, each pair of numbers represents the pair of symbol indices in a STBC

3.7.3 Set partitioning for super-orthogonal codewords

This section provides set partitioning for super-orthogonal codes and shows how to maximize the coding gain without sacrificing the rate. In constructing codes based on a super-orthogonal set, we assign a constituent STBC to all branches diverging from a state. The adjacent states are typically assigned to one of the other constituent STBC from the super-orthogonal code. Similarly, we can assign the same STBC to branches that are merging into a state. This allows us to assure that every pair of codewords diverging from (or merging to) a state achieves full diversity because the pair is from the same orthogonal code with same rotation parameter θ.

Similar to the case of orthogonal designs, set partitioning is done in such a way that the minimum CGD should be maximized at each level of partitioning. This set partitioning should be done for all possible orthogonal 2×2 codewords, for every possible rotation. In other words, we need to partition the set of all possible 2×2 matrices generated by the class of code in (3.80) with different rotation parameter θ.

Following the design criteria proposed in [15, Ch: 3] to achieve full diversity, first, we partition the set of all codewords into subsets with the same rotation. It means, the first step of the set partitioning is only based on the rotation parameter θ. Then, we partition the set of all codewords with the same rotation parameter θ as we did for the case of orthogonal designs with $\theta = 0$. In what follows, we show that optimal set partitioning for the set of codewords with different rotations results in the same set partitioning tree of section 3.7.2.1 with $\theta = 0$.

Similar to the case of $\theta = 0$, we consider two distinct pairs of constellation symbols $(x_1^1 = e^{j2\pi k_1/M}, x_2^1 = e^{j2\pi l_1/M})$ and $(x_1^2 = e^{j2\pi k_2/M}, x_2^2 = e^{j2\pi l_2/M})$. We denote the corresponding codewords by $\boldsymbol{X}_1^\theta$ and $\boldsymbol{X}_2^\theta$, and the corresponding difference matrix by B^θ. For parallel transitions in a trellis, we have

$$B^\theta = \begin{pmatrix} e^{j2\pi k_1/M}e^{j\theta} - e^{j2\pi k_2/M}e^{j\theta} & e^{j2\pi l_1/M} - e^{j2\pi l_2/M} \\ e^{-j2\pi l_2/M}e^{j\theta} - e^{-j2\pi l_1/M}e^{j\theta} & e^{-j2\pi k_1/M} - e^{-j2\pi k_2/M} \end{pmatrix} = B.U \qquad (3.93)$$

where U represents the rotation matrix in (3.79) and B is the difference matrix for $\theta = 0$ in (3.87). To calculate the CGD, we need to compute matrix $A^\theta = B^\theta.(B^\theta)^\dagger$ by using the relation. $B^\theta = B.U$

$$A^{\theta} = B^{\theta}.\left(B^{\theta}\right)^{\dagger} = \left(B.U\right).\left(B.U\right)^{\dagger} = B.U.U^{\dagger}.B^{\dagger} = B.B^{\dagger} = A \tag{3.94}$$

Therefore, $\det A^{\theta} = \det \mathrm{A}$. So the CGD between two codewords is only function of the corresponding constellation symbols and will not change whatever be the value of θ. Therefore, the optimal set partitioning for $\theta = 0$, presented in section 3.7.2.1, is equivalently optimal for other values of θ.

Figure 3.24 illustrates the set partition of a super-orthogonal code for a BPSK modulation using rotation angle as 0 and π. In this figure, instead of pair of indices for codeword symbols we have presented the equivalent 2×2 matrices. The superscripts in figure 3.24 represent the angle of rotation. Therefore, the left half of the tree of figure 3.24 is the same as that of the tree drew in figure 3.21 for $\theta = 0$. Similarly, the right half of the tree in figure 3.24 is the same as that of the tree depicted in figure 3.21 for $\theta = \pi$. Therefore we can equivalently consider fig. 3.21 as a compact representation of set partitioning of a super orthogonal code.

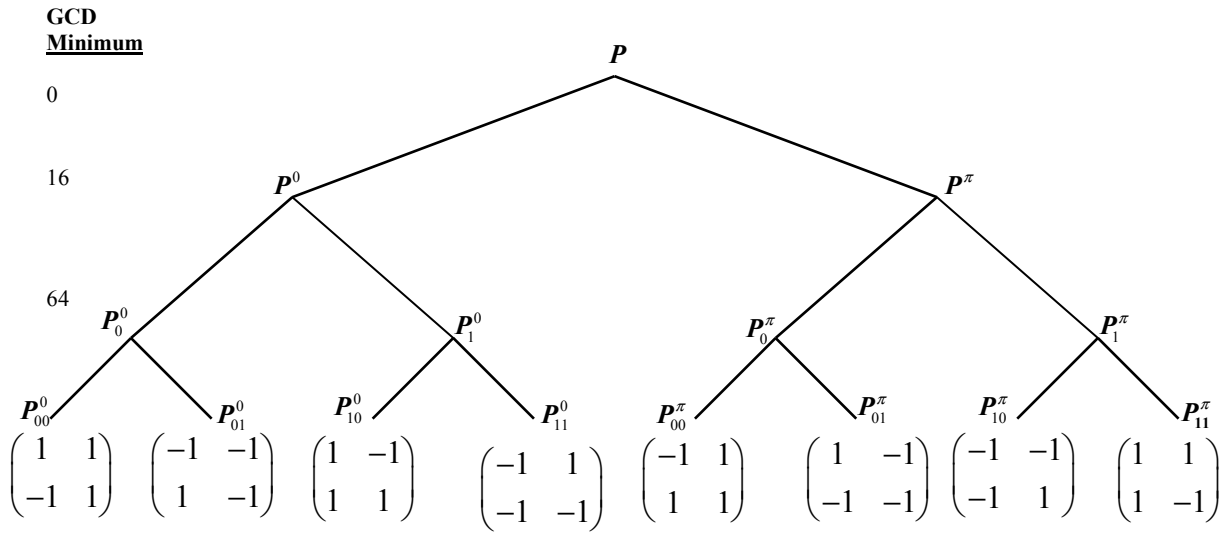

Figure 3.24 Set partitioning of super-orthogonal codewords for BPSK, and $\theta = 0, \pi$

3.7.4 Super-orthogonal STTCs

With the help of different examples, in this section we try to show how to use the proposed set-partitioning scheme to design full diversity, full rate space-time trellis codes. After the illustration of some examples, we lay down some general rules for construction of SOSTTCs

for a given trellis and required rate. In all examples of SOSTTCs illustrated below, we assign one subset P_i to each branch of the trellis. Each subset is composed of a certain number of 2×2 orthogonal matrices. Equivalently, each subset corresponds to a rotation parameter and a set of possible symbol pairs. The superscript of the subset corresponds to the rotation parameter θ. If the superscript of the subset is θ, we transmit $\mathcal{G}(x_1,x_2,\theta)$, *i.e* the STBC given in (3.80). The set of all the pairs of modulated symbols x_1 and x_2 for a given rotation parameter θ is the same as $\theta=0$. These subsets are presented in section 3.7.2 and are depicted in figures 3.21 and 3.23. For example, P_{10}^{π} for QPSK modulation corresponds to matrix $\mathcal{G}(x_1,x_2,\pi)$ and the subset P_{10} in figure 3.23.

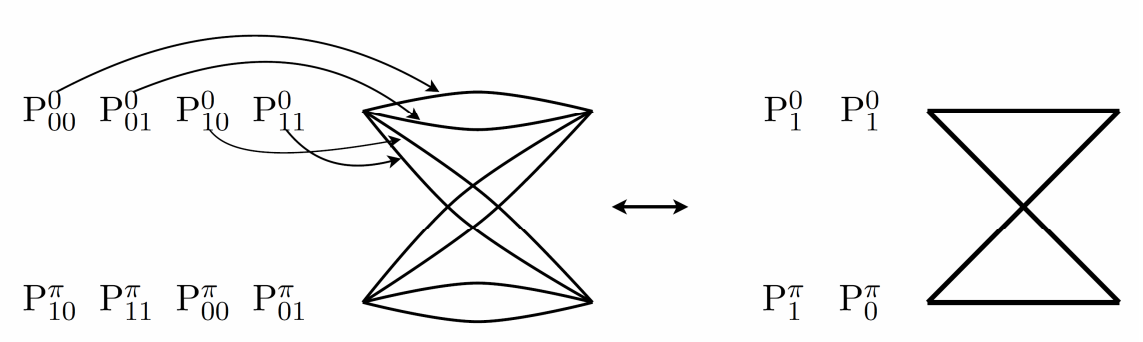

Figure 3.25 A 2-states SOSTTC with BPSK, r =1 bits/s/Hz

The left hand side view of figure 3.25 depicts an example of SOSTTC using a 2-states trellis with BPSK modulation. This trellis code is constructed from set-partitioning technique given in figure 3.24. For a transition from one state to other of the trellis, all the parallel branches with their associated subsets, where each subset contains a single codeword, are explicitly mentioned. The RHS view of figure 3.25 shows an equivalent and more compact view of the code. In this figure, each branch of the trellis which has a subset of two associated codewords represents two parallel branches.

In figure 3.26 we have given an example of SOSTTC with 4-states using BSPK and QPSK modulation. The figure contains two different representation of the same code. In LHS view, the STBCs $\mathcal{G}(x_1,x_2,\theta)$ are explicitly mentioned and the subsets are shown in figure 3.21 for BPSK modulation and in figure 3.23 for QPSK modulation. In RHS part of the same figure, the rotation parameters are indicated in superscripts of the corresponding subset.

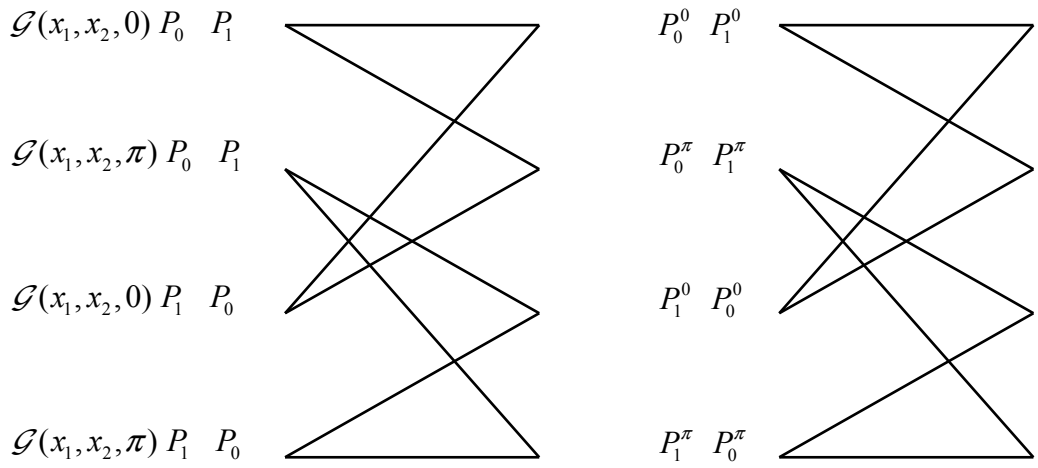

Figure 3.26 4-states SOSTTC , r =1 bits/s/Hz using BPSK and r = 2 bits/s/Hz using QPSK

In this example, when we use a BPSK modulation with the corresponding set partitioning presented in figure 3.21, the rate of the code is 1 bit/s/Hz. We use $\mathcal{G}(x_1,x_2,0)$ when departing from states zero or two, and $\mathcal{G}(x_1,x_2,\pi)$ when departing from states one or three. Here we add that this code uses eight possible 2×2 orthogonal matrices instead of four in case of trellis code of figure 3.22. The minimum CGD of such code is 64, as indicated in figure 3.21.

Now if we use a QPSK modulation, with the corresponding set partitioning in figure 3.26, the result is a four-state SOSTTC code with a rate of 2 bits/s/Hz. The minimum CGD in this case will be 16 which is greater than 4.

Some degrees of freedom in choosing the rotations and the sets exist in design of SOSTTCs. In other words the codes based on different choices of the rotation parameters and the sets, may give the same coding gain. For example, the code with 8-state and 3 bits/s/Hz, depicted on LHS of figure 3.27 provides same performances as that of sketched on RHS in same figure. This is due to the fact that the number of available 2×2 orthogonal matrices is more than what we needed. One limitation in picking different options is the possibility of a catastrophic code. To avoid a catastrophic code, a change of a few input bits should not create an infinite number of different symbols. In other words, the same input bits should not create the same codeword when starting from different states. To achieve this goal, either the rotation parameter θ assigned to different states should be different or the assigned subsets should be different.

One strategy is to pick up a small number of rotation parameters for creating the required number of orthogonal matrices and then making a permutation in subsets when same rotation

parameter is assigned to various states (figure 3.27, LHS). Another strategy of construction is to select a different rotation parameter for each state. Hence there is no need of permutation of subsets (figure 3.27, RHS). For designing a SOSTTC with higher states, if it possible to combine these two strategies, and by doing so one should be careful to select appropriate angles to avoid small CGD.

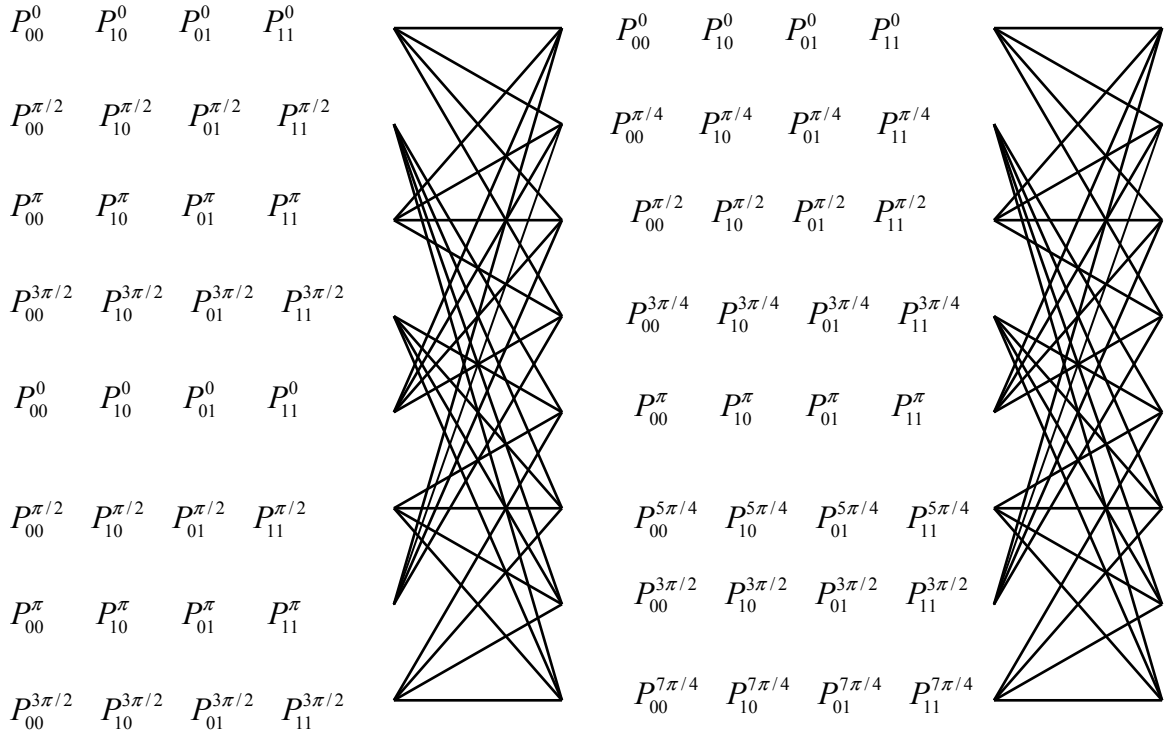

Figure 3.27 A 8-states SOSTTC , r =3 bits/s/Hz using 8-PSK

3.7.5 Encoding and decoding

So far we have considered SOSTTCs for two transmit antennas. Every path in the trellis corresponds to a block of two symbols for transmission over two time slots. Therefore, if a data frame includes $2Lm$ bits, L orthogonal blocks corresponding to $2L$ symbols are transmitted. We assign same rotation parameter θ to the branches leaving from a state of trellis, and this parameter should be predefined. We consider that the transmission of a frame always start at state zero and return to state zero at the end.

We use the notation, $l \in \{1,2,...,L\}$ to index the transmission of l-th orthogonal block. To transmit $2m$ bits of block l, first of all we select two symbols x_1^l and x_2^l from the constellation using the $2m$ input bits. For example in case of QPSK, $x_1^l, x_2^l \in \{1, j, -1, -j\}$. The rotation

parameter used to transmit *l*-th block is denoted by θ^l. The selected symbols and the rotation parameter are used for transmission over two time slots. During the first time slot, the symbols $x_1^l e^{j\theta^l}$ and x_2^l are transmitted from the first and second transmit antennas, respectively. Then, at the second time slot, the other two symbols $-(x_2^l)^* e^{j\theta^l}$ and $(x_1^l)^*$ are transmitted from the first and second transmit antennas, respectively. Similar to the case of STTC, the ML decoding finds the most likely valid path that starts from state zero and merges to state zero.

Let $r_{1,j}^l$ and $r_{2,j}^l$ be the received signals at receive antenna *j*, at the two time slots of block *l*. we have

$$\begin{cases} r_{1,j}^l = h_{j,1} x_1^l e^{j\theta^l} + h_{j,2} x_2^l + n_{1,j}^l \\ r_{2,j}^l = -h_{j,1} (x_2^l)^* e^{j\theta^l} + h_{j,2} (x_1^l)^* + n_{2,j}^l \end{cases} \tag{3.95}$$

where $h_{j,i}$ are channel coefficient from transmit antenna *i* to receive antenna *j*, $n_{i,j}^l$ represents noise samples for block *l*. The Viterbi algorithm can be used for the ML decoding of SOSTTCs.

In each transition from one state to other in the trellis of SOSTTC, we find various parallel braches. For example we consider a case of 2-state trellis with two parallel branches. All the parallel branches of transition from state s_1^l and s_2^l at instant *l* leading to state s_1^{l+1} and s_2^{l+1} are well indicated in figure 3.28., where a, *b* and *c*, *d* are the calculated branch metric for the parallel branches of transition from s_1^l and s_2^l to s_1^{l+1} respectively.

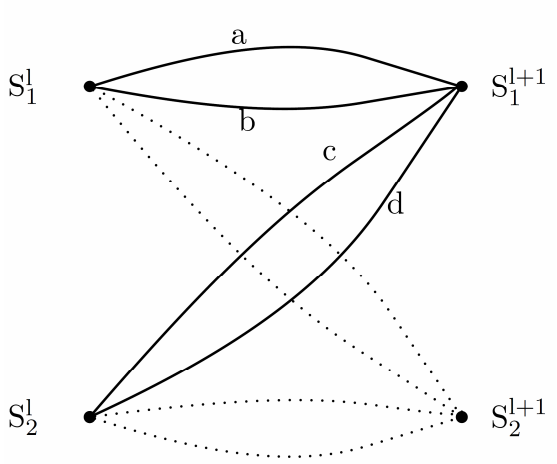

Figure 3.28 2-states trellis with two parallel branches

Let M_1^l be the cumulative metric at node S_1^l and M_2^l at node S_2^l, therefore if we want to search the cumulative metric M_1^{l+1} at node S_1^{l+1} we can calculate in following two ways :

$$1\text{-}\ M_1^{l+1} = \min(M_1^l + a, M_1^l + b, M_2^l + c, M_2^l + d) \Rightarrow 4 \text{ sums and 3 comparisons}$$

$$2\text{-}\ M_1^{l+1} = \min(M_1^l + \min(a,b), M_2^l + \min(c,d)) \Rightarrow 2 \text{ sums and 3 comparisons}$$

One can observe that calculating cumulative metric at node S_1^{l+1} using the second method needs less operation as compare to first method. In each state of decoding, to reduce the decoding complexity first of all we find out the best branch from all parallel branches of the transitions, *i.e.* the branch with smallest branch metric. Then, Viterbi algorithm uses this branch to calculate cumulative metric to find out most likely path in the trellis.

As a general case, the branch metric corresponding to *l*-th block is given by

$$\sum_{j=1}^{N_R} \left| r_{1,j}^l - h_{j,1}\hat{x}_1^l e^{j\hat{\theta}^l} - h_{j,2}\hat{x}_2^l \right|^2 + \left| r_{2,j}^l - h_{j,1}(\hat{x}_2^l)^* e^{j\hat{\theta}^l} - h_{j,2}(\hat{x}_2^l)^* \right|^2 \tag{3.96}$$

Expanding the branch metric in (3.96) and removing the constant terms results in the following branch metric:

$$\begin{aligned} &-\sum_{j=1}^{N_R} \Big[r_{1,j}^l h_{j,1}^* (\hat{x}_1^l)^* e^{-j\hat{\theta}^l} + r_{1,j}^l h_{j,2}^* (\hat{x}_2^l)^* + (r_{1,j}^l)^* h_{j,1} \hat{x}_1^l e^{-j\hat{\theta}^l} + (r_{1,j}^l)^* h_{j,2} \hat{x}_2^l - r_{2,j}^l h_{j,1}^* \hat{x}_2^l e^{-j\hat{\theta}^l} \\ &+ r_{2,j}^l h_{j,2}^* \hat{x}_1^l - (r_{2,j}^l)^* h_{j,1} (\hat{x}_2^l)^* e^{j\hat{\theta}^l} + (r_{2,j}^l)^* h_{j,2} (\hat{x}_1^l)^* \Big] + \left(\left|\hat{x}_1^i\right|^2 + \left|\hat{x}_2^i\right|^2 \right) \sum_{j=1}^{N_R} \sum_{i=1}^{2} \left| h_{j,1} \right|^2 \end{aligned} \tag{3.97}$$

This expression is divided in two parts. The first part depends only on $\hat{x}_1^l$

$$J_1^l(\hat{x}_1^l) = -\sum_{j=1}^{N_R} \left[2\Re\left(r_{1,j}^l h_{j,1}^* (\hat{x}_1^l)^* e^{-j\hat{\theta}^l} + r_{2,j}^l h_{j,2}^* \hat{x}_1^l \right) + \left|\hat{x}_1^l\right|^2 \sum_{j=1}^{N_R} \sum_{i=1}^{2} \left| h_{j,1} \right|^2 \right. \tag{3.98}$$

and the second part depends only on $\hat{x}_2^l$

$$J_2^l(\hat{x}_2^l) = -\sum_{j=1}^{N_R}\left[2\Re\left(r_{1,j}^l h_{j,2}^*(\hat{x}_2^l)^* + r_{2,j}^l h_{j,1}^* \hat{x}_2^l e^{-j\hat{\theta}^l}\right)\right] + \left|\hat{x}_2^l\right|^2 \sum_{j=1}^{N_R}\sum_{i=1}^{2}\left|h_{j,1}\right|^2 \quad (3.99)$$

The first state finds out the pair $(\hat{x}_1^l, \hat{x}_2^l)$ from all the parallel branches which minimize the function $J^l(\hat{x}_1^l, \hat{x}_2^l) = J_1^1(\hat{x}_1^l) + J_2^1(\hat{x}_2^l)$.

After finding the best parallel branch of all transitions, the ML decoder finds the most likely path in trellis. The path metric of a valid path is the sum of the branch metrics for the branches that form the path. The most likely path is the one which has the minimum path gain. The ML decoder finds the set of constellation symbols $(\hat{x}_1^l, \hat{x}_2^l)$, $l = 1, 2, ..., L$, which constructs a valid path and solves the following minimization problem:

$$\min_{\hat{x}_1^1, \hat{x}_2^1, \hat{x}_1^2, \hat{x}_2^2, ... \hat{x}_1^L, \hat{x}_2^L} \sum_{l=1}^{L} J^l\left(\hat{x}_1^l, \hat{x}_2^l\right) \quad (3.100)$$

Shortly, the decoding is done in following two steps

- Find out the best branch among all parallel transitions in the trellis
- Search for the best path with the smallest path metric among all valid paths.

3.7.6 Extension to more than two antennas

In this section, we extend the general approach for designing SOSTTCs to more than two transmit antennas.

3.7.6.1 Real constellations

As we discussed in section 3.5.3 that rate one real $N_T \times N_T$ orthogonal design only exists for $N_T = 2, 4, 8$. An example of a 4×4 real orthogonal design is given in (3.51). To expand the orthogonal matrices, similar to the case of two antennas in (3.80), we use the following phase rotations:

$$\mathcal{G}\left(x_1,x_2,x_3,x_4,\theta_1,\theta_2,\theta_3,\theta_4\right)=\begin{bmatrix} x_1e^{j\theta_1} & x_2e^{j\theta_2} & x_3e^{j\theta_3} & x_4e^{j\theta_4} \\ -x_2e^{j\theta_1} & x_1e^{j\theta_2} & -x_4e^{j\theta_3} & x_3e^{j\theta_4} \\ -x_3e^{j\theta_1} & x_4e^{j\theta_2} & x_1e^{j\theta_3} & -x_2e^{j\theta_4} \\ -x_4e^{j\theta_1} & -x_3e^{j\theta_2} & x_2e^{j\theta_3} & x_1e^{j\theta_4} \end{bmatrix} \tag{3.101}$$

Since the constellation is real, for example BPSK or PAM, and we do not want to expand the constellation symbols, we pick $\theta_i=0,\pi$, where $i=1,2,3,4$. This means that we only potentially use a sign change for each column. Note that (3.51) is a part of the super-orthogonal sets which can be obtained in (3.101) for $\theta_1=\theta_2=\theta_3=\theta_4=0$.

Similar to the case of two transmit antennas, we use CGD instead of Euclidean distance to define a set partitioning. An example of set partition using BPSK constellation is shown below in figure 3.29.

The group of binary numbers given at the roots of the tree, represent 4 indices of transmitted symbols. At the first level of partitioning, the highest minimum CGD that can be obtained is 4096, which is obtained by creating subsets P_0 and P_1 with transmitted symbol elements differing at least in two positions. At the last level of partitioning, we have eight sets P_{000}, P_{001}, P_{010}, P_{011}, P_{100}, P_{101}, P_{110}, and P_{111} with two elements per set that differ in all positions. The resulting minimum CGD is 65536.

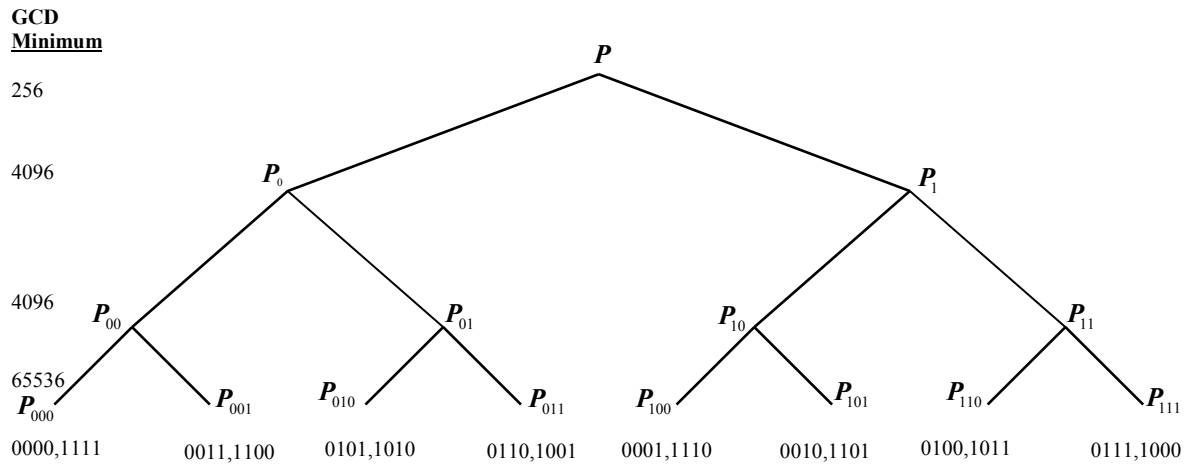

Figure 3.29 Set partitioning for BPSK. Each group of binary numbers represents the four symbols indices in a STBC with four transmit antennas

For constructing codes based on super-orthogonal sets, we use the same rule as we developed for case of two antennas. We assign a constituent STBC to all branches leaving from same

state. The adjacent states are typically assigned to one of the other constituent STBC from the super-orthogonal codes. Similarly, we can assign the same STBC to the branches that are merging into a state.

Figures 3.30 and 3.31 show the examples of two-state and four-state SOSTTC, respectively, for transmitting r = 1 bit/s/Hz using BPSK constellation.

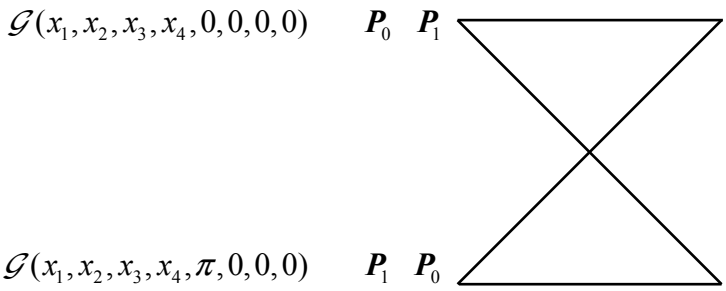

Figure 3.30 A 2-states code, four transmit antennas; r =1 bits/s/Hz (BPSK)

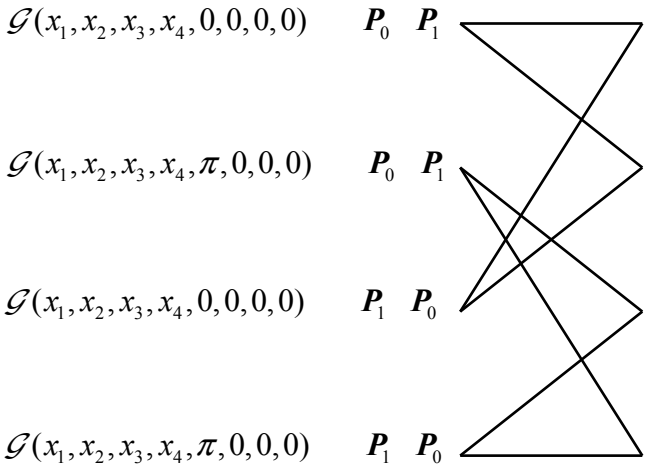

Figure 3.31 A 4-states code, four transmit antennas; r =1 bits/s/Hz (BPSK)

3.7.6.2 Complex constellations

As we discussed in section 3.5.3 that the complex OSTBCs with maximum rate of one is only the Alamouti code [34]. Rate 3/4 codes are there for 3 and 4 transmit antennas. In this section, we discuss how to design full rate complex SOSTTCs for more than two transmit antennas. Like that of real constellation, we use the rotation parameter to increase the number of orthogonal matrices. We use the following rotations:

$$G(x_1,x_2,x_3,\theta_1,\theta_2,\theta_3,\theta_4)=\begin{bmatrix} x_1e^{j\theta_1} & x_2e^{j\theta_2} & x_3e^{j\theta_3} & 0 \\ -x_2^*e^{j\theta_1} & x_1^*e^{j\theta_2} & 0 & x_3e^{j\theta_4} \\ x_3^*e^{j\theta_1} & 0 & -x_1^*e^{j\theta_3} & x_2e^{j\theta_4} \\ 0 & x_3^*e^{j\theta_2} & -x_2^*e^{j\theta_3} & -x_1e^{j\theta_4} \end{bmatrix} \quad (3.102)$$

Again, we only use rotations that do not expand the constellation. For example, in case of QPSK modulation, $\theta_1,\theta_2,\theta_3,\theta_4$ can only be limited to $0,\pi/2,\pi,3\pi/2$. We can systematically design rate 3/4 SOSTTCs for any trellis and complex constellation through set partitioning and assigning sets to different branches of the trellis.

The nice structure of SOSTTCs makes it possible to design rate one codes for specific trellises. An example of such a code for four transmit antennas can be seen in [15]. In constructing said code, the author in [15] proposes that instead of assigning the same STBC to all the branches leaving a given state, different STBCs belonging to a set of super orthogonal codes should be assigned to the branches leaving from the same state.

Another method to design full-diversity, rate one codes for more than two transmit antennas is the use of QOSTBCs. Such a method of code construction is called Super-Quasi-Orthogonal Space Time Trellis Code (SQOSTTC). For detail examples on SQOSTTCs, the reader is referred to [58] and [59] where SQOSTTCs for three and four transmit antennas, respectively have been discussed in detail.

3.7.7 Performance analysis of SOSTTCs

In this section we illustrate the simulation results of SOSTTCs with two transmit antennas and one receive antenna. A slow Rayleigh fading channel has been taken into account. Therefore, the channel coefficients are independent complex Gaussian random variables and fixed during the transmission of one frame. In analyzing the performances of such codes, simulations are driven for the Frame Error Rate (FER) as a function of received SNR. Then we compare the obtained results with performances of STTCs. In all simulations we have considered a frame length of 130 symbols.

Figure 3.32 shows the performance graph of the codes presented in figures 3.25 and 3.26, using BPSK modulation and the corresponding set partitioning of figure 3.21. Both of these codes are rate one and have a spectral efficiency of 1 bit/s/ Hz.

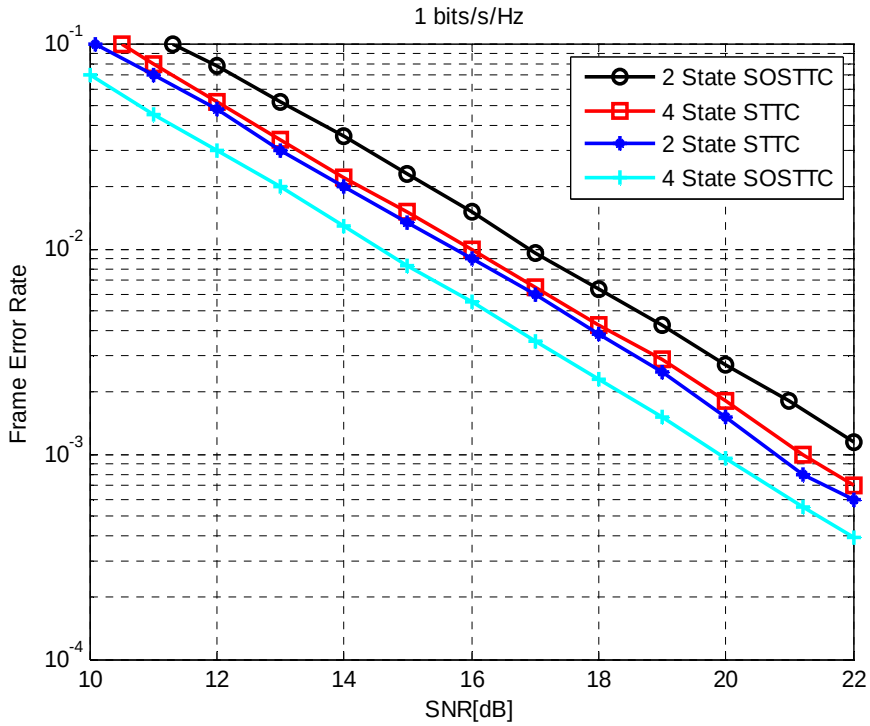

Figure 3.32 SOSTTC and STTC performance analysis at 1 bit/s/Hz using BPSK; two transmit and one receive antenna

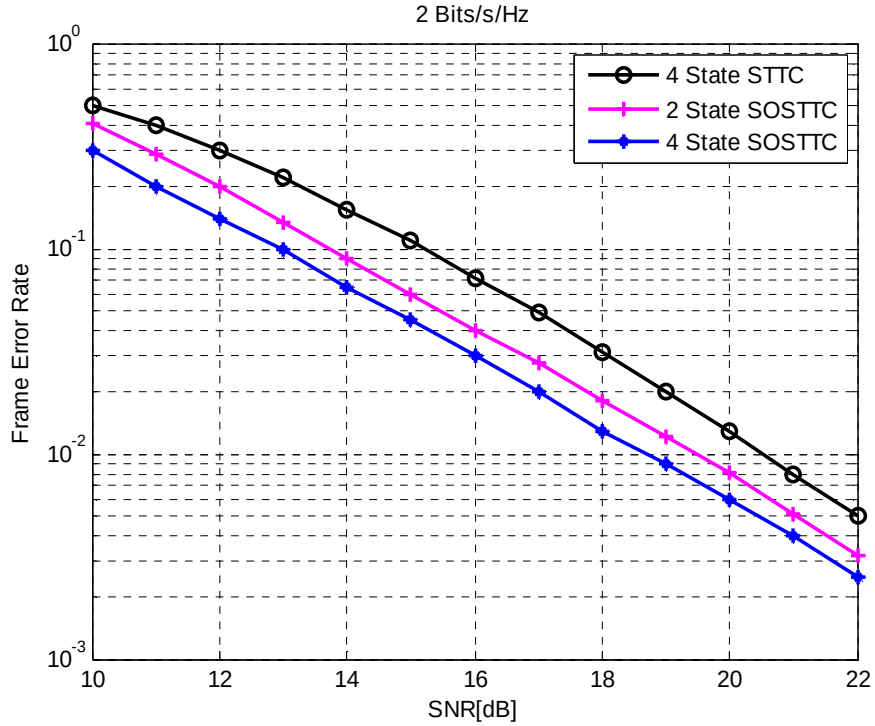

Figure 3.33 SOSTTC and STTC performance analysis, 2 bits/s/Hz using QPSK, two transmit and one receive antenna

Figure 3.33 shows the simulation results of transmitting 2 bits/s/Hz using a QPSK constellation. In this figure, 2-state SOSTTC and 4-state SOSTTC, corresponding to the code in figures 3.25 and 3.26 respectively, are taken into consideration. In this figure we have also shown the result for a 4-state STTC proposed by Chen [50], which is considered the best STTC for two transmit antennas.

3.8 Conclusions

This chapter starts with the basic concept of space time coding. Different types and techniques for construction of space time codes are discussed in detail. Some examples of full rate, maximum diversity and higher spectral efficiency codes are also presented. From the upper bound expressions of the error probability theory, various criteria of space time codes construction over slow and fast fading channels are discussed. In case of slow fading channels, the construction criteria are rank and determinant criteria whereas in case of fast fading channels, the Hamming and product distance criteria are privileged. In case of large number of antennas, the criteria of trace is applicable for both slow and fast fading channels. The construction and performances of some codes like STBCs, STTCs and SOSTTCs LDSTBCs are discussed in detail. The STBCs can achieve a maximum diversity gain with a simple decoding but they do not offer coding gain. We also presented a technique for building spectrally efficient STBCs for four transmit antennas scheme.

The STTCs offer a high coding gain, a good spectral efficiency and an improved diversity at the cost of complex decoding. The advantages of these two techniques can be combined to obtain a new class of code, *i.e.* SOSTTC. We also discussed the construction principle of SOSTTCs. The chapter is ended by presenting the simulation results of performances analyses for different space time codes.

Although the space time codes can get maximum diversity and rates when used over a MIMO channels but unfortunately they may lose their credibility when used over relay networks. So in next chapter we develop different technique for construction of space time codes which offer same performance over relays networks as they would give over MIMO channels.

Chapter 4

Construction of delay tolerant TAST codes

4.1 Introduction

In chapter 3, we discussed in detail the construction criteria and the properties of orthogonal space time codes. The orthogonality of OSTBCs makes it possible to decouple different symbols at receiving end by simple ML decoding. But on the other hand simple ML decoding restricts the cardinality of transmitted symbols and imposes a limit on the performance of the codes. STBCs do not provide coding gain for more than two transmit antenna schemes, whereas STTCs confront the problem of decoding complexity. Linear Dispersion Space Time Block Codes (LDSTBCs) do not respect the condition of orthogonality and are not flexible in term of number of receive antennas.

Layering architecture in space time coding [60], [61] has opened a new dimension in designing full rate and full diversity codes irrespective of number of transmit/receive antennas and signalling constellations. Diagonal Algebraic Space Time (DAST) codes [62] constructed from rotated constellation and Hadamard transformation, may achieve full rate and maximum diversity for 1, 2 and multiple of 4, number of transmit antennas. Threaded Algebraic Space Time (TAST) codes [60] [63] [64] may obtain a code rate $R = N_T$ and the diversity order equals to $N_T N_R$ for any number of transmit/receive antennas.

In [66],[67] Y. Lie et al. proved that all the so-called fully diverse space time codes are fundamentally asynchronous and loose their reliability (*viz*. diversity and coding gain) at the reception when used over distributed cooperative networks. In [68], the authors proposed the use of guard bands between successive transmissions to avoid timing offset. The technique proposed by [68] may be applicable for short length codes, but for lengthy codewords, the use of guard bands dramatically reduce the code rate. In [69] Damen et al. extended the work of [63] and introduced the design of TAST codes for unsynchronized cooperative network. The distributed TAST codes of [69] preserve the rank of the space-time codewords under arbitrary delays at the reception of different rows of the codeword matrices. A lattice base decoder is used for decoding the delayed codewords, which is computationally more complex than the decoupled decoding.

In this chapter we propose some easy and useful techniques for construction of delay tolerant TAST block codes which retain their maximum diversity under arbitrary delays at receiver. Our codes have simple structures and get better performance than existing codes in literature.

For the sake of completeness, we begin with some basic review over the construction of DAST and TAST codes from [62] and [63]. In section 4.2.3 we present a novel approach for construction TAST codes using fewer numbers of threads. Our principal work starts with the construction of delto code from section 4.4. The mathematical analyses followed by computer simulations confirm that our proposed codes obtain better performances as compare to the codes introduced in [69] and [80]. For example the error performance of our code proposed for three transmit antennas is improved by about 2 dB at the BER of 10^{-5}.

4.2 Algebraic space time coding structure

Conventional space time codes, discussed in last chapter, obtain full rate and maximum diversity for two transmit antennas schemes. For more than two transmit antennas they either lose the rate or diversity. With the help of algebraic codes, constructed from layering architecture, we can design full rate and full diversity space time codes for any number of transmit antennas. In fact in this architecture the individual SISO constituent encoders are combined in such a way that the composite space time code could achieve full spatial diversity for any number of transmit antennas.

The layering concept in space time codes for the first time was introduced by G.J. Foschini in [60]. Figures 4.1 illustrate horizontal layering (H-BLAST) and diagonal layering (D-BLAST) architecture in space time codes, where each colour represents an independent encoder. A layer is defined as a part of transmission in which each time slot is allocated to at most one transmit antenna. In other words, at each time slot, only one of the transmit antennas is utilized by each layer.

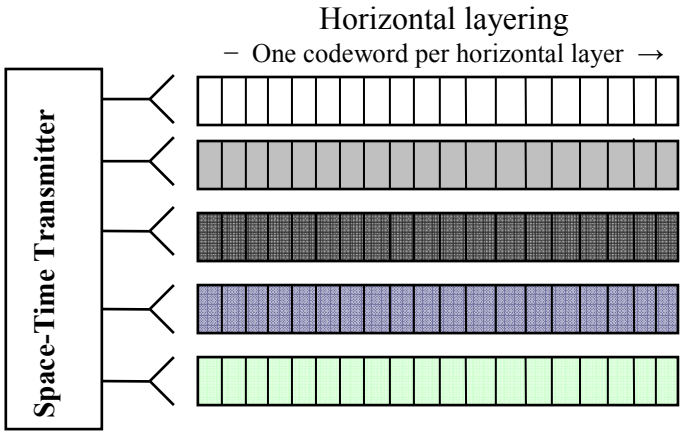

Figure 4.1(a) Horizontal layering architecture in space time coding

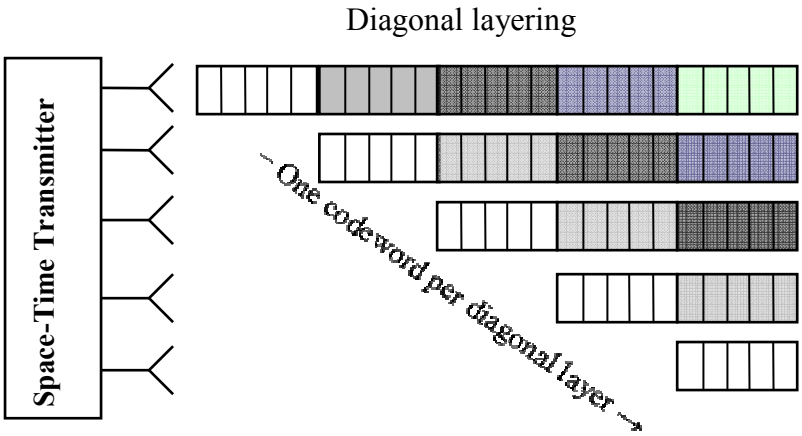

Figure 4.1(b) Diagonal layering architecture in space time coding

To be more specific, a layer, in an $N_T \times T$ transmission resource array, is identified by an indexing set $l \subset I_{N_T} \times I_T$ where $I_{N_T} = (1,...,N_T)$ and *t*-th-symbol interval on antenna *a* belongs to the layer if and only if $(a,t) \in l$. This indexing set must satisfy the requirement that if $(a,t) \in l$ and, $(a',t') \in l$, then either $t \neq t'$ or $a \neq a'$ (*i.e.*, that *a* is a function of *t*).

A layer with full spatial span N_T and full temporal span *l* is known as thread [61]. To make the above argument more clear, we define a layer/thread l_i $(i = 1,2,...,L)$ of the codeword, the set of the matrix entries in positions

$$l_i = \left\{ \left(\left\lfloor t + i - 1 \right\rfloor_{N_T} + 1, t \right) : 1 \le t \le T \right\} \qquad \text{for } 1 \le i \le L \tag{4.1}$$

where $\left\lfloor \cdot \right\rfloor_{N_T}$ denotes the modulo-N_T operation and $L \le N_T$ the total number of threads. An example for a system with four transmit antennas and four threads is provided in table 4.1. one can see from the table that each layer extends to all available time slots. Therefore it is possible to provide maximum diversity. It is possible to use coding at each layer to improve the performance. In fact, since each layer includes transmission from different transmit antennas, a space time code can be utilized at each layer.

Table 4.1 Distribution of threads for a system with $N_T = L = 4$

Time slot	Antenna 1	Antenna 2	Antenna 3	Antenna 4
1	Thread 1	Thread 4	Thread 3	Thread 2
2	Thread 2	Thread 1	Thread 4	Thread 3
3	Thread 3	Thread 2	Thread 1	Thread 4
4	Thread 4	Thread 3	Thread 2	Thread 1

As an example one can see that in case of one thread $L = 1$, in (4.1) and $T = N_T$, transmissions occur only on the principal diagonal of the $N_T \times N_T$ space time matrix.

The main idea in layering architecture is to assign the constituent codes in each thread l_i to a different algebraic subspace through the appropriate selection of some algebraic numbers in such a way that at receiving end one can separate them easily.

Now suppose that a $K \times 1$ information symbol vector $\boldsymbol{x} = (x_1, ..., x_K)^T$, belong to a given alphabet $\mathcal{V}^K$ is mapped by a channel encoder $\boldsymbol{\gamma}$ into an $N_T T \times 1$ output vector $\boldsymbol{\gamma}(\boldsymbol{x})$ from the output alphabet $\mathcal{S}^{N_T T}$ (*i.e.* $\boldsymbol{\gamma}: \mathcal{V}^K \to \mathcal{S}^{N_T T}$). Then a space time Mapper $\mathcal{M}$ maps each encoded symbol vector $\boldsymbol{\gamma}(\boldsymbol{x})$ to an $N_T \times T$ space time block code, $\boldsymbol{B}_{\boldsymbol{x}} = \mathcal{M}(\boldsymbol{\gamma}(\boldsymbol{x}))$ where N_T encoded symbols $s_{i,t}$ (i=1,…,N_T) are transmitted simultaneously from all transmit antennas at time t (t=1,…,T). There is a one to one correspondence between the information symbol vector $\boldsymbol{x}$ and $\boldsymbol{B}_{\boldsymbol{x}}$.

4.2.1 Diagonal algebraic space time block codes

In [62], the authors have proposed a new family of linear STBCs by the use of rotated constellation and the Hadamard transformation, and named it as Diagonal Algebraic Space Time (DAST) block codes. The DAST block codes get a normalized rate of 1 symbol/s and achieve full diversity over N_T transmit and N_R receive antennas. The DAST block codes outperform the orthogonal ST codes for $N_T > 2$. In fact DAST codes are constructed by sending the components of a rotated version of the information symbol vector over the diagonal of an $N_T \times N_T$ ST codeword matrix. The rotated constellations guarantee the maximum diversity whereas Hadamard transformation the coding gains. DAST codes can be developed for 1, 2 and multiple of 4 number of transmit antennas.

The idea behind the DAST code is not very difficult. First the DAST encoder selects a vector of N_T modulated complex symbols $\boldsymbol{s} = \left[s_1, s_2, ..., s_{N_T} \right]^T$. After multiply it with an N_T dimension full rank rotation matrix $\boldsymbol{M}$, we get the complex rotated symbols, $\boldsymbol{x} = \boldsymbol{M}\boldsymbol{s}$. The final DAST codewords are obtained after multiplication the rotated symbols by N_T – dimension diagonal matrix followed by the multiplication with N_T –dimension Hadamard transformation.

Now if we put the above definition into mathematical form, a DAST code can be represented by the following generating matrix.

$$\mathcal{G}_{N_T} = \begin{bmatrix} x_1 & 0 & \cdots & 0 \\ 0 & x_2 & \cdots & 0 \\ \vdots & \vdots & \ddots & \vdots \\ 0 & 0 & \cdots & x_{N_T} \end{bmatrix} . \mathcal{H}_{N_T} \tag{4.2}$$

where

$$\left[x_1, x_2, ..., x_{N_T} \right]^T = \boldsymbol{M}_{N_T} . \left[s_1, s_2, ..., s_{N_T} \right]^T \tag{4.3}$$

and $\mathcal{H}_{N_T}$ is an $N_T \times N_T$ Hadamard matrix.

A 2×2 Hadamard matrix has the following format

$$\mathcal{H}_2 = \begin{bmatrix} 1 & 1 \\ 1 & -1 \end{bmatrix} \tag{4.4}$$

Similarly higher dimension Hadamard matrices can be built by an easy method given below.

$$\mathcal{H}_{2^{N_T}} = \begin{bmatrix} \mathcal{H}_{2^{N_T-1}} & \mathcal{H}_{2^{N_T-1}} \\ \mathcal{H}_{2^{N_T-1}} & -\mathcal{H}_{2^{N_T-1}} \end{bmatrix} = \mathcal{H}_2 \otimes \mathcal{H}_{2^{N_T-1}} \tag{4.5}$$

where $\otimes$ denotes the Kronecker product. Here we may clear that the Hadamard transform is a real unitary transformation that exists for 1, 2 and all the dimensions multiple of 4, that is why DAST codes can be constructed for N_T=2 , 4 and multiple of 4 transmit antennas

In (4.3) $\boldsymbol{M}_{N_T}$ represent an $N_T \times N_T$ orthogonal rotation matrix. This rotation matrix should be designed so ingenious that it could maximize the minimum product distance and obtain full diversity. For 2 and 4 transmit antennas following two rotation matrices for real constellation, proposed in [70] can be used

$$\boldsymbol{M}_2 = \begin{bmatrix} 0.5257 & 0.8507 \\ -0.8507 & 0.5257 \end{bmatrix} \tag{4.6}$$

$$\boldsymbol{M}_4 = \begin{bmatrix} 0.2012 & 0.3255 & -0.4857 & -0.7859 \\ -0.3255 & 0.2012 & 0.7859 & -0.4857 \\ 0.4857 & 0.7859 & 0.2012 & 0.3255 \\ -0.7859 & 0.4857 & -0.3255 & 0.2012 \end{bmatrix} \tag{4.7}$$

Due to the lattice structure of the DAST block codes, the ML decoding can be implemented by the sphere decoder [73] at moderate complexity.

Example 4.1

As an example suppose that we have a system with two transmit antennas, then using $\boldsymbol{M}_2$ in (4.6) and $\mathcal{H}_2$ in (4.4), we get

$$\begin{aligned} x_1 &= 0.5257 s_1 + 0.8507 s_2 \\ x_2 &= -0.8507 s_1 + 0.5257 s_2 \end{aligned} \tag{4.8}$$

and

$$\mathcal{G}_2 = \begin{bmatrix} x_1 & x_1 \\ x_2 & -x_2 \end{bmatrix} \tag{4.9}$$

In figure 4.2, we have compared the performances of DAST code with that of Alamouti code with two transmit antennas and one and two receiver antennas using 4-QAM modulation. At the same spectral efficiency of 2 bits/s/Hz, the Alamouti scheme shows about 1dB of gain over the DAST code but in case of NT > 2, DAST code outperform orthogonal codes. For example in figure 4.3 we have evaluated the performance between DAST codes having a normalized rate of 1 symbol/s , and the orthogonal codes having a normalized rate of 1/2 symbol/s with 4 transmit antennas and one receive antenna with different spectral efficiencies.

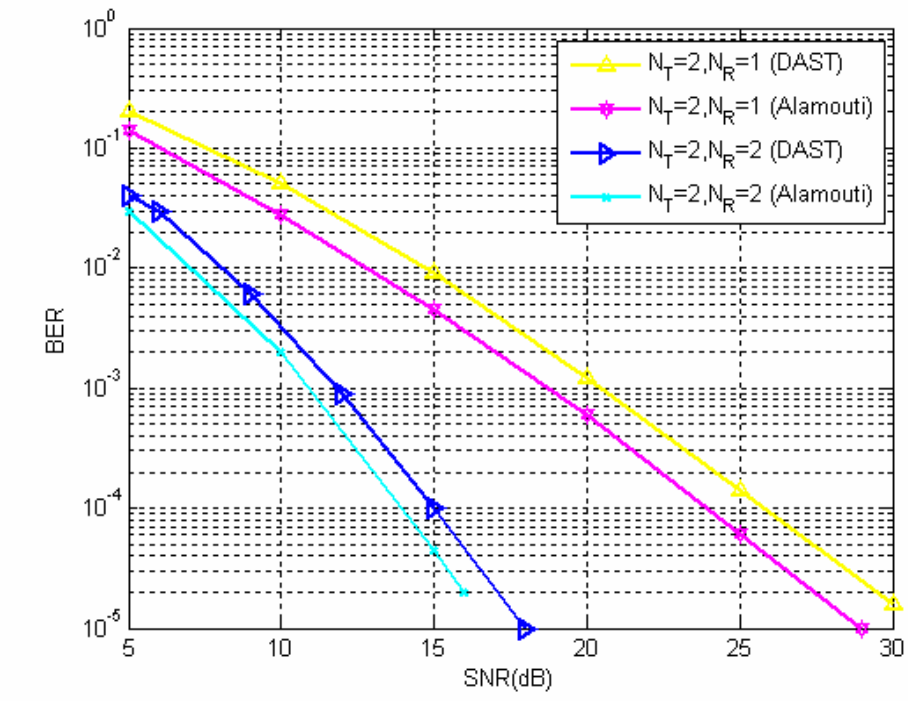

Figure 4.2 Performances analysis of DAST code

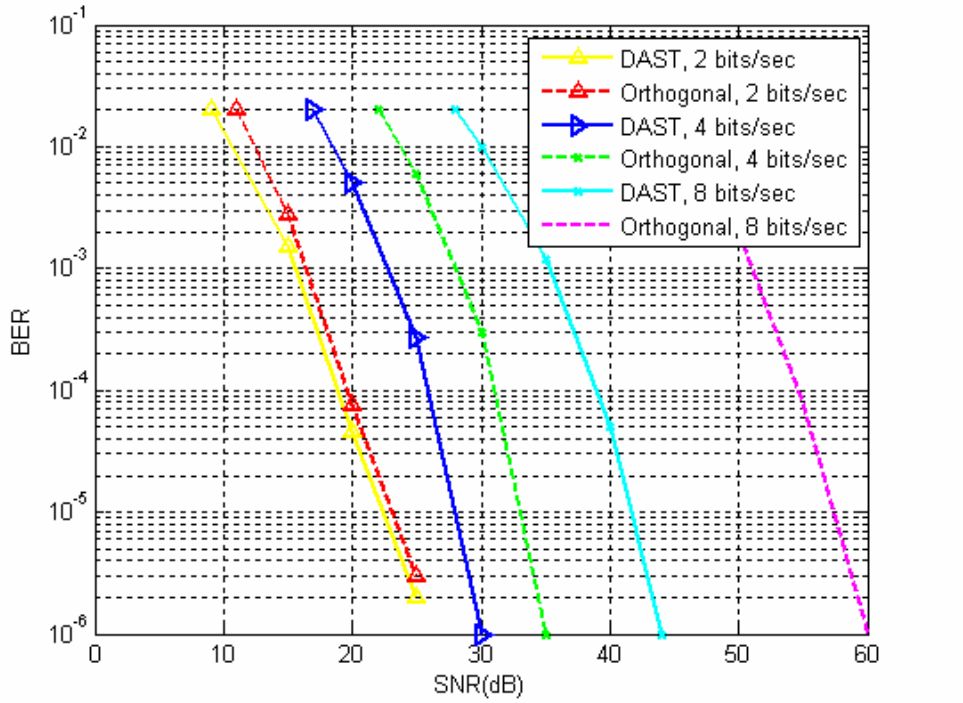

Figure 4.3 Performances analysis of DAST code

The two codes are compared at the same spectral efficiency. For example at a spectral efficiency of 2 b/s/Hz, the DAST code uses the normalized 4-QAM modulation, and the orthogonal code uses the normalized 16-QAM modulation. The DAST code has a gain of about 1 dB over the orthogonal code at 2 b/s/Hz. This gain is enhanced when increasing the size of constellation. For example, it reaches almost 5 dB at 4 b/s/Hz, and 16 dB at 8 b/s/Hz.

4.2.2 Threaded algebraic space time block codes

In [63] a novel class of space time coding system, known as Threaded Algebraic Space Time (TAST) code is proposed. In this coding technique different fully diverse SISO constituent codes γ_i's are transmitted in different threads at different algebraic sub-spaces in such a way that the composite space time block code achieves the maximum diversity of $N_T N_R$ and the rate equals to N_T.

In this technique of coding, the source information vector is first partitioned into a set of L disjoint component vectors $\boldsymbol{x}_i$, $i = 1,...,L$, $L \leq N_T$, where each vector $\boldsymbol{x}_i$ indicates a sub-space of the TAST code and is called a layer. Each layer $\boldsymbol{x}_i$ undergoes through an independently

DAST code with a rotation matrix $\boldsymbol{M}_i$ and constituent encoder γ_i. Different layers are separated by appropriate algebraic number ϕ. The composite channel encoder $\boldsymbol{\gamma}$ will, therefore, consist of L constituent encoders $\gamma_1, \gamma_2, ..., \gamma_L$ operating on independent information streams, and there is a corresponding partitioning of the composite codeword $\boldsymbol{\gamma}(\boldsymbol{x})$ into a set of constituent codewords $\gamma_i(\boldsymbol{x}_i)$. Here we may add that higher rate code can be designed by increasing the number of threads. For $L \leq \min(N_R, N_T)$, it is always possible to design a full-diversity TAST code [61]. Therefore, to maximize the rate, a good choice for the number of threads is $L = \min(N_R, N_T)$.

If we consider only one thread (*i.e.* $L = 1$), transmissions occur only on the principal diagonal of the $N_T \times N_T$ space time matrix (see table 4.1). That is why it is said that TAST codes are scaled version of DAST codes with more than one thread.

As stated in previous section, DAST codes are obtained by rotating an N_T-dimensional information symbol vector $\boldsymbol{s} = \left[s_1, s_2, ..., s_{N_T} \right]^T$ by an $N_T \times N_T$ rotation $\boldsymbol{M}$ in such a way that it maximizes the associated minimum product distance defined in [71].

$$d_{N_T} = \min_{\boldsymbol{x}=\boldsymbol{M}(\boldsymbol{s}-\boldsymbol{s}'), \boldsymbol{s}\neq\boldsymbol{s}'} \prod_{i=1}^{N_T} |x_i| \tag{4.10}$$

where $\boldsymbol{s}$ and $\boldsymbol{s}'$ belong to the considered multidimensional constellation (QAM or PAM). The rotation matrix $\boldsymbol{M}$ (complex or real) is constructed on an algebraic number field $\mathbb{Q}(\theta)$ with θ an algebraic number of degree n. [70], [71] and [74] discuss the construction of such rotation matrices in detail.

With an arbitrary number of threads, the TAST codes are constructed by transmitting a scaled DAST code in each thread, *i.e.*

$$\gamma_i(\boldsymbol{s}_i) = \phi_i \boldsymbol{x}_i = \phi_i \boldsymbol{M}_i \boldsymbol{s}_i \tag{4.11}$$

is transmitted over thread l_i, where $\boldsymbol{M}_i$ is an $N_T \times N_T$ real or complex rotation that achieves full diversity as a DAST code, and the numbers $\phi_i \in \mathbb{C}$, i =1,….L, are chosen to ensure full diversity and maximize the coding gain for the composite code. If same rotation matrix *i.e* $(\boldsymbol{M} = \boldsymbol{M}_1 = \boldsymbol{M}_2 = ... = \boldsymbol{M}_L)$ is used in all threads, the code is called symmetric TAST code, otherwise asymmetric. We denote the TAST codes by $\mathcal{T}_{N_T, L, R}$, where the subscript N_T, L, R

denote number of transmit antennas, layers and code rate, respectively. Since the rate of symmetric TAST codes is L symbols per channel use, so one may denote the symmetric codes as $\mathcal{T}_{N_T,L,L}$.

The algebraic numbers $\{\phi_1,....,\phi_L\}$, generally referred as Diophantine numbers, are chosen in such a way that the efficient separation of different layers at the receiver is assured.

A TAST code $\mathcal{T}_{N_T,L,L}$ using the full diversity algebraic rotation matrix $\boldsymbol{M}_{NT}$, a QAM constellation carved from $\mathbb{Z}[i]$,($\mathbb{Z}$ denotes ring of rational integers) and the Diophantine numbers

$$\left\{\phi_1 = 1, \phi_2 = \phi^{1/N_T}, ..., \phi_L = \phi^{(L-1)/N_T}\right\} \tag{4.12}$$

achieves full diversity if $\phi = e^{i\lambda}$ and $\lambda \neq 0$ is an algebraic number (*i.e.*, ϕ is transcendental). [63, th.2]

To make above discussion more clear, here we provide some examples.

Example 4.2

$$\underset{\text{Full diversity}}{\begin{bmatrix} x_1 & 0 \\ 0 & x_1 \end{bmatrix}} \oplus \underset{\text{Full diversity}}{\begin{bmatrix} 0 & x_2 \\ x_2 & 0 \end{bmatrix}} \Rightarrow \underset{\text{Not full diversity}}{\begin{bmatrix} x_1 & x_2 \\ x_2 & x_1 \end{bmatrix}} \tag{4.13}$$

One can see, the first two codeword matrices are fully diverse but when we combine them, the resultant codeword matrix loses its maximum diversity. If we separate the two threads by a Diophantine approximation as

$$\begin{bmatrix} x_1 & \theta x_2 \\ \theta x_2 & x_1 \end{bmatrix} \tag{4.14}$$

then (4.14) will be fully diverse if $\left\{1, \theta^2\right\}$ are algebraically independent over the set containing x_1, x_2.

Example 4.3

Using the above guidelines for TASTBC construction for $N_T = 2$ transmit and more than one receive antenna N_R, we have $L = 2$ [15]

$$\begin{bmatrix} \phi_1 x_{11} & \phi_2 x_{22} \\ \phi_2 x_{21} & \phi_1 x_{12} \end{bmatrix} \tag{4.15}$$

where x_{11} and x_{12} belong to the first thread, and x_{21} and x_{22} to second thread, and

$$x_1 = \begin{bmatrix} x_{11} \\ x_{12} \end{bmatrix} = \boldsymbol{M}_2 \begin{bmatrix} s_{11} \\ s_{12} \end{bmatrix} \tag{4.16}$$

and

$$x_2 = \begin{bmatrix} x_{21} \\ x_{22} \end{bmatrix} = \boldsymbol{M}_2 \begin{bmatrix} s_{21} \\ s_{22} \end{bmatrix} \tag{4.17}$$

and $s_{11},...,s_{22}$ belongs to the constellation considered. The appropriate selection of $\boldsymbol{M}_2$ and ϕ_i are the basic design parameters in construction of TASTBC. A good choice of $\boldsymbol{M}_2$ for complex symbols is the following matrix from [71]

$$\boldsymbol{M}_2 = \frac{1}{2}\begin{bmatrix} 1 & e^{j\pi/4} \\ 1 & -e^{j\pi/4} \end{bmatrix} \tag{4.18}$$

By choosing $\phi_1 = 1$ and $\phi_2 = \phi^{1/2}$, we can pick up the best parameter ϕ to maximize the coding gain. In this case, the coding gain distance is

$$CGD = \min\left|(x_{11} - x'_{11})(x_{12} - x'_{12}) - \phi(x_{21} - x'_{21})(x_{22} - x'_{22})\right| \tag{4.19}$$

For QPSK, the optimal choice is $\phi = e^{i\pi/6}$. Sphere decoding is used for decoding the transmitted symbols.

Example 4.4

For three transmit antennas, the number of threads depends on the number of receive antennas. For N_R = 2 receive antennas, we have L = min(N_T, N_R) = 2 threads while for N_R > 2 receive antennas, we have L = 3 threads.

For N_T = 3 transmit and $N_R \geq 2$ receive antennas, the following TASTBC is proposed in [63], [15].

$$\begin{bmatrix} x_{11} & \phi^{1/3}x_{21} & \phi^{2/3}x_{31} \\ \phi^{2/3}x_{32} & x_{12} & \phi^{1/3}x_{22} \\ \phi^{1/3}x_{23} & \phi^{2/3}x_{33} & x_{13} \end{bmatrix} \tag{4.20}$$

where

$$x_i = \begin{bmatrix} x_{i1} \\ x_{i2} \\ x_{i3} \end{bmatrix} = \boldsymbol{M}_3 \begin{bmatrix} s_{i1} \\ s_{i2} \\ s_{i3} \end{bmatrix} \qquad i=1,2,3 \tag{4.21}$$

and $s_{11},...,s_{33}$ belongs to the constellation used. By using the algebraic rotation from [70], [71] and setting $\phi = e^{i\pi/12}$, the TAST code (4.20) get full diversity.

For more examples on TASTBCs interested reader is referred to [63]

In figure 4.4 we have simulated the performance of TAST code with two transmit and two receive antennas and compared it with the performances of LDSTBC [46] and V-BLAST [60] codes. One can see that that TAST code outperforms both codes.

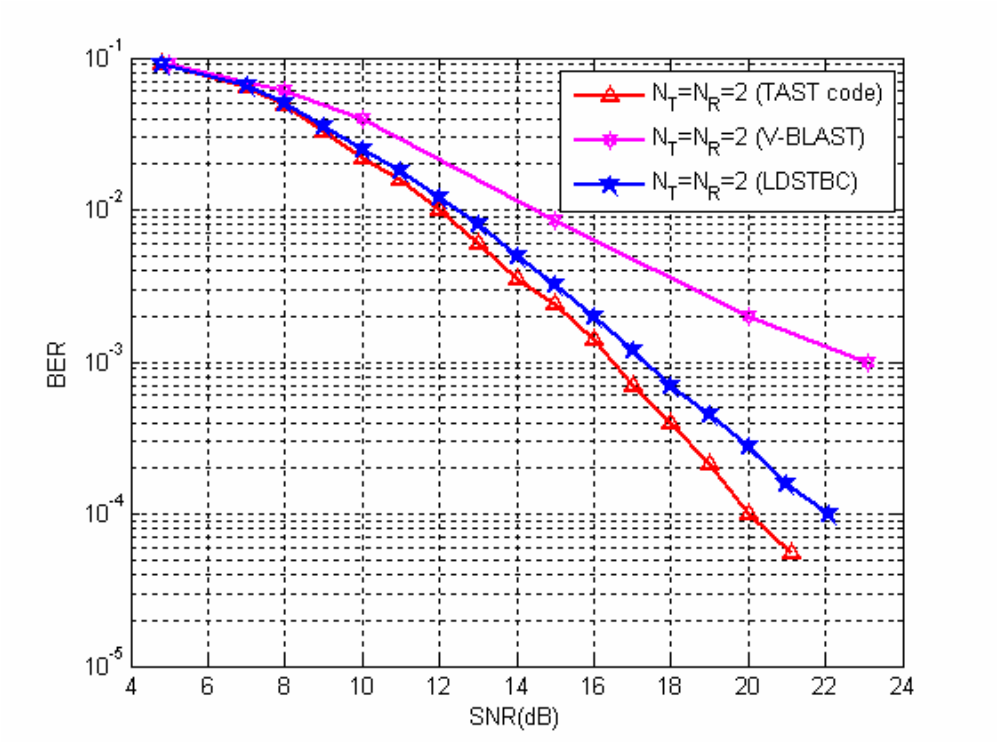

Figure 4.4 Performances analysis of DAST code

4.2.3 Block layering approach in TAST codes

The TAST codes discussed above is a powerful class of space time codes in which different layers are combined and separated by appropriate Diophantine numbers ϕ. In this section we present a technique of block layering in TAST codes. In this technique a series of layers (we call them block layers) has more than one transmit antenna at the same time instant. Therefore as a result we use less number of layers (Diophantine numbers) for four transmit antennas scheme, which enhances the coding gain for mentioned scheme. In each block layer we incorporate Alamouti transmit diversity scheme which decreases the decoding complexity. We start with basic simple Alamouti code.

$$A_1 = \phi_l \begin{bmatrix} s_1 & s_2 \\ -s_2^* & s_1^* \end{bmatrix} \quad (4.22) \quad , \quad A_2 = \phi_l \begin{bmatrix} s_3 & s_4 \\ -s_4^* & s_3^* \end{bmatrix} \quad (4.23)$$

$$A_3 = \phi_l \begin{bmatrix} s_5 & s_6 \\ -s_6^* & s_5^* \end{bmatrix} \quad (4.24) \quad , \quad A_4 = \phi_l \begin{bmatrix} s_7 & s_8 \\ -s_8^* & s_7^* \end{bmatrix} \quad (4.25)$$

For $1 \le l \le L$ (L being the numbers of layers)

It is not difficult to verify that considering any matrix from (4.22) to (4.25) results a simple Alamouti code. An additional advantage of such type of code structure is that they are flexible with respect to number of antennas. For example by simple reshuffles of (4.22) to (4.25) we get different structure of TAST codes for different set up of transmit/receive antennas. Below is a body of a simple program that might be used for this purpose.

Let N_T, N_R, L, A, denote number of transmit antennas, number of receive antennas, number of layers, and number of Alamouti matrices (given in (4.22) to (4.25)) respectively.

Initialization, N_T, N_R
Condition (No.of transmit & receive antenna)
Select (value for L and A)
Process (build TAST codeword matrix with given no. of L ,and N_T)
end

Note that for all the codes we consider Diophantine number ϕ_l in (4.12).

In section 4.2.2 we demonstrated some examples of TAST codes, in what follows, we focus a special case for $N_T = 4$ and $L = 2$.

The necessary condition of layering concept that "more than one antenna cannot transmit symbols from a given layer at a given time instant" is relaxed. A group of transmit antennas may now belong to a series (block) of layers for a given symbol period.

A block layer is indexed by a set b, $b = (a,t) \in \{1,2,...,N_T\} \times \{t_1, t_2, ..., t_T\}$, where a represents the transmit antenna and t the symbol interval. Like TAST codes [63], the idea is to map each block layer to a different subspace so that they are as far away from each other as possible. With the concept of block layers, the total number of layers becomes less and consequently fewer number of Diophantine numbers are required which increases the coding gain. Real or complex rotated symbols are used to further increase the coding gain. In each block we use Alamouti transmit diversity scheme that ensures simple decoding at the receiver.

Combining (4.22) to (4.25), we get

$$\mathcal{T}_{N_T,L,L} = \begin{vmatrix} \phi_1(A_1) & \phi_2(A_2) \\ \phi_2(A_4) & \phi_1(A_3) \end{vmatrix} \tag{4.26}$$

or more precisely

$$\mathcal{T}_{N_T,L,L} = \begin{bmatrix} \phi_1 s_1 & \phi_1 s_2 & \phi_2 s_3 & \phi_2 s_4 \\ -\phi_1 s_2^* & \phi_1 s_1^* & -\phi_2 s_4^* & \phi_2 s_3^* \\ \phi_1 s_5 & \phi_1 s_6 & \phi_2 s_7 & \phi_2 s_8 \\ -\phi_1 s_6^* & \phi_1 s_5^* & -\phi_2 s_8^* & \phi_2 s_7^* \end{bmatrix} \tag{4.27}$$

One can see that codeword matrix (4.27) has the same structure as original Alamouti code. However, this representation clearly falls within the scope of the threaded coding framework. In (4.27) ϕ_1 and ϕ_2 are two Diophantine numbers and $[s_1, s_2, ..., s_8]$ is rotated information vector to be transmitted. Table 4.2 shows the distribution of the blocks layers for code structure derived in (4.27).

The transmitted symbol $\boldsymbol{x}_l$ corresponding to source information symbol $\boldsymbol{s}_l$ over l^{th} block layer is

$$x_l(\boldsymbol{s}_l) = \phi_l \boldsymbol{x}_l = \phi_l \boldsymbol{M}_l \boldsymbol{s}_l \quad , \; l = 1, ..., L \tag{4.28}$$

where L represents the total number of block layers and $\boldsymbol{x}_l = \boldsymbol{M}_l \boldsymbol{s}_l$ is the rotated information symbol vector, and $\boldsymbol{M}_l$ is an $N_T \times N_T$ real or complex rotation matrix built on an algebraic number field $\mathbb{Q}(\theta)$ with θ an algebraic number of degree n.

Table 4.2.(Threaded structure in TAST block layering N_T =4, L = 2)

1	1	2	2
1	1	2	2
2	2	1	1
2	2	1	1

Decoding

The received signal can be written as

$$Y = \boldsymbol{H}\mathcal{T}_{N_T,L} + N \tag{4.29}$$

where $\boldsymbol{H}$ is the $N_R \times N_T$ complex Gaussian random channel matrix with element $h_{j,i}$, $j = 1, 2, ..., N_R$ and $i = 1, 2, ..., N_T$, and N is a complex Gaussian random noise vector. Let

$$y = vec(Y^T) \tag{4.30}$$

be the operation that arranges the matrix Y^T in one column vector by stacking its columns one after other, and let

$$\boldsymbol{y} = \left[y_1, y_2, ..., y_{N_R N_T} \right] \tag{4.31}$$

Simplifying equation (4.28) and (4.29), we get

$$\boldsymbol{y}' = \boldsymbol{H}'\phi'\boldsymbol{M}'\boldsymbol{s} + N \tag{4.32}$$

where

$$\boldsymbol{M}' = \begin{vmatrix} \boldsymbol{M} & \boldsymbol{A} \\ \boldsymbol{A} & \boldsymbol{M} \end{vmatrix} \tag{4.33}$$

where $\boldsymbol{A}$ is a $\mathbf{0}_{4\times4}$ matrix, $\boldsymbol{M}'$, ϕ' and $\boldsymbol{H}'$ are respectively rotation, Diophantine and the channel matrices given in (4.33) , (4.34) and (4.37), and N is obtained by converting $\text{vec}(N^T)$ into column vector by stacking its columns one after other, and $\boldsymbol{s}$ is a vector carrying source information symbols.

$$\phi' = \begin{bmatrix} \phi_1 \\ \phi_2 \end{bmatrix} \tag{4.34}$$

where

$$\phi_1 = \begin{vmatrix} \phi_1 & 0 & 0 & 0 & 0 & 0 & 0 & 0 \\ \phi_1^* & 0 & 0 & 0 & 0 & 0 & 0 & 0 \\ 0 & \phi_1 & 0 & 0 & 0 & 0 & 0 & 0 \\ 0 & \phi_1^* & 0 & 0 & 0 & 0 & 0 & 0 \\ 0 & 0 & \phi_1 & 0 & 0 & 0 & 0 & 0 \\ 0 & 0 & \phi_1^* & 0 & 0 & 0 & 0 & 0 \\ 0 & 0 & 0 & \phi_1 & 0 & 0 & 0 & 0 \\ 0 & 0 & 0 & \phi_1^* & 0 & 0 & 0 & 0 \end{vmatrix} \tag{4.35}$$

and

$$\phi_2 = \begin{vmatrix} \phi_2 & 0 & 0 & 0 & 0 & 0 & 0 & 0 \\ \phi_2^* & 0 & 0 & 0 & 0 & 0 & 0 & 0 \\ 0 & \phi_2 & 0 & 0 & 0 & 0 & 0 & 0 \\ 0 & \phi_2^* & 0 & 0 & 0 & 0 & 0 & 0 \\ 0 & 0 & \phi_2 & 0 & 0 & 0 & 0 & 0 \\ 0 & 0 & \phi_2^* & 0 & 0 & 0 & 0 & 0 \\ 0 & 0 & 0 & \phi_2 & 0 & 0 & 0 & 0 \\ 0 & 0 & 0 & \phi_2^* & 0 & 0 & 0 & 0 \end{vmatrix} \tag{4.36}$$

$$\boldsymbol{H}' = [h_1 \; h_2] \tag{4.37}$$

where

$$h_1 = \left(\begin{bmatrix} h_{ij} & 0 & h_{ij+1} & 0 & 0 & 0 & 0 & 0 \\ 0 & h_{ij+1}^* & 0 & -h_{ij}^* & 0 & 0 & 0 & 0 \\ 0 & 0 & 0 & 0 & h_{ij+2} & 0 & h_{ij+3} & 0 \\ 0 & 0 & 0 & 0 & & h_{ij+3}^* & 0 & -h_{ij+3}^* \end{bmatrix} \right)_{\substack{i=1,2,3,4 \\ j=1}} \tag{4.38}$$

$$h_2 = \left(\begin{bmatrix} h_{ij-1} & 0 & h_{ij} & 0 & 0 & 0 & 0 & 0 \\ 0 & h_{ij}^* & 0 & -h_{ij-1}^* & 0 & 0 & 0 & 0 \\ 0 & 0 & 0 & 0 & h_{ij-3} & 0 & h_{ij-2} & 0 \\ 0 & 0 & 0 & 0 & 0 & h_{ij-2}^* & 0 & -h_{ij-3}^* \end{bmatrix} \right)_{\substack{i=1,2,3,4 \\ j=4}} \tag{4.39}$$

Note that h_1 and h_2 are stacked into column for different values of i.

Figure 4.5 shows the simulation result of the proposed block layering scheme. For comparison we have included the results for TAST codes with two and four layers. For all cases the number of transmit and receiver antennas are taken as four.

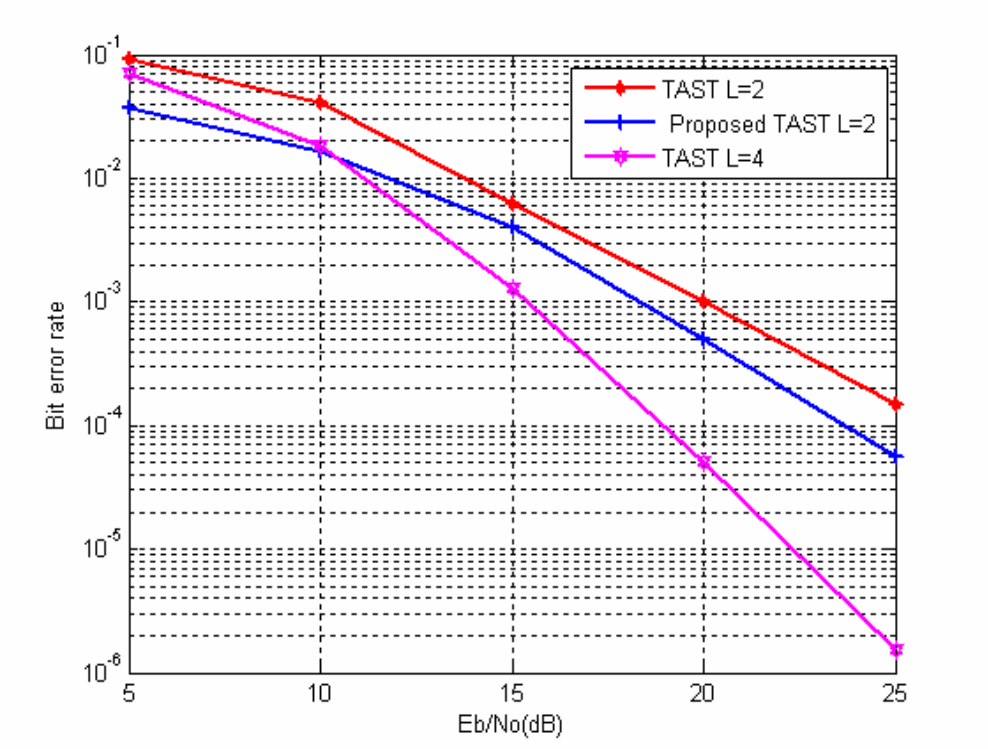

Figure 4.5 Comparison of different TAST codes

4.3 Construction of STBCs from cyclic division algebras

Algebraic codes can also be constructed from cyclic division algebra. Cyclic division algebra is itself a vast field, so it is beyond the scope of this report to elaborate it in depth. In what follows, we put a bird eye view over the subject and for detail interested reader is referred to [17], [65].

In fact cyclic division algebra is particular family of division algebras which are built over the number fields, with base field $\mathbb{Q}(i)$ or $\mathbb{Q}(j)$, with $i^2 = -1$ and $j^3 = 1$, which are helpful in describing QAM or HEX constellations.

Before starting our main topic of discussion, here we would like to lay down definitions of some basic terms which would help us to understand the main topic without any confusion.

Number field: Let $\mathbb{Q}$ denotes the set of rational numbers, which can be verified to be a field. Other fields can be built from $\mathbb{Q}$. For example the element *i*, such that $i^2 = -1$, which is not an element of $\mathbb{Q}$ can be used to build a new field by adding *i* to $\mathbb{Q}$, and is generally denoted by $\mathbb{Q}(i)$. Similarly adding *i* to $\mathbb{R}$ can create a new field $\mathbb{C}$. Where $\mathbb{R}$ and $\mathbb{C}$ denote real and complex fields, respectively.

Fields extension: Let $\mathbb{F}$ and $\mathbb{K}$ be two fields. If $\mathbb{F} \subseteq \mathbb{K}$, we say that $\mathbb{K}$ is a field extension of $\mathbb{F}$, and is denoted by $\mathbb{K}/\mathbb{F}$.

Algebraic fields extension: If all element of $\mathbb{K}$ are algebraic over $\mathbb{F}$, we say that $\mathbb{K}$ is an algebraic extension of $\mathbb{F}$. Remember that an algebraic number *r* is a root of a non-zero polynomial equation with degree *n*, who does not satisfies any other similar equation of degree < *n*,

Degree of Filed: Let $\mathbb{K}/\mathbb{F}$ be a field extension. The dimension of $\mathbb{K}$ as vector space over $\mathbb{F}$ is called the degree of $\mathbb{K}$ over $\mathbb{F}$, and is denoted by $[\mathbb{K}:\mathbb{F}]$.

Galois group: Let X^2+1 is a minimum polynomial of *i* over $\mathbb{Q}$, and *i* is algebraic over $\mathbb{Q}$. X^2+1 has exactly two embeddings, *i.e.* $X^2+1=(X+i)(X-i)$ and both embeddings are also mapping from $\mathbb{Q}(i)$ to itself, in other words both roots of the minimal polynomial X^2+1 belong to $\mathbb{Q}(i)$. Thus $\mathbb{Q}(i)/\mathbb{Q}$ is called Galois extension. The two embeddings σ_1 and

σ_2 of $\mathbb{Q}(i)$ form a group of two elements where σ_2 is invertible. Such a group is called Galois group. One may have noticed that Galois group is generated by one element and all the other elements of the group are obtained as the power of one element of the group. Such a group is called cyclic. A Galois cyclic group is denoted by $\langle\sigma\rangle$, where σ is generator of the group.

4.3.1 Perfect STBCs

Given a field $\mathbb{F}$, let $\mathbb{K}$ be a cyclic extension of $\mathbb{F}$ of degree *n* such that its Galois group $G = Gal(\mathbb{K}/\mathbb{F})$ is cyclic, with generator σ. Then we define a non-commutative algebra $\mathrm{A} = (\mathbb{K}/\mathbb{F}, \sigma, \gamma)$ as

$$\mathrm{A} = 1.\mathbb{K} \oplus e.\mathbb{K} \oplus ..... \oplus e^{n-1}.\mathbb{K} \tag{4.40}$$

Such that

$\gamma \in \mathbb{F}^*$ (Non-zero elements of $\mathbb{F}$ (resp.$\mathbb{K}$), $e^n = \gamma$, $\forall x \in \mathbb{K}$, $xe = e\sigma(x)$ and $\oplus$ denotes the direct sum.

Such an algebra is called a cyclic algebra [17] and algebra A encompasses the direct sum of copies of $\mathbb{K}$, which means that an elements *x* in the algebra is written as

$$x = x_0 + ex_1 + ... + e^{n-1}x_{n-1}\ , \qquad x_i \in \mathbb{K} \tag{4.41}$$

Now if we do left multiplication of an element of the algebra by *x* in the basis $\{1, e, e^2, .., e^{n-1}\}$, we get

$$\begin{bmatrix} x_0 & \gamma\sigma(x_{n-1}) & \gamma\sigma^2(x_{n-2}) & \dots & \gamma\sigma^{n-1}(x_1) \\ x_1 & \sigma(x_0) & \gamma\sigma^2(x_{n-1}) & \dots & \gamma\sigma^{n-1}(x_2) \\ \vdots & & \vdots & & \vdots \\ x_{n-2} & \sigma(x_{n-3}) & \sigma^2(x_{n-4}) & \dots & \gamma\sigma^{n-1}(x_{n-1}) \\ x_{n-1} & \sigma(x_{n-2}) & \sigma^2(x_{n-3}) & \dots & \sigma^{n-1}(x_0) \end{bmatrix} \tag{4.42}$$

An example for $n = 2$

$$\begin{aligned} xy &= (x_0 + ex_1)(y_0 + ey_1) \\ &= x_0 y_0 + x_0 ey_1 + ex_1 y_0 + ex_1 ey_1 \\ &= x_0 y_0 + e\sigma(x_0) y_1 + ex_1 y_0 + \gamma\sigma(x_1) y_1 \\ &= (x_0 y_0 + \gamma\sigma(x_1) y_1) + e(\sigma(x_0) y_1 + x_1 y_0) \end{aligned}$$

Since $e^2 = \gamma$. We represent it in matrix form, in the basis $\{1, e\}$ as follows:

$$xy = \begin{bmatrix} x_0 & \gamma\sigma(x_1) \\ x_1 & \sigma(x_0) \end{bmatrix} \begin{bmatrix} y_0 \\ y_1 \end{bmatrix} \tag{4.43}$$

One can see that the structure of (4.43) is same as that of Alamouti code. Of course this representation is within the framework of cyclic algebra. So the codebooks for two antennas yield:

$$C = \left\{ \begin{bmatrix} x_0 & \gamma\sigma(x_1) \\ x_1 & \sigma(x_0) \end{bmatrix}^T \middle| x_0, x_1 \in \mathbb{K} \right\} \tag{4.44}$$

In general, if $\mathbb{K}/\mathbb{F}$ has degree n, each coefficient x_i of $x = \sum_{i=0}^{n-1} e^i x_i$ ($x_i, i = 0,...,n-1$ are coefficient of field $\mathbb{F}$) will encode n information symbols. Since the element $x \in$ A has n coefficients, it encodes n^2 information symbols. Codes obtained from cyclic algebras are said to be full rate in the sense that they transmit n^2 signals that encode n^2 information symbols. In other words perfect codes have a diversity order of $N_T N_R$ and a rate $R = N_T$. Perfect codes possess another advantage that with an optimal choice of rotation parameter, their coding gains do not decrease with the size of constellation. Full rate perfect STBCs constructed from cyclic algebras are possible for 2×2 , 3×3 , 4×4 and 6×6 systems.

4.3.2 Golden code

The golden code is 2×2 perfect code, and was independently proposed by three groups, Dayal and Varanasi [75], Yao and Wornell [76] optimized the rotations and Diophantine numbers (*i.e.* θ and ϕ) in a general 2×2 linear TAST code, whereas Belfiore et al. constructed the code from a cyclic division algebra [77]. The name golden was given because of the usage of golden number in its construction.

Let $\mathbb{K}/\mathbb{Q}(i)$ be a relative extension of degree 2 of $\mathbb{Q}(i)$ of the form $\mathbb{K}=\mathbb{Q}\left(i,\sqrt{5}\right)$, then $\mathbb{K}$ can be represented as a vector space over $\mathbb{Q}(i)$ [17]

$$\mathbb{K}=\left\{x_1+x_2\sqrt{5}\ \ \middle|x_1,x_2\in\mathbb{Q}(i)\right\} \tag{4.45}$$

Its Galois group $Gal\left(\mathbb{K}/\mathbb{Q}\right)=\langle\sigma\rangle$ is generated by $\sigma:\sqrt{5}\to-\sqrt{5}$. The correspondence cyclic algebra of degree 2 is $\mathrm{A}=\left(\mathbb{K}=/\mathbb{Q}(i,\sqrt{5})/\mathbb{Q}(i),\sigma,\gamma\right)$.

With $\gamma=i$ and using a suitable ideal $\mathcal{I}\subseteq\mathcal{O}_{\mathbb{K}}$, we get

$$\mathcal{O}_{\mathbb{K}}\left\{x_1+x_2\theta\middle|x_1,x_2\in\mathbb{Q}(i)\right\} \tag{4.46}$$

Before shaping, the codeword has the form as:

$$\begin{bmatrix} x_1+x_2\theta & x_3+x_4\theta \\ i(x_3+x_4\sigma(\theta)) & (x_1+x_2\sigma(\theta)) \end{bmatrix} \tag{4.47}$$

After rotation and normalization by factor of $\frac{1}{\sqrt{5}}$, weget

$$\frac{1}{\sqrt{5}}\begin{bmatrix} \alpha[x_1+x_2\theta] & \alpha[x_3+x_4\theta] \\ i\sigma(\alpha)[x_3+x_4\sigma(\theta)] & \sigma(\alpha)[x_1+x_2\sigma(\theta)] \end{bmatrix} \tag{4.48}$$

where

- x_1,x_2,x_3,x_4 are information symbols which can be taken from QAM constellation carved from $\mathbb{Z}[i]$
- $i=\sqrt{-1}$
- $\theta=\frac{1+\sqrt{5}}{2}=1.618$ (Golden number)
- $\sigma(\theta)=\frac{1-\sqrt{5}}{2}=1-\theta$
- $\alpha=1+i-i(\theta)=1+i\sigma(\theta)$
- $\sigma(\alpha)=1+i-i\sigma(\theta)=1+i(\theta)$

Using the relation $\theta\sigma(\theta)=-1$ and $\theta+\sigma(\theta)=1$ we can write (4.48) as

$$\frac{1}{\sqrt{5}}\begin{bmatrix}[1+i\sigma(\theta)]x_1+[\theta-i]x_2 & [1+i\sigma(\theta)]x_3+[\theta-i]x_4\\ [i-\theta]x_3+[1+i\sigma(\theta)]x_4 & [1+i\theta]x_1+[\sigma(\theta)-i]x_2\end{bmatrix} \tag{4.49}$$

The golden code is full rate (since it contains 4-information symbols) and fully diverse. The minimum determinant of the Golden code $\frac{1}{\sqrt{5}}$

4.4 Delay tolerant distributed TAST codes

In a distributed cooperative communication system, since the distances between the individual transmitting nodes and the receiving nodes may be different, so the performances of STBCs at receiving nodes may severely be degraded if timing synchronization is not assured. In this section we present some useful techniques for construction of TAST codes, which are delay tolerant and hence suitable to be used in distributed cooperative networks. Our proposed codes achieve full diversity for arbitrary number of relays, and arbitrary number of transmit/receive antennas and input alphabets.

As we discussed in chapter 2, in a cooperative communication system, the communication between source and destination is modelled in two phases.

In phase-I: the source sends information to intended destination and at the same time this information is also received by the relays.

In phase-II: The relays help the source by forwarding or retransmitting the received information to destination.

Relays use different protocols for processing and re-transmitting the received signal from source to destination [21]. In the sequel, we mainly focus on DF relaying protocol.

Since the relay nodes use common time slots and frequency bandwidth for retransmissions of their signals, therefore the relays may expose to overlap both in time and frequency, *i.e.* each node transmits a distinctly coded bit stream, the superposition of which forms a space time code. In what follows, the design and performance analysis of such distributed STBCs will be our main focus.

We assume the conventional MIMO system modelled with N_T transmit antennas corresponding to N relays and N_R receive antennas at the destination. At time instant t, the received signal can be expressed in vector notation as

$$\overline{r}_t = H_t \overline{x}_t + \overline{n}_t \tag{4.50}$$

where $\overline{r}_t \in \mathbb{C}^{N_R \times 1}$ is received vector at time t, $\overline{x}_t \in \mathbb{C}^{N_T \times 1}$ is modulated signal vector transmitted during the t-th symbol interval, $H_t \in \mathbb{C}^{N_R \times N_T}$ is the channel matrix, and $\overline{n}_t \in \mathbb{C}^{N_R \times 1}$ denotes AWGN. The $N_T \times T$ modulated space time codeword matrix $\boldsymbol{x}$ is transmitted over T symbol intervals by taking $\overline{x}_t$ to be the t-th column of $\boldsymbol{x}$. The channel is assumed to be quasi-static, *i.e.* the channel transfer matrix H_t is constant over a codeword interval but is random and independent from codeword to codeword. We further assume that no errors occur between source and relays.

The nature of processing strategies at relays greatly impact the code design and decoding complexity. In the simplest case, the communication system design may be based on a postulated worst case in which the delay among different relay transmissions at the intended receivers extend the space time codeword transmissions using either arbitrary fill symbols or silent guard intervals to cover this worst case timing uncertainty [68]. If the maximum possible timing offset among the different relay's transmissions is L symbol intervals and a pad of duration L' symbols is used by each relay between its coded transmissions, then, as shown in figure 4.6(a), the different composite space time codewords never overlap in time. Each space time codeword can be decoded individually. For short STBCs, the significant rate loss induced by the use of fill symbols or guard intervals can be mitigated, as proposed in [68], by allowing the relays to transmit its coded streams one after another. Of course, for long block size the code rate loss is an open problem. Figure 4.6(b) depicts a view of transmission without guard intervals in which the composite space time codewords may potentially interfere with one another, so decoding is more complex.

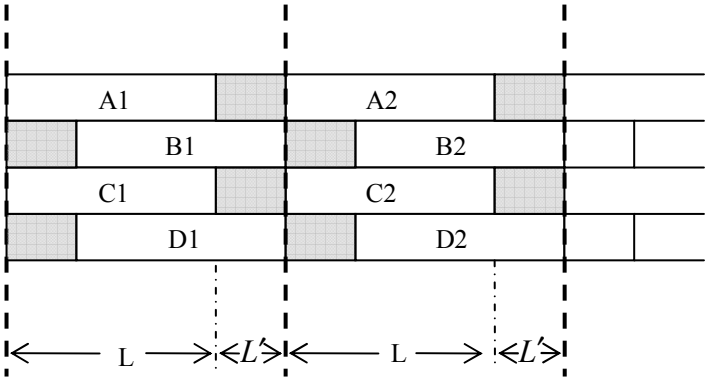

Figure 4.6(a) Transmission using pad between codes words

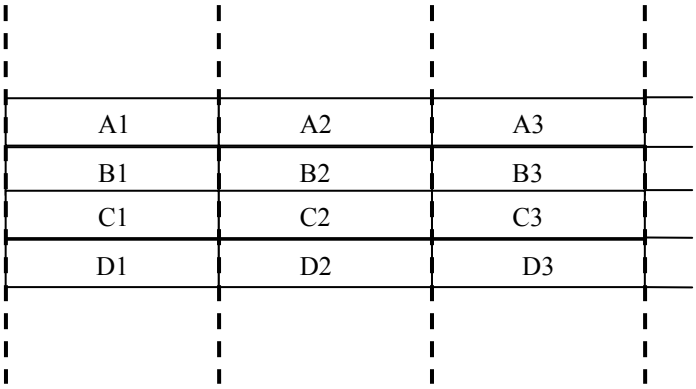

Figure 4.6(b) Transmission without pad between codes words

4.4.1 Delay tolerance of space time codes

Now let $\mathcal{X}$ be a STBC for N_T transmit antennas and T channel uses, and assume that $\boldsymbol{x}_1$ and $\boldsymbol{x}_2$ are two distinct codewords of $\mathcal{X}$. The diversity order of $\mathcal{X}$ is minimum rank of the difference matrix $\boldsymbol{x}_1 - \boldsymbol{x}_2$ over all pairs of distinct codeword in $\mathcal{X}$. This condition is referred as baseband rank criterion [38].

For our purpose, the transmitted symbols will be finitely generated from an underlying finite constellation using algebraic number field constructions. Let $\mathcal{A}$ denote the two-dimensional constellation chosen from $\mathbb{Z}[i]$ or $\mathbb{Z}[j]$, and let $\mathbb{F} = \mathbb{Q}(i)$ or $\mathbb{Q}(j)$ denote the field of complex rational numbers and complex Eisenstein rational numbers[2], respectively. Let $\mathbb{F}(\theta)$ be an extension field of degree $[\mathbb{F}(\theta):\mathbb{F}]$.Then the fundamental alphabet for our constructions is given by

$$\Omega = \left\{ s = \sum_{k=0}^{P-1} u_k \theta^k \ : u_k \in \mathcal{A} \right\} \tag{4.51}$$

where integer $P \le [\mathbb{F}(\theta):\mathbb{F}]$. Each transmitted symbol $x \in \boldsymbol{x}$ is from Ω or, more generally, is from its image $f(\Omega)$ under some specified one-to-one mapping $f : \Omega \to \mathbb{C}$.

A space time code $\mathcal{X}$ is τ-delay tolerant for the quasi-synchronous cooperative diversity scenario, if the difference between every nontrivial pair of codewords in $\mathcal{X}$ retains full rank

[2] Eisenstein numbers are complex numbers of the form $z = a+bw$. Where a and b are integers and $w = 1/2(-1+i\sqrt{3}) = e^{2\pi i/3}$

even though its rows are transmitted with arbitrary delays of duration at most τ symbols [69],[78].

To make this definition more clear, suppose that an $N_T \times T$ modulated codeword matrix $\boldsymbol{x} \in \mathcal{X}$, consisting of rows $\overline{r}_1, \overline{r}_2, ..., \overline{r}_{N_T}$, is transmitted cooperatively by N relays, whose various transmissions are received with delay profile $\Delta = (\delta_1, \delta_2, ...\delta_{N_T})$, where δ_i denotes the relative delay of the signal received from the i-th relay as reference to the earliest received relay signal. This is equivalent to receive the $N_T \times (T + \delta_{\max})$ matrix

$$\boldsymbol{x}^{\Delta} = \begin{bmatrix} \mathbf{0}^{\delta_1} & \overline{r}_1 & \mathbf{0}^{\delta_{\max} - \delta_1} \\ \mathbf{0}^{\delta_2} & \overline{r}_2 & \mathbf{0}^{\delta_{\max} - \delta_2} \\ \vdots & \vdots & \vdots \\ \mathbf{0}^{\delta_{N_T}} & \overline{r}_{N_T} & \mathbf{0}^{\delta_{\max} - \delta_{N_T}} \end{bmatrix} \tag{4.52}$$

where $\mathbf{0}^{\delta_i}$, $i = 1, ..., N_T$ denotes an all-zero vector of length δ_i (0 means no transmission) and $\delta_{\max}$ denotes the maximum of the relative delays. Now, a space-time code $\mathcal{X}$ is called τ-delay tolerant if for all delay profiles Δ with $\delta_{\max}(\Delta) \le \tau$, the effective space-time code $\mathcal{X}^{\Delta}$ achieves same spatial diversity as that of $\mathcal{X}$. A space-time code is fully delay tolerant if it is delay tolerant for any positive integer τ. For ease to write from now on we use the term delto as short form for **de**lay **to**lerant.

To have a clearer concept on delay tolerant codes, consider the following 3×3 STBC examples consisting of the BPSK modulated matrices [69]

$$\boldsymbol{x} = \begin{bmatrix} (-1)^a & (-1)^b & (-1)^c \\ (-1)^c & (-1)^{a+c} & (-1)^b \\ (-1)^b & (-1)^{b+c} & (-1)^{a+c} \end{bmatrix} \qquad \forall a, b, c \in GF(2) \tag{4.53}$$

By the Hammons–El Gamal binary rank criterion [79], the STBC achieves full spatial diversity since the corresponding unmodulated binary codewords are of full rank over the finite field GF(2) when nonzero.

$$\boldsymbol{s} = \begin{bmatrix} a & b & c \\ c & a+c & b \\ b & b+c & a+c \end{bmatrix} \tag{4.54}$$

In particular, one notes that $det\ \boldsymbol{s} = a+b+c+ab+ac+bc+abc$, which is equal to zero if and only if $a=b=c=0$. Suppose that, in the cooperative scenario, the first transmission (first row) is delayed by one symbol compared to the second and third transmissions. In this case, we say that the relative delay profile for these transmissions is $\Delta=(1,0,0)$. Then the unmodulated binary codeword matrices effectively become

$$\boldsymbol{s}^{\Delta}=\begin{bmatrix} 0 & a & b & c \\ c & a+c & b & 0 \\ b & b+c & a+c & 0 \end{bmatrix} \tag{4.55}$$

Now suppose, $a=1$ and $b=c=0$, we get

$$\boldsymbol{s}^{\Delta}=\begin{bmatrix} 0 & 1 & 0 & 0 \\ 0 & 1 & 0 & 0 \\ 0 & 0 & 1 & 0 \end{bmatrix} \tag{4.56}$$

One can see that (4.56) lost its rank from 3 to 2. Thus, this code is not delay tolerant. Similarly the TAST codes obtained from titled-QAM proposed by [76] lose their diversity when minimum delay is observed. The TAST codes constructed from cyclic algebra [17], [65] are also not delto. Consider the code given in (4.42)

$$\begin{bmatrix} x_0 & \gamma\sigma(x_{n-1}) & \gamma\sigma^2(x_{n-2}) & \cdots & \gamma\sigma^{n-1}(x_1) \\ x_1 & \sigma(x_0) & \gamma\sigma^2(x_{n-1}) & \cdots & \gamma\sigma^{n-1}(x_2) \\ \vdots & & \vdots & & \vdots \\ x_{n-2} & \sigma(x_{n-3}) & \sigma^2(x_{n-4}) & \cdots & \gamma\sigma^{n-1}(x_{n-1}) \\ x_{n-1} & \sigma(x_{n-2}) & \sigma^2(x_{n-3}) & \cdots & \sigma^{n-1}(x_0) \end{bmatrix} \tag{4.57}$$

Consider $x_1 = x_2 .... = x_{n-1} = 0$ yields codeword matrix of the form

$$\begin{bmatrix} x_0 & 0 & \cdots & 0 \\ 0 & \sigma(x_0) & \cdots & 0 \\ \vdots & \vdots & \ddots & \vdots \\ 0 & 0 & \cdots & \sigma^{n-1}(x_0) \end{bmatrix} \tag{4.58}$$

Delaying the first row of (4.58) by one symbol interval produces codeword matrix of the following form

$$\begin{bmatrix} 0 & x_0 & \dots & 0 & 0 \\ 0 & \sigma(x_0) & \dots & 0 & 0 \\ \vdots & \vdots & \ddots & \vdots & \vdots \\ 0 & 0 & \dots & \sigma^{n-1}(x_0) & 0 \end{bmatrix} \tag{4.59}$$

Hence TAST codes constructed from cyclic algebra are also not delay tolerant.

In what follows, we provide some easy and useful technique for constructing TAST codes which are delto for arbitrary delay profile.

4.4.2 Construction of delto codes

In this section we try to develop two useful techniques for construction of general STBCs based on threads that are delay tolerant. The constructed codes achieve maximal spatial diversity and are fully delto. They are also flexible with respect to signalling constellation, transmission rate, number of transmit and receive antennas, and decoder complexity. For most of the cases, we use the fundamental signalling alphabet Ω derived from constellation $\mathcal{A}$ in accordance with (4.51).

A layer is a mapping strategy that assigns a particular transmit antenna to be used at each individual time interval of a code word [60]. A layer is called a thread when it spans in spatial and temporal dimensions in such a way that at each time instant: $1 \le t \le T$ at most one antenna is used [61]. With a minor modification, we relax the condition of antenna usage at each time interval and allow signalling intervals to be empty, *i.e.* no symbol be transmitted from any antennas during certain signalling intervals.

We use a technique very similar to that of Huffman (HM) binary tree. We develop a HM binary tree of N_T+1 nodes. We assume that nodes 2 (node 1 is discarded) to N_T+1 of the HM binary tree represents the rows 1 to N_T of codeword matrix, respectively. We further assume that the weights or more precisely Hamming weights of nodes $m_i \; i=1,2,...,N_T+1$ are such that $m_i > m_{i+1} > .... > m_{N_T+1}$ and $m_{N_T-1} > +m_{N_T} + m_{N_T+1}$. With these assumptions, we may construct the HM tree in a straightforward manner starting from bottom node coming up to top node.

As an example, consider the Huffman (HM) thread Λ defined for N_T transmit antennas, where

$$T_{N_T}^{HM} = N_T \times \left\lceil \frac{N_T}{2} \right\rceil + \left(\frac{1+(-1)^{N_T}}{2} \right) \left\lceil \frac{N_T}{2} \right\rceil \tag{4.60}$$

For $N_T = 3$ and 4, we draw the following two HM binary trees to obtain HM threads

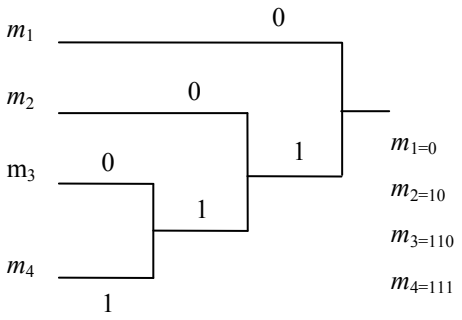

Figure 4.7(a) construction of HM binary tree for 3 transmit antennas

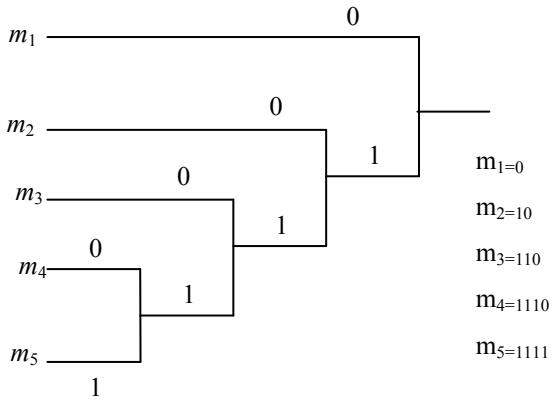

Figure 4.7(b) construction of HM binary tree for 4 transmit antennas

Putting the obtained numerical values in matrix form in a row end-to-start manner by non-zero elements, *i.e.* after discarding the first node of the tree, the m_{i+2}-th row is started immediately from next column in which m_{i+1}-th has its last non-zero element. The process is repeated till m_{N_T+1}-th row. The empty positions are filled by zeros, for $N_T = 3$ we get

$$\Lambda_3^{HM} = \begin{bmatrix} 1 & 0 & 0 & 0 & 0 & 0 \\ 0 & 1 & 1 & 0 & 0 & 0 \\ 0 & 0 & 0 & 1 & 1 & 1 \end{bmatrix} \tag{4.61}$$

and for $N_T = 4$, we have

$$\Lambda_4^{HM} = \begin{bmatrix} 1 & 0 & 0 & 0 & 0 & 0 & 0 & 0 & 0 & 0 \\ 0 & 1 & 1 & 0 & 0 & 0 & 0 & 0 & 0 & 0 \\ 0 & 0 & 0 & 1 & 1 & 1 & 0 & 0 & 0 & 0 \\ 0 & 0 & 0 & 0 & 0 & 0 & 1 & 1 & 1 & 1 \end{bmatrix} \tag{4.62}$$

As an alternate method, we can develop such type of codeword matrices by using the following expression, where the thread Λ_{HM} has (i, j) entry as

$$\Lambda(i,j) = \begin{cases} 1, \ if \quad i = \left(\lfloor \log_2 j + \delta_{j,7} \rfloor + 1 \right) \\ 0 \ , \ \text{otherwise} \end{cases} \tag{4.63}$$

where the Kronecker delta function is defined as

$$\delta_{j,7} = \begin{cases} 1 \ , \ \text{if} \, j = 7 \\ 0 \ , \ \text{otherwise} \end{cases} \tag{4.64}$$

Lemma 1: Let $\mathcal{X} = \Omega\Lambda_{HM}$ denote the space time code in which the repetition code over alphabet Ω is used over the thread Λ_{HM}, then $\mathcal{X}$ achieves full spatial diversity and is fully delto.

Proof: One can see that $\mathcal{X}$ encompasses multiples of Λ_{HM}, so all the differences between codeword in $\mathcal{X}$ are multiples of Λ_{HM}^{Δ}, hence it is easy to show that Λ_{HM}^{Δ} is of full rank for all delay profiles. One can see that regardless of delay profile Δ size, the *i*-th row of Λ_{HM}^{Δ} always contains the same number of ones as its position in that matrix. (*i.e.* $m_i = i$) whereas the total number of nonzero elements in all lower numbered rows is $i(i-1)/2$. Hence, for each *i*, there is a column in Λ_{HM}^{Δ} for which the entry in the *i*-th row is 1 and all the elements above it are zeros. The set of these columns for $i = 1$ to N_T forms an $N_T \times N_T$ submatrix that is lower-triangular with ones on the diagonal. Since this submatrix has determinant 1, so we can say that Λ_{HM}^{Δ} is of full rank.

As we see from the codeword matrices (4.61) and (4.62) that any permutation of rows or columns may be done in Λ_{HM} to produce an equivalent thread yet preserving the properties of its parent code, deletion of rows in Λ_{HM} also would not affect the delto property.

Now generalizing the obtained results over DAST codes [62], for $t = 1, 2, ...T_{N_T}^{HM}$. Consider $f_t : \Omega \to \mathbb{C}$ be a one to one function, and we derive the corresponding thread function matrix $\mathbf{F}_{\Lambda}(x)$ for thread Λ_{HM} by replacing the non-zero element in matrix Λ_{HM} by the function $\mathbf{F}_{\Lambda}(x)$. For example for $N_T = 4$, we have

$$\mathbf{F}_\Lambda(x)=\begin{bmatrix} f_1(x) & 0 & 0 & 0 & 0 & 0 & 0 & 0 & 0 & 0 \\ 0 & f_2(x) & f_3(x) & 0 & 0 & 0 & 0 & 0 & 0 & 0 \\ 0 & 0 & 0 & f_4(x) & f_5(x) & f_6(x) & 0 & 0 & 0 & 0 \\ 0 & 0 & 0 & 0 & 0 & 0 & f_7(x) & f_8(x) & f_9(x) & f_{10}(x) \end{bmatrix} \quad (4.65)$$

Lemma 2*:* let $\mathcal{X}$ denote space time code of form $\boldsymbol{x}_a=\mathbf{F}_\Lambda(a)$ for some $a\in\Omega$. Then $\mathcal{X}$ achieves full diversity and is delto.

Proof: If *a* and *b* are two distinct code word of $\mathcal{X}$, then the difference codeword matrix $f_\Lambda(a)$ and $f_\Lambda(b)$, will adopt the same form as Λ_{HM}, by replacing 1 for $t=1,2,...,T_{N_T}^{HM}$ by the difference matrix $f_t(a)-f_t(b)$.

Let an arbitrary delay profile Δ be applied to the difference matrix $f_\Lambda(a)-f_\Lambda(b)$ to produce the matrix $\mathbf{F}^\Delta$, then as proved before the columns $t_1,t_2,...t_{N_T}$ in $\mathbf{F}^\Delta$ form a lower triangular matrix with diagonal entries equal to $f_{ti}(a)-f_{ti}(b)$ for $i=1,2,...,N_T$ and this matrix has determinant

$$D=\prod_{i=1}^{N_T}(f_{t_i}(a)-f_{t_i}(b)) \quad (4.66)$$

Since all the functions f_{t_i} are one to one, so the determinant *D* will be zero subject to condition if *a* = *b*, likewise $\mathbf{F}_\Lambda(a)$ will be equal to $\mathbf{F}_\Lambda(b)$ if *a*=*b*. Therefore the matrix $\mathbf{F}^\Delta$ is of full rank.

Another Method

The HM method for codeword matrices construction may be lethargic for large value of N_T. As one can see from code structure, there is a large disparity or unevenness in usage of antennas. Here we develop another method of thread matrix construction in which each antenna is used for the same number of time. We call this technique of thread construction as Uniform Use (UU) generalized threads. In this particular scheme each transmit antenna is used twice per codeword. The two non-zero elements of the codeword matrix in row i $(i=1,2,...,N_T)$ are spanned by $u_i=\left\lfloor 2^{i-2}+\frac{i}{N_T}\right\rfloor$[3], where u is the number of zeros between two non-zero elements in row i. The first non-zero element in row i lies in columns j according to table 4.3.

[3] For $N_T>4$, plus sign is replaced by minus sign.

For example for $N_T = 3$ and 4, we have the following two matrices, where $T_{N_T}^{UU} = 2N_T$

$$\Lambda_{UU} = \begin{bmatrix} 0 & 1 & 1 & 0 & 0 & 0 \\ 0 & 0 & 0 & 1 & 0 & 1 \\ 1 & 0 & 0 & 0 & 1 & 0 \end{bmatrix} \tag{4.67}$$

$$\Lambda_{UU} = \begin{bmatrix} 0 & 1 & 1 & 0 & 0 & 0 & 0 & 0 \\ 0 & 0 & 0 & 1 & 0 & 1 & 0 & 0 \\ 0 & 0 & 0 & 0 & 1 & 0 & 0 & 1 \\ 1 & 0 & 0 & 0 & 0 & 0 & 1 & 0 \end{bmatrix} \tag{4.68}$$

The UU design is fully delto and offers full diversity.

Equivalently we can construct such codeword matrices for UU threads as follow, where (*i*,*j*)th entry is defined as

$$\Lambda_{(i,j)} = \begin{cases} 1\ , \text{ if } i_{del \bmod_{N_T}} = \lfloor \log_2 j + \delta_j \rfloor \\ 0\ , \text{ otherwise} \end{cases} \tag{4.69}$$

where *delmod* is an ordinary modulo function, and is not taken into account when kronecker delta function δ_j is active, and the Kronecker delta function is defined as

$$\delta_j = \begin{cases} P_{(i+2)}, \ if \ \ P_i = j \\ 0\ , \quad \text{otherwise} \end{cases} \tag{4.70}$$

where, *P* is a vector of first *T* elements of safe prime numbers[4].

Table 4.3. (Positions of leading nonzero elements in respective UU threads matrices)

I/J	$N_T = 3$	$N_T = 4$	$N_T = 5$
1	2	2	2
2	4	4	6
3	1	5	4
4	-	1	5
5	-	-	1

*Lemma:*3 Let $\mathcal{X} = \Omega\Lambda_{UU}$ be the $N_T \times T_{N_T}^{UU}$ space time code in which the repetition code is used over the thread Λ_{UU}. Then $\mathcal{X}$ achieves full spatial diversity and is fully delto.

Proof: as one can see from code structure, it is easy to show that for any delay profile Δ, the *i*-th row of the thread matrix cannot be expressed as a linear combination of rows 1 through $N_T - 1$.

[4] A safe prime is a prime number of the form 2*p* + 1, where *p* is also a prime. For example first 7 Safe prime no. are [5,7,11,23,47,59,83]

The two non-zero elements in *i*-th row are separated by *u* zero elements, where *u* given by:

$$u_i = \begin{cases} 0 \text{ if } i = 1 \\ 2^{i-2}+1 \text{ if } i = N_T \\ 2^{i-2} \text{ if } 2 \le i < N_T \end{cases} \tag{4.71}$$

or more precisely

$$u_i = \left\lfloor 2^{i-2} + \frac{i}{N_T} \right\rfloor \tag{4.72}$$

Furthermore the leading non-zero element in row i_1 and i_{N_T} always starts from column j_2 and j_1 respectively, whereas the second non-zero element of same rows lies in j_2 and j_{2N_T-1} respectively. Likewise for the rest of the rows the second non-zero elements lay in position $j_i + \varpi$, where ϖ is position of leading non-zero element in that row.

We know that in the linear combination of even weight rows, if the leading non-zero element in row N_T lies in column j_i, then there must be an odd number of rows having a non-zero element in column j_i[69]. Therefore we say that our proposed codeword is fully delto.

4.4.3 Construction of multiple thread delto code

In previous section, we discussed different techniques for construction of single thread delto codes. To improve the rate of these codes, we combine multiple delay tolerant threads in single codeword matrices. There are more than one ways of packing such threads. Here we discuss two methods similar to [69], as follows:

A-cyclic shift method

This method has a very simple and interesting structure. We use to shift each column of thread matrix Λ_k $(k = 1, 2, ..., N_T)$ by one element in thread matrix Λ_{k+1}. We repeat the process till the last thread Λ_{N_T}.

Let Λ_k be thread k for N_T transmit antennas and T vector channel uses. Then for $N_T = 4$ and $T_{N_T}^{HM} = N_T \times \left\lceil \frac{N_T}{2} \right\rceil + \left(\frac{1+(-1)^{N_T}}{2} \right) \left\lceil \frac{N_T}{2} \right\rceil$, for thread matrix Λ_1^{HM}, we get

$$\Lambda_1^{HM} = \begin{bmatrix} 1 & 0 & 0 & 0 & 0 & 0 & 0 & 0 & 0 & 0 \\ 0 & 1 & 1 & 0 & 0 & 0 & 0 & 0 & 0 & 0 \\ 0 & 0 & 0 & 1 & 1 & 1 & 0 & 0 & 0 & 0 \\ 0 & 0 & 0 & 0 & 0 & 0 & 1 & 1 & 1 & 1 \end{bmatrix} \tag{4.73}$$

For ease to understand, we replace the non-zero elements in their respective locations by letters *a*, *b* ,*c* and *d* in Λ_1 to Λ_4 respectively. Hence the above codeword matrix is represented by:

$$\Lambda_1^{HM} = \begin{bmatrix} a_{1,1} & 0 & 0 & 0 & 0 & 0 & 0 & 0 & 0 & 0 \\ 0 & a_{2,2} & a_{2,3} & 0 & 0 & 0 & 0 & 0 & 0 & 0 \\ 0 & 0 & 0 & a_{3,4} & a_{3,5} & a_{3,6} & 0 & 0 & 0 & 0 \\ 0 & 0 & 0 & 0 & 0 & 0 & a_{4,7} & a_{4,8} & a_{4,9} & a_{4,10} \end{bmatrix} \tag{4.74}$$

After making a shift by one element in each column in above codeword matrix, we get

$$\Lambda_2^{HM} = \begin{bmatrix} 0 & 0 & 0 & 0 & 0 & 0 & b_{1,7} & b_{1,8} & b_{1,9} & b_{1,10} \\ b_{2,1} & 0 & 0 & 0 & 0 & 0 & 0 & 0 & 0 & 0 \\ 0 & b_{3,2} & b_{3,3} & 0 & 0 & 0 & 0 & 0 & 0 & 0 \\ 0 & 0 & 0 & b_{4,4} & b_{4,5} & b_{4,6} & 0 & 0 & 0 & 0 \end{bmatrix} \tag{4.75}$$

After making a shift by one element in each column in above codeword matrix, we get

$$\Lambda_3^{HM} = \begin{bmatrix} 0 & 0 & 0 & c_{1,4} & c_{1,5} & c_{1,6} & 0 & 0 & 0 & 0 \\ 0 & 0 & 0 & 0 & 0 & 0 & c_{2,7} & c_{2,8} & c_{2,9} & c_{2,10} \\ c_{3,1} & 0 & 0 & 0 & 0 & 0 & 0 & 0 & 0 & 0 \\ 0 & c_{4,2} & c_{4,3} & 0 & 0 & 0 & 0 & 0 & 0 & 0 \end{bmatrix} \tag{4.76}$$

After making a shift by one element in each column in above codeword matrix, we get

$$\Lambda_4^{HM} = \begin{bmatrix} 0 & d_{1,2} & d_{1,3} & 0 & 0 & 0 & 0 & 0 & 0 & 0 \\ 0 & 0 & 0 & d_{2,4} & d_{2,5} & d_{2,6} & 0 & 0 & 0 & 0 \\ 0 & 0 & 0 & 0 & 0 & 0 & d_{3,7} & d_{3,8} & d_{3,9} & d_{3,10} \\ d_{4,1} & 0 & 0 & 0 & 0 & 0 & 0 & 0 & 0 & 0 \end{bmatrix} \tag{4.77}$$

Equivalently we can construct such a codeword threads matrix $\Lambda_{N_T}^{HM}$ by following expression

$$(a_{i,j})_k = \begin{cases} 1, \ if \quad i = Xm\,\mathrm{od}_{N_T}\left(\lfloor \log_2 j + \delta_{j,7} \rfloor + k\right) \\ 0\ , \ otherwise \end{cases} \tag{4.78}$$

where *Xmode* is ordinary modulo function with a small difference that it replaces the output zero by N_T and the Kronecker delta function is defined as

$$\delta_{j,7} = \begin{cases} 1 \ if \quad j = 7 \\ 0, \ \ otheriwse \end{cases} \tag{4.79}$$

From this packing of threads, we get an $N_T \times T$ space time code $\mathcal{X}$ which transmits N_T repetition codes simultaneously, one per thread by selecting the code codewords.

$$\boldsymbol{x} = a_1\Lambda_1 + a_2\Lambda_2 + ... + a_{N_T}\Lambda_{N_T} \tag{4.80}$$

For $a_1, a_2, ..., a_{N_T} \in \Omega$ arbitrary.

For HM thread structure when N_T = 4 and $T = N_T \times \left\lceil \frac{N_T}{2} \right\rceil + \left(\frac{1+(-1)^{N_T}}{2} \right) \left\lceil \frac{N_T}{2} \right\rceil$, by packing threads Λ_1^{HM} to Λ_4^{HM} we get

$$\boldsymbol{x} = \begin{bmatrix} a & d & d & c & c & c & b & b & b & b \\ b & a & a & d & d & d & c & c & c & c \\ c & b & b & a & a & a & d & d & d & d \\ d & c & c & b & b & b & a & a & a & a \end{bmatrix} \tag{4.81}$$

Similarly for N_T = 3, we have

$$\boldsymbol{x} = \begin{bmatrix} a & c & c & b & b & b \\ b & a & a & c & c & c \\ c & b & b & a & a & a \end{bmatrix} \tag{4.82}$$

and when $N_T = 2$, we have

$$\boldsymbol{x} = \begin{bmatrix} a & b & b \\ b & a & a \end{bmatrix} \tag{4.83}$$

For UU Threads

UU threads can also be packed in the same way as we did above for HM threads.

For $N_T = 4$ and $T = 2N_T$, we may write (4.68) as:

$$A = \Lambda_1^{UU} = \begin{bmatrix} 0 & a_{1,2} & a_{1,3} & 0 & 0 & 0 & 0 & 0 \\ 0 & 0 & 0 & a_{2,4} & 0 & a_{2,6} & 0 & 0 \\ 0 & 0 & 0 & 0 & a_{3,5} & 0 & 0 & a_{3,8} \\ a_{4,1} & 0 & 0 & 0 & 0 & 0 & a_{4,7} & 0 \end{bmatrix} \tag{4.84}$$

$$B = \Lambda_2^{UU} = \begin{bmatrix} b_{1,1} & 0 & 0 & 0 & 0 & 0 & b_{1,7} & 0 \\ 0 & b_{2,2} & b_{2,3} & 0 & 0 & 0 & 0 & 0 \\ 0 & 0 & 0 & b_{3,4} & 0 & b_{3,6} & 0 & 0 \\ 0 & 0 & 0 & 0 & b_{4,5} & 0 & 0 & b_{4,8} \end{bmatrix} \tag{4.85}$$

$$C = \Lambda_3^{UU} = \begin{bmatrix} 0 & 0 & 0 & 0 & c_{1,5} & 0 & 0 & c_{1,8} \\ c_{2,1} & 0 & 0 & 0 & 0 & 0 & c_{2,7} & 0 \\ 0 & c_{3,2} & c_{3,3} & 0 & 0 & 0 & 0 & 0 \\ 0 & 0 & 0 & c_{4,4} & 0 & c_{4,6} & 0 & 0 \end{bmatrix} \tag{4.86}$$

$$D = \Lambda_4^{UU} = \begin{bmatrix} 0 & 0 & 0 & d_{1,4} & 0 & d_{1,6} & 0 & 0 \\ 0 & 0 & 0 & 0 & d_{2,5} & 0 & 0 & d_{2,8} \\ d_{3,1} & 0 & 0 & 0 & 0 & 0 & d_{3,7} & 0 \\ 0 & d_{4,2} & d_{4,3} & 0 & 0 & 0 & 0 & 0 \end{bmatrix} \tag{4.87}$$

and packing all the four threads into a single codeword matrix, we get

$$\boldsymbol{x}=\begin{bmatrix} b & a & a & d & c & d & b & c \\ c & b & b & a & d & a & c & d \\ d & c & c & b & a & b & d & a \\ a & d & d & c & b & c & a & b \end{bmatrix} \tag{4.88}$$

For $N_T = 3$, we get

$$\boldsymbol{x}=\begin{bmatrix} b & a & a & c & b & c \\ c & b & b & a & c & a \\ a & c & c & b & a & b \end{bmatrix} \tag{4.89}$$

and for $N_T = 2$, get

$$\boldsymbol{x}=\begin{bmatrix} b & a & a & b \\ a & b & b & a \end{bmatrix} \tag{4.90}$$

B. Algebraically packed multiple-threads method

The codes constructed in section 4.4.2 are individually delto and fully diverse, but when they are packed together in a single codeword matrix in a way as we did above, it is not guaranteed that they are delto and fully diverse because the threads may interact in a detrimental way [69]. The remarkable work of El Gamal and Damen [63] can be used to make it sure that the packed codewords are delto and fully diverse.

Let Λ be the HM thread for N_T transmit antennas and $T = N_T \times \left\lceil \frac{N_T}{2} \right\rceil + \left(\frac{1+(-1)^{N_T}}{2} \right) \left\lceil \frac{N_T}{2} \right\rceil$ vector channel uses. Let $f_{i,j} : \Omega \to \mathbb{C}$ be a one-to-one function for each choice $i = 1, 2, ..., N_T$ and $j = 1, 2, ..., T$. For each thread Λ_k, derived from Λ in accordance with (4.78), form the threaded matrix function $\mathbf{F}_k(x)$ whose $(i, j)th$ entry is $f_{i,j}(x).\Lambda_k(i, j)$ [69, th:12].

Assuming ϕ be an algebraic number of suitable degree over the number field $\mathbb{F}(\theta)$, we build an $N_T \times T$ space time code $\mathcal{X}$ with $L \le N_T$ active threads consisting of all modulated codewords of the form

$$\boldsymbol{x}(a_1, a_2, ..., a_L) = \mathbf{F}_1(a_1) + \phi \mathbf{F}_2(a_2) + ... + \phi^{L-1} \mathbf{F}_L(a_L) \tag{4.91}$$

for $a_1, a_2, ..., a_L \in \Omega$ arbitrary.

Then $\mathcal{X}$ achieve full spatial diversity and is fully delto.

Proof: Assume *a* and *b* are two distinct codewords and are subjected to the delay profile Δ.

Then $\boldsymbol{x}^{\Delta}$ is given as

$$\boldsymbol{x}^{\Delta} = \boldsymbol{x}^{\Delta}\left(a_1, a_2, ..., a_L\right) - \boldsymbol{x}^{\Delta}\left(a_1', a_2', ..., a_L'\right)$$

$$= \sum_{i=1}^{L} \phi^{i-1} \mathbf{F}_i^{\Delta}(a_i, a_i') \tag{4.92}$$

where

$$\mathbf{F}_i^{\Delta}(a_i, a_i') = \mathbf{F}_i^{\Delta}(a_i) - \mathbf{F}_i^{\Delta}(a_i') \tag{4.93}$$

Let *m* denote the largest index for which $a_m \neq a_m'$ but $a_i = a_i'$ for $i > m$. Then

$$\boldsymbol{x}^{\Delta} = \sum_{i=1}^{m} \phi^{i-1} \mathbf{F}_i^{\Delta}(a_i, a_i') \tag{4.94}$$

The non-zero elements in main diagonal form a submatrix, and are given by

$$\phi^{m-1}\left[f_{i,j_i}(a_m) - f_{i,j_i}(a_m')\right] \qquad \text{for } i = 1, 2, ..., N_T \tag{4.95}$$

This sub-matrix has determinant

$$D(\phi) = G(\phi) + \phi^{N_T(m-1)} \prod_{i=1}^{N_T} \left(f_{i,j_i}(a_m) - f_{i,j_i}(a_m')\right) \tag{4.96}$$

where $G(\phi)$ is a polynomial in ϕ over $\mathbb{F}(\theta)$ of degree $< N_T(m-1)$. Since the functions f_{i,j_i} are all one-to-one and $a_m \neq a_m'$, (4.96) is a nontrivial polynomial in ϕ of degree $N_T(m-1)$ over $\mathbb{F}(\theta)$.

By design choice, ϕ is not the root of any nontrivial polynomial of degree $N_T(m-1)$ over $\mathbb{F}(\theta)$. Hence $D(\phi) \neq 0$, so the matrix is of full rank. We conclude that $\mathcal{X}$ achieves full spatial diversity and is fully delto.

Code rate

In the multiple thread code construction, the rate of the space time code $\mathcal{X}$ is given as [69]

$$R = \frac{PL}{T}\log_2 \mathcal{A} \quad \text{bpcu} \tag{4.97}$$

Thus we can make $\mathcal{X}$ full rate by proper selection of parameters L and P for a given set of codes parameters N_T, N_R, and T. In other words, we make the modulation parameters flexible to match the specified spatio-temporal structure. This selection of modulation parameters can be done in different ways, a natural choice is to take $L = min\ (N_T, N_R)$ and $P=T$.

C. Packing of threads (when $L < N_T$)

In previous section, we developed a technique of packing the single thread codeword matrices into $L = N_T$ threads codeword matrices. Selecting fewer threads than N_T may increase the spectral efficiency of the code without increasing the constellation size by reducing the code interval length, but for that we have to relax the condition of antenna usage per time unit within each thread. In this section we pack the threads in such a way that we allow the usage of more than one antenna per time unit within each thread.

I. HM thread

We denote the *smallest* code length for transmission of L threads from N_T transmit antennas by $T^{SHM}_{N_T,L}$. From section 4.4.2 we know that for HM threads the total number of channel uses is $n_1 + n_2 + ... + n_{N_T} = N_T(N_T+1)/2$, where $n_i = i$.

Now let $\eta_1, \eta_2, ..., \eta_L$ denote permutation assigning the values $n_1 + n_2 + ... + n_{N_T}$ to the transmit antennas $1, 2, ..., N_T$ then according to [69], we may write

$$T^{SHM}_{N_T,L} = \min_{\eta_1,\eta_1,...,\eta_L} \max_{m=1,2,...,N_T} \left\{ \sum_{i=1}^{L} \eta_i(m) \right\} \tag{4.98}$$

From (4.98) for L=1 , we have.

$$T^{SHM}_{N_T,1} = N_T \tag{4.99}$$

and for L > 1, we have

$$T_{N_T,L}^{SHM} = \left\lceil \frac{L\left(N_T \times \left\lceil \frac{N_T}{2} \right\rceil + \left(\frac{1+(-1)^{N_T}}{2} \right) \left\lceil \frac{N_T}{2} \right\rceil \right)}{N_T} \right\rceil \tag{4.100}$$

For $N_T = 4$ and $L = 1$ and 2, we have for example

$$\boldsymbol{x}_{4,1}^{SHM} = \begin{bmatrix} a & 0 & 0 & 0 \\ a & a & 0 & 0 \\ a & a & a & 0 \\ a & a & a & a \end{bmatrix} \tag{4.101}$$

$$\boldsymbol{x}_{4,2}^{SHM} = \begin{bmatrix} a & b & b & b & b \\ a & a & b & b & b \\ a & a & a & b & b \\ a & a & a & a & b \end{bmatrix} \tag{4.102}$$

II- UU thread

We denote the *smallest* code length for transmission of L threads from N_T transmit antennas by $T_{N_T,L}^{SUU}$. From section-4.4.2 we saw that for UU thread, the maximum expansion between two channel uses is: $2N_T - 1$. so we may deduce that

$$T_{N_T,L}^{SUU} = \left\lceil \left\lfloor \frac{L}{N_T} \right\rfloor + \left(2N_T - 1\right) \right\rceil \tag{4.103}$$

For $N_T = 4$ and $L = 1$, we have for example:

$$\boldsymbol{x}_{4,1}^{SUU} = \begin{bmatrix} 0 & a & a & 0 & 0 & 0 & 0 \\ a & 0 & a & 0 & 0 & 0 & 0 \\ a & 0 & 0 & a & 0 & 0 & 0 \\ a & 0 & 0 & 0 & 0 & 0 & a \end{bmatrix} \tag{4.104}$$

For $N_T = 4$, $L = 2$

$$\boldsymbol{x}_{4,2}^{SUU} = \begin{bmatrix} b & a & a & 0 & 0 & 0 & b \\ a & 0 & a & b & 0 & 0 & b \\ a & 0 & 0 & a & b & 0 & b \\ a & b & b & 0 & 0 & 0 & a \end{bmatrix} \tag{4.105}$$

When $N_T = 4$ and $L = 4$

$$\boldsymbol{x}_{4,4}^{SUU} = \begin{bmatrix} d & a & c & c & a & b & d & b \\ c & b & d & d & b & a & c & a \\ b & c & a & a & c & d & b & d \\ a & d & b & b & d & c & a & c \end{bmatrix} \tag{4.106}$$

Example for $N_T = 3$ and $L = 3$

$$\boldsymbol{x}_{3,3}^{SUU} = \begin{bmatrix} b & a & a & c & b \\ c & b & b & a & c \\ a & c & c & b & a \end{bmatrix} \tag{4.107}$$

Such type of codes will work efficiently for larger value of L. For smaller value of L, we can delete zero columns (*i.e.* columns whose all elements are zeros) in (4.104) and (4.105), even after amputation of these columns the obtained codes still retain their properties of full diversity and delto.

4.4.4 Construction of delto codes with minimum length

The delto codes discussed in previous sections have a codes length $T > N_T$, therefore for large size N_T their performances may decrease. In this section we extend our work and propose a technique for constructing delto codes with minimum delay length $T = N_T$. Our construction method is based on tight packing of the HM threads developed in subsection 4.4.2.

In fact, an $N_T \times T$ MIMO codeword matrix is a strand of algebraic SISO codes separated by Diophantine numbers ϕ, and the difference between distinct $N_T \times N_T$ submatrices is the diversity order of the codeword matrix [63, th: 4].

In [80], the authors show that the minimum length delto full diversity STBC $\mathcal{X}$ can be constructed by multiplying the designed thread codeword matrix with an $N_T \times T$ matrix C, whose entries are re-arrangement of $\overline{c} \in C$, (C being a full diversity one dimensional block code of length $N_T T$).

Of course the main problem in designing such type of codes is the design of thread codeword matrix. In [80], the authors have proposed two types of such matrices for two and three active relays. In what follows, we discuss a new technique for construction of thread codeword matrices, and by simulation results at the end of this chapter, we show that our proposed codes get better performance than the codes presented in [80].

Construction of thread codeword matrix

Recall from section 4.4.2 for HM generalized thread construction, here we develop a simple construction method for $T_{N_T}^{ML} = N_T$ as follows:

- For row i, $(i = 2,..., N_T)$, define a complex number ϕ whose power of 2 is simple addition of non-zero elements of row i in HM single thread codeword matrix.
- In the first row of HM single thread codeword matrix, the i-tuples of zeros above the non-zero elements in i-th row $(i = 2,..., N_T)$ are replaced by ϕ^{i-1}.
- Fill the empty positions by 1.

For example for $N_T = 3$, the Λ_3^{HM} matrix from (4.61) can be represented as

$$\Lambda_3^{ML} = \begin{bmatrix} 1 & \phi & \phi^2 \\ 1 & \phi^4 & 1 \\ 1 & 1 & \phi^8 \end{bmatrix} \tag{4.108}$$

For ease to understand, let $\alpha_{i,j}$ represents the location of ϕ in (4.108).

We show that by an appropriate selection of parameters ϕ and one dimensional code C, the resulted space-time code $\mathcal{X}$ is delto for every delay profile.

Now let Ξ denote those N_T-tuples of $\alpha_{i,j}$ in Λ_{ML}, which are taken from different rows, and let $\phi^{\alpha_{\max}}$ be the highest number used, where $\alpha_{\max} = 2^{N_T}$.

Lemma 4: Let $\mathcal{X} = \Omega\Lambda_{ML}$ denote the space time code in which the repetition code (with codewords of length N_T^2) over alphabet Ω is used as one dimensional SISO code in conjunction with thread Λ_{ML}, then $\mathcal{X}$ achieves full spatial diversity and is fully delto, if the following conditions are satisfied.

- ϕ is chosen as an algebraic or transcendental number such that the numbers $\{1, \phi, ..., \phi^{\alpha_{\max}}\}$ are algebraically independent over the field $\mathbb{F}(\theta)$ that contains Ω [74].
- The parameters $\alpha_{i,j}$ are chosen such that the summation of the entries of every N_T-tuples in Ξ is unique.

Since the one-dimensional code C is a repetition code, it is sufficient to show that Λ_{ML}^{Δ} is full rank for every arbitrary delay profiles $\Delta = (\delta_1, \delta_2, .., \delta_{N_T})$. To verify the diversity order of the code, we need to find out the largest square submatrix in Λ_{ML}^{Δ} which is full rank.

- First column is chosen such that it contains a non-zero element in row N_T.
- j-th column is chosen such that it contains a power of ϕ at i-th row $(i, j = 2, ..., N_T - 1)$
- As the last step chose N_T-th column (for which we have only one choice).
- Arrange the columns in reverse order.

As a result, the obtained $N_T \times N_T$ submatrix has at least one thread L with all non-zero elements containing N_T elements of power ϕ.

If the sum of the powers of ϕ in L threads is m, then the determinant of the submatrix is given by

$$det(D) = g(\phi) + \phi^m \tag{4.109}$$

where $g(\phi)$ is a polynomial of ϕ with degree less than or equal to $\alpha_{\max}$. Since m is unique, $g(\phi)$ does not contain any term in ϕ^m. Therefore, if the numbers $\{1, \phi, ..., \phi^{\alpha_{\max}}\}$ are algebraically independent over $\mathbb{F}(\theta)$, det(D) is not zero and the code achieves full diversity

for every delay profile. Due to the nice structure of our codes, we may use more than one method to verify the determinant of the largest $N_T \times N_T$ submatrix, for example we can use (4.96) or the same proof as developed in *lemma* 1.

Examples

In this section we lay down some examples of delto distributed TAST codes. Like that of TAST codes [63], the construction of delto codes are carried out by appropriate selection of the SISO codes and the numbers ϕ. Full-diversity SISO codes over fading channels can be constructed by applying full-diversity unitary transformations to input signals drawn from lattices or multidimensional constellations carved from a ring. In [74], Damen et al. provided a systematic way of constructing $N_T \times N_T$ fully diverse unitary transformations over the field that contains the elements of information symbols, as.

$$\boldsymbol{X} = \boldsymbol{R}.\boldsymbol{U} \tag{4.110}$$

where $\boldsymbol{R}$ is the $P \times P$ discrete Fourier transform with entries

$$W(k,l) = 1/\sqrt{P}.\exp(-2j\pi.(k-1).(l-1)/P) \quad , \quad k,l = 1,2,..,P \tag{4.111}$$

and $\boldsymbol{U}$ is a vector of the following form

$$\boldsymbol{U} = \text{diag}[1, \theta^{1/P}, \theta^{2/P}, ..., \theta^{(P-1)/P}] \tag{4.112}$$

where θ is a transcendental or an algebraic number of suitable degree to guarantee the full diversity of the rotation [74].

For $N_T = N_R = L = 2$, $P = T = 3$, using HM thread construction guideline from section-4.5.2, we get delto distributed TAST code as follow

$$\begin{bmatrix} x_1 & \phi y_2 & \phi y_3 \\ \phi y_1 & x_2 & x_3 \end{bmatrix} \tag{4.113}$$

where $\boldsymbol{X} = (x_1, x_2, x_3)^T = \boldsymbol{R}.\boldsymbol{U}$ and $\boldsymbol{Y} = (y_1, y_2, y_3)^T = \boldsymbol{R}.\boldsymbol{V}$, $\boldsymbol{U}, \boldsymbol{V}$ are two 3×1 vectors of QAM symbols and $\boldsymbol{R}_3$ is optimal 3×3 complex rotation according to (4.110). By setting

$\phi = \exp(2\pi i/15)$, this code provides the rate of 2-QAM symbols per channel use and achieves a transmit diversity of 2 regardless of the delay profile.

Another example is the well known Alamouti code, which is not delto, but its extension to HM threads makes it delto, as shown below in (4.114)

$$\begin{bmatrix} x_1 & -x_2^* & -x_2^* \\ x_2 & x_1^* & x_1^* \end{bmatrix} \tag{4.114}$$

For $N_T = 3$, $N_R = L = 2$, $P = T = 5$, we have the SUU STBC (4.107) with codeword matrix

$$\begin{bmatrix} x_1 & \phi y_2 & \phi y_3 & 0 & x_5 \\ 0 & x_2 & x_3 & \phi y_4 & 0 \\ \phi y_1 & 0 & 0 & x_4 & \phi y_5 \end{bmatrix} \tag{4.115}$$

where $\boldsymbol{X} = (x_1, x_2, x_3, x_4, x_5)^T = \boldsymbol{R}.\boldsymbol{U}$ and $\boldsymbol{Y} = (y_1, y_2, y_3, y_4, y_5)^T = \boldsymbol{R}.\boldsymbol{V}$, $\boldsymbol{U}, \boldsymbol{V}$ are two 5×1 vectors of QAM symbols and $\boldsymbol{R}_5$ is optimal 5×5 complex rotation according to (4.110). By setting $\phi = \exp(2\pi i/25)$, this code provides the rate of 2-QAM symbols per channel use and achieves a transmit diversity of 3 regardless of the delay profile.

In (4.115), the number of active threads L are less than the number of transmit antennas N_T. One can re-construct (4.115) to get a delto distributed TAST code of smaller latency by reducing the number of zeros in transmission.

Thus for $N_T = 3$, $N_R = L = 2$, $P = 5$ and $T = 4$, one has the STBC with codeword matrix

$$\begin{bmatrix} x_1 & \phi y_2 & \phi y_3 & 0 \\ 0 & x_2 & \phi y_4 & x_5 \\ \phi y_1 & x_3 & x_4 & \phi y_5 \end{bmatrix} \tag{4.116}$$

In this case, by setting $\phi = \exp(2\pi i/36)$, code (4.116) guarantees full diversity irrespective of the delay profile. This code provides the rate of 2.5-QAM symbols per channel use.

Although the above examples are independently deriven from the thread construction techniques discussed in section 4.4.2 and 4.4.3, they resemble to that of Damens' codes designed in [69], and it was also confirmed by simulation results that they have exactly same performances as that of [69], but we hope that the simplicity in construction techniques of our codes may reduce hardware complexity.

In section 4.4.4, we introduced a technique for $T = N_T$ codeword matrix construction. Where the information symbols are chosen from $\mathbb{Z}[i]$ for $N_T = 2$ with a required full-diversity rotations of 4×4, and $\mathbb{Z}[j]$ when $N_T = 3$, with a required full-diversity rotations of size 9×9.

For $N_T = N_R = T = 2$, we get a delto STBC codeword matrix of the form

$$\begin{bmatrix} x_1 & \phi x_3 \\ x_2 & \phi^4 x_4 \end{bmatrix} \tag{4.117}$$

where $\boldsymbol{X} = (x_1, x_2, x_3, x_4)^T = \boldsymbol{R}.\boldsymbol{U}$, U is 4×1 vectors of QAM symbols and $\boldsymbol{R}_4$ is optimal 4×4 complex rotation according to (4.110). By setting $\phi = \exp(2\pi i/3)$, this code provides a rate of 2-QAM symbols per channel use and achieves a transmit diversity of 2 regardless of the delay profile among its rows.

The noiseless received signal from (4.117) can be written as:

$$\boldsymbol{Z}_{N_R\times2} = \boldsymbol{H}_{N_R\times2}.\begin{bmatrix} x_1 & \phi.x_3 \\ x_2 & \phi^4.x_4 \end{bmatrix}_{2\times2} \tag{4.118}$$

We remark that: $x_1 = \boldsymbol{R}(1,:)_{1\times4}.\boldsymbol{U}_{4\times1}$, $x_2 = \boldsymbol{R}(2,:)_{1\times4}.\boldsymbol{U}_{4\times1}$, $x_3 = \boldsymbol{R}(3,:)_{1\times4}.\boldsymbol{U}_{4\times1}$ and $x_4 = \boldsymbol{R}(4,:)_{1\times4}.\boldsymbol{U}_{4\times1}$ with $\boldsymbol{U}_{4\times1} = [u_1, u_2, u_3, u_4]^T$ denoting the vector of transmitted QAM symbols. Hence, we have :

$$\begin{aligned} \boldsymbol{Z}_{N_R\times2} &= \boldsymbol{H}_{N_R\times2}.\begin{bmatrix} \boldsymbol{R}(1,:)_{1\times4}.\boldsymbol{U}_{4\times1} & \phi.\boldsymbol{R}(3,:)_{1\times4}.\boldsymbol{U}_{4\times1} \\ \boldsymbol{R}(2,:)_{1\times4}.\boldsymbol{U}_{4\times1} & \phi^4.\boldsymbol{R}(4,:)_{1\times4}.\boldsymbol{U}_{4\times1} \end{bmatrix}_{2\times2} \\ &= \begin{bmatrix} \boldsymbol{H}(1,1) & \boldsymbol{H}(1,2) \\ \boldsymbol{H}(2,1) & \boldsymbol{H}(2,2) \\ \vdots & \vdots \\ \boldsymbol{H}(N_R,1) & \boldsymbol{H}(N_R,2) \end{bmatrix}_{N_R\times2} . \begin{bmatrix} \boldsymbol{R}(1,:)_{1\times4}.\boldsymbol{U}_{4\times1} & \phi.\boldsymbol{R}(3,:)_{1\times4}.\boldsymbol{U}_{4\times1} \\ \boldsymbol{R}(2,:)_{1\times4}.\boldsymbol{U}_{4\times1} & \phi^4.\boldsymbol{R}(4,:)_{1\times4}.\boldsymbol{U}_{4\times1} \end{bmatrix}_{2\times2} \end{aligned} \tag{4.119}$$

This can be equivalently written in columns as :

$$\begin{aligned}
&\boldsymbol{Z}(1,1) = \boldsymbol{H}(1,1).\boldsymbol{R}(1,:)_{1\times4}.\boldsymbol{U}_{4\times1} + \boldsymbol{H}(1,2).\boldsymbol{R}(2,:)_{1\times4}.\boldsymbol{U}_{4\times1} \\
&\boldsymbol{Z}(1,2) = \boldsymbol{H}(1,1).\phi.\boldsymbol{R}(3,:)_{1\times4}.\boldsymbol{U}_{4\times1} + \boldsymbol{H}(1,2).\phi^4.\boldsymbol{R}(4,:)_{1\times4}.\boldsymbol{U}_{4\times1} \\
&\vdots \\
&\boldsymbol{Z}(N_R,1) = \boldsymbol{H}(N_R,1).\boldsymbol{R}(1,:)_{1\times4}.\boldsymbol{U}_{4\times1} + \boldsymbol{H}(N_R,2).\boldsymbol{R}(2,:)_{1\times4}.\boldsymbol{U}_{4\times1} \\
&\boldsymbol{Z}(N_R,2) = \boldsymbol{H}(N_R,1).\phi.\boldsymbol{R}(3,:)_{1\times4}.\boldsymbol{U}_{4\times1} + \boldsymbol{H}(N_R,2).\phi^4.\boldsymbol{R}(4,:)_{1\times4}.\boldsymbol{U}_{4\times1}
\end{aligned} \tag{4.120}$$

This can be summarized in matrix form as :

$$\begin{aligned}
&\boldsymbol{Z}(1,1) = (\boldsymbol{H}(1,1).\boldsymbol{R}(1,:)_{1\times4} + \boldsymbol{H}(1,2).\boldsymbol{R}(2,:)_{1\times4}).\boldsymbol{U}_{4\times1} \\
&\boldsymbol{Z}(1,2) = (\boldsymbol{H}(1,1).\phi.\boldsymbol{R}(3,:)_{1\times4} + \boldsymbol{H}(1,2).\phi^4.\boldsymbol{R}(4,:)_{1\times4}).\boldsymbol{U}_{4\times1} \\
&\vdots \\
&\boldsymbol{Z}(N_R,1) = (\boldsymbol{H}(N_R,1).\boldsymbol{R}(1,:)_{1\times4} + \boldsymbol{H}(N_R,2).\boldsymbol{R}(2,:)_{1\times4}).\boldsymbol{U}_{4\times1} \\
&\boldsymbol{Z}(N_R,2) = (\boldsymbol{H}(N_R,1).\phi.\boldsymbol{R}(3,:)_{1\times4} + \boldsymbol{H}(N_R,2).\phi^4.\boldsymbol{R}(4,:)_{1\times4}).\boldsymbol{U}_{4\times1}
\end{aligned} \tag{4.121}$$

$$\begin{bmatrix} \boldsymbol{Z}(1,1) \\ \boldsymbol{Z}(1,2) \\ \vdots \\ \boldsymbol{Z}(N_R,1) \\ \boldsymbol{Z}(N_R,2) \end{bmatrix}_{2.N_R\times1} = \begin{bmatrix} \boldsymbol{H}(1,1).\boldsymbol{R}(1,:)_{1\times4} + \boldsymbol{H}(1,2).\boldsymbol{R}(2,:)_{1\times4} \\ \boldsymbol{H}(1,1).\phi.\boldsymbol{R}(3,:)_{1\times4} + \boldsymbol{H}(1,2).\phi^4.\boldsymbol{R}(4,:)_{1\times4} \\ \vdots \\ \boldsymbol{H}(N_R,1).\boldsymbol{R}(1,:)_{1\times4} + \boldsymbol{H}(N_R,2).\boldsymbol{R}(2,:)_{1\times4} \\ \boldsymbol{H}(N_R,1).\phi.\boldsymbol{R}(3,:)_{1\times4} + \boldsymbol{H}(N_R,2).\phi^4.\boldsymbol{R}(4,:)_{1\times4} \end{bmatrix}_{2.N_R\times4} .\boldsymbol{U}_{4\times1} \tag{4.122}$$

So, the transformation of the transmit constellation is obtained by multiplication with the equivalent matrix :

$$\boldsymbol{B} = \begin{bmatrix} \boldsymbol{H}(1,1).\boldsymbol{R}(1,:)_{1\times4} + \boldsymbol{H}(1,2).\boldsymbol{R}(2,:)_{1\times4} \\ \boldsymbol{H}(1,1).\phi.\boldsymbol{R}(3,:)_{1\times4} + \boldsymbol{H}(1,2).\phi^4.\boldsymbol{R}(4,:)_{1\times4} \\ \vdots \\ \boldsymbol{H}(N_R,1).\boldsymbol{R}(1,:)_{1\times4} + \boldsymbol{H}(N_R,2).\boldsymbol{R}(2,:)_{1\times4} \\ \boldsymbol{H}(N_R,1).\phi.\boldsymbol{R}(3,:)_{1\times4} + \boldsymbol{H}(N_R,2).\phi^4.\boldsymbol{R}(4,:)_{1\times4} \end{bmatrix} \tag{4.123}$$

Note that when the number of equations is less than the number of unknowns it is necessary to use a decision feedback equalization (DFE) to help the sphere decoding to converge. For example it is possible to proceed like this:

At each time the first n_m transmitted symbols in a packet correspond to the last n_m decoded symbols in the last packet. The matrix $\boldsymbol{B}$ can be partitioned in the following way:

$$\boldsymbol{B} = [[\boldsymbol{B}_1]_{2N_R \times n_m}, [\boldsymbol{B}_2]_{2N_R \times (4-n_m)}]_{2N_R \times 4} \tag{4.124}$$

and the transmitted symbol vector can be partitioned as: $\boldsymbol{U} = [\boldsymbol{C}_{n_m \times 1}; \boldsymbol{D}_{4-n_m \times 1}]$; where $\boldsymbol{C}_{n_m \times 1}$ is the last n_m decoded symbols in the last packet, we have thus :

$$\boldsymbol{Z} = \boldsymbol{B}_1.\boldsymbol{C} + \boldsymbol{B}_2.\boldsymbol{D} \tag{4.125}$$

and we can run the sphere decoding algorithm with the following transformation: $\boldsymbol{Z}' \rightarrow \boldsymbol{Z} - \boldsymbol{B}_1.\boldsymbol{C}$ and $\boldsymbol{U} \rightarrow \boldsymbol{D}$ The new system involves the calculation of vector $\boldsymbol{D}$ of lower size and this can be done with the classical sphere decoding algorithm.

In the case of delay tolerant TAST codes:

We suppose that first row of codeword matrix (4.118) is delayed by one symbol period. In this case the new space time code can be written as:

$$\begin{bmatrix} 0 & x_1 & \phi.x_3 \\ x_2 & \phi^4.x_4 & 0 \end{bmatrix} \tag{4.126}$$

The noiseless received signal can then be written:

$$\boldsymbol{Z}_{N_R \times 3} = \boldsymbol{H}_{N_R \times 2}.\begin{bmatrix} 0 & x_1 & \phi.x_3 \\ x_2 & \phi^4.x_4 & 0 \end{bmatrix}_{2 \times 3} \tag{4.127}$$

We can remark that: $x_1 = \boldsymbol{R}(1,:)_{1\times 4}.\boldsymbol{U}_{4\times 1}$, $x_2 = \boldsymbol{R}(2,:)_{1\times 4}.\boldsymbol{U}_{4\times 1}$, $x_3 = \boldsymbol{R}(3,:)_{1\times 4}.\boldsymbol{U}_{4\times 1}$ and $x_4 = \boldsymbol{R}(4,:)_{1\times 4}.\boldsymbol{U}_{4\times 1}$. Hence, we have :

$$\boldsymbol{Z}_{N_R \times 3} = \boldsymbol{H}_{N_R \times 2}.\begin{bmatrix} 0 & \boldsymbol{R}(1,:)_{1\times 4}.\boldsymbol{U}_{4\times 1} & \phi.\boldsymbol{R}(3,:)_{1\times 4}.\boldsymbol{U}_{4\times 1} \\ \boldsymbol{R}(2,:)_{1\times 4}.\boldsymbol{U}_{4\times 1} & \phi^4.\boldsymbol{R}(4,:)_{1\times 4}.\boldsymbol{U}_{4\times 1} & 0 \end{bmatrix}_{2 \times 3}$$

$$= \begin{bmatrix} \boldsymbol{H}(1,1) & \boldsymbol{H}(1,2) \\ \boldsymbol{H}(2,1) & \boldsymbol{H}(2,2) \\ \vdots & \vdots \\ \boldsymbol{H}(N_R,1) & \boldsymbol{H}(N_R,2) \end{bmatrix}_{N_R \times 2} . \begin{bmatrix} 0 & \boldsymbol{R}(1,:)_{1\times 4}.\boldsymbol{U}_{4\times 1} & \phi.\boldsymbol{R}(3,:)_{1\times 4}.\boldsymbol{U}_{4\times 1} \\ \boldsymbol{R}(2,:)_{1\times 4}.\boldsymbol{U}_{4\times 1} & \phi^4.\boldsymbol{R}(4,:)_{1\times 4}.\boldsymbol{U}_{4\times 1} & 0 \end{bmatrix}_{2\times 3} \tag{4.128}$$

This can be equivalently written in column:

$$\begin{aligned} &\boldsymbol{Z}(1,1) = \boldsymbol{H}(1,2).\boldsymbol{R}(2,:)_{1\times 4}.\boldsymbol{U}_{4\times 1} \\ &\boldsymbol{Z}(1,2) = \boldsymbol{H}(1,1).\boldsymbol{R}(1,:)_{1\times 4}.\boldsymbol{U}_{4\times 1} + \boldsymbol{H}(1,2).\phi^4.\boldsymbol{R}(4,:)_{1\times 4}.\boldsymbol{U}_{4\times 1} \\ &\boldsymbol{Z}(1,3) = \boldsymbol{H}(1,1).\phi.\boldsymbol{R}(3,:)_{1\times 4}.\boldsymbol{U}_{4\times 1} \\ &\vdots \\ &\boldsymbol{Z}(N_R,1) = \boldsymbol{H}(N_R,2).\boldsymbol{R}(2,:)_{1\times 4}.\boldsymbol{U}_{4\times 1} \\ &\boldsymbol{Z}(N_R,2) = \boldsymbol{H}(N_R,1).\boldsymbol{R}(1,:)_{1\times 4}.\boldsymbol{U}_{4\times 1} + \boldsymbol{H}(N_R,2).\phi^4.\boldsymbol{R}(4,:)_{1\times 4}.\boldsymbol{U}_{4\times 1} \\ &\boldsymbol{Z}(N_R,3) = \boldsymbol{H}(N_R,1).\phi.\boldsymbol{R}(3,:)_{1\times 4}.\boldsymbol{U}_{4\times 1} \end{aligned} \tag{4.129}$$

This can be summarized in matrix form as :

$$\begin{bmatrix} \boldsymbol{Z}(1,1) \\ \boldsymbol{Z}(1,2) \\ \boldsymbol{Z}(1,3) \\ \vdots \\ \boldsymbol{Z}(N_R,1) \\ \boldsymbol{Z}(N_R,2) \\ \boldsymbol{Z}(N_R,3) \end{bmatrix}_{3.N_R\times 1} = \begin{bmatrix} \boldsymbol{H}(1,2).\boldsymbol{R}(2,:)_{1\times 4} \\ \boldsymbol{H}(1,1).\boldsymbol{R}(1,:)_{1\times 4} + \boldsymbol{H}(1,2).\phi^4.\boldsymbol{R}(4,:)_{1\times 4} \\ \boldsymbol{H}(1,1).\phi.\boldsymbol{R}(3,:)_{1\times 4} \\ \vdots \\ \boldsymbol{H}(N_R,2).\boldsymbol{R}(2,:)_{1\times 4} \\ \boldsymbol{H}(N_R,1).\boldsymbol{R}(1,:)_{1\times 4} + \boldsymbol{H}(N_R,2).\phi^4.\boldsymbol{R}(4,:)_{1\times 4} \\ \boldsymbol{H}(N_R,1).\phi.\boldsymbol{R}(3,:)_{1\times 4} \end{bmatrix}_{3.N_R\times 4} .\boldsymbol{U}_{4\times 1} \tag{4.130}$$

For $N_T = N_R = T = 3$, we get delto STBC codeword matrix of the form from

$$\begin{bmatrix} x_1 & \phi x_4 & \phi^2 x_7 \\ x_2 & \phi^4 x_5 & x_8 \\ x_3 & x_6 & \phi^8 x_9 \end{bmatrix} \tag{4.131}$$

where $\boldsymbol{X} = (x_1, x_2, ..., x_9)^T = \boldsymbol{R}.\boldsymbol{U}$, $\boldsymbol{U}$ is a 9×1 vector of information symbols belonging to a 4-array constellation in $\mathbb{Z}[j]$ and $\boldsymbol{R}_9$ is optimal 9×9 complex rotation according to (4.110). By setting $\phi = \exp(\pi i/12)$, this code provides the rate of 3 symbols per channel use and achieves a transmit diversity of 3 regardless of the delay profile.

Simulation results

Like that of TAST codes, we use sphere decoder for decoding our delto codes. In case of delay profiles where the received signals may contain some unknown equations, are dealt by the use of minimum mean square error-decision feedback equalization (MMSE-DFE) processing, as explained above and originally can be found in [81], [82].

The simulation figures illustrated below show bit and symbol error rates as function of E_b / N_0 in decibels, which is adjusted as follows.

$$\left.\frac{E_b}{N_0}\right|_{dB} = \left.\frac{E_s}{N_0}\right|_{dB} - 10\log_{10} R$$

where E_s is the average signal energy per receive antenna and R is the code rate in bit per channel use (bpcu).

Figure 4.8, shows the bit error rate (BER) and symbol error rate (SER) of the delto distributed TAST code of (4.113) with and with out delay. We repeat that the code parameters for the code (4.113) are $N_T = N_R = L = 2$ and $P = T = 3$. In case of delay, the first row is shifted by one symbol right to the second row.

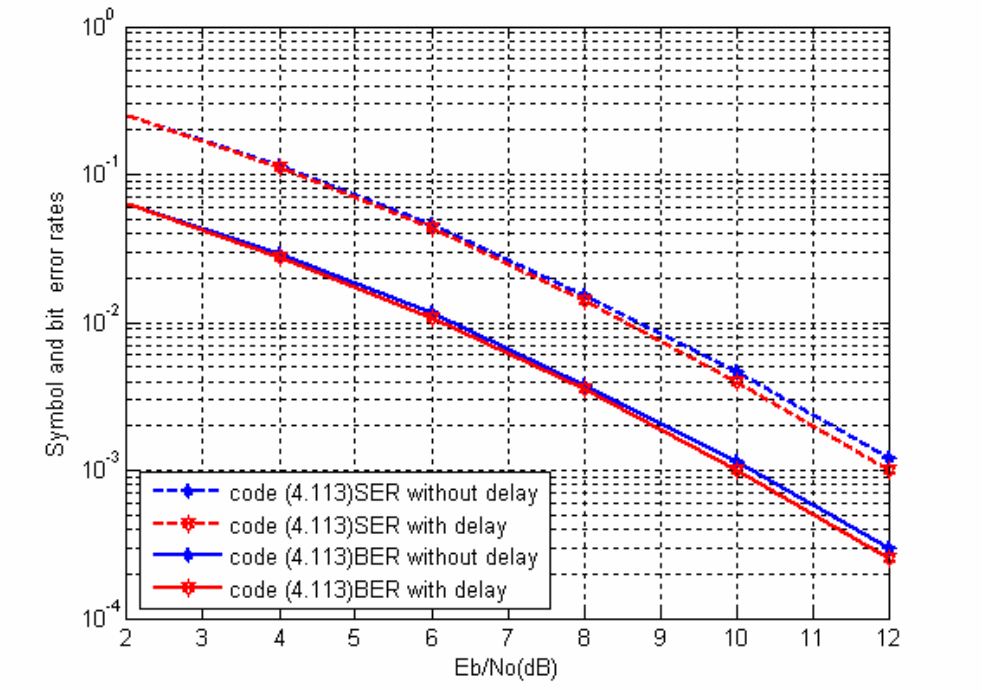

Figure 4.8 Performance of the delto codeword matrix (4.113) with and with out delay

In figure 4.9, we simulated the bit error rate (BER) and symbol error rate (SER) performances of delto distributed TAST code (4.115) with and without delay. The code parameters of (4.115) are $N_T = 3$, $N_R = L = 2$, and $P = T$=5. For delay profile, the first row is shifted by one symbol right to the second row

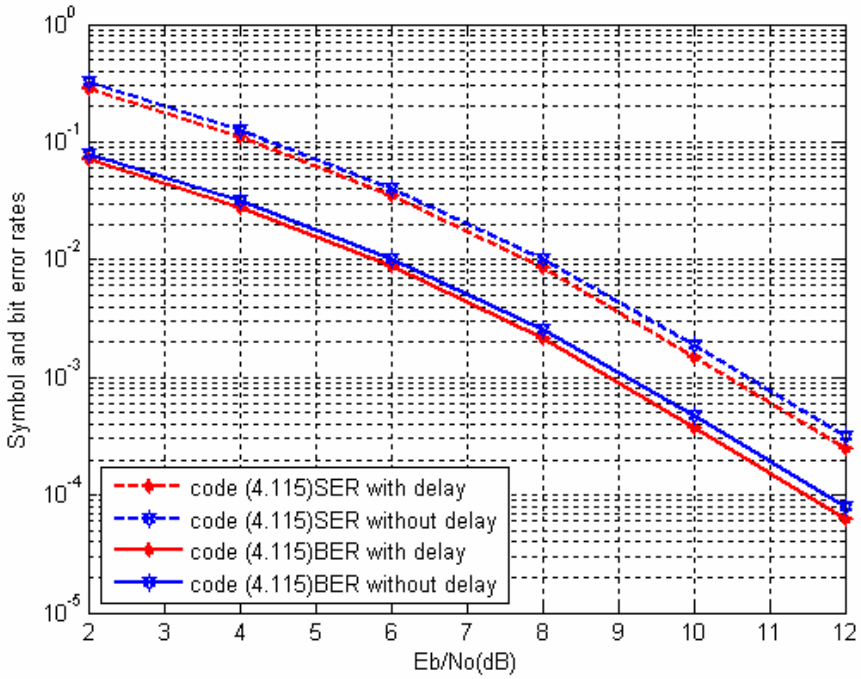

Figure. 4.9 Performance of delto codeword matrix (4.115) with and with out delay

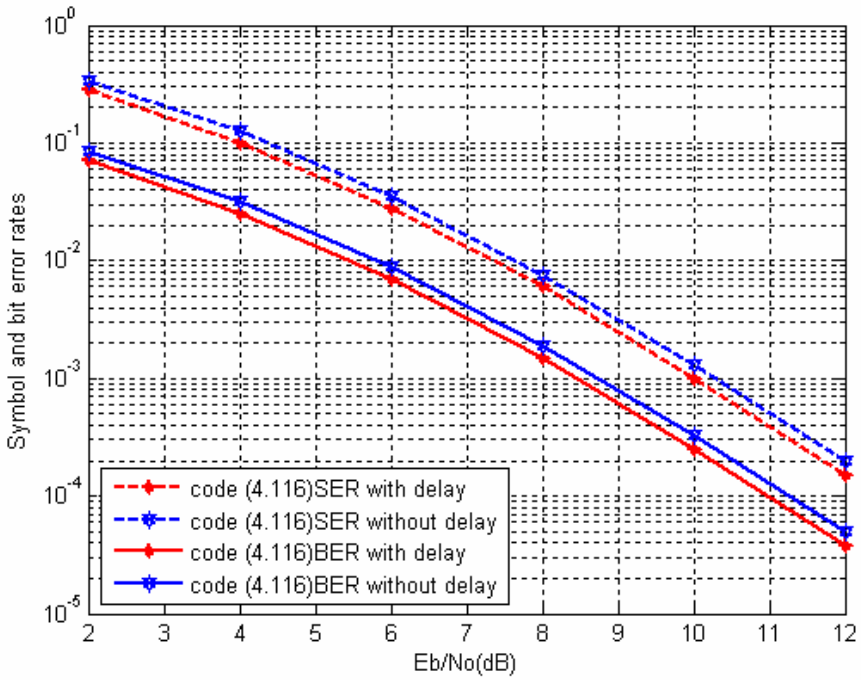

Figure 4.10 Performance of delto codeword matrix (4.116) with and with out delay

In figure 4.10, we considered the bit error rate (BER) and symbol error rate (SER) performances of delto distributed TAST code of (4.116) with and without delay. The code parameters of (4.116) are $N_T = 3$, $N_R = L = 2$, $P = 5$, and $T = 4$. For delay profile, the first row is shifted by one symbol right to the second row

Figure 4.11 shows the bit error rate (BER) and symbol error rate (SER) performances for codeword matrix (4.117) without delay. The results are compared with the result of the well known golden code [77] and the code proposed in [80]. The associated code parameters of (4.117) are $N_T = N_R = T = 2$.

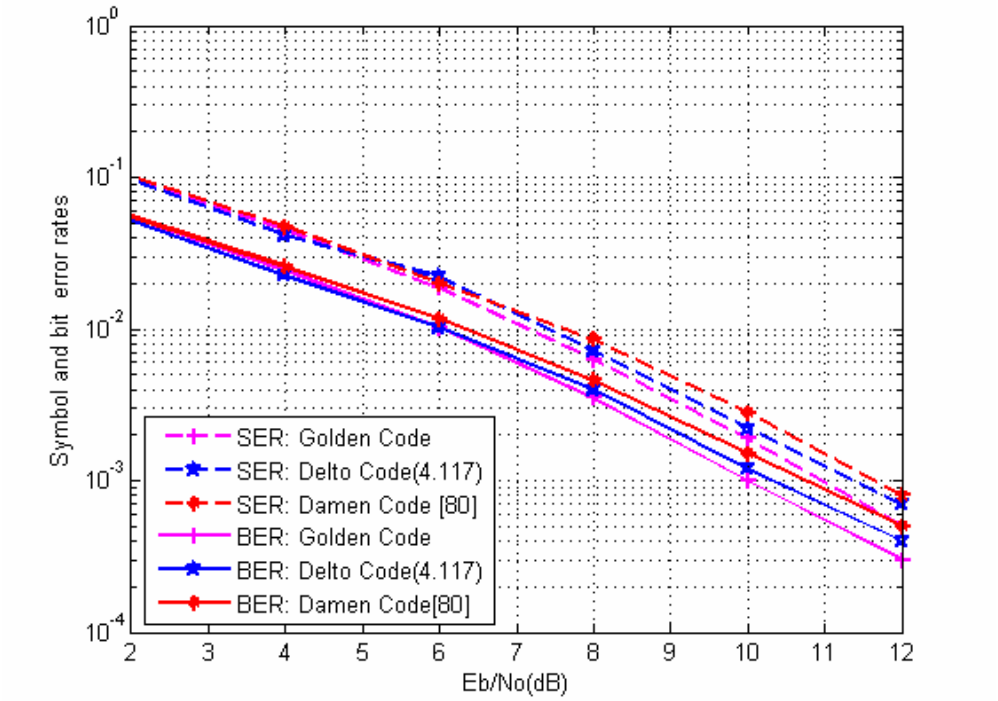

Figure 4.11 Performances of delto codeword matrix (4.117) without delay (perfect synchronization) with two transmit two receive antennas (4 bpcu)

Figure 4.12 shows the bit error rate (BER) and symbol error rate (SER) performances for codeword matrix (4.117) with delay. For delay case, we shifted the first row by one symbol interval as shown in (4.126). The results are compared with the result of well known golden code [77] and the code given in [80]. One can see that at high SNR's our proposed codes (4.117) get better performances.

Figure 4.13 shows the bit error rate (BER) and symbol error rate (SER) performances for codeword matrix (4.131) without delay. The associated code parameters (4.131) are $N_T = T = 3$,

and N_R = 2. The results are compared with the result of the code given in [80]. From the figure, one can observe that our proposed code get better performance by 0.5 dB at the BER of 10^{-3}.

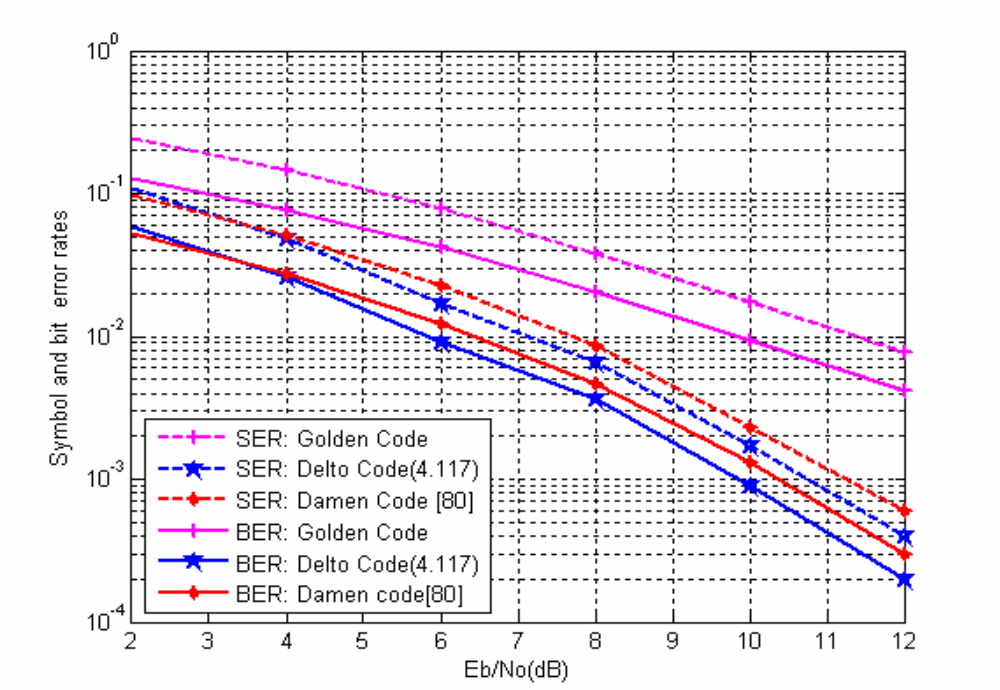

Figure 4.12 Performances of delto codeword matrix (4.117) with delay (asynchronous relays) with two transmit two receive antennas (8/3 bpcu)

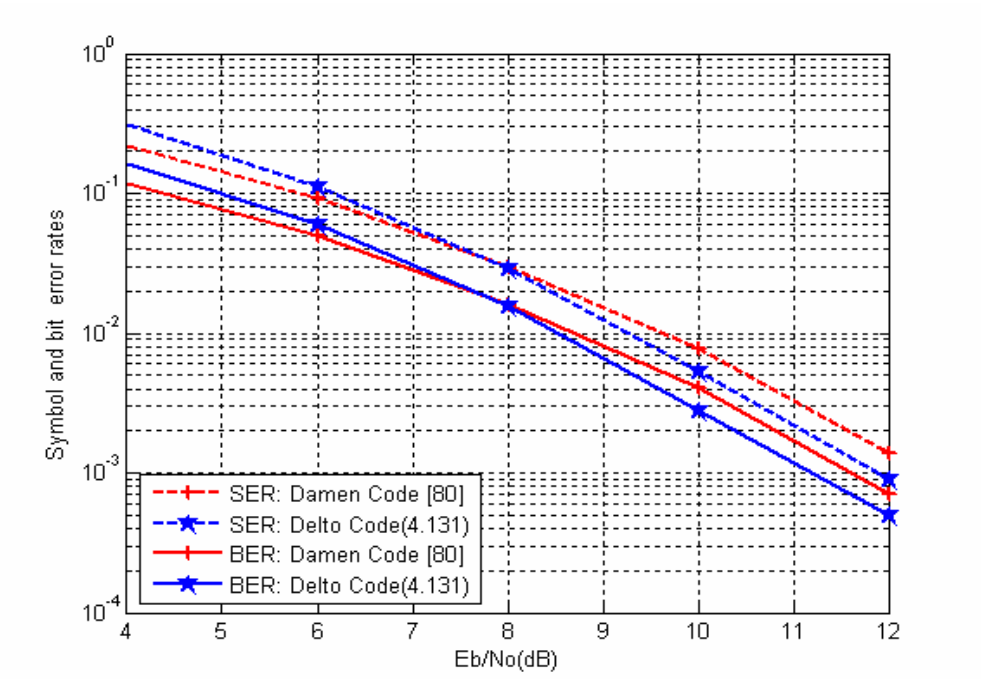

Figure 4.13 Performances of delto codeword matrix (4.131) without delay (perfect synchro:) with 3-transmit 2-receive antennas(8/3 bpcu due to DFE equalization)

Figure 4.14 shows the bit error rate (BER) and symbol error rate (SER) performances for codeword matrix (4.131) with delay. The code parameters for (4.131) are $N_T = T = 3$, and N_R=2. For delay case, we shifted the first row by one symbol interval. The results are compared with that of the code given in [80].

Figure 4.15 shows the bit error rate (BER) and symbol error rate (SER) performances for codeword matrix (4.131) with delay. Delay profile is obtained by shifting the first row in (4.131) by one symbol to the right of other rows. The associated code (4.131) parameters are N_T= N_R=T=3. The results are compared with that of the code in [80]. Our proposed delto distributed TAST code (4.131) get better performances of 1 dB at a BER of 10^{-5}.

Figure 4.16 shows the bit error rate (BER) and symbol error rate (SER) performances for codeword matrix (4.131) without delay. In this case the associated code (4.131) parameters are N_T= N_R=T=3. The results are compared with that of the code in [80]. One can see that the error performance of our proposed delto distributed TAST code (4.131) is improved by about 2dB at the BER of 10^{-5}.

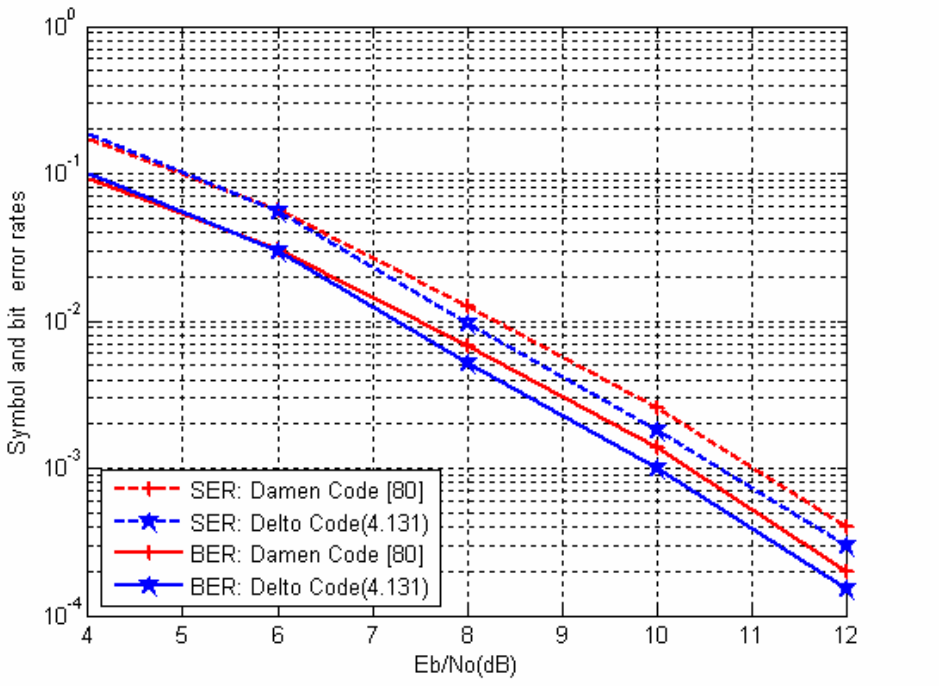

Figure 4.14 Performances of delto codeword matrix (4.131) with delay (asynchronous relays) with 3-transmit 2-receive antennas (3 bpcu due to DFE equalization)

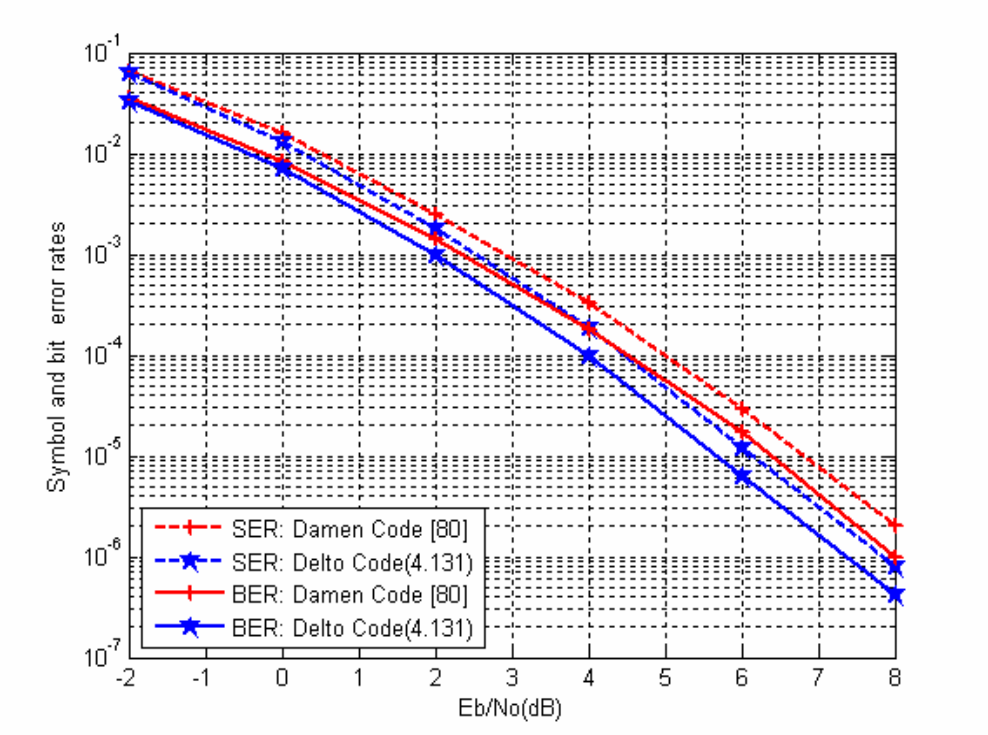

Figure 4.15 Performances of delto codeword matrix (4.131) with delay (asynchronous relays) with three transmit three receive antennas (9/2 bpcu)

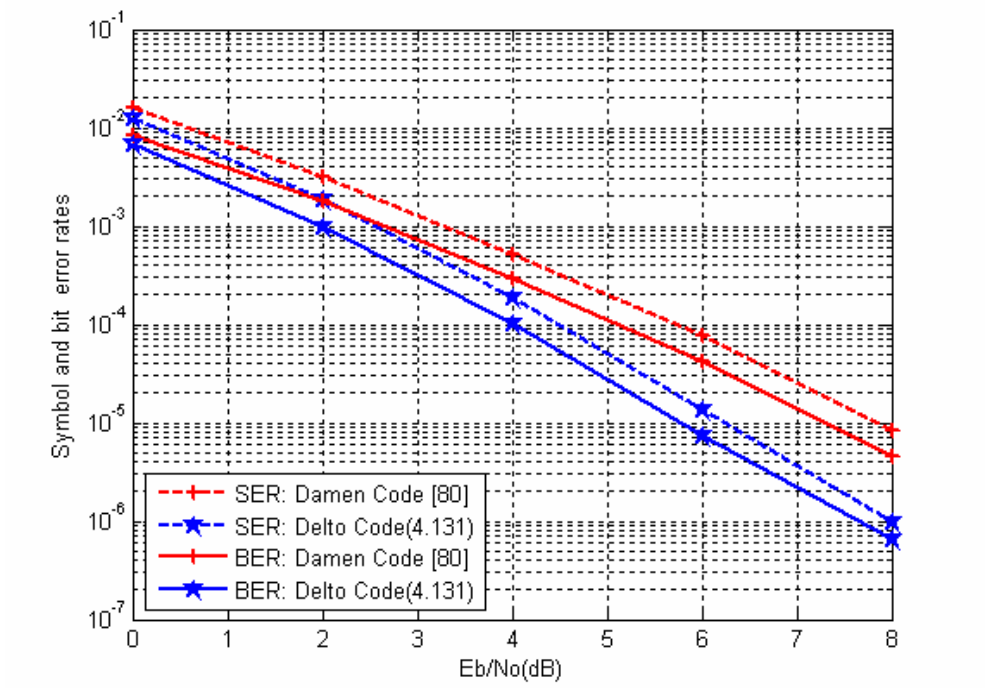

Figure 4.16 Performances of delto codeword matrix (4.131) with out delay (perfect synchronization) with three transmit three receive antennas (6 bpcu)

4.5 Conclusion

One of the recentl discussed problems of the cooperative communication is the asynchronization of the relaying nodes. Due to the asynchronous transmissions a traditionally designed structure of distributed space-time code is destroyed at the reception and it loses the diversity and coding gain. This point is thoroughly explained in [66]. In a delay constrained cooperative system, the data from different relays reach the destination after different delays. It is shown in [69] that the received delayed distributed space-time block code loses diversity for all well-known codes. The first reported delay tolerant codes for asynchronous cooperative network were proposed in [66]. In [69], delay tolerant distributed space-time block codes based on threaded algebraic space-time (TAST) codes [63] are designed for unsynchronized cooperative network. The distributed TAST codes of [69] preserve the rank of the space-time codewords under arbitrary delays at the reception of different rows of the codeword matrix. Within the framework developed in [69], we introduced some easy and useful techniques for the construction of delto distributed STBCs which are delto for arbitrary delay profile. Like their brethren codes, our proposed codes are flexible with respect to constellation size, number of receive/transmit antennas. We introduced two useful techniques for constructing threads codewords matrices. The packing of different threads into a single codeword matrix provides different codes structures to be used over cooperative networks with different setup of relays and antennas. In term of error rates, the codes with $T > N_T$ developed in (4.113) to (4.116) do not outperform the codes introduced by Damen in [69] but we hope that their simple structures may reduce the hardware complexity. The codes with $T = N_T$ developed in (4.117) and (4.131) outperform the existing codes in literature without sacrificing decoding complexity and other nice characteristics. For example the error performance of the code proposed in (4.131) is improved by about 2 dB at the BER of 10^{-5} when $N_T = N_R = 3$, and 0.5 dB at 10^{-3} when $N_T = N_R = 2$ as compared to most recent published delto codes in [80].

In the beginning of this chapter we briefly discussed DAST codes. For completeness we also discussed perfect and golden codes constructed from cyclic algebra. We have also introduced a block layering concept in TAST codes which gains better performance, in addition of reducing the decoding complexity.

Due to the lattice structure of algebraic space time codes, the ML decoding can be implemented by the use of sphere decoding, hence in next chapter we review the concept of sphere decoding, its complexity and performance.

Chapter 5

Sphere decoding

5.1 Introduction

In communication systems where the signals are transmitted using digital modulation like QPSK or QAM, the signal space diagram forms a regular grid. On certain applications such a grid can be described with the help of lattice theory [83]. In doing so, the maximum-likelihood detection is equivalent to the task of finding the closest point in a lattice.

Actually the maximum likelihood decoder for multi-receivers operates by comparing the received signal vector with all possible noiseless received signals corresponding to all possible transmitted signals. Under certain assumptions, a receiver may achieve optimal performance in the sense of maximizing the probability of correct data detection. However, the complexity of this decoder increases exponentially with the number of transmit antennas, and hence makes its usage almost impossible for large array size and high order digital modulation schemes.

The principal idea of the Sphere Decoder (SD) [84] is to reduce the computational complexity of the maximum likelihood detector by only searching over the noiseless received signals that lie within a hypersphere of radius d around the received signal. Normally SD algorithm is implemented as a depth first tree search, where each level in the search represents one transmit antenna's signal. Figure 5.1 depicts the tree of sphere decoding. If at a given level, a given branch exceeds the radius constraint, then that part of the tree is removed from further consideration.

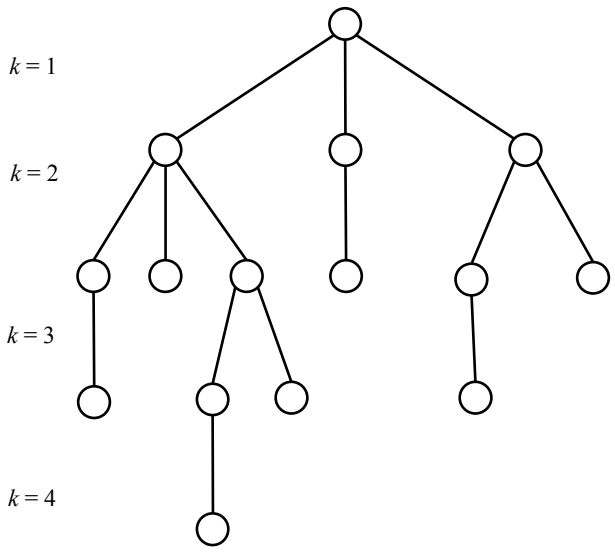

Figure 5.1 Sample tree generated to determine lattice points in a four dimensional sphere

5.2 Introduction to lattice

The concept of lattice is very important in shape coded modulation (SCM). Talking loosely, a lattice is a set of points that have some regularness. For example figure 5.2 demonstrates two examples of general two dimensional lattices and are denoted by $\mathbb{Z}^2$, where $\mathbb{Z}$ shows the field consisting of integers and 2 is the dimension order of the lattice.

Now let, $\boldsymbol{h}_1, \boldsymbol{h}_2, ..., \boldsymbol{h}_m$ be m linearly independent vectors of the n-dimensional Euclidean space $\mathbb{R}^n$, with $m \le n$. A lattice is the set Λ of vectors

$$\lambda_1 \boldsymbol{h}_1 + \lambda_2 \boldsymbol{h}_2 + ... + \lambda_m \boldsymbol{h}_m, \quad \lambda_i \in \mathbb{Z} \text{ with } i = 1,\ldots,m \tag{5.1}$$

The set of vectors $\{\boldsymbol{h}_1, \boldsymbol{h}_2, ..., \boldsymbol{h}_m\}$ is called the basis of Λ, and the generator matrix of Λ is given by

$$\boldsymbol{G}_\Lambda^T = [\boldsymbol{h}_1 \boldsymbol{h}_2 ..... \boldsymbol{h}_m] \tag{5.2}$$

Hence for any point $\boldsymbol{x} \in \Lambda$, there exist a unique $\boldsymbol{u} \in \mathbb{Z}^m$ such that $\boldsymbol{x} = \boldsymbol{u}\boldsymbol{G}_\Lambda$

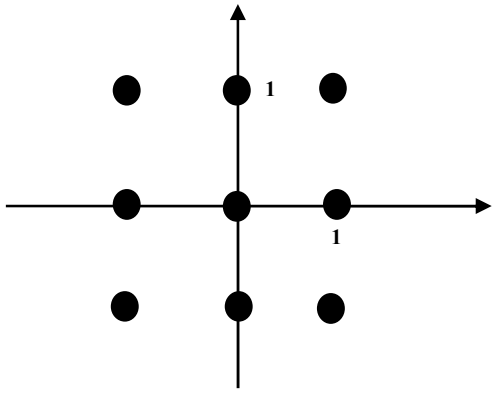

$\mathbb{Z}^2$-Lattice

$$\boldsymbol{G} = \begin{bmatrix} 1 & 0 \\ 0 & 1 \end{bmatrix}$$

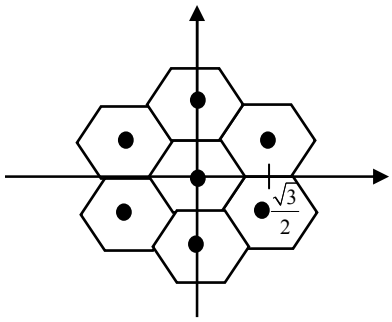

Hexagonal lattice

$$\boldsymbol{G} = \begin{bmatrix} \frac{\sqrt{3}}{2} & 0 \\ \frac{1}{2} & 1 \end{bmatrix}$$

Figure 5.2 2-dimensional lattices and their generator matrices.

5.2.1 Real representation of a complex system

The lattices briefly discussed above are real, *i.e.* the points are taken from $\mathbb{R}^n$, whereas in a communication system, one usually has to deal with complex systems as well. To circumvent this contrariety, it is possible to use an equivalent real-valued model. Taking the complex valued *n*-dimensional model

$$\boldsymbol{r} = \boldsymbol{H}\boldsymbol{x} + \boldsymbol{N} \tag{5.3}$$

the real model has 2*n*-dimensions and can be obtained by separating real and imaginary parts.

$$\begin{bmatrix} \Re(\boldsymbol{r}) \\ \Im(\boldsymbol{r}) \end{bmatrix} = \begin{bmatrix} \Re(\boldsymbol{H}) & \Im(\boldsymbol{H}) \\ -\Im(\boldsymbol{H}) & \Re(\boldsymbol{H}) \end{bmatrix} \begin{bmatrix} \Re(\boldsymbol{x}) \\ \Im(\boldsymbol{x}) \end{bmatrix} + \begin{bmatrix} \Re(\boldsymbol{N}) \\ \Im(\boldsymbol{N}) \end{bmatrix} \tag{5.4}$$

5.3 System model

We consider the multi-antenna system of N_T transmitters and N_R receivers over the Rayleigh fading channel, and for simplicity here we consider the case when $N_R = N_T$.

The received signal at each time instant is given by

$$\boldsymbol{r} = \boldsymbol{H}\boldsymbol{x} + \boldsymbol{N} \tag{5.5}$$

where $\boldsymbol{x} = (x_1, ..., x_{N_T})^T$ denotes the transmitted vector which belongs to the QAM constellation carved from $\mathbb{Z}(i)$, $\boldsymbol{N}$ is $N_R \times 1$ complex column vector AWGN with a variance σ^2 per dimension.

Equivalently, one can write the system (5.5) as

$$\begin{aligned} \boldsymbol{r}' &\triangleq \left[\Re(\boldsymbol{r}^T)\ \Im(\boldsymbol{r}^T)\right] \\ &= \boldsymbol{u}\begin{bmatrix} \Re(\boldsymbol{H}^T) & \Im(\boldsymbol{H}^T) \\ -\Im(\boldsymbol{H}^T) & \Re(\boldsymbol{H}^T) \end{bmatrix} + \boldsymbol{N}' \\ &= \boldsymbol{u}\boldsymbol{G}_H + \boldsymbol{N}' \end{aligned} \tag{5.6}$$

where $\boldsymbol{u} = \left[\Re(\boldsymbol{x})\ \Im(\boldsymbol{x})\right] \in \mathbb{Z}^{2N_T}$ and $\boldsymbol{N}' = \left[\Re(\boldsymbol{N}^T)\ \Im(\boldsymbol{N}^T)\right] \in \mathbb{R}^{2N_T}$

5.4 Sphere decoding algorithm

Initially the sphere decoding algorithm was proposed to determine the shortest vector in a given lattice [84], [85]. Its applications in digital communication systems and vector quantization were introduced in [86] where the problem of decoding lattice codes over the Gaussian channel was shown to be equivalent of finding the shortest vector problem.

In this sequel we consider the case that $N_T \leq N_R$ within the framework provided by [87]. For the case when $N_T > N_R$, the interested reader is referred to [88].

The principle of the sphere algorithm is to search only those lattice points that lay in the jurisdiction of a sphere with radius *d* around the given vector ***r***, thereby reducing the search space and, hence the required computations. Figure 5.3 shows a pictorial view of above definition.

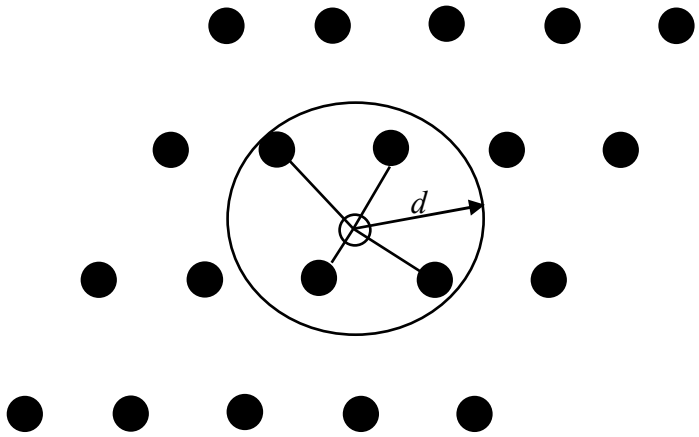

Figure 5.3. Schematic of the SD, only the points inside the circle are searched

Note that the lattice points will lie inside the sphere of radius *d* subject to condition, if

$$d^2 \geq \|\boldsymbol{r} - \boldsymbol{H}\boldsymbol{x}\|^2 \tag{5.7}$$

Every $N_T \times N_R$ (with $N_T \leq N_R$) channel matrix $\boldsymbol{H}$ with linearly independent columns can be factorized as [85]

$$\boldsymbol{H} = \boldsymbol{Q}\begin{bmatrix} \boldsymbol{R} \\ \boldsymbol{0} \end{bmatrix} \tag{5.8}$$

where $\boldsymbol{Q}$ is $N_R \times N_R$ and orthogonal, $\boldsymbol{R}$ is $N_T \times N_T$, upper triangular and $\mathbf{0}$ is an $(N_R - N_T) \times N_T$ matrix of zeros. Further partitioning $\boldsymbol{Q} = [\boldsymbol{Q}_1 \;\; \boldsymbol{Q}_2]$, where $\boldsymbol{Q}_1$ is $N_R \times N_T$ and $\boldsymbol{Q}_2$ is $N_R \times (N_R - N_T)$. We get

$$d^2 \geq \left\| \boldsymbol{r} - [\boldsymbol{Q}_1 \;\; \boldsymbol{Q}_2] \begin{bmatrix} \boldsymbol{R} \\ \mathbf{0} \end{bmatrix} \boldsymbol{x} \right\|^2 = \left\| \begin{bmatrix} \boldsymbol{Q}_1^\dagger \\ \boldsymbol{Q}_2^\dagger \end{bmatrix} \boldsymbol{r} - \begin{bmatrix} \boldsymbol{R} \\ \mathbf{0} \end{bmatrix} \boldsymbol{x} \right\|^2$$

$$= \left\| \boldsymbol{Q}_1^\dagger \boldsymbol{r} - \boldsymbol{R}\boldsymbol{x} \right\|^2 + \left\| \boldsymbol{Q}_2^\dagger \boldsymbol{r} \right\|^2 \tag{5.9}$$

where $(\cdot)^\dagger$ denotes Hermitian matrix transposition. In other words

$$d^2 - \left\| \boldsymbol{Q}_2^\dagger \boldsymbol{r} \right\|^2 \geq \left\| \boldsymbol{Q}_1^\dagger \boldsymbol{r} - \boldsymbol{R}\boldsymbol{x} \right\|^2 \tag{5.10}$$

Note that the first term is independent of $\boldsymbol{x}$, defining $\boldsymbol{y} = \boldsymbol{Q}_1^\dagger \boldsymbol{r}$ and $d'^2 = d^2 - \left\| \boldsymbol{Q}_2^\dagger \boldsymbol{r} \right\|^2$, the integer least square problem (5.7) is then reduced to the following integer least square problem:

$$d'^2 \geq \left\| \boldsymbol{y} - \boldsymbol{R}\boldsymbol{x} \right\|^2 \tag{5.11}$$

(5.11) can expanded as

$$\begin{bmatrix} y_1 \\ \vdots \\ y_{N_T-2} \\ y_{N_T-1} \\ y_{N_T} \end{bmatrix} \approx \begin{bmatrix} r_{1,1} & \cdots & r_{1,N_T-2} & r_{1,N_T-1} & r_{1,N_T} \\ & \ddots & \vdots & \vdots & \vdots \\ & & r_{N_T-2,N_T} & r_{N_T-2,N_T-1} & r_{N_T-2,N_T} \\ & & & r_{N_T-1,N_T-1} & r_{N_T-1,N_T} \\ & & & & r_{N_T,N_T} \end{bmatrix} \begin{bmatrix} x_1 \\ \vdots \\ x_{N_T-2} \\ x_{N_T-1} \\ x_{N_T} \end{bmatrix} \tag{5.12}$$

Since $\boldsymbol{R}$ is upper triangular, we can write (5.11) as

$$d'^2 \geq \sum_{i=1}^{N_T} \left| y_i - \sum_{j=i}^{N_T} r'_{i,j} x_j \right|^2 \tag{5.13}$$

where $r'_{i,j}$ denotes an (i, j) entry of $\boldsymbol{R}$. The above inequality can be expanded as

$$d'^2 \geq \left| y_{N_T} - r'_{N_T,N_T} x_{N_T} \right|^2 + \left| y_{N_T-1} - r'_{N_T-1,N_T-1} x_{N_T-1} - r'_{N_T-1,N_T} x_{N_T} \right|^2 + \ldots \tag{5.14}$$

The first term in (5.14) depends only on N_T-th entry x_{N_T} of lattice point x, the second term depends on the entries $\{x_{N_T}, x_{N_T-1}\}$, and so on.

We can see that a necessary condition for $\boldsymbol{Rx}$ to lie inside the hypersphere of a given radius d is $d'^2 \geq \left| y_{N_T} - r'_{N_T,N_T} x_{N_T} \right|^2$, which is equivalent to the following condition for entry x_{N_T}:

$$\left\lceil \frac{-d' + y_{N_T}}{r'_{N_T,N_T}} \right\rceil \leq x_{N_T} \leq \left\lfloor \frac{d' + y_{N_T}}{r'_{N_T,N_T}} \right\rfloor \tag{5.15}$$

where $\lceil \cdot \rceil$ denotes rounding to the nearest larger element in the set of numbers that spans the lattice, and $\lfloor \cdot \rfloor$ denotes rounding to the nearest smaller element in the set of numbers that spans the lattice.

Furthermore for each integer x_{N_T} satisfying (5.15), define $d'^2_{N_T-1} = d'^2 - \left| y_{N_T} - r'_{N_T,N_T} x_{N_T} \right|^2$ and $y_{N_T-1|N_T} = y_{N_T-1} - r'_{N_T-1,N_T} x_{N_T}$, a stronger necessary condition can be found by looking at the first two terms in (5.14), which leads to x_{N_T-1} belonging to the interval

$$\left\lceil \frac{-d'_{N_T-1} + y_{N_T-1|N_T}}{r'_{N_T-1,N_T-1}} \right\rceil \leq x_{N_T-1} \leq \left\lfloor \frac{d'_{N_T-1} + y_{N_T-1|N_T}}{r'_{N_T-1,N_T-1}} \right\rfloor \tag{5.16}$$

Following the above procedure, we can obtain the intervals for x_{N_T-2} and so on until x_1. Then we would be able to determine all the lattice points in the hypersphere of radius d.

Algorithm

Input : R , d , r , $y = Q_1^{\dagger} r$ and $Q = [Q_1 \;\; Q_2]$

Output : x or *null*

1. *set* $k = N_T$

$d'^2_{N_T} = d^2 - \left\| Q_2^{\dagger} r \right\|^2$, $y_{N_T | N_T+1} = y_{N_T}$

2.(set b*ounds for* x_k)

$$z = \frac{d'_k}{r_{N_T, N_T}}$$

$UB(x_k) = \lfloor (z + y_{k|k+1}) \rfloor$, $x_k = \lceil (-z + y_{k|k+1}) \rceil - 1$

3.(*increase* x_k) $x_k = x_k + 1$.

If $x_k \le UB(x_k)$ *go to* 5; *else go to* 4

4.(*increase* k)

$k = k + 1$;

if $k = N_T + 1$ *terminate algorithm*;

else go to 3

5.(decrease k)

if $k = 1$ *Go to* 6

else $k = k - 1$, $y_{k|k+1} = y_k - \sum_{j=k+1}^{N_T} r'_{k,j} x_j$, $d'^2_k = d'^2_{k+1} - \left| y_{k+1|k+2} - r'_{k+1,k+1} x_{k+1} \right|^2$

and go to 2.

6. *solution found*. *Save x and its distance from r*,

$d'^2_{N_T} - d'^2_1 + \left| y_1 - r'_{1,1} x_1 \right|^2$ *and go to* 3.

The subscript $k \,|\, k+1$ in above algorithm is used to denote the received signal y_k adjusted with the already estimated symbol components $x_{k+1}, ..., x_{N_T}$. To help us to understand the algorithm in a better way, we draw the flowchart of the algorithm in figure 5.4, followed by a work example.

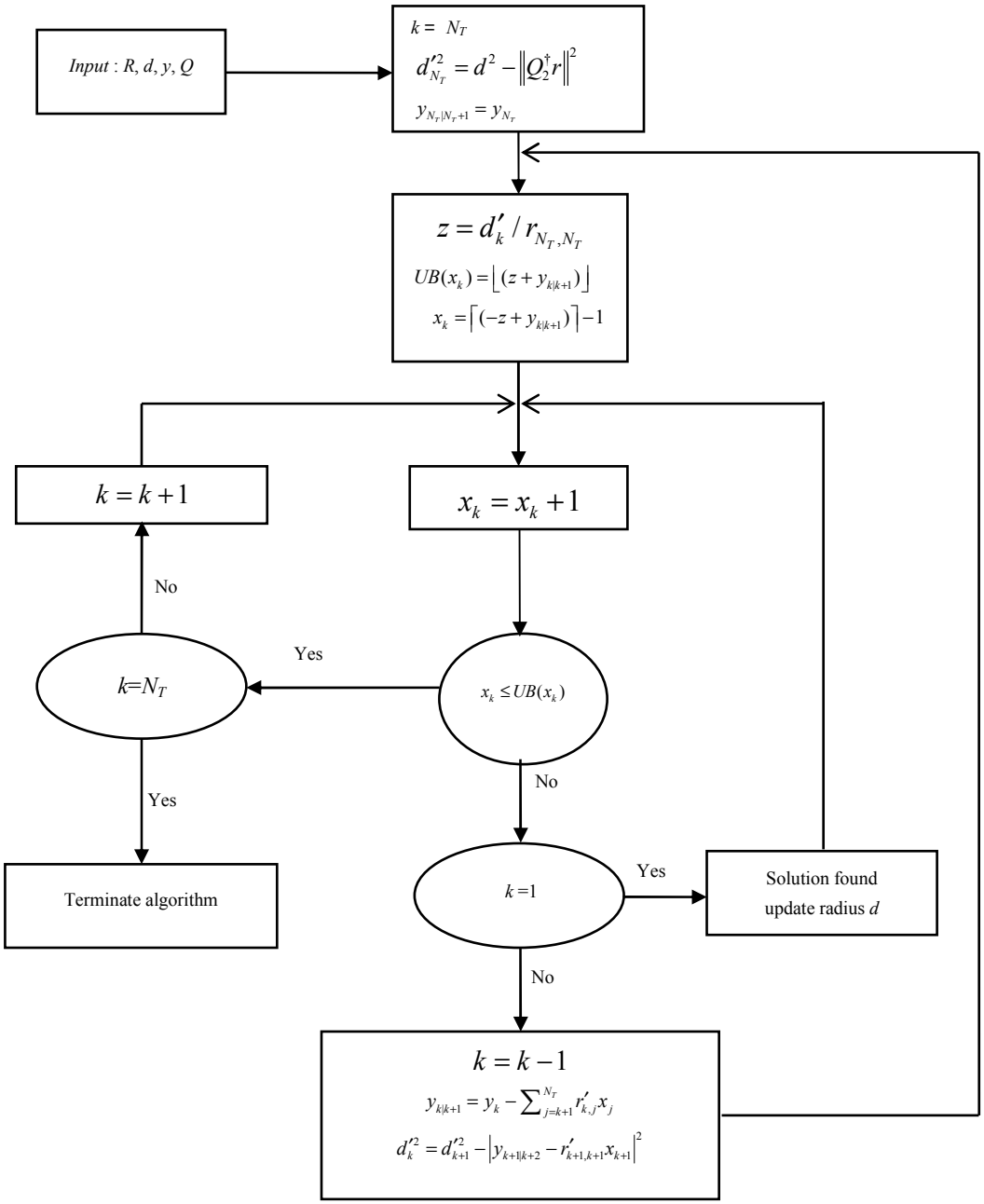

Figure 5.4 Flowchart of SD algorithm

Work example 5.1

To have a better concept about SD, here we present a simple work example. Considering (5.7) and using BPSK modulation with level $x \in \{1, -1\}$ for three binary input data, suppose we have channel matrix as

$$\boldsymbol{H} = \begin{bmatrix} -0.97 & -0.09 & -0.29 \\ -1.51 & -1.68 & -1.13 \\ 1.41 & 1.14 & 0.4 \end{bmatrix}$$

and the output signal is

$$\boldsymbol{r} = \begin{bmatrix} 0.747 \\ 2.49 \\ -2.40 \end{bmatrix}$$

Searching for the most likely bit sequence using SD by taking its radius as $d = 1$

The problem to be solved can be formulated as

$$\hat{\boldsymbol{x}} = argmin\left\{\left|\boldsymbol{r} - \boldsymbol{H}\boldsymbol{x}\right|^2\right\}$$

Decomposing $\boldsymbol{H}$ in to $\boldsymbol{QR}$ factors

$$\boldsymbol{H} = \boldsymbol{QR} = \begin{bmatrix} -0.425 & 0.838 & 0.341 \\ -0.661 & -0.545 & 0.515 \\ 0.618 & 0.006 & 0.787 \end{bmatrix} \begin{bmatrix} 2.28 & 1.85 & 1.12 \\ 0 & 0.84 & 0.37 \\ 0 & 0 & -0.367 \end{bmatrix}$$

We search for all bit sequences for which

$$\left|\boldsymbol{r} - \boldsymbol{H}\boldsymbol{x}\right|^2 < d$$

From (5.9), the above equation can be written as

$$\left|\boldsymbol{Q}^{\dagger}\boldsymbol{r} - \boldsymbol{Q}^{\dagger}\boldsymbol{Q}\boldsymbol{R}\boldsymbol{x}\right|^2 = \left|\boldsymbol{r}' - \boldsymbol{R}\boldsymbol{x}\right|^2 < d$$

$$\boldsymbol{Q}^{\dagger}\boldsymbol{r} = \boldsymbol{r}' = \begin{bmatrix} -3.45 \\ -0.72 \\ -0.35 \end{bmatrix}$$

Now we have

$$\left\| \begin{bmatrix} -3.45 \\ -0.72 \\ -0.35 \end{bmatrix} - \begin{bmatrix} 2.28 & 1.85 & 1.12 \\ 0 & 0.84 & 0.37 \\ 0 & 0 & -0.367 \end{bmatrix} \begin{bmatrix} x_1 \\ x_2 \\ x_3 \end{bmatrix} \right\|^2 < d$$

From (5.14) we know

$$\left|-0.35+0.367x_3\right|^2+\left|-0.72-0.84x_2-0.37x_3\right|^2+\left|-3.45-2.28x_1-1.85x_2-1.12x_3\right|^2$$

For 3 bits sequence we may have 8 possible different sequences.

Now we fix one bit position and see whether it exceeds the value of *d* or not. In case if any bit alone exceed *d*, then we do not further consider that bit and so we limit our search space. *e.g.* fixing x_3 , we have

$$\boldsymbol{x}=\begin{bmatrix}\times\\ \times\\ -1\end{bmatrix}=\left|-0.35+0.367x_3\right|^2=0.717$$

This is less than *d*, so we save it and fix x_2 or x_1, and see whether it exceed the value of *d* or not. So in this way we test different sequences and discard the specific bit value not satisfying the condition. In this way our search space will be limited.

For example

$$\begin{bmatrix}-1\\ -1\\ -1\end{bmatrix}=2.76$$

has a value greater than *d*, so this cannot be a possible sequence, and is discarded.

5.5 Sphere decoding of algebraic ST codes

In this section we consider the sphere decoding of algebraic space-time (ST) codes $\mathcal{T}_{N_T,L}$ discussed in previous chapter.

The decoding is applied to the scheme where the number of receive antennas are equal to the number of transmit antennas, *i.e.* $N_R = N_T$.

The lattice sphere packing representation of the algebraic space-time codes is done in two steps:

- Represent $\mathcal{T}_{N_T,L}$ by its equivalent uncoded system (N_T , N_R)→ (LN_T , LN_R),
- Represent the resulted uncoded system by its lattice form (5.6): $n = 2LN_T$.

Example 5.2

Consider the system with, $N_T = N_R = L = 2$, the received signal is given by

$$\boldsymbol{r} = \begin{bmatrix} h_{11} & h_{12} \\ h_{21} & h_{22} \end{bmatrix} \begin{bmatrix} y_1 & -y_3 \\ y_2 & y_4 \end{bmatrix} + \boldsymbol{N} \tag{5.17}$$

where $\boldsymbol{N}$ is a 2×2 matrix of complex Gaussian noise and $y^T = [y_1, y_2, y_3, y_4]^T = \boldsymbol{R}_4 \boldsymbol{x}^T$, $\boldsymbol{R}_4$ is optimal rotation matrix of dimension 4, and $x = [x_1, x_2, x_3, x_4] \in$ QAM the uncoded symbols vector.

The equivalent uncoded system is given by

$$Vec(\boldsymbol{r}^T) = \begin{bmatrix} h_{11} & h_{12} & 0 & 0 \\ 0 & 0 & h_{11} & h_{12} \\ h_{21} & h_{22} & 0 & 0 \\ 0 & 0 & h_{21} & h_{22} \end{bmatrix} . R_4' \boldsymbol{x}^T + vec(\boldsymbol{N}^T)$$

$$= \boldsymbol{H}_4 \boldsymbol{R}_4' \boldsymbol{x}^T + vec(\boldsymbol{N}^T) \tag{5.18}$$

where $vec(\boldsymbol{r}^T)$ is the vector representation of the matrix $\boldsymbol{r}^T$ by putting all its columns one after another in one vector column. $\boldsymbol{R}_4'$ is the rotation matrix $\boldsymbol{R}_4$ with the third line multiplied by -1. The received signal can be written as

$$\boldsymbol{r}' = vec(\boldsymbol{r}^T) = \boldsymbol{H}' \boldsymbol{x}^T + \boldsymbol{N}' \tag{5.19}$$

where $\boldsymbol{H}' = \boldsymbol{H}_4 \boldsymbol{R}_4'$ of rank 4 almost always, since the rank of $\boldsymbol{H}_4$ is 4 almost always.

Finally, the lattice sphere packing representation of the resulted system is given by

$$\begin{aligned} \boldsymbol{r}'' &\triangleq \left[\Re(\boldsymbol{r}'^T) \;\; \Im(\boldsymbol{r}'^T)\right] \\ &= \boldsymbol{u}\begin{bmatrix} \Re(\boldsymbol{H}'^T) & \Im(\boldsymbol{H}'^T) \\ -\Im(\boldsymbol{H}'^T) & \Re(\boldsymbol{H}'^T) \end{bmatrix} + \boldsymbol{N}'' \\ &= \boldsymbol{u}\boldsymbol{G}_{\boldsymbol{H}'} + \boldsymbol{N}'' \end{aligned} \tag{5.20}$$

where $\boldsymbol{u} = \left[\Re(\boldsymbol{x}) \;\; \Im(\boldsymbol{x})\right] \in \mathbb{Z}^{2LN_T}$, and $\boldsymbol{N}'' = \left[\Re(\boldsymbol{N}'^T) \;\; \Im(\boldsymbol{N}'^T)\right] \in \mathbb{R}^{2LN_T}$. The dimension increase for lattice representation is $N_T = 2 \rightarrow 2LN_T = 8$.

Work example 5.3

Suppose a system with $N_T = N_R = L = 2$. The two threads are separated by the algebraic number $\phi = i$

The two binary symbols with possible values $x \in \{-1,1\}$ are mapped into one thread. So in one block we may transmit 4 bits of information.

The rotation matrix for two threads is

$$\boldsymbol{M} = \begin{bmatrix} 1 & i \\ 1 & i \end{bmatrix}$$

and the channel matrix is assumed as

$$\boldsymbol{H} = \begin{bmatrix} -0.58 + 0.37i & 0.32 - 0.37i \\ 0.061 + 0.56i & -0.27 + 0.55i \end{bmatrix}$$

The threads are mapped as follows:

Threads-I= {1, 2} meaning that in first interval, stream 1 is transmitted from antenna 1 and in the second interval from antenna 2.

Threads-II= {2, 1} meaning that in first interval, stream 2 is transmitted from antenna 2 and in second interval from antenna 1.

Hence the matrix $\boldsymbol{H}$ for first thread is

$$\boldsymbol{H}_1 = \begin{bmatrix} -0.58+0.37i & 0 \\ 0 & 0.051+0.56i \\ 0.32-0.37i & 0 \\ 0 & -0.27-0.55i \end{bmatrix}$$

and for second thread

$$\boldsymbol{H}_2 = \begin{bmatrix} 0.051+0.56i & 0 \\ 0 & -0.58+0.37i \\ -0.27-0.55i & 0 \\ 0 & 0.32-0.37i \end{bmatrix}$$

The combined matrix is

$$\boldsymbol{H} = \begin{bmatrix} -0.58+0.37i & 0 & 0.051+0.56i & 0 \\ 0 & 0.051+0.56i & 0 & -0.58+0.37i \\ 0.32-0.37i & 0 & -0.27-0.55i & 0 \\ 0 & -0.27-0.55i & 0 & 0.32-0.37i \end{bmatrix}$$

Rotation matrix for thread one and two is

$$\boldsymbol{M} = \begin{bmatrix} 1 & i & 0 & 0 \\ 1 & -i & 0 & 0 \\ 0 & 0 & i\begin{bmatrix} 1 & i \\ 1 & -i \end{bmatrix} \end{bmatrix} = \begin{bmatrix} 1 & i & 0 & 0 \\ 1 & -i & 0 & 0 \\ 0 & 0 & i & -1 \\ 0 & 0 & -i & 1 \end{bmatrix}$$

Because of the structure of rotation, the data streams are arranged as

$$s = \begin{bmatrix} \boldsymbol{s}_{th,1} \\ \boldsymbol{s}_{th,2} \end{bmatrix} = \begin{bmatrix} s_{th,1,bit1} \\ s_{th,1,bit2} \\ s_{th,2,bit1} \\ s_{th,2,bit2} \end{bmatrix}$$

Multipling the channel matrix $\boldsymbol{H}$ by rotation matrix $\boldsymbol{M}$, we get

$$\boldsymbol{H'} = \boldsymbol{HM} = \begin{bmatrix} -0.58+0.37i & -0.37-0.58i & -0.56+0.051i & -0.051+0.56i \\ 0.051+0.56i & 0.56-0.051i & -0.37-0.58i & -0.58+0.37i \\ 0.32-0.37i & 0.37-0.32i & 0.55-0.27i & 0.27+0.55i \\ -0.27-0.55i & -0.55+0.27i & 0.37+0.32i & 0.32-0.37i \end{bmatrix}$$

From section 5.2.1 matrix $\boldsymbol{H'}$ can be converted into real form as

$$\boldsymbol{H}_{real} = \begin{bmatrix} \Re(\boldsymbol{H'}) & -\Im(\boldsymbol{H'}) \\ \Im(\boldsymbol{H'}) & \Re(\boldsymbol{H'}) \end{bmatrix}_{8\times 8}$$

$$= \begin{bmatrix} -0.58 & -0.37 & -0.56 & -0.051 & -0.37 & 0.58 & -0.051 & 0.56 \\ 0.051 & 0.56 & -0.37 & -0.58 & -0.56 & 0.051 & 0.58 & -0.37 \\ 0.32 & 0.37 & 0.55 & 0.27 & 0.37 & 0.32 & 0.27 & -0.55 \\ -0.27 & -0.55 & 0.37 & 0.32 & 0.55 & -0.27 & -0.32 & 0.37 \\ 0.37 & -0.58 & 0.051 & -0.56 & -0.58 & -0.37 & -0.56 & -0.051 \\ 0.56 & -0.051 & -0.58 & 0.37 & 0.051 & 0.56 & -0.37 & -0.58 \\ -0.37 & -0.32 & -0.27 & 0.55 & 0.32 & 0.37 & 0.55 & 0.27 \\ -0.55 & 0.27 & 0.32 & -0.37 & -0.27 & -0.55 & 0.37 & 0.32 \end{bmatrix}$$

Then the above matrix is split into $\boldsymbol{QR}$ factors.

The received vector $\boldsymbol{r}$ is also converted into real form as

$$\boldsymbol{r}_{real} = \begin{bmatrix} \Re(\boldsymbol{r}) \\ \Im(\boldsymbol{r}) \end{bmatrix}$$

The search has now the form

$$\left|\boldsymbol{r}-\boldsymbol{H}\boldsymbol{x}\right|^2 < d$$

where $\boldsymbol{x}$ is calculated from $\boldsymbol{x} = \boldsymbol{M}\boldsymbol{s}$.

Further calculation can be done in same way as we did in work example 5.1.

5.6 Performance of sphere decoding

For performance analysis of SD, we consider (5.5) and its equivalent lattice representation in (5.6). Performing SD needs additional operations to compute the ***QR*** factorization of matrix ***H***. The additional computational complexity is $O(n^3)$ arithmetical operations [85],[89], where $n = 2N_T$. Over a quasi-static fading where the channel is fixed during a long period of time, this additional computation is performed once at the beginning of each received block.

In simulation we have considered the 16-QAM modulation. The average energy per bit is fixed to $E_b = 1$. The matrix ***H*** is modelled by independent Gaussian random variables of variance 0.5 per dimension. The curves are plotted as a function of SNR, and the variance σ^2 of the AWGN per dimension is adjusted by the formula

$$\sigma^2 = \frac{N_T E_{S_{av}}}{2\log_2(16)} 10^{\frac{-SNR}{10}} \tag{5.21}$$

where $E_{S_{av}}$ is the average symbol energy of the 16-QAM modulation, when $E_b = 1$.

Fig. 5.5 shows the average symbol error rate of SD, ML and V-BLAST detector for the uncoded system with $N_T = N_R = 2$ and for the algebraic ST code with $N_T = N_R = L = 2$, using 16-QAM modulation. One may notice both SD and ML have same performances and both of them outperform the V-BLAST decoder.

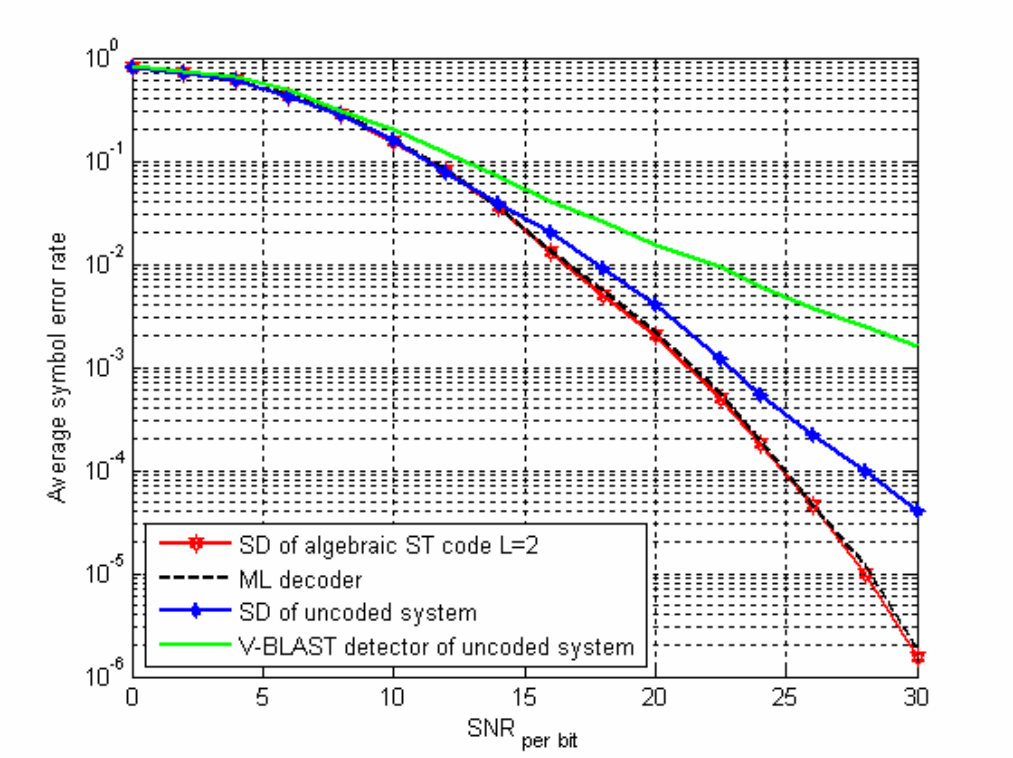

Figure 5.5: Performance analysis of different decoders

5.7 Conclusion

In this chapter we discussed the sphere decoding and its application generally in multiple antennas communication system and particularly in algebraic space time codes. The interesting point of SD algorithm is this, that it is independent of the size of the constituent QAM constellation. Hence, a very high throughput could be achieved along with ML performance. For performances analysis we simulated the performances of four decoders, including zero-forcing, V-BLAST [90], maximum likelihood and sphere decoding algorithm. The zero-forcing and V-BLAST decoder are simple decoders with low complexities. But their performances are low as compared to the maximum likelihood decoder, which in some sense is the optimal decoder, but it has high decoding complexity. The sphere decoding solves the intricate problems of decoding the algebraic space time codes up to dimensions $LN_T \leq 16$ [89]. The main advantage of sphere decoding is the achievement of the full diversity in a multi-antenna system without adding any redundancy, and performing the ML decoding with low computational complexity.

Conclusions and Perspectives

Recent advances in wireless communication systems show that the use of multiple antennas at both link ends can achieve impressive increases in overall system performances. Hence to meet the fast growing demand for high data rate and reliable communication, the use of multiple antennas both at transmitter and receiver has become inevitable. Since last decade MIMO technology has brought revolutionary changes in wireless communication systems. MIMO system provides high data rate by exploiting the spatial domain under the constraints of limited bandwidth and transmit power. Space-time coding [15] is a MIMO transmit strategy which exploits transmit diversity and high reliability. In literature one can find different space time coding techniques for different network topologies and schemes. Through out the evolutionary period both MIMO and space time coding systems have confronted numerous constraints and problems, and perhaps yet there is room for improvement and advancement. Initially full rate and full diversity space time codes were available only for two transmit antenna schemes, but today we have algebraic space time codes [62] which provide high performances irrespective of number of transmit/receive antennas. Cooperative diversity [19] is benefited to compensate the use of multiple antennas at certain small devices. After finding the solutions to get maximum diversity and full rate space time codes, delay constraints over asynchronous network is recent topic of discussion.

In fact in a delay constrained cooperative system the data from different relays reach the destination after different times, hence as a result all the so-called powerful space time codes lose their reliability if timing offset is not assured. This gloomy aspect of space time codes for the first time was studied in [67]. In [68] the authors propose the use of guard bands between successive transmissions. Obviously the technique proposed in [68] drastically reduces the code rates. In [69] delay tolerant distributed space-time block codes based on threaded algebraic space-time (TAST) codes [63] are presented for unsynchronized cooperative networks. The codes developed in [69] preserve the rank of the space-time codewords under arbitrary delays at the reception of different rows of the codeword matrices.

In this work, we have proposed some easy and useful techniques for construction of delay tolerant space time block codes which are delay tolerant for arbitrary delays. We claim that our codes obtain better performances as compare to the codes introduced in [69]. But yet there is a big room for improvement, because we think that the construction of thread codeword

matrices for higher number of antennas may create some complexities. Therefore one should focus to construct simple and more efficient delay tolerant codeword matrices for larger number of antennas. Secondly, of course the construction of the codes having the property to retain the coding rate is a great challenge. Some type of advance timing protocols or artificial intelligent detectors at relays and receivers may be considered to study this blemishing aspect of the codes. Similarly the performances of delay non-constraint codes over trellis codes can be further improved by improving the structure of trellis codes in a way as we did in case of traditional space time trellis codes in chapter 3 by the introduction of super orthogonal trellis codes.

Appendices

Appendix-A

Slow fading channels

In case of slow fading channels, the fading coefficients of the channel are constant during a frame length L. Its mean the fading $h_{j,i}^{t}$ does not depend on temporal superscript t, *i.e.* $h_{j,i}^{1} = h_{j,i}^{2} = ... = h_{j,i}^{L} = h_{j,i}$, $i = 1,2,...,N_T$, $j = 1,2,...,N_R$

Hence the expression for calculating Euclidean distance between two sequences of space time codes can be written as:

$$d_h^2\left(\boldsymbol{X},\hat{\boldsymbol{X}}\right) = \sum_{t=1}^{L}\sum_{j=1}^{N_R}\left|\sum_{i=1}^{N_T} h_{j,i}\left(\hat{x}_t^i - x_t^i\right)\right|^2 \tag{A.1}$$

Defining a matrix $\boldsymbol{B}$ as difference matrix between two sequences of space time symbols $\boldsymbol{X}$ and $\hat{\boldsymbol{X}}$:

$$\boldsymbol{B}\left(\boldsymbol{X},\hat{\boldsymbol{X}}\right) = \boldsymbol{X} - \hat{\boldsymbol{X}} = \begin{bmatrix} x_1^1 - \hat{x}_1^1 & x_2^1 - \hat{x}_2^1 & \dots & x_L^1 - \hat{x}_L^1 \\ x_1^2 - \hat{x}_1^2 & x_2^2 - \hat{x}_2^2 & \dots & x_L^2 - \hat{x}_L^2 \\ \vdots & \vdots & \ddots & \vdots \\ x_1^{N_T} - \hat{x}_1^{N_T} & x_2^{N_T} - \hat{x}_2^{N_T} & \dots & x_L^{N_T} - \hat{x}_L^{N_T} \end{bmatrix} \tag{A.2}$$

The square matrix ***A,*** which is called as distance matrix of $N_T \times N_T$ dimension, is given by

$$\boldsymbol{A}\left(\boldsymbol{X},\hat{\boldsymbol{X}}\right) = \boldsymbol{B}\left(\boldsymbol{X},\hat{\boldsymbol{X}}\right).\boldsymbol{B}^{\dagger}\left(\boldsymbol{X},\hat{\boldsymbol{X}}\right) \tag{A.3}$$

where $(\cdot)^{\dagger}$ denotes the conjugate transpose.

It is clear that $\boldsymbol{A}(\boldsymbol{X},\hat{\boldsymbol{X}})$ is non-negative definite Hermitian, as $\boldsymbol{A}(\boldsymbol{X},\hat{\boldsymbol{X}}) = \boldsymbol{A}^{\dagger}(\boldsymbol{X},\hat{\boldsymbol{X}})$ and the eigenvalues of $\boldsymbol{A}(\boldsymbol{X},\hat{\boldsymbol{X}})$ are non-negative real numbers, therefore, there exist a unitary matrix $\boldsymbol{V}$ and a real diagonal matrix $\boldsymbol{D}$ such that [4].

$$\boldsymbol{V}\boldsymbol{A}(\boldsymbol{X},\hat{\boldsymbol{X}})\boldsymbol{V}^{\dagger} = \boldsymbol{D} \tag{A.4}$$

The rows of $\boldsymbol{V}, (\boldsymbol{v}_1, \boldsymbol{v}_2, \ldots, \boldsymbol{v}_{\mathrm{N_T}})$ are the eigenvectors of $\boldsymbol{A}(\boldsymbol{X}, \hat{\boldsymbol{X}})$ forming a complete orthonormal basis of an N_T -dimensional vector space. The diagonal elements of $\boldsymbol{D}$ are the eigvalues $\lambda_i \geq 0, i = 1, 2, ..., N_T$, of $\boldsymbol{A}(\boldsymbol{X}, \hat{\boldsymbol{X}})$.

The diagonal matrix is represented as

$$\boldsymbol{D} = \begin{bmatrix} \lambda_1 & 0 & \ldots & 0 \\ 0 & \lambda_2 & \ldots & 0 \\ \vdots & \vdots & \ddots & \vdots \\ 0 & 0 & \ldots & \lambda_{N_T} \end{bmatrix} \tag{A.5}$$

Let $\boldsymbol{h}_j = \left(h_{j,1}, h_{j,2}, ..., h_{j,N_T}\right)$ represents the j-th row of the channel matrix $\boldsymbol{H}$, Then PEP can be upper bounded to obtain the relation [4], [5]

$$\begin{aligned} P\left(\boldsymbol{X}, \hat{\boldsymbol{X}} \mid \boldsymbol{H}\right) &\leq \sum_{j=1}^{N_R} \exp\left(-\boldsymbol{h}_j A(\boldsymbol{X}, \hat{\boldsymbol{X}}) \boldsymbol{h}_j^{\dagger} \frac{E_s}{4N_0} \right) \\ &= \sum_{j=1}^{N_R} \sum_{i=1}^{N_T} \exp\left(-\frac{E_s}{4N_0} \sum_{i=1}^{N_T} \lambda_i \left|\beta_{j,i}\right|^2 \right) \end{aligned} \tag{A.6}$$

where E_s is energy per symbol, and $\beta_{j,i} = \boldsymbol{h}_j . \boldsymbol{v}_i$

Inequality (A.6) is an upper bound on the conditional PEP expressed as a function of $\beta_{j,i}$. If $\beta_{j,i}$ follows a Rayleigh distribution, the upper bound of the PEP becomes

$$P\left(\boldsymbol{X}, \hat{\boldsymbol{X}}\right) \leq \left(\prod_{i=1}^{N_T} \frac{1}{1 + \frac{E_S}{4N_0} \lambda_i} \right)^{N_R} \tag{A.7}$$

Let r_A be the rank of matrix $\boldsymbol{A}$. One can see that $\boldsymbol{A}$ possesses exactly $N_T - r_A$ zero eigenvalues, hence at high SNR (A.7) can be written as

$$P(\boldsymbol{X}, \hat{\boldsymbol{X}}) \leq \left[\underbrace{\left(\prod_{i=1}^{r_A} \lambda_i \right)^{1/r_A}}_{\text{Coding gain}} \frac{E_s}{4N_0} \right]^{\overbrace{-r_A N_R}^{\text{Diversity order}}} \tag{A.8}$$

Appendix-B

Fast fading channels

Now suppose that the channel fading coefficients $h_{j,i}^{t}$ varies from one symbol to other. So the Euclidean distance $d_h^2\left(\boldsymbol{X},\hat{\boldsymbol{X}}\right)$ can be written as:

$$d_h^2\left(\boldsymbol{X},\hat{\boldsymbol{X}}\right)=\sum_{t=1}^{L}\sum_{j=1}^{N_R}\left|\sum_{i=1}^{N_T}h_{j,i}^{t}\left(\hat{x}_t^i-x_t^i\right)\right|^2 \tag{B.1}$$

At each time *t*, we define a space time symbol difference vector $\boldsymbol{F}\left(\boldsymbol{x}_t,\hat{\boldsymbol{x}}_t\right)$ as

$$\boldsymbol{F}\left(\boldsymbol{x}_t,\hat{\boldsymbol{x}}_t\right)=\left[x_t^1-\hat{x}_t^1,x_t^2-\hat{x}_t^2,.....,x_t^{N_T}-\hat{x}_t^{N_T}\right]^T \tag{B.2}$$

Let us consider an $N_T\times N_T$ matrix $\boldsymbol{C}_t\left(\boldsymbol{x}_t,\hat{\boldsymbol{x}}_t\right)$ defined as

$$\boldsymbol{C}\left(\boldsymbol{x}_t,\hat{\boldsymbol{x}}_t\right)=\boldsymbol{F}\left(\boldsymbol{x}_t,\hat{\boldsymbol{x}}_t\right).\boldsymbol{F}^{\dagger}\left(\boldsymbol{x}_t,\hat{\boldsymbol{x}}_t\right) \tag{B.3}$$

From (B.3) it is clear that the matrix $\boldsymbol{C}\left(\boldsymbol{x}_t,\hat{\boldsymbol{x}}_t\right)$ is Hermitian. Therefore, there exist a unitary matrix $\boldsymbol{V}_t$ and a diagonal matrix $\boldsymbol{D}_t$ such that

$$\boldsymbol{V}_t.\boldsymbol{C}\left(\boldsymbol{x}_t,\hat{\boldsymbol{x}}_t\right).\boldsymbol{V}_t^{\dagger}=\boldsymbol{D}_t \tag{B.4}$$

The diagonal elements of $\boldsymbol{D}_t$ are the eigenvalues, $D_t^i, i=1,2,....,N_T$, and the rows of $\boldsymbol{V}_t,\left\{\boldsymbol{v}_t^1,\boldsymbol{v}_t^2,....,\boldsymbol{v}_t^{N_T}\right\}$ are the eigenvectors of $\boldsymbol{C}\left(\boldsymbol{x}_t,\hat{\boldsymbol{x}}_t\right)$.

In the case if $\boldsymbol{x}_t=\hat{\boldsymbol{x}}_t$, then $\boldsymbol{C}\left(\boldsymbol{x}_t,\hat{\boldsymbol{x}}_t\right)$ will be an all-zero matrix and all the eigenvalues D_t^i, $i=1,2,....,N_T$, are zero. If $\boldsymbol{x}_t\neq\hat{\boldsymbol{x}}_t$, the matrix $\boldsymbol{C}\left(\boldsymbol{x}_t,\hat{\boldsymbol{x}}_t\right)$ will observe a single nonzero eigenvalue and the other N_T-1 eigenvalues are zero.

Let D_t^1 be the nonzero eigenvalue element which is equal to the squared Euclidean distance between the two space-time symbols $\boldsymbol{x}_t$ and $\hat{\boldsymbol{x}}_t$.

$$D_t^1 = \left| \boldsymbol{x}_t - \hat{\boldsymbol{x}}_t \right|^2 = \sum_{i=1}^{N_T} \left| x_t^i - \hat{x}_t^i \right|^2 \tag{B.5}$$

The eigenvector of $\boldsymbol{C}\left(\boldsymbol{x}_t, \hat{\boldsymbol{x}}_t\right)$ corresponding to the nonzero eigenvalue D_t^1 is denoted by $\boldsymbol{v}_t^1$.

Let

$$\boldsymbol{h}_t^j = \left[h_{j,1}^t, h_{j,2}^t, ..., h_{j,N_T}^t \right] \tag{B.6}$$

be the *j*-th row of channel matrix $\boldsymbol{H}$ at *t* instant.

Then the Euclidean distance between two distinct space time matrices can be written as

$$d_h^2\left(\boldsymbol{X}, \hat{\boldsymbol{X}}\right) = \sum_{t=1}^{L} \sum_{j=1}^{N_R} \sum_{i=1}^{N_T} \left| \beta_{j,i}^t \right|^2 . D_t^i \tag{B.7}$$

where

$$\beta_{j,i}^t = \boldsymbol{h}_t^j . \boldsymbol{v}_t^i \tag{B.8}$$

Since at each time *t* there is at most only one nonzero eigenvalue, D_t^1, the expression (B.7) can be represented by

$$d_h^2\left(\boldsymbol{X}, \hat{\boldsymbol{X}}\right) = \sum_{\substack{t=1 \\ \boldsymbol{x}_t \neq \hat{\boldsymbol{x}}_t}}^{L} \sum_{j=1}^{N_R} \left| \beta_{j,1}^t \right|^2 . D_t^i \tag{B.9}$$

Hence the conditional error probability can be upper bounded by

$$P\left(\boldsymbol{X}, \hat{\boldsymbol{X}} \mid \boldsymbol{H}\right) \leq \frac{1}{2} \exp\left(- \sum_{\substack{t=1 \\ \boldsymbol{x}_t \neq \hat{\boldsymbol{x}}_t}}^{L} \sum_{j=1}^{N_R} \left| \beta_{j,1} \right|^2 \left| \boldsymbol{x}_t - \hat{\boldsymbol{x}}_t \right|^2 \frac{E_s}{4N_0} \right) \tag{B.10}$$

We define $d_H(\boldsymbol{X}, \hat{\boldsymbol{X}})$ as the Hamming distance between two codewords $\boldsymbol{X}$ and $\hat{\boldsymbol{X}}$ of length *L*.

$$d_H(\boldsymbol{X},\hat{\boldsymbol{X}}) = \sum_{t=1}^{L} h(\boldsymbol{x}_t,\hat{\boldsymbol{x}}_t) \tag{B.11}$$

where h is defined as

$$h(\boldsymbol{x}_t,\hat{\boldsymbol{x}}_t) = \begin{cases} 0 & \text{if } \boldsymbol{x}_t = \hat{\boldsymbol{x}}_t \\ 1 & \text{otherwise} \end{cases}$$

In case, if $\left|\beta_{j,i}^{t}\right|$ follows a Rayleigh distribution, we get

$$P\left(\boldsymbol{X},\hat{\boldsymbol{X}}\right) \le \left(\prod_{\substack{t=1 \\ \boldsymbol{x}_t \neq \hat{\boldsymbol{x}}_t}}^{L} \left|\boldsymbol{x}_t - \hat{\boldsymbol{x}}_t\right|^2 \right)^{-N_R} \left(\frac{E_s}{4N_0}\right)^{-N_R d_H(\boldsymbol{X},\hat{\boldsymbol{X}})} \tag{B.12}$$

and the Euclidean distance $d_h^2\left(\boldsymbol{X},\hat{\boldsymbol{X}}\right)$ becomes [5]

$$d_P^2\left(\boldsymbol{X},\hat{\boldsymbol{X}}\right) = \prod_{\substack{t=1 \\ \boldsymbol{x}_t \neq \hat{\boldsymbol{x}}_t}}^{L} \left(\sum_{i=1}^{N_T} \left|\boldsymbol{x}_t^i - \hat{\boldsymbol{x}}_t^i\right|^2 \right) \tag{B.13}$$

For small value of $N_R.d_H(\boldsymbol{X},\hat{\boldsymbol{X}})$ the inequality (B.12) at high SNR can be written as [4]

$$P(\boldsymbol{X},\hat{\boldsymbol{X}}) \le \left[\underbrace{\left(d_p^2(\boldsymbol{X},\hat{\boldsymbol{X}})\right)^{1/d_H(\boldsymbol{X},\hat{\boldsymbol{X}})}}_{\text{Coding gain}} \frac{E_s}{4N_0} \right]^{\underbrace{-d_H(\boldsymbol{X},\hat{\boldsymbol{X}})N_R}_{\text{Diversity order}}} \tag{B.14}$$

Appendix-C

Trace criteria

Trace is also an important parameter to judge the power of space time codes. From appendix A, we know that the matrix $\boldsymbol{A}$ is Hermitian, and can written as

$$\boldsymbol{A} = \boldsymbol{V}\boldsymbol{D}\boldsymbol{V}^{\dagger} \tag{C.1}$$

where $\boldsymbol{V}$ is an $N_T \times N_T$ matrix of eigenvectors of $\boldsymbol{A}$, and $\boldsymbol{D}$ is an $N_T \times N_T$ diagonal matrix comprising the real eigenvalues λ_i of matrix $\boldsymbol{A}$.

Defining $\boldsymbol{h}_j = \left(h_{j,1}, h_{j,2}, ..., h_{j,N_T}\right)$ as the j-th row of matrix $\boldsymbol{H}$, the Euclidean distance between two symbol sequences can be written as

$$\begin{aligned} d_h^2\left(\boldsymbol{X}, \hat{\boldsymbol{X}}\right) &= \sum_{j=1}^{N_R} \boldsymbol{h}_j \boldsymbol{A}\left(\boldsymbol{X}, \hat{\boldsymbol{X}}\right) \boldsymbol{h}_j^{\dagger} \\ &= \sum_{j=1}^{N_R} \boldsymbol{h}_j \boldsymbol{V}\boldsymbol{D}\boldsymbol{V}^{\dagger} \boldsymbol{h}_j^{\dagger} \\ &= \sum_{j=1}^{N_R} (\boldsymbol{h}_j \boldsymbol{V}) \boldsymbol{D} (\boldsymbol{h}_j \boldsymbol{V})^{\dagger} \\ &= \sum_{j=1}^{N_R} \sum_{i=1}^{r_A} \lambda_i \left|\beta_{j,i}\right|^2 \end{aligned} \tag{C.2}$$

where $\beta_{j,i} = \boldsymbol{h}_j . \boldsymbol{v}_i$ represents the product of row vector $\boldsymbol{h}_j$ with the i-th column vector $\boldsymbol{v}_i$ of $\boldsymbol{V}$. Substituting (C.2) into (3.16) we get

$$P\left(\boldsymbol{X}, \hat{\boldsymbol{X}} \mid \boldsymbol{H}\right) \le \prod_{j=1}^{N_R} \exp\left(-\frac{E_s}{4N_0} \sum_{i=1}^{r_A} \lambda_i \left|\beta_{j,i}\right|^2 \right) \tag{C.3}$$

As the channel coefficient $h_{j,i}$ are zero mean complex Gaussian variables, and 1/2 variance per dimension, it is possible to show that the coefficients $\left|\beta_{j,i}\right|$ follow Rayleigh distribution. Applying the central limit theorem, when $r_A N_R \ge 4$, the expression

$$\sum_{j=1}^{N_R}\sum_{i=1}^{r_A}\lambda_i\left|\beta_{j,i}\right|^2 \tag{C.4}$$

approaches a Gaussian random variable, D with mean

$$\mu_D = N_R\sum_{i=1}^{r_A}\lambda_i \tag{C.5}$$

and the variance

$$\sigma_D^2 = N_R\sum_{i=1}^{r_A}\lambda_i^2 \tag{C.6}$$

Hence the PEP can then be upper bounded by

$$P\left(\boldsymbol{X},\hat{\boldsymbol{X}}\right)\le\frac{1}{2}\int_0^{\infty}\exp\left(-\frac{E_s}{4N_0}D\right)p(D)dD \tag{C.7}$$

where $p(D)$ is the PDF of the Gaussian random variable D.

We can derive [4], [5]

$$P\left(X,\hat{X}\right)\le\frac{1}{2}\exp\left(\frac{1}{2}\left(\frac{E_s}{4N_0}\right)^2\sigma_D^2-\frac{E_s}{4N_0}\mu_D\right)Q\left(\frac{\frac{E_s}{4N_0}\sigma_D^2-\mu_D}{\sigma_D}\right) \tag{C.8}$$

Using inequality

$$Q(x)\le\frac{1}{2}e^{-x^2/2},\qquad x\ge 0 \tag{C.9}$$

We can get the following equation

$$P\left(\boldsymbol{X},\hat{\boldsymbol{X}}\right)\le\frac{1}{4}\exp\left(-N_R\frac{E_s}{4N_0}\sum_{i=1}^{r_A}\lambda_i\right) \tag{C.10}$$

In order to minimize the error probability, the minimum sum of all eigenvalues of matrices $\boldsymbol{A}(\boldsymbol{X},\hat{\boldsymbol{X}})$ among all the pair of distinct codewords should be maximized. For a square matrix the sum of all the eigenvalues is equivalent to the sum of all the elements on the matrix main diagonal, which is called the *trace of the matrix* [4] and can be expressed as

$$tr\left(\boldsymbol{A}\left(\boldsymbol{X},\hat{\boldsymbol{X}}\right)\right)=\sum_{i=1}^{r_A}A_{ii}=\sum_{i=1}^{r_A}\sum_{t=1}^{L}\left|x_i^t-\hat{x}_i^t\right|^2=\sum_{t=1}^{L}d_E^2\left(x_t,\hat{x}_t\right) \tag{C.11}$$

It can be seen from (C.11) that the trace of matrix $\boldsymbol{A}(\boldsymbol{X},\hat{\boldsymbol{X}})$ is equivalent to the squared Euclidean distance between the codeword $\boldsymbol{X}$ and $\hat{\boldsymbol{X}}$. It is also important to note that the condition $r_A N_R \ge 4$ is verified for various MIMO systems. Most of the time, if $r_A = N_T$, the condition $r_A N_R \ge 4$ can be transferred to $N_T N_R \ge 4$.

References

[1] Ezio Biglieri, Robert Calderbank, Andrea Goldsmith, Arog Yaswami, Paulraj and H. Vincent Poor, " *MIMO Wireless Communications* " Cambridge University Press, 2007

[2] George Tsoulos, "*MIMO System Technology For Wireless Communications*" CRC Press, USA ,2006

[3] C. Comaniciu, N. Mandayam, and H. V. Poor, " *Wireless Networks: Multi-user Detection in Cross-layer Design.*" New York: Springer, 2005.

[4] Jakes W. C. "*Microwave Mobile Communication*", Wiley, 1974

[5] Fatma Kharrat-Kammoun, "*Adaptive techniques and classification for MIMO systems*" PhD Thesis ENST Paris, 2006

[6] Proakis, J. G. "*Digital Communications*", McGraw-Hill Inc., 1989.

[7] C.E. Shannon, "A Mathematical Theory of Communication," *Bell Systems Technical Journal*, vol. 27, July and October 1948.

[8] T. M Cover, J.A. Thomas, " *Elements of Information theory* " John Wiley & Sons, 1991.

[9] J. Proakis, " *Digital Communications* ", 4th edition, McGrawHill, New York, 2000.

[10] G.J. Foschini and M.J. Gans, "On Limits of Wireless Communications in a Fading Environment when Using Multiple Antennas", *Wireless Personal Communications*, vol. 6, no. 3, pp. 311-335, March 1998.

[11] A. Paulraj, R. Nabar, and D. Gore, "*Introduction to Space-Time Wireless communications*," Cambridge University Press, New York, 2003.

[12] I.E. Telatar, "Capacity of multi-antenna Gaussian Channels," *European Transactions on Telecommunications*, vol. 10, no. 6, pp. 585-595, November-December 1999.

[13] A. Leon-Garcia, "*Probability and Random Processes for Electrical Engineering*" Addison Wesley, New York, 2nd edition, 1994.

[14] A. Papoulis," *Probability, Random Variables, and Stochastic Processes* " McGraw Hill, New York, NY, 1984.

[15] H.Jaffarkhani "*Space time coding: theory and practice*", Cambridge university press UK, 2005.

[16] Branka Vucetic, Jinhong Yuan, "*Space Time Coding*" New York John Wiley and sons 2003

[17] Frédérique Oggier, Jean-Claude Belfiore, Emanuele Viterbo, " *Cyclic Division Algebras*: *A Tool for Space Time Coding*", now, Boston – Delft, 2007

[18] David Tse and Pramod Viswanath, " *Fundamentals of Wireless Communication*," Cambridge University Press, September 2004.

[19] E. C. van der Meulen, " *Transmission of Information in a T-Terminal Discrete Memoryless Channel*", PhD thesis, University of California at Berkeley, Berkeley, CA, June 1968.

[20] K.J.Ray Liu, Ahmed K. Sadek, Weifeng Su, and Andres Kwasinski, "*Cooperative Communications and Networking*", Cambridge University Press 2009.

[21] T.M. Cover and Abbas A. EL Gamal, "Capacity Theorems for the Relays Channel " *IEEE transaction on information Theory* vol. 25 no.5 September 1979.

[22] J.N. Laneman, David Tse, and G.W. Wornell, "Cooperative Diversity in Wireless Networks: Efficient protocols and outage Behabior", *IEEE Trans on Info Theory*, vol. 50, no.12 December 2004.

[23] M. K. Simon and M. S. Alouini , "A unified approach to the performance analysis of digital communication over generalized fading channels", *Proceedings of the IEEE*, 86(9):1860–1877, September 1998

[24] M. O. Hasna and M. S. Alouini, "Performance analysis of two-hop relayed transmissions over rayleigh fading channels,". *In Proceedings of the IEEE Vehicular Technology Conference*, vol. 4, pp. 1992–1996, 2002.

[25] Murat Uysal, "*Cooperative Communications for Improved wireless Network Transmission*" , Information Science Reference USA 2010.

[26] Gerhard Kramer, Ivana Maric and Roy D. Yates, "*Cooperative Communications*", now Publishers Inc. USA 2006

[27] Christoph F.M. and Markus Rupp, "Generalized Alamouti Codes for Trading Quality of Service against Data Rate in MIMO UMTS ", *Eurasip Journal on applied signal processing* 2004, pp 662-675

[28] Mohammad A. Khojastepour, Ashutosh Sabharwal, Behnaam Aazhang, "Bounds on Achievable Rates for General Multi-terminal Networks with Practical Constraints", 2nd *International Workshop on Information Processing in Sensor Networks* (IPSA '03), Pale Alto, California, USA, April (2003)

[29] Wyner, A. and Ziv, J, " The rate-distortion function for source coding with side information at the decoder", *IEEE Trans. on Inform. Theory*, 22(1):pp. 1–10. 1976.

[30] Lai, Liu K. and H. Gamal, "The three node wireless network: Achievable rates and cooperation strategies", *IEEE Transactions on Information Theory*, vol. 52 issue 3, 2006.

[31] Jhong Sam Lee and Leonard E. Miller, "*CDMA Systems Engineering HANDBOOK*," Artech House Publishers, New York, 1998.

[32] Kamran Etemad, "*CDMA 2000 Evolution: System Concept and Design Principles*", Wiley-Interscience 1st edition, 2004

[33] Abbas E. Gamal and Sina Zahedi, "Capacity of a class of relay channels with orthogonal components", *IEEE Trans. on info theory* vol.51 no.5 May 2005

[34] S.M.Alamouti , "A simple diversity technique for wireless communications" *selected area in communications IEEE journal* vol.16 pages 1451-1458 October 1998.

[35] V.Tarokh, H.Jaffarkhani et A.R.Calderbank, " Space Time Block Codes from Orthogonal design" , *Information Theory, IEE transaction*, vol. 45, no.5 pages1456-1467 July 1999.

[36] Thi Minh Hien NGO, "*Study and construction a new class of space time trellis codes for future MIMO system*" Phd Thesis INSA Rennes, 2009.

[37] Xhue-Bin Liang and Xiang-gen Xia, " On the Non-existence of rate-One Generalized Complex Orthogonal Design," *IEEE Trans. on Info Theory*. vol.49, no.11 Nov. 2003.

[38] V. Tarokh, N. Seshadri et A. Calderbank, "Space-time codes for high data rate wireless communication: performance criterion and code construction", *IEEE Trans.Inform. Theory*, vol. 44, no. 2, pp. 744-765, March 1998.

[39] B.Hochwald, T.L. Marzetta et C.B. Papadias, " A transmitter diversity scheme for wideband CDMA systems based on space time spreading", *selected area in communication IEEE journal* vol. 19 no.1 pages 48-60 Jan 2001

[40] Weifeng Su, X.G.Xia and K.J. Ray Liu, "A systematic Design of High Rate Complex orthogonal Space-Time Block Codes" , *IEEE Comm. Lett*, vol.8,no.6 June 2004

[41] Haiquan Wang et Xiang-Gen Xia, " Upper bound of rates of complex orthogonal space-time block codes" *Information theory IEEE transaction* on vol. 49 no.10 pages 2788-2796, October 2003

[42] H.Jaffarkhani "A quasi orthogonal space time block code", *communication IEEE Trans*. vol. 49, no. 1, pages 1-4 jan 2001

[43] N. Sharma and C.B. Papadias, "Improved quasi orthogonal codes through constellation rotation" *communication IEEE transaction on* vol. 51 no.3 pages 332-335 March 2003

[44] Weifeng Su et Xiang-Gen Xia, "Signal constellation for quasi orthogonal space time block codes with full diversity " *Information theory IEEE transaction on* vol. 50 no.10 pages 2331-2347 October 2004

[45] L.A. Dalton et C.N. Georghiades, "A full rate, full diversity, four antennas quasi orthogonal space time block codes" *Wireless communication IEEE transaction on* vol. 4 no.2 pages 363-366 March 2005

[46] Hassibi, B. and Hochwald, B, " High-rate codes that are linear in space and time," *IEEE Trans. on Information Theory*, vol. 48 no. 7, pages 1804-1824, July 2002.

[47] Jr. Heath, R.W. and A.J. Paulraj, "Linear dispersion codes for MIMO systems based on frame theory" Signal processing *IEEE transaction on* vol. 50 no.10 pages 2429-2441 October 2002

[48] Qi Ling and Tongtong Li , " Efficiency Improvement for Alamouti codes", *IEEE 40th annual conference on Information Sciences and systems*, pages 569-572, 22-24 March 2006 .

[49] S. Baro, G.bauch et Hansmann, " Improved codes for Space Time Trellis Coded Modulation*" IEEE commun. Lett*. vol. 4, no.1 pages 20-22 Jan 2000

[50] Z.Chen, J. Yuan et B. Vuceutic "improved Space Time trellis coded modulation scheme on slow fading channels" *Electron. Lett*. vol. 37, no. 7 pages 440-441 March 2001.

[51] W. Fermanto, B.S. Vuceutic et J.Yuan , " Space Time TCM with improved performance on fast fading channels" *IEEE Commun. Lett*. vol. 5, no.4 pages 154-156 April 2001

[52] Q.Yan and R.S. Blum, "Optimum Space Time Convolutional codes" *in proc. IEEE WCNC 2000 Wireless Communication and networking Conference*, vol. 3, pages 1351-1355, 2002.

[53] Yi Hong, J. Yuan, Z. Chen et B. Vuceutic, "Space Time turbo trellis coded Codes for Two, Three and Four transmit antennas" *Electron. Trans*. *On Vehicular Technology* vol. 53, no. 2 pages 318-328 March 2004.

[54] Y.S Jung, et J.H. Lee, "Hybrid-ARQ scheme employing different Space Time trellis coded in slow fading channels" *In proc. IEEE VTC* 2002-fall vol. 1, pages 247-251, Sept. 2002.

[55] H.Jaffarkhani and N.Seshadri, " Super-orthogonal Space Time trellis Codes" *Information Theory, IEEE transactions*, vol. 49, no.4 pages 937-950 April 2003.

[56] S.M. Alamouti,V. Tarokh, and P. Poon," Trellis-coded modulation and transmit diversity: design criteria and performance evaluation" *IEEE International Conference on Universal Personal Communication* (ICUPC-98), pages 917–920 October 1998.

[57] Ungerboeck, G, "Channel coding for multilevel/phase signals", *IEEE Trans. on Information Theory*, vol. 28 no. 1, pages 55-67 Jan. 1982.

[58] G. Ferré, J.P. Cances, V. Meghdadi and J.M. Dumas, "STBC based (Turbo) STTC Codes built by Set Partitioning for Three Transmit Antennas: Construction and Performances" *Wireless Communications, IEEE Transactions* on, vol. 6, no3, pages 827–832, March 2007.

[59] H. Jafarkhani and N. Hassanpour, " Super-Quasi-Orthogonal Space-Time Trellis Codes for Four Transmit Antennas, " *Wireless Communications, IEEE Transactionson*, vol. 4, no.1, pages 215–227, Jan. 2005.

[60] G.J. Foschini, "Layered space time architecture for wireless communication in a fading environment when using multiple antennas", *Bell Lab. Tech. Journal*. vol. 2 Autumn 1996.

[61] H.Gamal and A.R. Hammon, "A New approach to Layered Space Time Coding and Signal Processing" *IEEE Trans info theory* vol. 47, no.6, pp 2321-2334, Sept. 2001.

[62] M.O.Damen, K.A. Meraim and J.C.Belfiore, " Diagonal Algebraic Sapce Time Block codes," *IEEE trans on info theory*, vol. 48, no.3, pp 628-636, March 2002.

[63] H.EL. Gamal, and M.O. Deman, " Universal Space Time Coding" *IEEE Trans. on Information theory*, vol. 49 no.5, pages 1097–1119 May. 2003

[64] Damen, M. O. , Tewfik, A. and Belfiore, J.-C. " A construction of a space-time code based on number theory".*IEEE Trans. on Information Theory*, vol.48 no.3 pages 753-760 March. 2002,

[65] B.A.Sethuraman, B.Sundar rajan and V.Shashidhar, " Full-Diversity, High-Rate Space Time Block codes From Division Algebras" , *IEEE trans. on info theory* vol.49, no.10 October 2003

[66] Y. Lie and X.G. Xia, "Full Diversity Distributed Space Time Trellis Codes for Asynchronous Cooperative Communication," 2004 reprint.

[67] Y. Mei, Y. Hua, A. Swami, and B. Daneshrad, "Combating synchronization errors in cooperative relays" , *in Proc. IEEE International Conference on Acoustic, Speech, and Signal Processing,* Philadelphia, PA, USA, pp. 1-6, Mar. 2005.

[68] A. R. Hammons, Jr. and R. E. Conklin, Jr., "Space-time block codes for quasi-synchronous cooperative diversity", *in Proc. Military Communications Conf.* (MILCOM), Washington, DC, pp. 1–7, October 2006.

[69] Mohamed Oussama Damen and A.Roger Hammons, "delay Tolerant Distributed TAST Codes for Cooperative Diversity", *IEEE trans on Info theory* vol. 53 no. 10 October 2007

[70] J. Boutros and E. Viterbo, "Signal space diversity: A power and bandwidth efficient diversity technique for the Rayleigh fading channel," *IEEE trans. Information theory*, vol. 44, pp. 1453-1467, July 1998

[71] X. Giraud, E. Boutillon, and J. C. Belfiore, "Algebraic tools to build modulation schemes for fading channels" , *IEEE trans. Inform. theory*, vol. 43, pp. 938-952, May 1997.

[72] J.-C. Belfiore, X. Giraud, and J. Rodriguez, "Linear labeling for joint source channel coding," *in Proc. ISIT* 2000, Sorrento, Italy, June 2000.

[73] M. O. Damen, A. Chkeif, and J. C. Belfiore, "Lattice codes decoder for space-time codes," *IEEE Communications Letters*, vol. 4, pp. 161-163, May 2000.

[74] M.O. Damen, H. E. Gamal and N.C. Beaulieu, "Systematic Construction of Full Diversity Algebraic Constellations", *IEEE trans: on info: theory* vol.49 no.12 December 2003

[75] P. Dayal and M. K. Varanasi, "An optimal two transmit antenna space time code and its stacked extensions" , *in Proc. Asilomar Conf. Signals,Systems and Computers*, Pacific Grove, CA, pp. 987–991, November 2003.

[76] H. Yao and G. W. Wornell, "Achieving the full MIMO diversity-multiplexing frontier with rotation-based space-time codes," *in Proc. Allerton Conf. Communication, Control, and Computing*, Monticello,IL, October 2003

[77] J. Belfiore, G. Rekaya, and E. Viterbo, "The Golden code: A 2×2 full-rate space–time code with nonvanishing determinants", *IEEE trans. Inf. theory*, vol. 51, no. 4, pp. 1432-1436, April 2005.

[78] A. R. Hammons, Jr., "Algebraic space-time codes for quasi-synchronous cooperative diversity" *in Proc. IEEE Int. Conf. Wireless Networks, Communications and Mobile Computing* (WirelessCom 2005), Maui, HI, vol. 1, pp. 11-15, June 2005.

[79] A. R. Hammons, Jr. and H. El Gamal, "On the theory of space-time codes for PSK modulation," *IEEE Trans. Inf. Theory*, vol. 46, no. 2, pp. 524-542, March 2000.

[80] Mehdi Torbatian and Mohamed Oussama, " On the design of Delay Tolerant Distributed Space Time Codes with Minimum Length", *IEEE trans on wireless comm.*: vol.8 no. 2 pages 931-939 February 2009

[81] A. D. Murugan, H. El Gamal, M. O. Damen, and G. Caire, "A unified framework for tree search decoding: Rediscovering the sequential decoder*," IEEE Trans. Inf. Theory*, vol. 52, no. 3, pp. 933-953, March 2006.

[82] M. O. Damen, H. El Gamal, and G. Caire, "On maximum-likelihood detection and the search for the closest lattice point," *IEEE Trans. Inf Theory*, vol. 49, no. 10, pp. 2389-2401, October 2003.

[83] Garrett Birkhoff, "*Lattice Theory*", Colloquium Publications, American Mathematical Society, 3rd edition 1967

[84] M. Pohst, "On the computation of lattice vectors of minimal length, successive minima and reduced basis with applications," *in ACM SIGSAM*, vol. 15, pp. 37-44, Bull, 1981.

[85] U.Fincke and M. Pohst, "Improved methods for calculating vectors of short length in a lattice, including a complexity analysis", *Mathematics of computation*, vol.44 no.170 pp. 463-471, April 1985

[86] E. Viterbo and J. Boutros, "A universal lattice code decoder for fading channel," *IEEE trans. Inform. theory*, vol. 45, pp. 1639–1642, July 1999.

[87] B. Hassibi and H. Vikalo, "On the Sphere-Decoding Algorithm-I. Expected Complexity", *IEEE Trans on signal processing* vol.53, no.8, pp. 2806-2818, Aug. 2005

[88] B. Hassibi and H. Vikalo, "On the Sphere-Decoding Algorithm-II. Generalizations, Second-Order Statistics, and Applications to Communications", *IEEE Trans on signal processing* vol.53, no.8, pp. 2819-2834, August 2005.

[89] M.O. Damen, "*Joint Coding/Decoding in a multiple Access System, Application to Mobile Communications*", PhD Dissertation, ENST Paris, October 1999.

[90] G. D. Golden, G. J. Foschini, R. A. Valenzuela, and P. W. Wolniasky, "Detection algorithm and initial laboratory results using V-BLAST space-time communication architecture," *Electronics Letters*, vol. 35, pp. 14-16, Jan. 1999

List of Publications

1. Zahoor Ahmed, J.P. Cances and V. Meghdadi," Delay Tolerant (delto) Distributed TAST Codes for Cooperative Wireless Networks," submitted to EURASIP Journal on Advances in Signal Processing

2. Zahoor Ahmed, J.P. Cances and V. Meghdadi," Block layering approach in TAST codes," published in International Journal of Communications, Network and System sciences, vol.3, no.10, October 2010

3. Zahoor Ahmed, M.Usamn and Noor Hussian,"Efficiency Improvement of Space Time Block Codes Block," published in International Journal of Communications, Network and System sciences, vol.3, no.6 June 2010.

4. Zahoor Ahmed, J.P. Cances and V. Meghdadi," Cryptographic Spread Spectrum Relay Communication," presented at 2nd International IEEE conference on Next generation Mobile application and services technologies (NGMAST) held at Cardiff UK from 16-19 September 2008

Étude et construction de codes spatio-temporels algébriques dans le contexte des communications asynchrones par relais coopératif

Résumé

Une des spécificités des communications coopératives par relais sans fil est l'asynchronisme des transmissions. A cause de ces transmissions asynchrones, les méthodes de conception traditionnelles des codes espace-temps distribués sont à revoir si on veut conserver des codes à gains de diversité maximale. Pour éviter ce décalage de synchronisation certains auteurs ont proposé l'utilisation de bandes de garde entre les transmissions successives. Cette technique peut être applicable pour les codes de longueur courte, mais pour de longs mots de code, l'utilisation de bandes de garde réduit considérablement le taux de codage.
En travaillant sur cette contrainte de délai pour les codes TAST, Damen et Hammons ont introduit une nouvelle classe de codes TAST qui sont robustes en terme de retards et donc adaptés aux réseaux coopératifs asynchrones. Ces codes préservent leur propriété de rang plein pour des retards arbitraires en réception sur les différentes lignes de la matrice de codage.
Bien que les codes distribués TAST mis en place par Damen et Hammons peuvent atteindre le maximum de diversité pour un profil de délai arbitraire, leur longueur temporelle n'est pas optimisée et peut s'avérer prohibitive. Pour aller plus loin dans le travail de Damen et Hammons, notre travail principal de cette thèse a consisté à construire des codes distribués TAST qui pourraient absorber des retards arbitraires et offrir de meilleurs taux de codage avec une longueur minimale. Nos codes proposés sont simples à construire, tolérants en terme de retard, et possèdent une longueur minimale au regard de la taille de la constellation et du nombre d'antennes d'émission et de réception.
Nous présentons différentes techniques pour la construction de codes TAST tolérants en retard. Les analyses mathématiques suivies par des simulations réalisées confirment que nos codes à longueur minimale dépassent les performances des codes existants dans la littérature sans pour autant sacrifier la complexité de décodage.

Mots clés : Algébrique STBC, communication asynchrones, code résistant au retard

---

Study and construction of delay tolerant (delto) distributed TAST codes for cooperative wireless networks.

Abstract

One of the recent discussed problems of the cooperative communication is the asynchronization of the relaying nodes. Due to the asynchronous transmissions all traditionally designed structure of distributed space-time codes are destroyed at the reception and they loose their reliability (*viz*. diversity and coding gain). To avoid this destructive effect some authors have proposed the use of guard bands between successive transmissions. This technique may be applicable for short length codes, but for lengthy codewords, the use of guard bands drastically reduces the code rate.
Working on delay constraint of TAST codes, Damen and Hammons introduced a new class of TAST codes which are delay resistant and hence suitable for unsynchronized cooperative network. These codes preserve their rank under arbitrary delays at the reception of different rows of the codeword matrices.
Although the distributed TAST codes introduced by Damen and Hammons can achieve maximum diversity under arbitrary delay profile but their delay time is not gnarly. Extending the work of Damen and Hammons, our principal work in this thesis is to build distributed TAST codes which could absorb arbitrary delays and offer better code rates. Our proposed codes are simple in construction, delay tolerant under arbitrary delays, better in rates, feasible in term of constellation size, number of receive/transmit antennas, and decoding complexity.
We introduce different techniques for constructing delay tolerant TAST codes. Mathematical analyses followed by computer simulations confirm that our codes with minimum code lengths outperform the existing codes in the literature without sacrificing decoding complexity and other nice characteristics.

Keywords: Algebraic STBC, asynchronization communication, delay tolerant STBC